ABSORPTION OF SULPHUR DIOXIDE INTO AQUEOUS MEDIA:

A MECHANISM STUDY

by

P.J. HETHERINGTON, B.Sc.(App.) Hons. (Tas.)

submitted in fulfilment of the requirements
for the Degree of

Doctor of Philosophy

UNIVERSITY OF TASMANIA

HOBART

July 1968

Except as stated herein, this thesis contains no material which has been accepted for the award of any other degree or diploma in any University. To the best of the candidate's knowledge and belief, it contains no copy or paraphrase of material previously published or written by another person, except when due reference is made in the text.

P.J. Hetherington

July 1968

CONTENTS

APPENDICES

FIGURES

PLATES

TABLES

CHAPTER 3

CHAPTER 5

CHAPTER 6

CHAPTER 7

CHAPTER 8

GRAPHS

CHAPTER 1

CHAPTER 3

ABSTRACT

A laminar jet technique is used to investigate the absorption of sulphur dioxide into aqueous media. Two new features of the technique are

(i) an improved nozzle design which minimizes boundary layer effects and

(ii) precision measurement of gas flow rates in the range 1 - 10 cc/sec.

Interpretation of the absorption measurements is based on new equilibrium solubility data for water and hydrochloric acid solutions.

Studies of absorption into water and hydrochloric acid solutions indicate that, although absorption into water appears to be a physical process, it is accompanied by a fast, reversible, pseudo first order reaction. The concentration dependence of the diffusion coefficients of the equilibrium species is determined by studying absorption of sulphur dioxide into its aqueous solution. This dependence explains the discrepancies between previously published measurements of these coefficients.

Lack of kinetic data prevents a complete analysis of the mechanisms of absorption into sodium hydroxide solutions. It appears that absorption rates are enhanced by interactions between diffusing ionic species.

Results obtained for absorption into water from mixtures with nitrogen indicate that unsteady-state gas-phase transfer cannot be

described in terms of Fick's law diffusion coefficients. These must be corrected to allow for changes in the partial pressure of the solute gas.

CHAPTER 1 STATEMENT OF THE PROBLEM

1.1 INTRODUCTION

Since the pioneering work of Whitman [1]* in 1923, numerous investigations of gas absorption processes have been reported. Until recently, the majority of these investigations were designed to improve the performance of industrial equipment and the results were reported in the form of empirical or semi-empirical correlations. Because of the complex gas- and liquid-phase hydronamics involved, these correlations can yield little information about the absorption mechanisms. Indeed, many predict quite different effects of the variables (e.g. gas- or liquid-phase diffusion coefficients) and much of the confusion which exists regarding these mechanisms can be traced to the differences between the correlations.

Many of the theories of gas absorption are basically very different and yet predict similar absorption rates. Consequently, to test these theories experimentally, it is necessary to use equipment in which both gas- and liquid-phase hydronamics can be adequately described and to obtain precise measurements of absorption rates. Many such 'fundamental' investigations have been reported more recently but these have been very restricted in the variety of solute gases studied. One process which has received little

---

* References are given in Appendix 1. Where direct access to a reference has not been possible, the actual source of the information has been indicated by the phrase 'quoted by Ref.[ ].'

attention, and about which there has been some controversy, is the absorption of sulphur dioxide into aqueous media. Evidence for the rate of ionization of sulphur dioxide in water is conflicting and most investigators have found it convenient to ignore the reaction and its possible effects on absorption rates. It is not altogether surprising then that, for example, diffusion coefficients of sulphur dioxide in water measured in absorption experiments differ markedly from those measured by other techniques. One of the aims of this investigation has been to resolve these and other discrepancies associated with the absorption of sulphur dioxide. Again, by far the greater proportion of these 'fundamental' investigations has been concerned with the study of liquid-phase mechanisms and there is still a dearth of reliable experimental data regarding transfer in the gas-phase. It has long been known that when sulphur dioxide is absorbed from mixtures with other gases the resistance to transfer in the gas-phase is of the same order of magnitude as that in the liquid-phase. The process therefore affords a good opportunity for study of gas-phase mechanisms and this has been the second aim of this investigation.

1.2 THEORIES OF GAS ABSORPTION

In most absorption processes, a liquid is exposed to a mixture of two or more gases, one of which is to be absorbed. The transfer process is often represented as in Figure 1.1 and described by the relationships

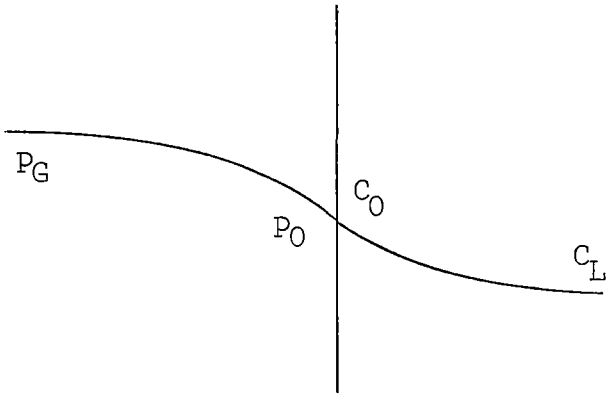

Gas Interface Liquid

Figure 1.1

$$N_A = k_G(P_G - P_0) = k_L(C_0 - C_L) \qquad (1.1)$$

This assumes that the interface offers no resistance to transfer, an assumption which recently has been seriously questioned and which is discussed in Section 1.2.3.

The oldest and most general theory, the two-film theory [1,2], suggests that transfer is controlled in each phase by a film of finite thickness across which well defined concentration profiles exist and that the rate of transfer across each film is proportional to the diffusion coefficient of the solute gas. The theory has been very useful as a basis for correlating data in industrial equipment [e.g. 3,4], but it is now accepted as being unrealistic, at least with respect to the liquid-phase [5]. Other theories are concerned specifically with only one of the phases and will be discussed accordingly.

1.2.1 LIQUID-PHASE THEORIES

1.2.1.1 Physical Absorption

If a gas is suddenly exposed to a liquid with which it does not react and if heat effects and volume changes can be ignored, then the liquid-phase absorption mechanism is one of unsteady state diffusion [6] and can be described by Fick's second equation

$$\frac{\partial C}{\partial \theta} = \left[\frac{\partial^2 C}{\partial x^2}\right] \tag{1.2}$$

with the following boundary conditions:

$$\theta = 0, \quad x \geqslant 0, \quad C = C_o \tag{1.3}$$

$$\theta \geqslant 0, \quad x = \infty, \quad C = C_o \tag{1.4}$$

$$\theta > 0, \quad x = 0, \quad C = C_s \tag{1.5}$$

If the diffusion coefficient is assumed independent of concentration, equations (1.2) to (1.5) can be solved for the instantaneous absorption rate, defined by

$$N(\theta) = - \mathcal{D}\left(\frac{\partial C}{\partial x}\right)_{x=0} \tag{1.6}$$

to give

$$N(\theta) = (C_o - C_L)\left[\frac{\mathcal{D}}{\pi\theta}\right]^{\frac{1}{2}} \tag{1.7}$$

and

$$k_L = \left[\frac{\mathcal{D}}{\pi\theta}\right]^{\frac{1}{2}} \tag{1.8}$$

Equation (1.7) is the basis of what is now known as penetration theory. It has been used by numerous investigators [e.g. 7-23] to interpret absorption mechanisms and is used in the present investigation. It can be used only when liquid-phase velocity

gradients are absent or can be well defined. Other theories (surface renewal [5,24,25], film-penetration [26] and random eddy [27]) have been developed to describe conditions with ill-defined hydronamics but are of no interest here.

1.2.1.2 Absorption With Chemical Reaction

Many processes are accompanied by a chemical reaction between the solvent and the dissolving gas. They can be classified first according to the order, rate and reversibility of the reaction and, because diffusion of the reaction products affects the absorption rate, they must also be classified according to the number and nature of these products. Two types of reaction are of interest in this investigation and a mathematical model of each will be described.

(a) Fast Reversible First Order Reaction with Two Products

Consider the reaction

$$R \rightleftarrows P_1 + P_2 \tag{1.9}$$

If the products P_1 and P_2 are univalent ions of opposite sign, they will diffuse together with a diffusion coefficient $\mathcal{D}_P$. If the reaction is very fast compared with the rate of diffusion, equilibrium conditions will be approached at all points along the diffusion path and the concentrations of reactant and product can be related by

$$K = \frac{C_{P_1} \cdot C_{P_2}}{C_R} = \frac{C_P^2}{C_R} \tag{1.10}$$

Olander [28] has presented a model for this type of reaction based on surface renewal theory. His derivation apparently contains an

error and this has been corrected, and the model adapted to penetration theory, in Appendix 3. The model is only an approximate one and a more accurate one has been obtained by inserting an empirical correction. This is also discussed in Appendix 3 and the final result can be stated as follows. If the instantaneous absorption rate is defined by

$$N(\theta) = -\mathcal{D}_R\left(\frac{\partial C_R}{\partial x}\right)_{x=0} - \mathcal{D}_P\left(\frac{\partial C_P}{\partial x}\right)_{x=0} \tag{1.11}$$

and if both diffusion coefficients are again independent of concentration, then

$$N(\theta) = (C_{RO} - C_{RL})\left[\frac{C_{RO}^{\frac{1}{2}} + \frac{K^{\frac{1}{2}}}{2}\cdot\frac{\mathcal{D}_P}{\mathcal{D}_R}}{\left(\frac{C_{RO}}{b}\right)^{\frac{1}{2}}\exp\left(\frac{a^2}{b}\right)\operatorname{erfc}\left(\frac{a}{b^{\frac{1}{2}}}\right)}\right]\left(\frac{\mathcal{D}_R}{\pi\theta}\right)^{\frac{1}{2}} \tag{1.12}$$

where the parameters a and b are given by

$$a = \frac{K^{\frac{1}{2}}\left(\frac{\mathcal{D}_P}{\mathcal{D}_R}\right)(C_{RO} - C_{RL})}{2C_{RO}\left(2C_{RO}^{\frac{1}{2}} + K^{\frac{1}{2}}\frac{\mathcal{D}_R}{\mathcal{D}_P}\right)\left(\frac{\pi}{b}\right)^{\frac{1}{2}}\exp\left(\frac{a^2}{b}\right)\operatorname{erfc}\left(\frac{a}{b^{\frac{1}{2}}}\right)} \tag{1.13}$$

$$b = \left(\frac{C_{RO}^{\frac{1}{2}} + \frac{K^{\frac{1}{2}}}{2}}{C_{RO}^{\frac{1}{2}} + \frac{K^{\frac{1}{2}}}{2}\cdot\frac{\mathcal{D}_R}{\mathcal{D}_P}}\right) + 6.60a^2\left(\frac{C_{RO} - C_{RL}}{C_{RO}}\right)\left(\frac{6C_{RO}^{\frac{1}{2}}}{K^{\frac{1}{2}}}\frac{\mathcal{D}_R}{\mathcal{D}_P} + 1\right) \tag{1.14}$$

Comparison of equations (1.7) and (1.12) shows that the effect of the reaction is to increase the liquid-film transfer coefficient by the factor

$$\frac{k_{LR}}{k_L} = F_{R1} \tag{1.15}$$

where F_{R1} is the expression in square brackets in equation (1.12). To the best of the writer's knowledge, no attempts have been made to investigate absorption processes in which this type of reaction occurs.

(b) Fast Irreversible Second Order Reaction with One Product

Consider the reaction

$$G + mS \rightarrow P \qquad (1.16)$$

in which one mole of gas G reacts instantaneously and irreversibly with m moles of solute in the liquid. The process is one of diffusion with a moving boundary, a general solution of which was given by Danckwerts [29]. It can be written for the above reaction as follows. The diffusion of gas and solute in the liquid (Figure 1.2) can be

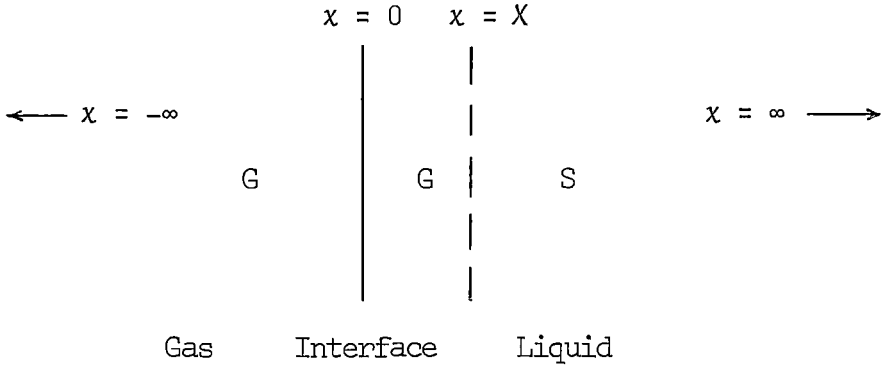

Figure 1.2

represented by

$$\frac{\partial C_G}{\partial \theta} = \mathcal{D}_G \cdot \frac{\partial^2 C_G}{\partial \chi^2} \qquad (1.17)$$

$$\text{and} \quad \frac{\partial C_S}{\partial \theta} = \mathcal{D}_S \cdot \frac{\partial^2 C_S}{\partial \chi^2} \qquad (1.18)$$

Any part of the liquid will contain G or S but not both. As absorption proceeds, a reaction plane at $x = X$ will move further into the liquid. The position of this plane is defined from conservation of diffusants by

$$\mathcal{D}_S\left(\frac{\partial C_S}{\partial x}\right)_{x=X} - m\mathcal{D}_G\left(\frac{\partial C_G}{\partial x}\right)_{x=X} + C_S(X)\frac{\partial X}{\partial \theta} - C_G(X)\frac{\partial X}{\partial \theta} = 0 \qquad (1.19)$$

Liquid for $x < X$ will contain only G; liquid for $x > X$ will contain only S and

$$C_G(X) = C_S(X) = 0 \qquad (1.20)$$

so that equation (1.19) becomes

$$\mathcal{D}_S\left(\frac{\partial C_S}{\partial x}\right)_{x=X} - m\mathcal{D}_G\left(\frac{\partial C_G}{\partial x}\right)_{x=X} = 0 \qquad (1.21)$$

The following boundary conditions will apply

$$\theta = 0;\quad x < 0,\ C_S = 0,\ C_G = C_G;\quad x > 0,\ C_S = C_{SL},\ C_G = 0 \qquad (1.22)$$

$$x = 0;\quad \text{all } \theta,\quad C_G = C_{GO} \qquad (1.23)$$

$$x = -\infty;\quad \text{all } \theta,\quad C_G = C_G \qquad (1.24)$$

$$x = \infty;\quad \text{all } \theta,\quad C_S = C_{SL} \qquad (1.25)$$

The instantaneous absorption rate is defined by

$$N(\theta) = -\mathcal{D}_G\left(\frac{\partial C_G}{\partial x}\right)_{x=0} \qquad (1.26)$$

and if both diffusion coefficients are again independent of concentration, (1.21) can be solved to give

$$N(\theta) = F_{R2} \cdot C_{GO}\left[\frac{\mathcal{D}_G}{\pi\theta}\right]^{\frac{1}{2}} \qquad (1.27)$$

where $F_{R2} = 1/\text{erf}\ \sigma$ (1.28)

and σ can be found by successive approximations from the equation

$$\frac{C_{SL}}{mC_{GO}}\left[\frac{\mathcal{D}_S}{\mathcal{D}_G}\right]^{\frac{1}{2}} = \frac{\operatorname{erfc}\left[\sigma\left(\frac{\mathcal{D}_S}{\mathcal{D}_G}\right)^{\frac{1}{2}}\right]}{\operatorname{erf}(\sigma)\exp\left[\sigma^2\left(1-\frac{\mathcal{D}_G}{\mathcal{D}_S}\right)\right]} \qquad (1.29)$$

Comparison of equations (1.7) and (1.27) shows that if $C_L = 0$, the effect of the reaction is to increase the liquid film coefficient by the factor F_{R2}. Equations (1.27) to (1.29) have been successfully tested and used by other investigators [22,30] to interpret absorption mechanisms for other systems.

1.2.2 GAS-PHASE THEORIES

The present understanding of gas-phase transfer mechanisms is limited. Much confusion seems to have arisen because many semi-empirical correlations have been based on an analogy between heat and mass transfer [3,4]. As Arnold [31] has pointed out, 'the analogy is not exact ... because a diffusing vapour (unlike heat) cannot merely penetrate a gas without causing volume changes, but must displace the gas while mixing with it. Fick's equation makes no allowance for this change in volume ... [and] at high concentrations [the analogy] becomes entirely inadequate.'

The writer knows of only one attempt [32] to investigate the transfer process under conditions of well-defined gas-phase hydrodynamics. Unfortunately this involved the absorption of carbon dioxide into water, a process which is 'liquid-phase controlled', and the results of the investigation were inconclusive.

It is obvious that more 'fundamental' investigations are required and it seems probable that many well-established concepts will have to be re-evaluated before much progress can be made.

1.2.3 INTERFACIAL CONDITIONS

1.2.3.1 Interfacial Resistance

Consider a liquid, unsaturated with respect to a gas, suddenly exposed to a pure atmosphere of that gas. If there were no transfer of gas from the interface into the liquid, the gas concentration at the interface would, after some finite time, reach its saturation value C_s. However, during this time, the gas molecules continuously move away from the interface and, because of this movement, the interface can never reach saturation. When dynamic equilibrium is established, the interfacial concentration is some lower value C_i and transfer across the interface can be described by the relationship

$$N_A = k_i(C_s - C_i) \tag{1.30}$$

The value of C_i is determined by the liquid-phase transfer rate and the upper limit to k_i is determined by the rate at which gas molecules can move to the interface and the condensation coefficient. It has been shown theoretically [33] that this upper limit is given by

$$k_i = \frac{\alpha H}{[2\pi R_c TM]^{\frac{1}{2}}} \tag{1.31}$$

and that, under normal conditions, the value of this limit is so large that the interface offers negligible resistance to transfer

and that equilibrium exists between material on either side of the interface (i.e. $C_i = C_s = C_o$).

It has also been suggested that an interfacial resistance may be caused by surface tension effects [34-36] and interfacial turbulence (Marangoni effect) [36]. However, quantitative prediction of the magnitude of such resistances has proved difficult.

There have been numerous attempts to measure interfacial resistances. Some [6,24,37-42] have yielded inconclusive results due to imprecise measurements but many [7-23,43,44] have indicated that, in the absence of surface active agents, the resistances are negligible. Resistances caused by surface active agents are difficult to measure because of the effects of the surfactants on liquid-phase hydronamics. However, results [45-51] appear to indicate that resistances decrease with decreasing contact time between the gas and liquid. The effects of interfacial turburlence have not been measured but it appears that the phenomenon is not important in most gas-liquid systems, especially with short contact times [52,53].

1.2.3.2 Heat Effects

If the heat of solution is high enough, or if a gas reacts with its solvent, absorption may be accompanied by a comparatively large temperature change at and near the interface. Chiang and Toor [54] considered the problem of simultaneous heat and mass transfer and showed that the temperature change at the interface, which is assumed to occur instantaneously, can be calculated by successive approximations from the equation

$$\Delta t_i = \beta H_s \rho_m \left[\frac{\pi \mathcal{D}}{C_p \rho k}\right]^{\frac{1}{2}} \tag{1.32}$$

where the dimensionless parameter β is also estimated by successive approximations from the equation

$$\frac{\beta \pi^{\frac{1}{2}} \exp(\beta^2)(1 + \operatorname{erf}\beta)}{1 + \beta \pi^{\frac{1}{2}} \exp(\beta^2)(1 + \operatorname{erf}\beta)} = a\beta H_s \left[\frac{\pi \mathcal{D}}{C_p \rho k}\right]^{\frac{1}{2}} \tag{1.33}$$

For physical absorption, the effect of this temperature change on the absorption rate can be represented by an equation of the form

$$N_h = K_1 K_2 N \tag{1.34}$$

where K_1, given by

$$K_1 = \frac{C_{o,h}}{C_o} = 1 + \frac{a H_s \beta \rho_m}{C_o} \left[\frac{\pi \mathcal{D}}{C_p \rho k}\right]^{\frac{1}{2}} \tag{1.35}$$

accounts for the influence of the temperature change on the interfacial gas concentration and K_2, given by

$$K_2 = \frac{1}{\exp(\beta^2)(1 + \operatorname{erf}\beta)} + \beta \pi^{\frac{1}{2}} \tag{1.36}$$

indicates the influence on transfer rates of convective effects due to heat transfer.

If absorption is exothermic, K_1 and K_2 tend to nullify each other and absorption rates may be similar to those that would occur if absorption were isothermal. Consequently, considerable care must be exercised when analysing experimental results for such an absorption process. Equations (1.32) and (1.33) were successfully used to analyse results for the absorption of ammonia into water.

1.3 INTERACTION OF SULPHUR DIOXIDE AND WATER

1.3.1 NATURE OF AQUEOUS SOLUTIONS OF SULPHUR DIOXIDE

Early ultraviolet absorption studies [55-61] of solutions of sulphur dioxide in water revealed only one absorption band. Because aqueous solutions of alkali metal sulphites and bisulphites gave no corresponding band, it was concluded that sulphur dioxide exists in water essentially as unreacted molecules. Some investigators [55,60] considered the molecules to be unaffected by the solvent while others [56-58,61] considered the molecules to be hydrated. Dietzel and Galanos [59] suggested that both free and hydrated molecules co-exist in solution.

Early Raman spectroscopic studies [62-65] were reviewed by Gerding and Nivjeld [65] who concluded that the three observed Raman shifts were attributable to free sulphur dioxide. The same conclusion was reached independently by Fadda [66] but Nisi [67], who examined the spectra of aqueous solutions of several compounds which contained both sulphur and oxygen, not only concluded that sulphurous acid is present in aqueous solutions of sulphur dioxide, but also suggested its structural formula.

In all these investigations comparatively dilute solutions were used. This was noted by Rao [68] who carried out a Raman study of aqueous solutions of different concentrations, the strongest of which was almost saturated. For each solution a single shift of constant wave number was observed and the intensities of the lines were approximately proportional to the sulphur dioxide concentration.

The lines were consequently attributed to free molecules. In a further Raman study, Simon and Waldmann [69] observed sets of lines of three different intensities and concluded that as well as unionised molecules, the solutions contain HSO_3^- ions and a very small proportion of $S_2O_5^=$ ions.

In his ultraviolet absorption work, DeMaine [70] studied the temperature dependence of the band which had been observed in earlier studies and suggested that the interaction between sulphur dioxide and water could be represented by the mechanism

$$SO_2(g) \rightleftarrows SO_2 + H_2O \rightleftarrows \text{complex(hydrate)} \rightleftarrows H_2SO_3 \rightleftarrows H^+ + HSO_3^- \rightleftarrows 2H^+ + SO_3^=$$

It should be noted however, that the validity of this mechanism is very sensitive to the equilibrium solubility data and ionization constants used to establish it. It will be shown later in this thesis that the solubility data used by DeMaine (taken from the International Critical Tables) are not very accurate.

An infrared absorption study by Jones and McLaren [71] provided little information but that of Falk and Giguere [72] was more conclusive. As well as examining aqueous sulphur dioxide solutions, these investigators also studied an equi-molar mixture of sulphur dioxide and water at -190°C. The absorption bands for the solutions occurred at wavelengths only slightly different from those for the bands of the gas phase, and this was interpreted to confirm 'the conclusions of earlier Raman investigations that sulphur dioxide molecules are not strongly hydrated in aqueous solution and do not form the compound H_2SO_3.' This interpretation was substantiated by

the solid state study because, although formation of H_2SO_3 would be more favoured in this state, its presence could not be detected.

It now appears to be generally accepted [e.g. 73-78] that, although H_2SO_3 molecules may have a transient existence as intermediates in the formation of HSO_3^- ions, the interaction between sulphur dioxide and water can be represented quantitatively by the classical reaction

$$SO_2 + H_2O \rightleftarrows H^+ + HSO_3^- \qquad (1)$$

and that the reactions

$$HSO_3^- \rightleftarrows H^+ + SO_3^= \qquad (2)$$

$$\text{and } 2HSO_3^- \rightleftarrows H_2O + S_2O_5^= \qquad (3)$$

occur to a negligible extent.

1.3.2 IONIZATION CONSTANTS

Early calculations [79-82] of the first ionization constant for sulphur dioxide in water gave results which differed by as much as forty percent. All these calculations were based on conductivity data and the discrepancies arose from three factors:

(a) inaccuracies in the experimental data

(b) differences between definitions of the constant and

(c) uncertainties regarding values given to the activity coefficients of the different species in solution.

Of these calculations, the most widely quoted are those of Johnstone and Leppla [82] which were based on the definition

$$K_a = \frac{a_{H^+} \cdot a_{HSO_3^-}}{a_{H_2SO_3}}$$

and the assumptions that $a_{H_2SO_3}$ is unity and that the mean activity coefficient for the hydrogen and bisulphite ions is the same as for hydrogen and chloride ions. The value calculated at 25°C was 0.0130.

However, Tartar and Garretson [83], using essentially the same definition

$$\text{i.e.} \qquad K_a = \frac{a_{H^+} \cdot a_{HSO_3^-}}{a_{SO_2}}$$

and the results of their E.M.F. measurements, calculated a value of 0.0172 at the same temperature. Because it does not involve any assumptions regarding activity coefficients, the latter value must be regarded as the more accurate.

Now the mass transfer equations given in Section 1.2.1 are derived using equilibrium constants based on concentrations rather than activities. For the sulphur dioxide - water system this requires

$$K_c = \frac{[H^+][HSO_3^-]}{[SO_2]}$$

Values of K_c, calculated from the conductivity data of Morgan and Maass [81] by the method of Johnstone and Leppla [82] are shown in Table 1.1. It is seen that K_c is constant over a wide range of concentrations and that the value at 25°C is not very different from Tartar and Garretson's value of K_a. Thus, because K_c is so small, its use in the mass transfer equations introduces very little error and the value of K_c = 0.0226 at 20°C was used in this investigation.

TABLE 1.1 IONIZATION CONSTANT FOR SO_2 IN WATER AT 20°C

From data of Sherril and Noyes [79],

$$\Lambda_o/\Lambda_{o,c} = 1.090C_t^{1/3}.$$

From data of Morgan and Maass [81];

C_t	$\Lambda_o/\Lambda_{o,c}$	κ	$\Lambda = \frac{\kappa}{C_t}$	$\alpha = \frac{\Lambda}{\Lambda_{o,c}}$	$K_c = \frac{\alpha^2 C_t}{1-\alpha}$
t = 10°C; Λ_o = 311.5					
0.4097	1.067	27.27	66.56	0.2280	0.0276
0.6784	1.078	36.58	53.63	0.1856	0.0287
0.9436	1.088	43.55	46.15	0.1612	0.0292
1.459	1.099	54.31	37.22	0.1313	0.0290
1.926	1.111	61.89	32.13	0.1145	0.0285
2.156	1.115	64.91	30.11	0.1078	0.0281
				Av. =	0.0285
t = 18°C; Λ_o = 359.3					
0.3877	1.065	28.32	73.05	0.2165	0.0232
0.6594	1.078	38.00	57.63	0.1729	0.0226
0.9255	1.087	45.56	49.23	0.1489	0.0241
1.186	1.094	51.69	43.58	1.327	0.0241
1.436	1.101	56.67	39.46	1.209	0.0239
1.687	1.107	61.08	36.21	0.1116	0.0237
				Av. =	0.0236
t = 25°C; Λ_o = 398.2					
0.2838	1.059	24.43	86.08	0.2290	0.0193
0.4918	1.070	33.55	68.22	0.1833	0.0202
0.7433	1.081	42.01	56.52	0.1534	0.0207
0.9906	1.089	48.66	49.12	0.1344	0.0207
1.233	1.096	54.16	43.93	0.1209	0.0205
1.420	1.100	57.69	40.63	0.1122	0.0201
				Av. =	0.0203

By graphical interpolation (see Graph 1.1)

$$t = 20°C, \quad K_c = 0.0226$$

Graph 1.1

Graph 1.1

Ionization Constant for SO_2 in Water

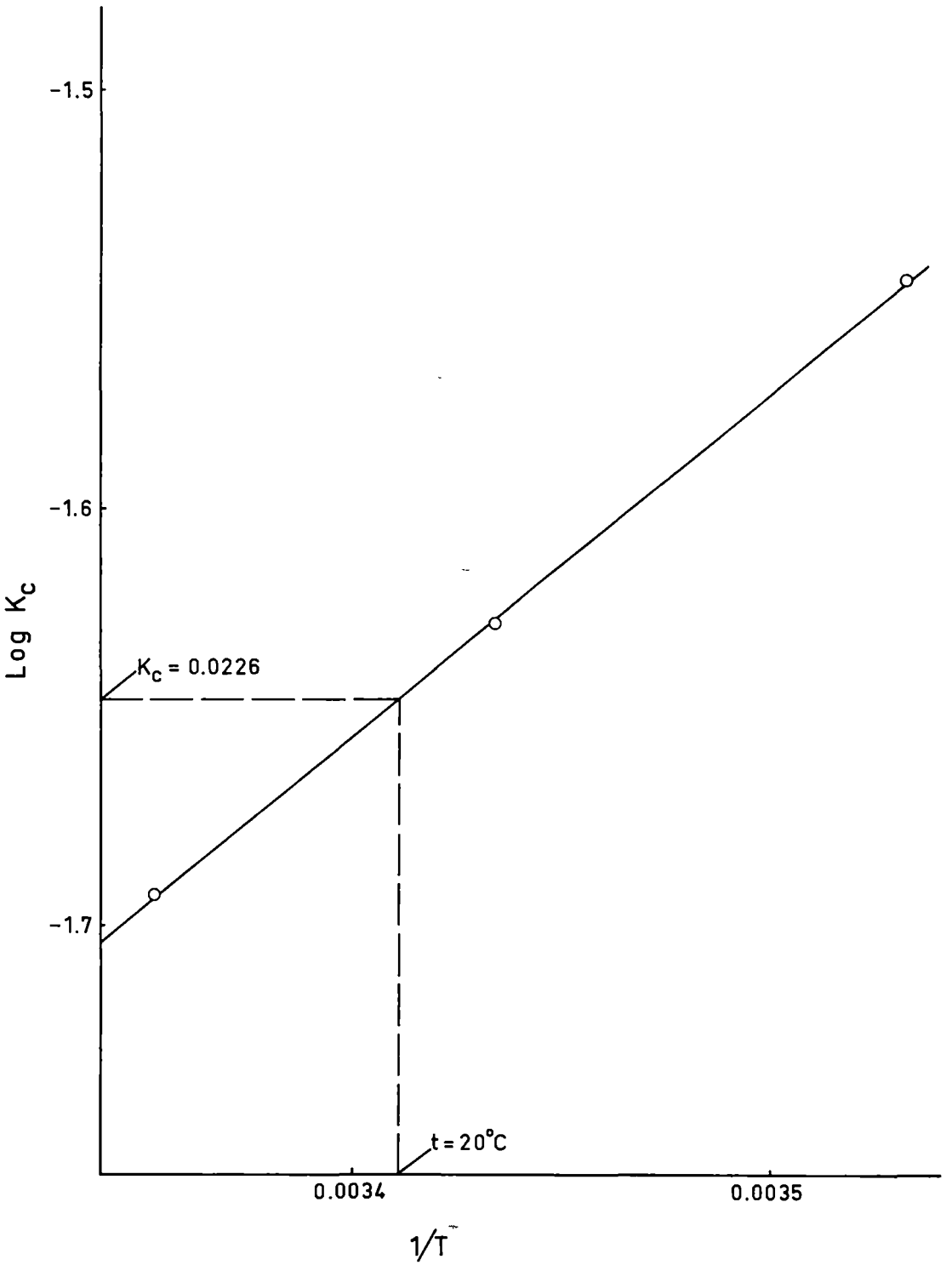
-1.5
-1.6
-1.7
Log K_c
K_c = 0.0226
t = 20°C
0.0034
0.0035
1/T

1.3.3 RATE OF IONIZATION

Studies of the rate of reaction of sulphur dioxide in water have yielded conflicting results. Thus Eigen et al. [75], using a relaxation technique obtained a value of the order of 10^6 sec^{-1} for the pseudo first order rate constant for the reaction

$$SO_2 + H_2O \rightleftarrows H^+ + HSO_3^-$$

while Wang and Himmelblau [84], using a radioactive tracer technique, obtained a value of the order of 10^{-3} sec^{-1}. Investigations involving mass transfer (absorption) have been no more enlightening. These are discussed in detail in Section 1.4 but it may be noted here that both Whitney and Vivian [85] and Chertkov [86] found that the performance of their packed towers could be explained more easily if a slow reaction was assumed. On the other hand, Lynn et al. [7] claim to have shown by experiments in a wetted-wall column that the reaction is fast. One of the main aims of this investigation has been to resolve these discrepancies.

1.4 PREVIOUS STUDIES OF SULPHUR DIOXIDE ABSORPTION

Despite its long established industrial importance, absorption of sulphur dioxide into water and aqueous electrolytes received little attention prior to 1949. Early investigations [87-90] were concerned with the design of industrial equipment and this has also been the subject of many recent studies [91-102].

1.4.1 ABSORPTION INTO WATER

Since the packed-tower study of Whitney and Vivian in 1949 [86], which is 'clearly the first serious attempt to relate the transport of sulphur dioxide to the flow conditions' [103], this process has been the subject of controversy.

Based on measured rates of desorption of oxygen from water, Whitney and Vivian predicted liquid-film coefficients for sulphur dioxide absorption. This gas was then absorbed from mixtures with air and overall coefficients were calculated. For this purpose, film-theory equations were used in which the driving force term was calculated from concentrations of sulphur dioxide. As a result of a previous study of chlorine absorption in the same tower [104], several assumptions were made and the individual film coefficients were calculated. Liquid-film coefficients were consistently lower than those predicted from the calibration.

From the study of chlorine absorption it had been concluded that hydrolysis of this gas in the liquid film is slow and a similar conclusion was reached for sulphur dioxide. The overall liquid-film coefficients were then recalculated 'using the same equations as for the normal coefficients but modifying the driving force term ... to include only the undissociated sulphur dioxide.' The re-calculated coefficients were converted to liquid-film coefficients as before and these 'pseudocoefficients' agreed well with predicted values.

Despite the apparent success of this treatment, Whitney and Vivian appear to have been undecided about the slow hydrolysis

reaction. They stated that 'this hypothesis is not proposed as a true representation of the facts ... but rather as an interesting contrast to the usual assumption that hydrolysis equilibrium has been established at the gas-liquid interface' and later that 'it appears ... that for this system the hydrolysis rate may be so slow as to be inconsequential with respect to the diffusion rate in controlling conditions within the liquid film.'

In a further packed-tower study carried out by Pearson et al. [105], sulphur dioxide was again absorbed from mixtures with air. Results were expressed as heights of transfer units and these were compared with values predicted by semi-empirical correlations. Agreement was poor but when the results were expressed as pseudo-heights of transfer units (corresponding to Whitney and Vivian's pseudocoefficients) agreement was better. Hikita et al. [106] absorbed pure sulphur dioxide in water in a packed tower and obtained similar results.

An extensive study was carried out by Lynn et al. [7] in 1955. Using a long wetted-wall column and with Teepol added to the water, rates of absorption of pure sulphur dioxide were measured for varying liquor flow rates. Predicted absorption rates, calculated from penetration theory equations in which the driving force term was based on concentrations of total sulphur dioxide, were shown to be in close agreement with measured values at low flow rates. Differences between measured and predicted values at higher flow rates were attributed to an 'increasingly greater effect of the

entrance conditions.' At the higher flows, where rippling did not occur, measured rates of absorption in water agreed well with those measured for the Teepol solutions and it was inferred that the effect of the Teepol was only to eliminate ripples. When a short wetted-wall column was used, deviations between measured and predicted absorption rates were attributed to an end effect caused by rippling and thickening of the film. For absorption into flow over a single sphere, deviations were assumed to be due to 'stretching' of the liquid film while, for a column of spheres, further deviations were thought to be 'due to the increasingly greater tendency of the liquid film to ripple at a given liquid flow rate as the number of spheres in the column is increased.'

To investigate the hydrolysis reaction rate, Lynn et al. considered absorption into solutions in which the extent of ionization should be suppressed and suggested that

(a) if the reaction is slow there should be little difference between absorption rates in water and in the solutions and

(b) if the reaction is fast, rates of absorption in the solutions should be lower than in water.

Using the long wetted-wall column, rates of absorption of pure sulphur dioxide into solutions of sodium bisulphite and hydrochloric acid of different strengths were measured. After accounting for the effect of ionic strength on the diffusion coefficients it was concluded that the results indicated a fast reaction. To obtain support for this conclusion, Lynn et al. measured the conductivities of

solutions of sulphur dioxide in water at temperatures as low as 4°C at times between 0.1 and 1.0 seconds after contact. The apparatus is not described and no experimental results are given, but it was claimed that the reaction was shown to be at least 90% complete after 0.1 seconds.

To explain the discrepancy between their results and those obtained by Whitney and Vivian, Lynn et al. pointed out that 'Whitney and Vivian made their assumption of a slow hydrolysis reaction in order to correlate their absorption data with those of other investigators ... [and] ... their data can be correlated just as easily by assuming a lower value of the diffusion coefficient than they used.' Lynn et al. then concluded that 'the rate of hydrolysis of SO_2 in water is fast relative to the diffusion process ... and ... the absorption of SO_2 in water may be treated as physical absorption.'

Several subsequent investigations have purported to provide support for this conclusion. Toor and Chiang [106] absorbed pure sulphur dioxide into a laminar water jet. Measured absorption rates were corrected for the increase in temperature at the jet surface and the results were shown to be in good agreement with penetration theory predictions for physical absorption. Using a disc column similar to that described by Stephens and MOrris [107], Novella and Simo [108] studied the absorption of sulphur dioxide into water from air mixtures over a wide range of operating conditions. Results were presented in semi-empirical correlations for the individual film coefficients. Whitney and Vivian's value

of the diffusion coefficient of sulphur dioxide in water was used and liquid-film coefficients thus calculated agreed well with those obtained by Whitney and Vivian. However, the hypothesis of a slow reaction was rejected and the explanation of Lynn et al. was accepted. A different design of disc column packing element was used by Norman and Sammak [109] to investigate the absorption of pure sulphur dioxide in water and of carbon dioxide in water and some organic liquids. Results were interpreted using the penetration theory for physical absorption and measured liquid-phase coefficients for sulphur dioxide absorption were lower than the corresponding coefficients for carbon dioxide. This could not be attributed entirely to the lower diffusion coefficient for sulphur dioxide. However, Norman and Sammak also rejected Whitney and Vivian's hypothesis and suggested that 'local variations in the film thickness over the packing surface cause a considerable temperature rise in the thinner parts of the film in the case of sulphur dioxide with a corresponding decrease in the rate of absorption.'

That the absorption of sulphur dioxide in water is a physical process was assumed by Matsuyama [42] in connection with his studies of absorption in laminar jets and by Ternovskaya and Belopolskii [110] in their wetted-wall column studies of the effect of surface active agents on gas absorption. To study absorption in single drops, Groothuis and Kramers [111] made the same assumption. Since 1955 several other investigators have used sulphur dioxide absorption to calibrate absorption equipment - viz. wetted-wall columns

[112,116], laminar jets [112-115] and stirred vessels [117].

In a theoretical study, Ratkowsky [73] showed that if sulphur dioxide absorption is accompanied by a fast reversible first order reaction and if the diffusion coefficients of the ionized and un-ionized species are the same, then the process can be described by the relationship

$$N/N_o = (C_{t,o} - C_{t,L})/(C_{u,o} - C_{u,L})$$

To test this relationship, Ratkowsky examined the data of Pearson et al. [105]. Semi-empirical correlations were used to calculate gas- and liquid-film coefficients and average values of N/N_o were predicted for each experimental condition. Corresponding values were calculated from the experimental data and agreement between the two sets of data was good. Attempts to apply the same treatment to the chlorine absorption data of Vivian and Whitney [104] were less successful and this was attributed to the more complicated hydrolysis reaction of chlorine. Ratkowsky thus agreed with Lynn et al. [7] that the reaction is fast, but pointed out the requirement of equal diffusion coefficients for the process to be considered as one of physical absorption. Essentially the same conclusion was reached by Thomas [103] who examined the data of Whitney and Vivian [86] and of Haslam et al. [87].

From the preceding review it appears that the evidence is strongly in favour of a fast ionization reaction. However, a closer examination of the packet tower studies reveals that many of the conclusions were based on 'agreements' of within only 5 to 10% and

in one case [103] there are discrepancies between 'agreeing' values of up to 60%. As only about 10% of the sulphur dioxide in solution is ionized the conclusions must be suspect.

If they are rejected then the only investigation which purports to offer any real evidence is that of Lynn et al. [7]. It is not possible to comment on their experimental work which is not described, but that which is described does not stand up very well under close scrutiny. Thus only the results of absorption into bisulphite solutions were offered as evidence of a fast reaction but it was not established whether the lowered absorption rates resulted from reduced ionization or from reduced solubility of unionized sulphur dioxide molecules. The situation is even more complicated when it is considered that the addition of sulphur dioxide to aqueous bisulphite solutions produces not a simple common ion effect but an increase in the concentration of $S_2O_5^=$ ions [118]. Again, Lynn et al. state that 'the rate of absorption by 3N HCl was found to be the same as that of water' and 'rough solubility measurements indicated, however, that the equilibrium concentration of SO_2 in 3N HCl is about 15% greater than that of water.' In view of their statement that 'the scatter of the data ... is very low for absorption work' it is difficult to accept their conclusion for HCl absorption that 'the agreement in rates of absorption is simply a coincidence.'

The conclusion must therefore be reached that there is insufficient evidence regarding the rate of ionization to make any decision about the absorption process. However, recent measurements by

Eriksen [119] indicate that the diffusion coefficients of unionized sulphur dioxide molecules and bisulphite ions are quite different so that, even if the ionization reaction is very fast, the absorption process should be regarded as one accompanied by a chemical reaction rather than as a physical process.

1.4.2 ABSORPTION INTO AQUEOUS ELECTROLYTES

The number of mechanism studies of these processes which have been reported is also very small. In fact, only two systems appear to have been investigated.

Johnstone and Coughanowr [120,121] studied the rates of absorption of sulphur dioxide from air by drops of water containing different catalysts (iron, copper, nickel and manganese sulphates) and a similar study using a wetted-wall column was carried out by Pritchett [122]. Comparatively long contact times are required to obtain a measurable influence of the catalytic reactions and such systems are outside the scope of the present work.

The other system which has been studied is the absorption into aqueous solutions of sodium hydroxide. This was reported by Takeuchi and Namba [123] and several aspects of the work are open to criticism.

(1) Very short liquid jets (1.13 and 2.58 cm) were used. As well as being difficult to measure accurately, such short lengths require comparatively large hydronamic correction factors (cf. Chapter 6).

(2) It was assumed that absorption of sulphur dioxide into water is a physical process and that absorption into hydroxide solutions involves only the reaction

$$SO_2 + 2OH^- \rightarrow SO_3^= + H_2O$$

(3) The theoretical analysis presented for this reaction was essentially that already given in this thesis (equations (1.27 to (1.29)), but the simplifying assumption was made that $\mathcal{D}_P/\mathcal{D}_R$ ($\mathcal{D}_{OH^-}/\mathcal{D}_{SO_2}$) was equal to unity while the experimental results indicated a value greater than three.

(4) The value of $\mathcal{D}_{OH^-}$ calculated from the experimental results was approximately three times the value in aqueous sodium hydroxide but no attempt was made to discuss the possible significance of this.

Because of these criticisms it would seem profitable to repeat the work. In particular, the process should offer a good opportunity to study the nature of ion diffusion during mass transfer.

CHAPTER 2 PROPERTIES OF SULPHUR DIOXIDE AND ITS AQUEOUS SOLUTIONS

2.1 EQUILIBRIUM SOLUBILITY DATA

2.1.1 SOLUBILITY IN WATER

If the normal sources [124-130] are consulted to ascertain the equilibrium solubility of sulphur dioxide in water at 20°C and gas pressures up to one atmosphere, variations of up to 15% may be found between the different sets of data. Reliable data are required in the present work and an exhaustive survey of the literature was undertaken in an effort to obtain them.

In the past forty years, four attempts have been made to correlate statistically the different experimental results. The first was presented in 1925 [131] and was subsequently incorporated into the second, which was published by Plummer in 1950 [132]. The equations used by Plummer are thermodynamically unsound [78], but this does not affect the results of the correlation. These were later assessed by Dzhabagin et al. [77] who made minor modifications but arrived at a correlation which predicts solubilities within one percent of those predicted by Plummer. The fourth review, which apparently was compiled before Plummer's results were known, was presented by Pearson et al. [105] in 1951. There is some overlap of experimental data used by Plummer and by Pearson et al. but there is sufficient difference between the two sets of data for the reviews to be considered independently. Despite this solubilities calculated from the two correlations agree almost within one percent at 20°C.

It should be noted however, that what Seidell [127] considered to be the most reliable experimental data [81,132] differ by as much as three percent from the two sets of calculated values.

The only experimental measurements published since 1951 which are of interest here are those of Rabe and Harris [78] and of Norman and Sammak [109]. Rabe and Harris used a new type of apparatus (a static cell in which mercury is used to sample the gas phase). Norman and Sammak do not describe their apparatus but it was most probably of the manometric-volumetric type. The results of the two investigations are compared with those already discussed in Tables 2.1 and 2.2 and in Graph 3.1. The reason for including data at 30°C is explained in Section 3.2.

It can be seen that there are differences of up to five percent between the sets of data. It is not possible to justify a choice of one set rather than another and it was consequently decided to obtain new experimental data. The methods of measurement and results are discussed in Section 3.2.

2.1.2 SOLUBILITY IN AQUEOUS ELECTROLYTES

The electrolytes of interest in this investigation are sodium chloride, hydrogen chloride and sodium hydroxide. Data for sodium chloride are available [134] and, although the absolute values given may be in error, it appears that the relationship between the solubilities in water and in the salt solutions has been well established. For salt concentrations up to 2 molar, the data can be correlated by the relationship

TABLE 2.1 SOLUBILITY OF SULPHUR DIOXIDE IN WATER AT 20°C

gm SO_2/100 gm H_2O

P_{SO_2}	Reference			
	[132]	[105]	[81,133]	[109]
3.0			1.0	
10.0	1.66	1.67		
11.0			2.0	
20.0	3.12	3.11		
27.0			4.0	
30.0	4.52	4.50		
40.0	5.85	5.89		
43.0			6.0	
50.0	7.17	7.22		
58.0			8.0	
60.0	8.46	8.56		
70.0	9.82	9.91		
76.0				10.57
80.0	11.16	11.24		

TABLE 2.2 SOLUBILITY OF SULPHUR DIOXIDE IN WATER AT 30°C

gm SO_2/100 gm H_2O

P_{SO_2}	Reference			
	[132]	[105]	[81,132]	[78]
4.1				0.59
7.0			1.0	
10.0	1.16	1.18		
17.0			2.0	
17.7				1.92
20.0	2.22	2.20		
30.0	3.24	3.18		
30.9				3.21
38.0			4.0	
40.0	4.22	4.14		
44.5				4.47
50.0	5.17	5.09		
58.0			6.0	
60.0	6.07	6.04		
70.0	6.98	6.98		
78.0			8.0	
80.0	7.88	7.92		

$$C_t(NaCl) = C_t(H_2O)[1 - 0.014\ M(NaCl)] \qquad (2.1)$$

Solubilities in aqueous hydrogen chloride do not appear to have been measured and these data were obtained in conjunction with those for water. Results are discussed in Section 3.2.

It is, of course, impossible to measure the physical solubility of a gas in a liquid with which it reacts. A method is available [135] for estimating the solubilities of gas in aqueous electrolytes and it was used by Takeuchi and Namba [123] to estimate the solubility of sulphur dioxide in aqueous sodium hydroxide solutions. However, it is shown later in this thesis (Section 8.6) that if absorption is characterized by a moving reaction zone (which is the case for absorption of sulphur dioxide into aqueous sodium hydroxide) it is the solubility in water and not in the electrolyte which determines the driving force.

2.2 DIFFUSION OF SULPHUR DIOXIDE

2.2.1 INTRODUCTION

Quantitative descriptions of diffusion are based on the fundamental transfer equation

$$J = \mathcal{D}.V \qquad (2.2)$$

where J is the flux of transfer (diffusive flux)

$\mathcal{D}$ is a constant (diffusion coefficient)

and V is a driving force.

The most convenient definition of the diffusion coefficient is that defined from equation (2.2) when the driving force is based on a concentration gradient. This was first defined by Fick [136]

in the equation

$$J = -\mathcal{D}.\frac{\partial C}{\partial x} \qquad (2.3)$$

where J is the uni-dimensional flux in the x-direction ($ML^{-2}T^{-1}$)

$\mathcal{D}$ is Fick's diffusion coefficient (L^2T^{-1})

and C is a concentration term (ML^{-3})

Because of their ease of measurement [137] and the widespread use of concentrations in chemical engineering, Fick coefficients have been used almost exclusively in mass transfer studies. References in this thesis are to such coefficients.

The equation describing changes at a point in a diffusing system can be written in differential form as

$$\frac{\partial C}{\partial t} = \frac{\partial}{\partial x}\left(\mathcal{D}.\frac{\partial C}{\partial x}\right) \qquad (2.4)$$

In this equation, $\mathcal{D}$, which may depend on the concentration of the diffusing species, is known as the differential diffusion coefficient. In many cases measured coefficients are based on observations of the rate of transfer between two concentration C_1 and C_2. Such coefficients represent some sort of average depending on the experimental technique. They are known as integral coefficients (denoted here by $\overline{\mathcal{D}}$) and are related to the differential coefficient by the equation [138]

$$\overline{\mathcal{D}}(C_1 - C_2) = \int_{C_1}^{C_2} \mathcal{D}.dC \qquad (2.5)$$

Equation (2.5) is non-linear and analytical solutions are available only for simplified cases of concentration dependence and boundary conditions [139]. Several approximate numerical

solutions have also been published [140-149].

In many applications diffusion coefficients are assumed independent of concentration. In this case equation (2.4) reduces to

$$\frac{\partial C}{\partial t} = \mathcal{D} \cdot \frac{\partial^2 C}{\partial x^2} \qquad (2.6)$$

and the solution to this equation is the basis of the penetration theory which has already been discussed.

2.2.2 DIFFUSION IN GASES

Early molecular theories [150-153] of diffusion in binary gas systems produced the Stefan-Maxwell equation. This contained a constant to be calculated from simple kinetic theory but different authors [151,154,155] disagreed as to its correct value.

More recent theories, accounting for molecular interactions, have led to the Chapman-Cowling equation [156]. Interactions are described in terms of force constants and a collision integral function, parameters which are characteristic of the model used to describe the potential field of the molecules. For non-polar gases the Lennard-Jones (12-6) model is used; collision functions have been tabulated [157] and force constants may be calculated from experimental viscosity data [157], second virial coefficients [157] or semi-empirical relationships [158-162]. A graphical correlation is also available [163]. For polar gases the Stockmayer (12-6-3) model is used [157] and collision functions are available [164]; other parameters may be estimated from viscosity data [164] or semi-empirical relationships [165]. For a mixture of a polar and a non-

polar gas it has been shown [164,166] that good agreement with experimental coefficients is obtained by using, for the non-polar component, a force constant calculated from the (12-6) model (viscosity data), for the polar component, a force constant calculated from the (12-6-3) model (viscosity data) and (12-6) collision functions. Coefficients for sulphur dioxide in air and nitrogen at 20°C, calculated using the data given in Ref.[166] are shown in Table 2.3.

TABLE 2.3 DIFFUSION COEFFICIENTS FOR SULPHUR DIOXIDE IN AIR AND NITROGEN AT 20°C

Values of $\mathcal{D}_G$ in cm^2/sec

Ref.	Air	Nitrogen	Method
[166]	0.122	0.123	Theoretical
[173]	0.122	0.120	Semi-empirical
[174]	0.108	0.106	"
[175]	0.127	0.129	"
[176]	-	0.122	"
[158]	0.133	0.133	"
[161]	0.129	0.129	"
[177]	0.116	-	"
Avge.	0.122	0.123	

Theoretical relationships describing the concentration dependence of binary coefficients for non-polar systems predict only a small dependence (approx. 3%) [157] and this has been confirmed

experimentally [167]. Similar data for systems containing polar components do not seem to be available.

For accurate measurement of diffusion coefficients, most investigators have used a Loschmidt type of apparatus [168]. Other techniques with comparable accuracy have recently been described [167, 169,170]. It appears, however, that no measurements for sulphur dioxide either in air or in nitrogen have been obtained by any of these methods. Reid and Sherwood [171] report a supposedly experimental value of 0.122 cm^2/sec for sulphur dioxide in air at 0°C, but attempts to trace the origin of this measurement have been unsuccessful. Using a simplified apparatus, Andrew [172] obtained 0.122 cm^2/sec for the same gases at 20°C and this appears to be the only reliable figure available.

With the Stefan-Maxwell equation as a basis, two semi-empirical relationships [173,174], a reference substance plot [175] and a reduced states correlation [176] have been published; the last is not applicable to systems containing air. In relationships based on the Chapman-Cowling equation [158,161,177], force constants for a polar gas are calculated from the (12-6) model and the relationships contain correction factors. The sources of many of the experimental data used in obtaining these correlations have been seriously questioned by Scott [178] and it is doubtful if they can be used with confidence. Coefficients for sulphur dioxide in air and in nitrogen at 20°C calculated from the correlations are shown in Table 2.3 and the agreement between average values and those pre-

dicted theoretically must be regarded as largely fortuitous.

Because the theoretical value for air agrees so well with the only experimental result, the theoretical value of 0.123 cm^2/sec for sulphur dioxide in nitrogen was accepted for the present investigation.

2.2.3 DIFFUSION IN LIQUIDS

Phenomenological approaches to liquid diffusion give different definitions of diffusion coefficients and it is not easy to relate these definitions to Fick coefficients. Of the equations available for calculating coefficients [179] lack of data prevents use of all but the modified Stokes-Einstein relationship

$$\mathcal{D} = \frac{1}{4\pi r} \cdot \frac{kT}{\eta} \qquad (2.7)$$

The coefficient for unionized sulphur dioxide in water at 20°C, calculated from this equation is given in Table 2.4.

In experimental determinations of gas-liquid coefficients, 'the most widely used techniques ... are (a) to measure the transfer of gas into or out of a liquid phase or (b) to measure concentration gradients in a diffusing system' [179]. Several authors [e.g. 17, 23,180-184] have discussed the experimental difficulties associated with the different techniques and it is generally agreed that most accurate results are obtained in type (a) experiments by measuring rates of gas absorption in laminar flow systems. Several such systems have been described and the most satisfactory are anular jets [180], flow over wetted spheres [17,44,181], flow in a rectangular duct [183, 185], moving band absorber [23] and laminar jets [e.g. 109,182,186-

TABLE 2.4 DIFFUSION COEFFICIENTS FOR SULPHUR DIOXIDE IN WATER AT 20°C

Calculated from theoretical and semi-empirical relationships for unionized sulphur dioxide

Ref.	$\mathcal{D} \times 10^5$ cm^2/sec	Method
[179]	1.53	Equation (2.6)
[194]	1.44	Semi-empirical
[195]	1.43	"
[196]	1.52	"
Avge.	1.48	

TABLE 2.5 DIFFUSION COEFFICIENTS FOR SULPHUR DIOXIDE IN WATER AT 20°C

Experimental Results

	Ref.	$\mathcal{D} \times 10^5$ cm^2/sec	Method	
	[7]	1.46	Absorption - W.W. Column	
	[19,106]	1.41	"	Jet
(a)	[109]	1.48	"	Jet
	[111]	1.40	"	Still liquid
	[123]	1.44	"	Jet
	[119]	1.45	Radioactive tracer	
(b)	[189]	1.78	Polarographic	
	[190]	1.62	Diaphragm Cell	

188 and others]. These are discussed in more detail in Chapter 5. For type (b) measurements an interferometric technique [179,184] appears to give best results. Experimental results reported for the diffusion of sulphur dioxide in water at 20°C are given in Table 2.5.

Several semi-empirical relationships for predicting liquid-phase diffusion coefficients have been derived [191-198]. Only three of these [194-196] have been tested for gas solutes and one [198] was based on a previously published relationship. Coefficients calculated from these 'cannot be used with any degree of certainty' [109] and values for unionized sulphur dioxide molecules in water are given in Table 2.4 for comparison only.

From Table 2.5 it is seen that the coefficients measured in absorption experiments, although agreeing well within themselves, differ quite markedly from those obtained by other techniques. This was noted in only one of the absorption studies [19,106] but no satisfactory explanation was given.

The present writer feels that it may be necessary to consider two separate phenomena to explain the discrepancy. First, it has been shown [199,200] that if liquid-phase coefficients are a function of concentration this may have a marked effect on absorption rates. Theoretical expressions [201-206] (which are essentially the same [179,188]) predict that such coefficients are influenced by solute activity coefficients and liquid-phase viscosities, parameters which depend on solute concentration. While these influences may be negligible in dilute solutions (e.g. carbon dioxide - water [188,

207]) their effects do not appear to have been measured for more soluble gases. Secondly, if the ionization of sulphur dioxide in water is fast compared with diffusion, coefficients measured in absorption experiments will not be integral coefficients for un-ionized sulphur dioxide but will be some average for all the diffusing species. One of the aims of this investigation has been to re-assess the diffusion of sulphur dioxide in water in the light of these comments.

CHAPTER 3 SOLUBILITY MEASUREMENTS

3.1 INTRODUCTION

The apparatus used to measure the required equilibrium solubilities of sulphur dioxide was a simplified version of that recently described by Dymond and Hildebrand [208]. Because the solubilities measured in this investigation were much greater than those measured by Dymond and Hildebrand, the dimensions of the apparatus were radically altered. Despite the simplifications in construction, the simple physical principle of measurement remained the same. It consisted of exposing a known weight of liquid to a known weight of the gas and allowing equilibrium to be established. The point of equilibrium was determined by noting when the pressure of the undissolved gas became constant and the amount of gas dissolved was calculated as the difference between that exposed and that which remained undissolved. The results obtained indicated that simplifying the apparatus did not reduce the precision of measurement.

3.2 DESCRIPTION OF APPARATUS

The apparatus, which is sketched in Figure 3.1, consisted of seven main components:

(i) sulphur dioxide gas supply

(ii) vacuum pump

(iii) water-jacketed 100 ml burette and water pump

(iv) mercury reservoir

(v) exposure cell and stirring equipment

Figure 3.1

Figure 3.1

Solubility Equipment

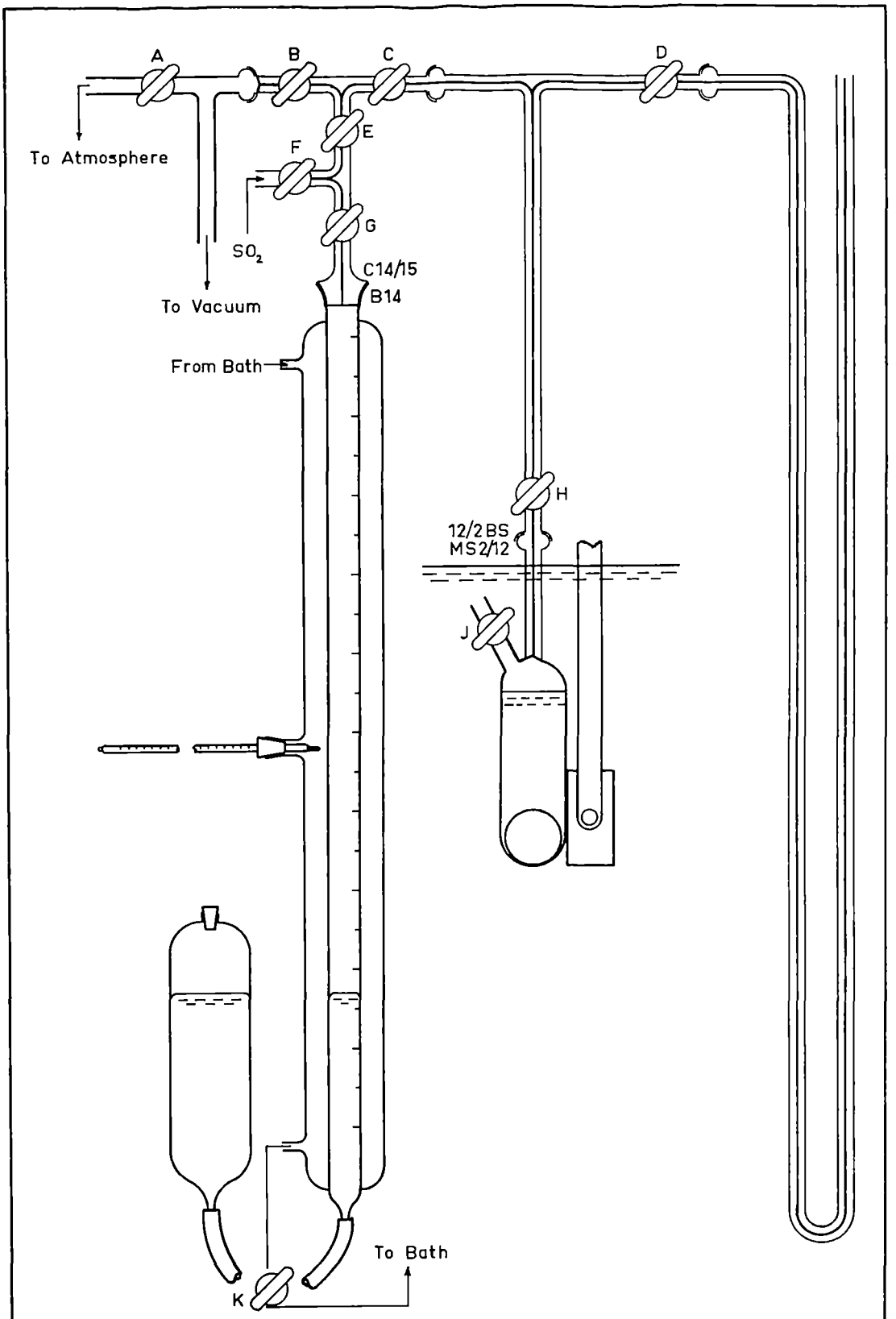

SOLUBILITY EQUIPMENT

(vi) open-ended mercury manometer

(vii) thermostat water bath.

All components which contained sulphur dioxide were constructed of glass and their volumes were measured accurately by displacement of mercury. To minimize experimental error, all glass connections were constructed of 2 mm I.D. capillary tube. All stopcock barrels were initially made of Teflon but these proved unsatisfactory because of their inability to maintain the required pressure differences for prolonged periods of time. 'Solva', high vacuum, matched stopcocks were finally used and the rate of uptake of sulphur dioxide by the 'Apiezon' grease lubricant used was so slow as to introduce no significant errors into the measurements.

The exposure cell, whose volume was approximately 6 ml, was immersed to a depth of about eight inches in the thermostat bath. The temperature of this bath was measured and controlled, by the technique described in Section 7.2.5, to within 0.05°C. The cell contained a steel ball enclosed in a spherical glass sheath and the liquid in the cell was stirred by up and down movement of the ball. This was effected by a reciprocating magnet which was eccentrically mounted on a fly wheel driven, through a reduction gear, by a variable speed electric motor mounted above the thermostat bath. Because of the small volume of liquid used (3 to 5 ml) stirring was very efficient and the method was probably just as effective as that described by Dymond and Hildebrand.

Water from the thermostat bath was circulated around the burette.

By using the apparatus in a room in which the temperature was the same (±0.5°C) as that of the bath, negligible error was introduced by assuming the gas in the burette and in the connecting tubes to be at the same temperature as the bath.

3.3 EXPERIMENTAL METHOD

The following procedure was used.

(i) The exposure cell was thoroughly washed with distilled water, flushed three times with each of alcohol and ether and dried under vacuum.

(ii) A known weight, ±0.0005 gm, of distilled, de-aerated water was placed in the cell with a 5 ml hypodermic syringe.

(iii) H and J were closed and the cell was attached to the apparatus via a spring-loaded, flexible, lightly greased ground glass elbow joint.

(iv) With A, F and K closed and B, C, D, E and G open, the pressure in the apparatus was reduced to less than 1 mm Hg. When this was attained, H was opened briefly (2-3 secs) and then closed.

(v) The liquid in the cell was stirred for 10 minutes to expel the small amount of absorbed air. After this time, H was again opened briefly to remove the expelled air. The loss of water vapour in this operation was insignificant.

(vi) B was closed, F was opened and sulphur dioxide gas* was

---

*All sulphur dioxide used in this investigation was Refrigeration Grade and was supplied by I.C.I.A.N.Z. Ltd. It meets the Australian Standards Specification EK 514 (1943). Viz: Sediment: Nil. Moisture: ≯ 0.002%. Acid: Nil. Non-condensible gases: ≯ 0.02%. Residue on evaporation: ≯ 0.002%.

admitted to a pressure of about one atmosphere as indicated by the manometer.

(vii) F was closed, B was opened and the pressure was again reduced to less than 1 mm Hg.

(viii) B was closed, F was opened and sulphur dioxide was again admitted. The level of the mercury in the burette was adjusted to just above the 100 ml mark and the burette reading noted. When the gas pressure was again about one atmosphere, F was closed.

(ix) H was opened cautiously to admit some of the gas to the cell and was then closed. C was closed, H was opened and the system on the manometer side of C was allowed to come to equilibrium.

(x) As soon as C was closed the gas in the burette was adjusted to atmospheric pressure with K which was finally closed. The burette reading and the atmospheric pressure were then noted. Performing this operation at this stage minimized the risk of gas leaks through B, E, F and G while equilibrium was being reached.

(xi) Equilibrium was taken to have been reached when the manometer reading did not change during a thirty minute period. The time for this to occur increased as the concentration of gas in the liquid increased, the longest time for all the measurements taken being about four hours. When equilibrium was reached, the manometer reading was noted.

(xii) Steps (ix) to (xi) were repeated while the burette reading was greater than zero. Two to four separate measurements were made with the same liquid sample and these were checked by taking a

further two to four measurements with a different sample of the same solvent. All results were calculated as gm sulphur dioxide dissolved per 100 gm of solvent at the equilibrium pressure.

3.4 RESULTS

3.4.1 SOLUBILITY IN WATER

Results obtained for the solubility of sulphur dioxide in water at 20°C are given in Appendix 5, Table A.5.1, and are shown in Graph 3.1 in which they are compared with the data of Table 2.1. The fact that the experimental results lie very close to a smooth curve through the origin is a good indication of the reproducibility of the measurements. However, the solubilities are consistently lower than those predicted by the empirical correlations and the interpolated solubility at 76 cm Hg is also lower than the recent experimental measurement. Again, although at higher concentrations the results agree well with the data quoted by Seidell [127], they are lower at lower concentrations. This suggested that some systematic error may have been included in the experimental technique and it was consequently decided to measure solubilities at 30°C for further comparison. The results obtained are also shown in Table A.5.1 and are compared with the data of Table 2.2 in Graph 3.1. In this case it can be seen that the position has been reversed although the results agree with Seidell's data over a wider range of concentrations. This discounted the possibility of a systematic error and it was decided to use the measured solubilities in the analysis of

Graph 3.1

Graph 3.1

Solubility of SO_2 in Water at 20°C and 30°C:

Experimental Results for 'Total' SO_2.

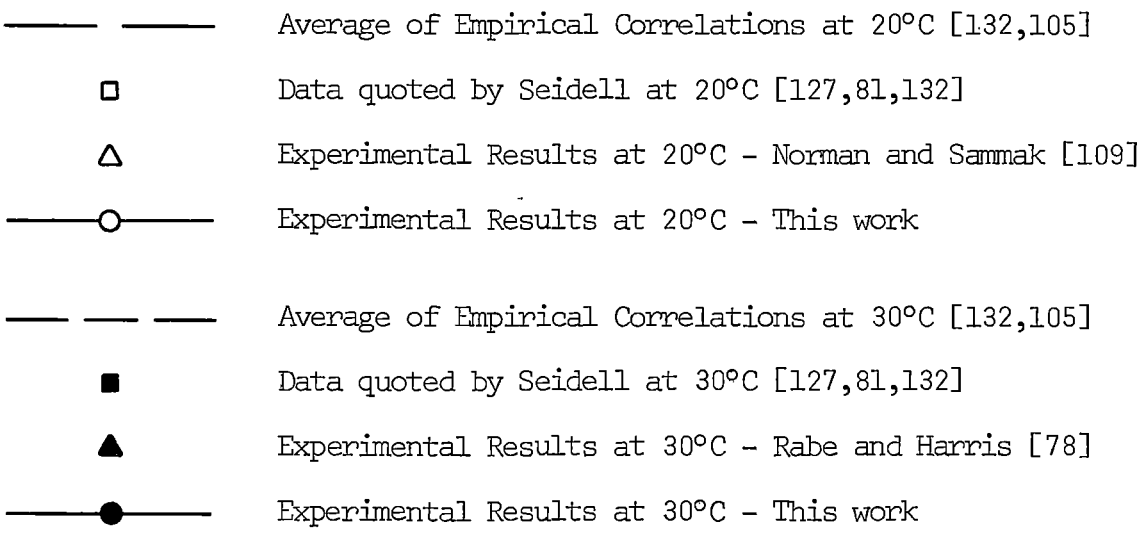

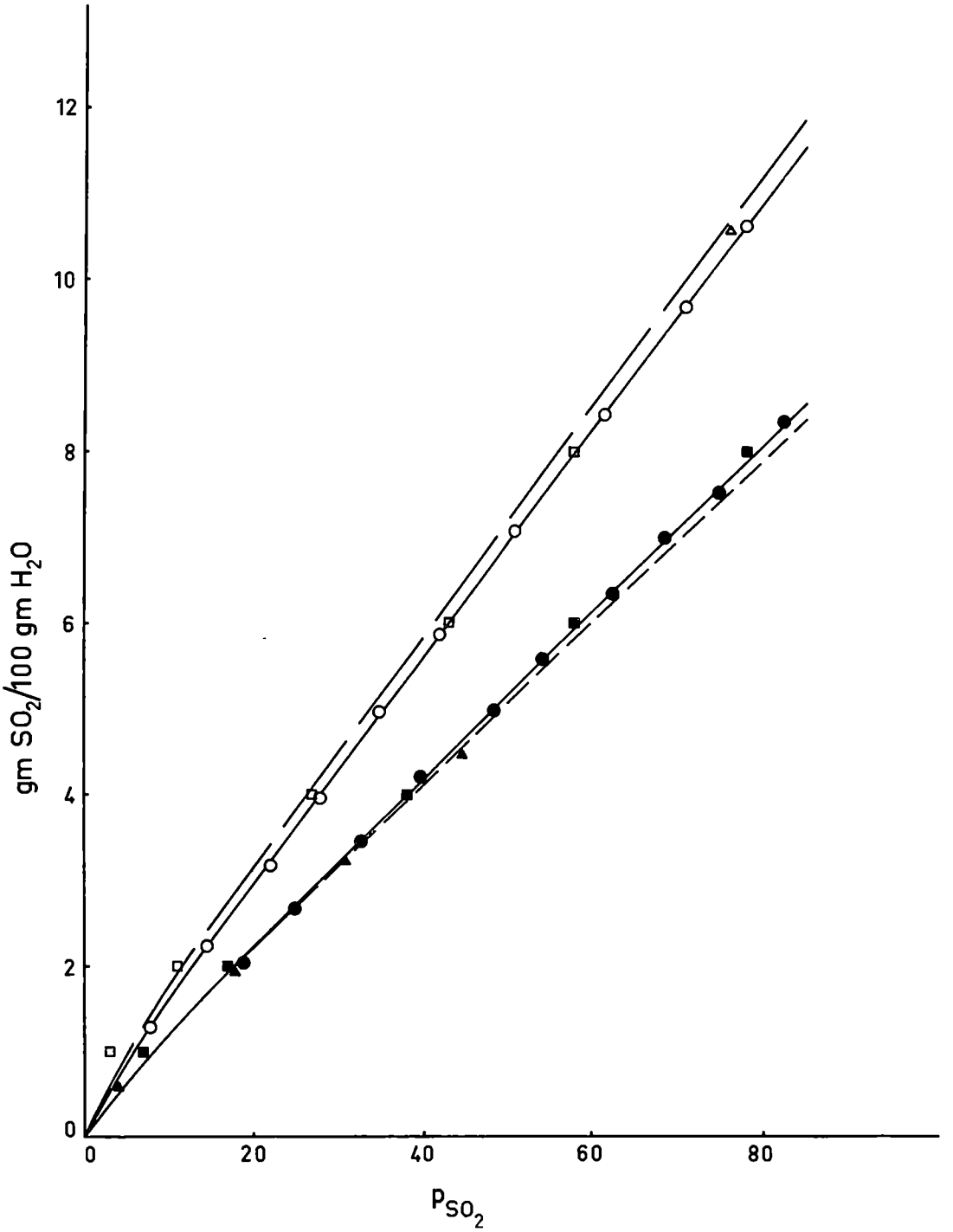
12
10
8
6
4
2
0
gm SO_2/100 gm H_2O
0
20
40
60
80
P_{SO_2}

absorption data. This decision was justified later by the fact that diffusion coefficients calculated from these results agreed much better with previously measured coefficients than they would have otherwise.

In order to use the data in the analysis of absorption results it was necessary to convert the concentrations to molar units and to estimate the concentrations of unionized sulphur dioxide molecules. For this purpose, the densities of the solutions were interpolated from the data of Morgan and Maass [81] and the ionization constant was taken as 0.0226. The results of these calculations are given in Table 3.1.

TABLE 3.1 SOLUBILITY OF SULPHUR DIOXIDE IN WATER AT 20°C

P_{SO_2}	gm SO_2 per 100 gm H_2O	ρ	C_t	C_u
7.8	1.29	1.0044	0.200	0.143
14.5	2.23	1.0088	0.343	0.266
22.0	3.17	1.0134	0.486	0.392
27.8	3.95	1.0170	0.603	0.497
34.8	4.96	1.0217	0.754	0.635
41.8	5.86	1.0258	0.886	0.756
51.0	7.08	1.0312	1.064	0.920
61.4	8.42	1.0370	1.257	1.100
70.9	9.67	1.0423	1.435	1.266
77.9	10.60	1.0461	1.565	1.388

Values of C_u are plotted against pressure in Graph 3.2. To demonstrate the validity of Henry's law, the units of C_u should be weight/weight. However, for the small range of densities involved, the use of molar units does not cause any significant deviation from a linear relationship and the straight line of Graph 3.2 was used to interpolate values for C_u at different pressures.

3.4.2 SOLUBILITY IN HYDROCHLORIC ACID SOLUTIONS

The results of these measurements are given in Appendix 5, Table A.5.2 and are shown in Graph 3.3. Again good reproducibility of measurement is indicated. Data required for the analysis of absorption measurements were the solubilities of unionized molecules in the solutions at a gas pressure of 76 cm Hg. Values of C_t were interpolated from Graph 3.3 and these were converted to molar units by assuming an independence of densities; i.e. assuming that when sulphur dioxide is added to a hydrochloric acid solution, the contribution to density by the sulphur dioxide is the same as if it were added to water. This assumption cannot be justified but, in view of the small range of densities involved, it should not have introduced any significant error into the calculations. Densities of the hydrochloric acid solutions were interpolated from the data given in Ref. [125]. The concentrations of unionized molecules were estimated on the basis of a simple common-ion effect, the concentrations of hydrogen ion in the acid solutions being calculated from the conductivity data of Ref. [209] as shown in Tables 3.2 and 3.3. The results of all these calculations are given in Table 3.4.

Graph 3.2

Graph 3.2

Solubility of SO_2 in Water at 20°C:

Experimental Results for Unionized SO_2

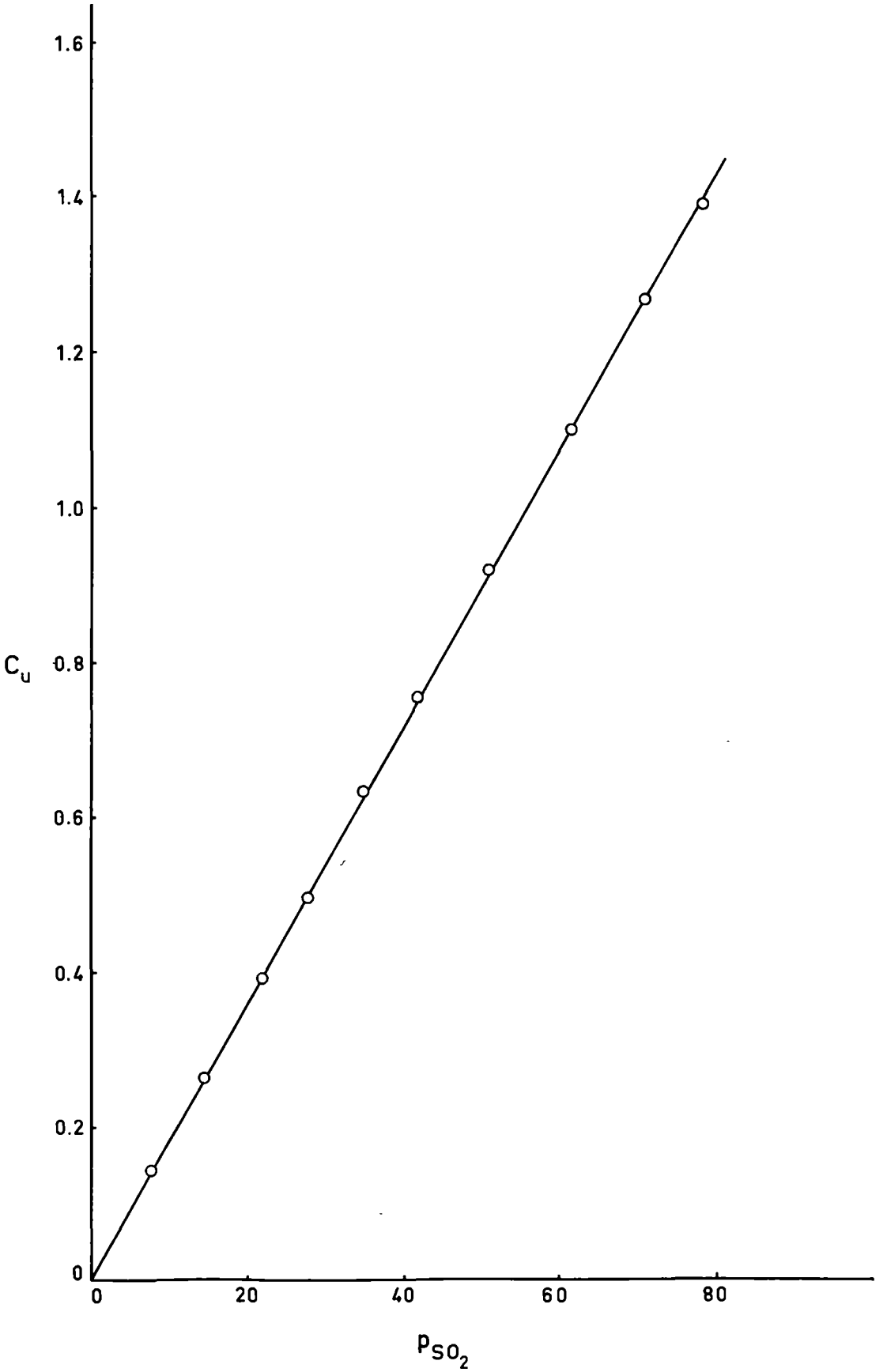
1.6
1.4
1.2
1.0
0.8
0.6
0.4
0.2
0
C_u
0
20
40
60
80
p_{SO_2}

Graph 3.3

Graph 3.3

Solubility of SO_2 in Hydrochloric Acid Solutions at 20°C:

Experimental Results for 'Total' SO_2

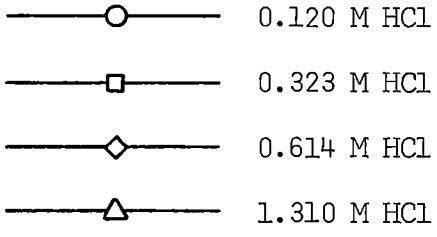

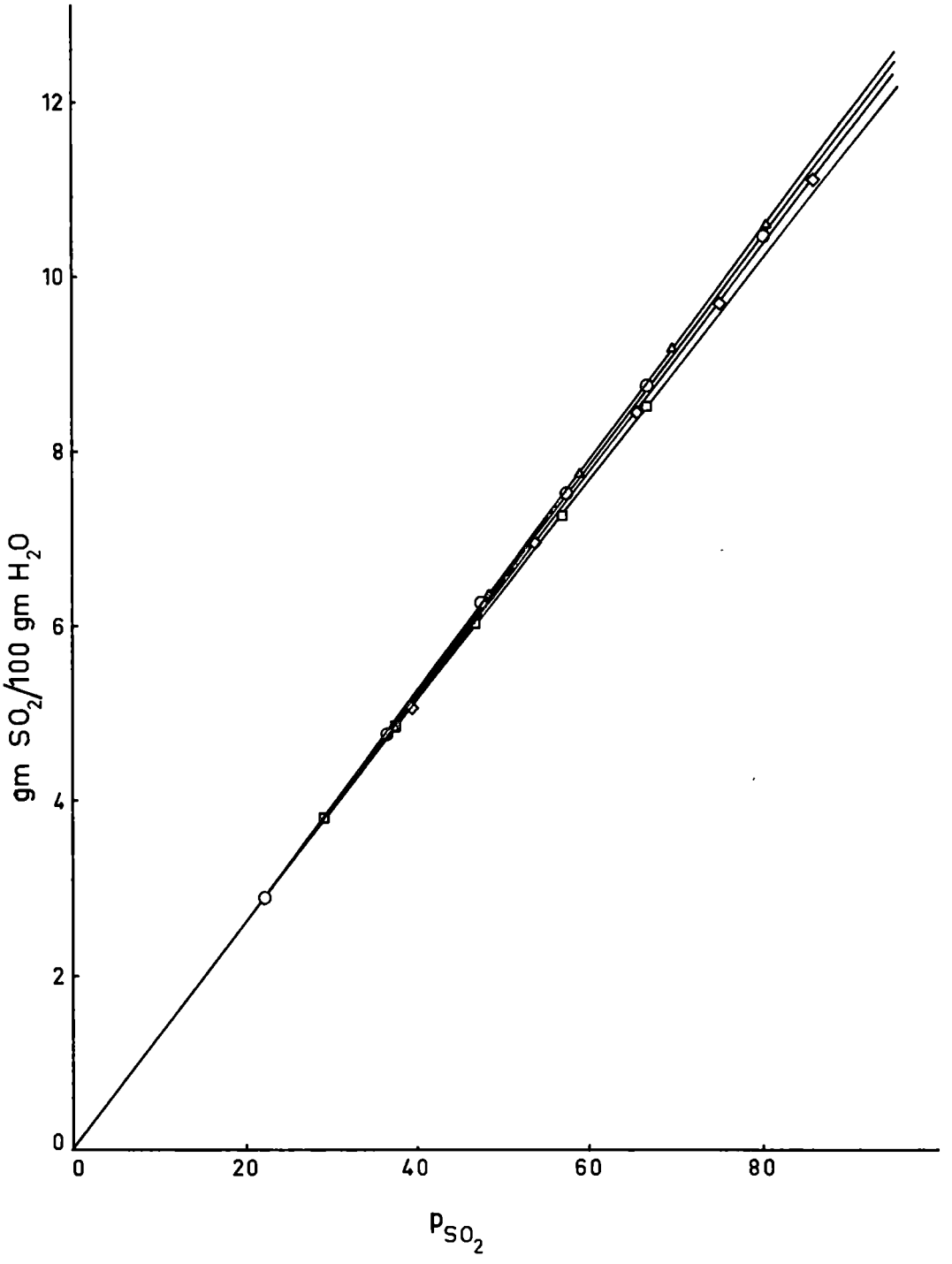
12
10
8
6
4
2
0
0
20
40
60
80
gm SO_2/100 gm H_2O
P_{SO_2}

TABLE 3.2 CONDUCTIVITIES OF HYDROCHLORIC ACID SOLUTIONS

From Graphical Interpolation of Data of Ref. [209]

M HCl	Λ
0	393
0.25	348
1.00	307
2.25	250

TABLE 3.3 HYDROGEN ION CONCENTRATIONS IN HYDROCHLORIC ACID SOLUTIONS

From Graphical Interpolation of Data of Table 3.2

M HCl	Λ	$\alpha = \frac{\Lambda}{\Lambda_o}$	M H^+
0.120	360	0.917	0.110
0.323	345	0.879	0.284
0.614	325	0.830	0.510
1.310	292	0.743	0.974

TABLE 3.4 SOLUBILITY OF SULPHUR DIOXIDE IN HYDROCHLORIC ACID SOLUTIONS AT 20°C and 76 cm Hg

M HCl	gm SO_2 per 100 gm soln	ρ (HCl)	ρ (SO_2)	ρ (Total)	C_t	C_u
0.120	9.943	1.000	1.043	1.043	1.473	1.345
0.323	9.672	1.003	1.042	1.045	1.439	1.356
0.614	9.813	1.007	1.043	1.050	1.465	1.409
1.310	10.008	1.020	1.044	1.064	1.512	1.479

A plot of C_u against the hydrogen ion concentration of the acid is shown in Graph 3.4 in which the 95% confidence limits are shown for each point. The two main features of this curve are the increase in solubility at higher hydrogen ion concentrations and the minimum at lower concentrations.

The increase is predicted by the empirical correlation given by van Krevelen and Hoftijser [135]. The measured rate of increase is somewhat less than that predicted but this is not surprising in view of the doubtful accuracy of the correlation. The increase is possibly caused by the effect of hydrogen ions on the structure of water. It is known [210] that an increase in the concentration of these ions caused increased 'clustering' of the water molecules but the effect of this on the space available for solute molecules does not seem to have been investigated. Such an investigation is outside the scope of this work but it is suggested that it may be profitable in relation to the structure of water and of other solvents.

The form of the empirical correlation does not allow for the minimum although it has been observed for other gases in hydrochloric acid (Cl_2, H_2S and N_2O) [127]. Locating with any precision the hydrogen ion concentration corresponding to the minimum is not possible because of the extremely accurate data that would be required. However, for SO_2, Cl_2 and H_2S, the minimum occurs at concentrations between 0.1 and 0.4 molar and it is probably not a coincidence that the activity coefficients for hydrogen ions in aqueous hydrochloric acid solutions also have a minimum in this range [211]. Further

Graph 3.4

Graph 3.4

Solubility of SO_2 in Hydrochloric Acid Solutions at 20°C:

Experimental Results for Unionized SO_2

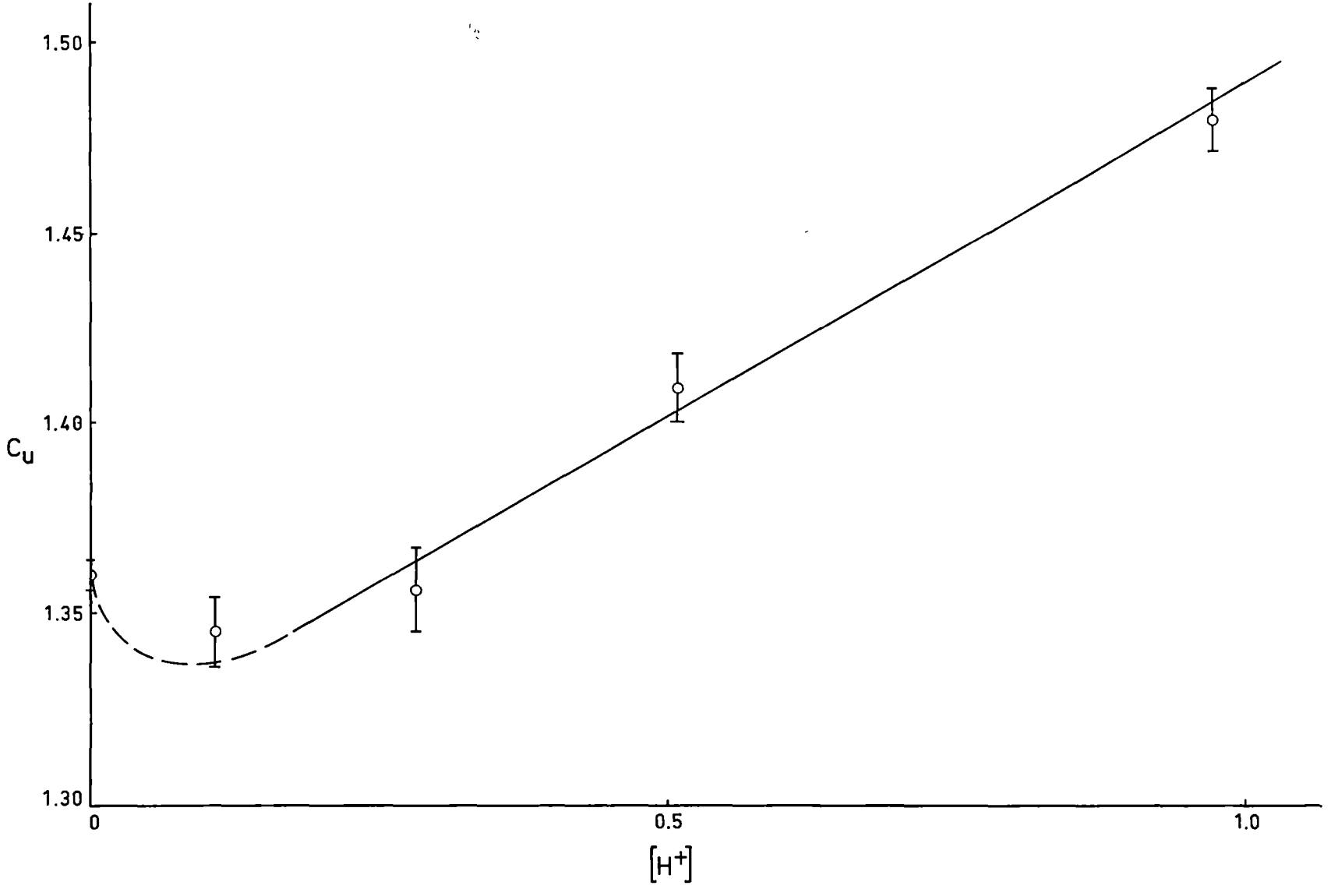
1.50
1.45
1.40
1.35
1.30
C_u
0
0.5
1.0
$[H^+]$

investigation of this phenomenon is again outside the scope of this work but it may also merit attention.

3.5 CONCLUSIONS

Equilibrium solubilities of sulphur dioxide in water and in aqueous hydrochloric acid solutions have been measured. The data for hydrochloric acid are believed to be the first obtained and there is evidence from the absorption experiments (Section 8.2) that the data for water are at least as accurate as any previously published.

CHAPTER 4 VISCOSITY MEASUREMENTS

4.1 INTRODUCTION

The discrepancies between measured diffusion coefficients for sulphur dioxide in water were noted in Section 2.2. A close examination of the original sources of these measurements revealed that they were obtained under a variety of conditions including different concentrations of dissolved gas. It was considered that the discrepancies may have arisen, at least partly, from a concentration dependence of the coefficients and this was confirmed by absorption measurements (Section 8.5).

The diffusion coefficient for a solute in a liquid is a function of the liquid viscosity and the relationship between the two parameters varies for different systems [119,179,194-196]. The viscosities of aqueous sulphur dioxide solutions do not appear to have been measured and to establish the relationship for this system it was first necessary to obtain these data.

4.2 EXPERIMENTAL

All measurements were made with a Hoeppler, Model BH, falling-ball viscometer. Briefly, the principle of measurement consists of filling a sloping glass tube with the liquid and measuring the time taken for a ball to fall between two marks on the tube. The viscosity of the liquid is then calculated from the expression

$$\eta = K_V.\theta.(\rho_B - \rho_L) \qquad (4.1)$$

where η is the viscosity (cp)

K_v is a 'ball constant'

θ is the time of fall (secs)

ρ_B is the density of the ball (gm/cc)

ρ_L is the density of the liquid (gm/cc)

The instrument used had the following characteristics:

Tube: Diameter: 1.594 cm

Capacity: 40 cc

Slope: 10° from vertical

Distance between marks: 10 cm

Ball: Material: Glass

Diameter: 1.581 cm

Density: 2.405 gm/cc

Constant K_v: 0.00912 calculated from measurements with water at 20°C using equation (4.1)

The tube was enclosed in a glass water bath through which water from a thermostated tank was circulated. The thermostat used was a 'Tempette' model whose sensing device is a bi-metallic strip. By manual control of this instrument the temperature of the water in the bath was maintained at 20±0.05°C. Times of fall were measured manually using a stopwatch which could be read to the nearest 0.1 second and, for all measurements, these times were in the range 75 to 90 seconds. Because of the small difference between the diameters of the tube and the ball, the measurements are especially sensitive to contamination of the liquid by suspended material. For this

reason the equipment was scrupulously cleaned before use and was situated in a dust-free area.

Distilled, de-aerated water was used and the following procedure was adopted. The tube, containing the ball, was filled with water and sulphur dioxide was bubbled through the water for several hours. Liquid spilled during this operation was replaced with water. Care was taken to avoid entrainment of air bubbles and the tube was sealed. It was inverted several times to ensure uniform mixing and the time of fall was measured. The seal was removed and, using a calibrated hypodermic syringe, two samples (approx. 1 cc) were immediately removed from the centre of the tube and analysed by iodiometric titration (Section 7.3). Portion of the liquid was decanted and was replaced with water and the above procedure was repeated for different concentrations of sulphur dioxide.

4.3 DISCUSSION

The results of these measurements are given in Table A.5.3 and the calculated viscosities are shown in Graph 4.1. The times in Table A.5.1 are the average of five independent readings and the 95% confidence limits shown in Graph 4.1 are based on these readings. The curve through the experimental points for aqueous sulphur dioxide solutions extrapolates smoothly to the tabulated viscosity of water [125] and this was taken to indicate that the experimental procedure did not introduce any systematic error into the measurements.

Eriksen [119] has shown that diffusion coefficients for bisulphite ions are much lower than for unionized sulphur dioxide molecules and

Graph 4.1

Graph 4.1

Viscosities of Aqueous Sulphur Dioxide Solutions

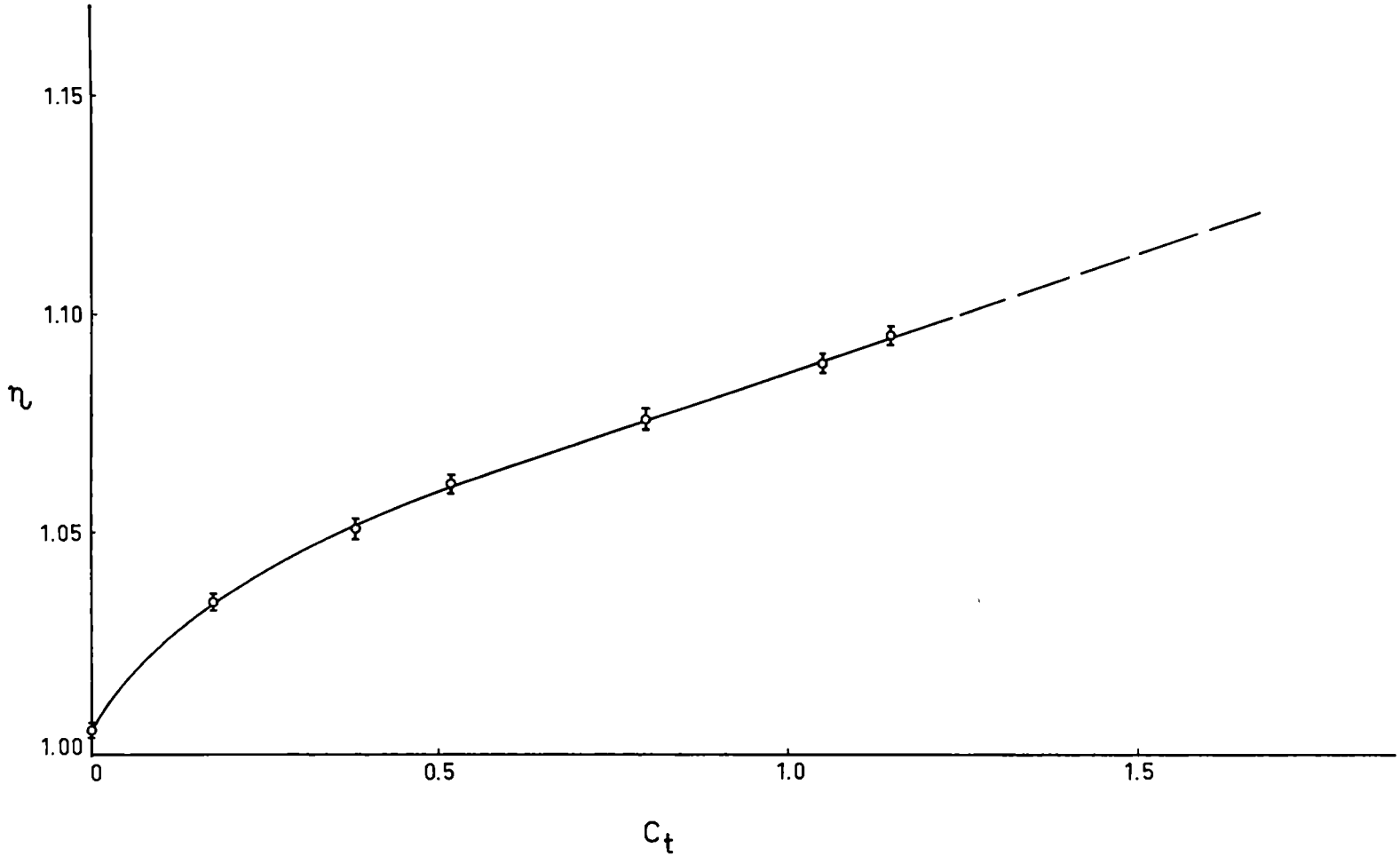
1.15
1.10
1.05
1.00
η
0
0.5
1.0
1.5
C_t

it is reasonable to expect (cf equation (2.7)) that the contribution to viscosity by these ions will be greater than that of unionized molecules at the same concentration. The proportion of these ions decreases with increased sulphur dioxide concentration and this is the most probable explanation for the shape of the curve in Graph 4.1. The relationship between viscosity and diffusion is discussed in Section 8.5.

CHAPTER 5 CHOICE OF ABSORPTION EQUIPMENT

5.1 INTRODUCTION

Experimental studies of absorption mechanisms have been carried out in many different types of equipment. Most have been designed to produce a liquid flow in which velocity gradients, and their effects on absorption rates can be estimated. In other designs, attempts have been made to eliminate hydronamic effects by studying absorption in stagnant liquids. In this chapter the characteristics of each type of equipment are discussed and finally the laminar jet apparatus is chosen for the present investigation.

5.2 ABSORPTION INTO FLOWING LIQUIDS

5.2.1 WETTED-WALL COLUMNS

The wetted-wall column has been used in absorption studies for many years and its general design features are well known. Early investigations [e.g. 212-217] were carried out in long columns (up to four feet) and the results were correlated in semi-empirical relationships; these were based on the assumption of a parabolic velocity distribution in the liquid film for Reynold's numbers up to 2100. However, Friedman and Miller [218] showed that, after a certain distance, waves were formed at much lower Reynold's numbers; subsequent investigations [219-229] have shown that not only waves, but also turbulence may develop at these low Reynold's numbers. The problem may be overcome by adding surface active agents to the liquid

[7,18,112,230-232] but this introduces uncertainties regarding interfacial resistance. A different approach has led to the development of the short column [37,38,190] and this has been used in many investigations [7,11,37,38,190,233-236].

A characteristic of wetted-wall columns, which is most pronounced in the short columns, is the existence of end effects. Two effects may be recognized:

(i) an entrance effect caused by liquid at the top of the column not reaching its terminal velocity immediately,

(ii) an exit effect caused by poor definition of the lowest level of exposed liquid. This is accentuated when surface active agents are used because of accumulation of surface active material at the bottom of the column which gives decreased local absorption rates in this region.

Some investigators [e.g. 7,18,231,232] have accounted for both effects together by calibrating their column under conditions of physical absorption and defining an effective column height. However, Roberts and Danckwerts [237] pointed out that this assumes a predictable influence of liquid flow rate on the exit effect. They demonstrated that this is not always true and designed a long column in which exit effects were virtually eliminated. Entrance effects were reduced by suitable design and estimated using the theoretical equations of Wilkes and Nedderman [227]. This design has not yet been extended to short columns.

5.2.2 FLOW IN RECTANGULAR CHANNELS

Laminar flow of liquids in rectangular channels which are slightly inclined to the horizontal is characterized by the absence of surface waves over a wide range of Reynold's numbers [183,185, 238]. Some investigators have therefore preferred this type of equipment to wetted-wall columns.

In a theoretical analysis based on laminar flow theory, Jaymond [238] showed that if wall effects are neglected and the liquid velocity is assumed constant near the surface, then the penetration theory equations can be applied to absorption in the liquid. He measured rates of absorption of carbon dioxide into aqueous solutions of sodium hydroxide in a channel inclined at angles of 1 to 15° and the results, although scattered, appear to support this conclusion. However, a definite end effect is evident from the results and this was not accounted for. In a subsequent investigation [185] wider channels were used and they were inclined at only 20 minutes. End effects were accounted for and it was claimed that the measured diffusion coefficient for carbon dioxide in water was accurate to within 1.5 percent.

A rigorous mathematical analysis of absorption in this type of apparatus has been presented by Tang and Himmelblau [183]. The mathematical model was solved by three methods - an eigensolution, boundary layer theory and penetration theory. They stated that the boundary layer solution may be subject to error and considered the eigensolution to give the most accurate results. Values of the

diffusion coefficient for carbon dioxide in water, calculated from experimentally determined absorption rates by the penetration theory, agreed well with those obtained from the eigensolution and they claimed that use of this theory for this type of apparatus is justified.

A modification of this type of apparatus, designed to give much shorter contact times, has been described by Savinova and Tovbin [239]. The channel, which is completely filled with liquid, is covered on top and exposure to the gas occurs through a rectangular hole in the covering. However, experimental results obtained by these investigators show a large degree of scatter and this was undoubtedly caused by end effects which would probably be difficult to estimate.

5.2.3 LAMINAR JETS

Laminar jets were first used in absorption studies in 1930 [240] and they have since proved increasingly popular. The technique requires a circular jet of liquid to issue in laminar flow from a nozzle. This is allowed to fall under gravity through the gas and is collected in such a way that the exposed liquid surface is well defined. The two main requirements of the technique are:

(i) a sufficiently long jet (at least 10 cm) so that end effects are minimized and the area of exposed liquid can be measured accuately.

(ii) a jet in which velocity gradients can be accurately predicted.

To interpret absorption measurements the penetration theory is used with the following additional assumptions:

(i) the depth of gas penetration is small and the curvature of the jet can be neglected; this fulfils the requirement that diffusion is uni-dimensional. Using a method given by Crank [139] it can be shown that, for most gases, (including sulphur dioxide) this assumption introduces errors of less than 1 percent in measured diffusion coefficients.

(ii) changes in jet density and viscosity due to the absorbed gas do not significantly alter the jet dimensions or hydronamics.

With these assumptions, the total absorption rate in a jet is given by

$$\Phi = \int_{X=0}^{X=L} N_X \cdot \pi \bar{D} \cdot dX \qquad (5.1)$$

To evaluate hydronamic effects it is convenient to define an ideal jet as one in which the velocity profile is flat and the diameter is constant throughout its length. In this case the penentration theory gives

$$N_{X,id} = (C_o - C_L)\left[\frac{\mathcal{D}.V_{id}}{\pi X}\right]^{\frac{1}{2}} \qquad (5.2)$$

and equation (5.1) reduces to

$$\Phi_{id} = 2(C_o - C_L)D_o[\pi \mathcal{D}.V_{id}L]^{\frac{1}{2}} \qquad (5.3)$$

which gives

$$\Phi_{id} = 4(C_o - C_L)\mathcal{D}^{\frac{1}{2}}(QL)^{\frac{1}{2}} \qquad (5.4)$$

In practice, hydronamic conditions are determined by two distinct influences; viscous drag in the nozzle which produces a boundary layer at the beginning of the jet and gravitational acceleration which causes thinning of the jet. To apply equation (5.1) to a non-ideal jet requires a knowledge of the dependence on jet length of both N and D. The latter dependence can be obtained from measurement of the jet profile but the former requires a knowledge of velocity gradients within the jet and a solution of the diffusion equation (equation (1.2)) for absorption into a liquid moving with these velocities.

Table 5.1 contains a summary of previous investigations in which laminar jets have been used. It can be seen that many jets were produced in glass tubes with either straigth or converging walls. Jets issuing from straight glass tubes most probably have a velocity profile at the nozzle face similar to that inside the tube - i.e. fully developed parabolic; unless converging nozzles are specially designed, jets issuing from them will most probably have a thick boundary layer at the nozzle face. Non-ideal behaviour of an uncertain nature will occur in both types of jets and accurate prediction of absorption rates is extremely difficult. Despite this the jets were assumed to be ideal in many investigations; in others, hydronamic effects were estimated by absorbing either carbon dioxide or sulphur dioxide into water and assuming both processes to be physical absorption.

TABLE 5.1 PREVIOUS USE OF LAMINAR JETS

Investigator	Nozzle diameter mm	Receiver diameter mm	Jet lengths cm	Contact times sec x 10^3	Jet hydronamics
TAPERED GLASS NOZZLES					
Dirken & Mook [240]	0.4	-	-	10	Assumed ideal
Onda et al [182]	0.6 - 1.8	-	0.6 - 3.3	2 - 20	Assumed ideal
Uhara [241]	0.3 - 0.5	-	0.5 - 1.1	5 - 8	Assumed ideal
Matsuyana [42]	0.7 - 0.8	-	0.7 - 2.5	5 - 18	Assumed ideal
Edwards et al [39]	0.8 - 1.6	-	2 - 10	1 - 18	Assumed ideal
Vielstich [12]	0.6 - 0.8	-	0.7 - 3.0	1 - 40	Assumed ideal
Hofmeister [242]	0.87	-	2 - 6	6 - 20	Assumed ideal
Yano & Kawai [243]	0.3 - 0.8	-	0.5 - 2.5	6 - 25	Empirical correlation
Scriven & Pigford [8,9,244]	1.41	1.94	1 - 16	3 - 50	Examined by CO_2 absorption
Raimondi & Toor [13,14]	-	-	1 - 4	2 - 20	Examined by CO_2 absorption
Sharma & Danckwerts [245]	0.7 - 1.8	-	1.5 - 7.1	4 - 60	Examined by CO_2 absorption
Manogue & Pigford [113,114]	0.63	0.78	0.1 - 8	-	Examined by SO_2 absorption
Nysing et al [18,112,231]	0.1 - 1.5	-	1 - 10	1 - 20	Examined by SO_2 absorption
Kramers et al [115]	1.01	1.5	2 - 8	6 - 25	Examined by SO_2 absorption
STRAIGHT GLASS NOZZLES					
Cullen & Davidson [16]	-	-	0.1 - 7.0	-	Examined by CO_2 absorption
Raimondi & Toor [13,14]	0.76	1.0	1 - 4	2 - 20	Examined by CO_2 absorption
Manogue & Pigford [113,114]	0.61	0.90	0.1 - 8	-	Examined by SO_2 absorption

TABLE 5.1 (cont.)

ORIFICE NOZZLES - SQUARE SECTION					
Raimondi & Toor [13,14]	0.57,0.85	1.0	0.6 - 4	1 - 20	Assumed ideal
Chiang & Toor [19,20,45,54,106]	0.83,0.91	1.1	0.4 - 6.2	1 - 20	Assumed ideal
Rehm et al [22]	1.40	1.70	0.8 - 8	1.5 - 22	Assumed ideal
Clarke [246]	1.11	-	1 - 10	3 - 20	Assumed ideal
ORIFICE NOZZLES - ELLIPTICAL SECTION					
Woods [32]	1.5	1.9	1 - 12	-	Theoretical analysis
Scriven & Pigford [8,9,244]	1.54	1.94	1 - 15	3 - 50	Theoretical analysis
Hatch & Pigford [247]	1.45	2.0	1.5 - 12	5 - 40	Theoretical analysis
Spalding [248]	1.65	-	2.5 - 9	8 - 40	Theoretical analysis
Vrentas [46]	1.54	2.0	1 - 12	2.5 - 50	Theoretical analysis
Onda et al [182]	0.80	-	0.6 - 3.3	2 - 30	Assumed ideal
Raimondi & Toor [13,14]	0.85	1.0	0.6 - 4	1 - 20	Assumed ideal
Astarita [249,250]	1.54	1.94	1 - 15	20 - 70	Assumed ideal
ORIFICE NOZZLES - SPECIAL DESIGN					
Cullen & Davidson [16]	3.73	-	1.6 - 13	15 - 250	Theoretical analysis
Briggs & Thompson [251]	3.7 - 4.0	-	-	-	Theoretical analysis
Tang & Himmelblau [187,188]	4.0	4.0	13	20.-25	Theoretical analysis
ORIFICE NOZZLES - DESIGN NOT KNOWN					
Takeuchi & Namba [123]	-	-	1.1 - 2.6	-	Assumed ideal
Thomas & Adams [186]	-	-	1 - 10	-	Assumed ideal
Jeffreys & Bull [252]	2.5	-	2.0 - 7.5	10 - 120	End effects accounted for

To produce jets with predictable velocity profiles, three types of nozzle have been used. The basic construction of each is similar (a tube sealed at one end by a flat plate with a small central orifice) and it is the shape of the orifice section which distinguishes them.

The simplest design is a square-edged orifice in a very thin plate. In all investigations using jets produced from these nozzles, rates of absorption of carbon dioxide into water were measured. Results agreed well with values predicted for ideal jets and the jets were consequently assumed to be ideal. However, several investigators [8,9,16,187,188,244] have shown that such agreement can be explained by the interaction of boundary layer and gravitational effects and need not necessarily indicate an ideal jet.

An elliptically shaped orifice section is only a small improvement in design and the main value of Scriven and Pigford's work [8, 9,244] lies in the method they give for analysing jet hydronamics. The method has been used in many investigations [e.g. 32,46,247, 248,251] and is used in the present study. Details are given in Appendix 4.

In a theoretical study, Southwell [253] analysed the shape of the free streamline in a jet of inviscid liquid issuing from a sharp orifice in the absence of a gravitational field. Cullen and Davidson [16] made the curve of their orifice section 'the same shape as the initial part of ... [this] streamline' and, from an analysis of measured jet diameters, claimed to have eliminated the

boundary layer. From measurements of the diameters of the jets used in the present investigation (see Chapter 4), it can be seen that if the boundary layer at the nozzle face is about ten percent of the jet radius, its influence on absorption rates will be substantial while its effect on the jet profile may be measurable only in the first few diameters of jet travel. The latter effect is masked by the influence of gravitational acceleration and this masking increases with increasing jet diameter. Because Cullen and Davidson used very large diameter jets, and because of uncertainties in the precision of their diameter measurements, their claim must be suspect. This is emphasized by the fact that Tang and Himmelblau [187,188] used the same design and measured a thin boundary layer while Briggs and Thompson [251] measured a much thicker boundary layer and used Scriven and Pigford's method to analyse hydronamic conditions.

Catching jets efficiently is not difficult. Except in three investigations [39,182,231] all jets were caught in a cylindrical tube whose diameter was slightly greater than that of the jet; in most cases a piece of glass capillary tube was used. By balancing the kinetic head of the jet against a potential head in the receiver outlet, a jet can be caught for extended periods without either entrainment of gas or liquid spill-over. Careful selection of the receiver diameter enables exit effects to be reduced to insignificance.

5.2.4 ANNULAR JETS

An annular jet is a 'cylindrical sheet of liquid issuing from an annular orifice. Surface tension makes the sheet converge to become an ordinary jet some distance below the orifice' [180]. If the jet is allowed to converge onto a tube, gas can flow into the space surrounded by the jet and out through the tube and the apparatus is suitable for absorption studies. In the only reported study [180], boundary layer effects were assumed absent and absorption rates were analysed by combining a simple hydronamic analysis with the penetration theory. That diffusion coefficients of some sparingly soluble gases in water did not agree with those determined in a wetted-sphere apparatus was tentatively attributed to interfacial resistances supposedly present during jet absorption but not during wetted-sphere absorption.

5.2.5 FLOW OVER WETTED SPHERES

In studying packed-tower absorption, many investigators [7, 254-259] simplified hydronamic conditions by using a model in which the liquid flows over spheres arranged in a vertical column. Some of the results obtained in these investigations were correlated in semi-empirical relationships [254-256] and attempts to obtain more fundamental analyses [7,257-259] showed that hydronamic uncertainties still existed. These resulted from mixing of the liquid between the spheres and ripples on the lower spheres which were not always eliminated by surface active agents.

Lynn et al [7] limited their column to a single sphere and

used a simple hydronamic analysis with the penetration theory to analyse their absorption data. Rates of absorption of sulphur dioxide into water were higher than predicted values and this was attributed to a stretching effect in the liquid film which was not considered in the hydronamic analysis. Subsequent investigators [10,17,44,180,181,260] claimed that, over a limited range of liquid flow rates, this effect can be minimized; Davidson and Cullen [260] claimed that it is possible to measure liquid-phase diffusion coefficients to within one percent using this type of apparatus.

5.3 ABSORPTION INTO STAGNANT LIQUIDS

Absorption into stagnant liquids at long exposure times is complicated by convection currents in the liquid which influence the absorption rate [261]. However, at sufficiently short exposure times, this influence is negligible and two types of apparatus have been designed to obtain these conditions.

In one [24,262] a film of liquid, picked up on a rotating drum and supposedly at rest relative to the drum, is briefly exposed to a gas. Measured absorption rates for carbon dioxide into water obtained by this method were consistently lower than values predicted by the penetration theory and this was attributed to 'end effects, such as the initial adjustment of the liquid velocity to that of the drum or "stagnant" surface near the exit' [262]. In a similar apparatus [23] the liquid is carried through the gas on a narrow rotating band. Again measured absorption rates for carbon dioxide

into water were lower than predicted values but in this case it was claimed that end effects were absent and the discrepancy was attributed to an interfacial resistance.

In their study of interfacial resistances, Harvey and Smith [15] described an interferometric technique in which gas is absorbed into a stagnant liquid and there is no relative motion between the two phases. However, to use the technique to measure absorption rates first requires accurate measurement of any interfacial resistances. In the absence of a resistance the technique cannot be used.

5.4 DISCUSSION

From the preceding review it can be seen that absorption data of comparable accuracy may be obtainable from the following types of equipment:

(i) a short wetted-wall column modified as suggested by Roberts and Danckwerts [237];

(ii) near-horizontal films flowing in a wide channel;

(iii) a laminar jet issuing from a carefully designed nozzle and

(iv) flow over a wetted sphere.

To investigate sulphur dioxide absorption the laminar jet technique was chosen for the following reasons:

(i) it allows the widest range of contact times to be used;

(ii) it exposes the smallest liquid surface and has the smallest contact time; because sulphur dioxide absorbs at a much greater rate than carbon dioxide, this makes available some of the techniques of

gas flow measurement that have been developed for carbon dioxide absorption at longer contact times and greater exposed liquid surfaces;

(iii) a technique for accurately estimately the effects of liquid phase hydronamics has been developed and widely tested;

(iv) an improved nozzle design was available;

(v) facilities were available for accurate nozzle construction and jet profiling.

CHAPTER 6 PRODUCTION AND ANALYSIS OF THE LAMINAR JET

6.1 CONSTRUCTION OF THE JET NOZZLE

The problem of producing a stable laminar jet of liquid is analogous to that of designing a cavitation-free contraction in a pipe. To avoid cavitation it is necessary that the fluid pressure at the pipe wall varies continuously from a maximum at the start of the contraction to a minimum just after the end. In other words, the shape of the contraction should be such that boundary layer separations are minimized. The hydronamic conditions in a jet are so critical that any upstream perturbations, such as would be caused by these separations, are greatly magnified with consequent loss in jet stability. A further requirement of the nozzle is that its inside edge at the jet exit should be as sharp as possible. This minimizes the effects of surface tension at the nozzle face which will also cause instability.

One contour which meets the requirements with regard to boundary layer separation is the so called 'double-cubic' (Figure 6.1). The characteristics of this contraction were studied by Rouse and Hassan [263] who showed that a favorable pressure gradient can be obtained if, for fixed values of D_1/D_2 and X_4/D_1, X_1/X_4 does not exceed a critical value. If this value is exceeded a pronounced pressure drop occurs just before the end of the contraction.

Jets produced in double cubic nozzles were examined in this investigation as follows. Two nozzles (Table 6.1) were constructed

Figure 6.1

Figure 6.2

Figure 6.3

Figure 6.1

Design of a 'Double-Cubic' Nozzle

Figure 6.2

Method of Mounting the Plastic Nozzles

Figure 6.3

Method of Mounting the Stainless Steel Mandrel

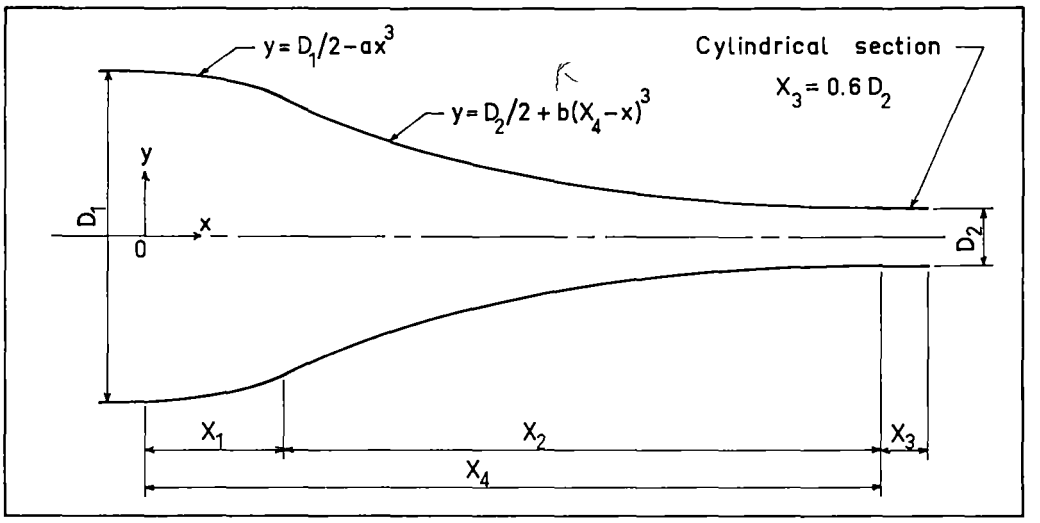
$y = D_1/2 - ax^3$
$y = D_2/2 + b(X_4 - x)^3$
Cylindrical section
$X_3 = 0.6\,D_2$
y
x
0
D_1
D_2
X_1
X_2
X_3
X_4

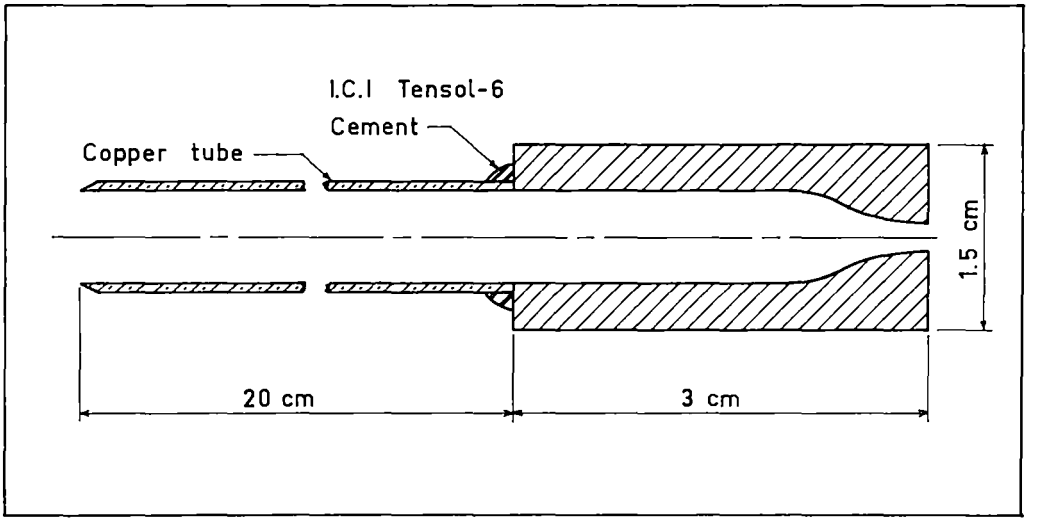
I.C.I Tensol-6
Cement
Copper tube
1.5 cm
20 cm
3 cm

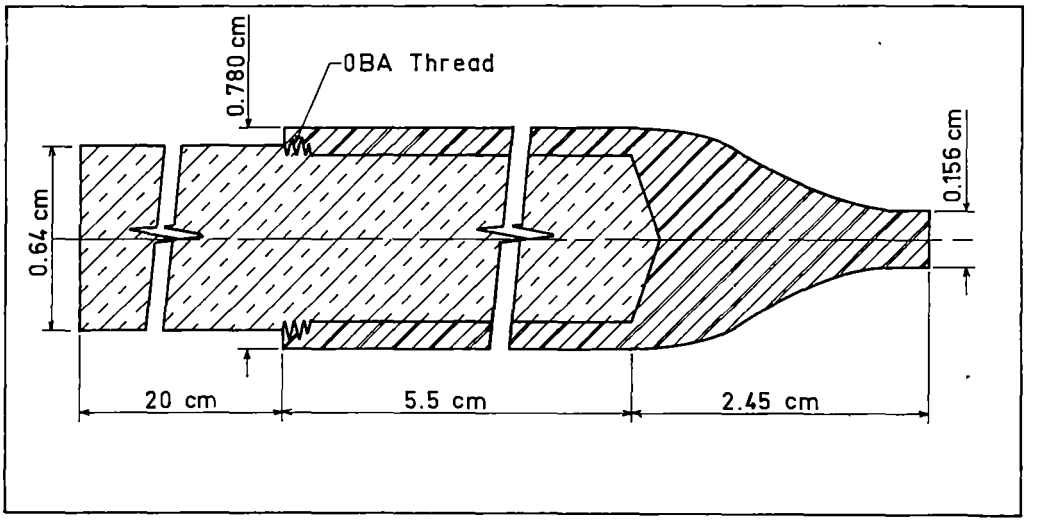
0.780 cm
0BA Thread
0.64 cm
0.156 cm
20 cm
5.5 cm
2.45 cm

TABLE 6.1 DIMENSIONS OF PLASTIC NOZZLES

Dimension	1	2
D_1 (cm)	0.635	0.710
D_2 (cm)	0.159	0.150
X_1 (cm)	0.143	0.420
X_2 (cm)	0.810	1.710
X_3 (cm)	0.095	0.090
X_4 (cm)	0.953	2.130
Constant a	12.25	0.746
Constant b	0.381	0.0450

by moulding Buehler Transoptic mounting powder around highly polished brass mandrels. The mounting powder, after moulding, has excellent machining properties and a very sharp inside edge was obtained by carefully machining the nozzle face followed by very light polishing with 'Brasso' on a hard, flat surface. The nozzles were mounted as shown in Figure 6.2. Jets produced in these nozzles were examined microscopically with carefully arranged illumination. For flow rates of 3 to 7 cc/sec (velocities of 170 to 400 cm/sec) there was no discernible disturbance of the jet surface for lengths of 20 to 30 cm. Although the nozzles exhibited a small degree of dimensional instability, this was not sufficient to cause any significant change in exit diameter over a short period of time and it was possible to measure jet diameters at different lengths to ± 0.0002 cm (Section 6.2). These measurements were analysed by the method described by

Scriven and Pigford [8,9,244] (Appendix 4) and it was shown that the boundary layer, which was never more than 7% of the jet radius, disappeared after 1.5 cm of travel. This indicated that the jets more closely approach ideal behaviour than any previously used in absorption studies.

Plate 6.1(a) shows 18 cm of a stable jet with a flow rate of 5 cc/sec. Plate 6.1(b) shows conditions at the nozzle face for the same jet and demonstrates the small amount of wetting of the nozzle face. Plates 6.1(c) and 6.1(d) are discussed in Section 7.2.1.

As well as being dimensionally unstable, the plastic nozzles also deteriorated on exposure to moist sulphur dioxide and it was necessary to select another material for the absorption studies. Metals were rejected because of uncertainties in chemical stability and, although glass nozzles could not be made with the same precision, they were chosen because they were subsequently shown to produce jets with only slightly inferior hydronamics.

Several attempts were made to collapse glass tubes onto a stainless steel mandrel with the same precision achieved in the plastic nozzles. All were unsuccessful because after collapse the mandrel could not be removed from the glass and, even with cooling rates less than 1°C per minute, small cracks formed in the nozzle. However, it was observed that if a piece of tubing is drawn carefully to a neck, the internal contour of the shoulder of the neck closely approximates a cubical arc. If the tube bore is chosen to allow easy removal of the mandrel, and the neck is collapsed over the lower

Plates 6.1 (a) to 6.1 (d)

Plate 6.1 (b)

Conditions at the Nozzle Face

Plate 6.1 (a)

Laminar Jet Produced in a Plastic Nozzle

Plate 6.1 (c)

Catching a 15 cm Jet

Plate 6.1 (d)

Catching an 18 cm Jet

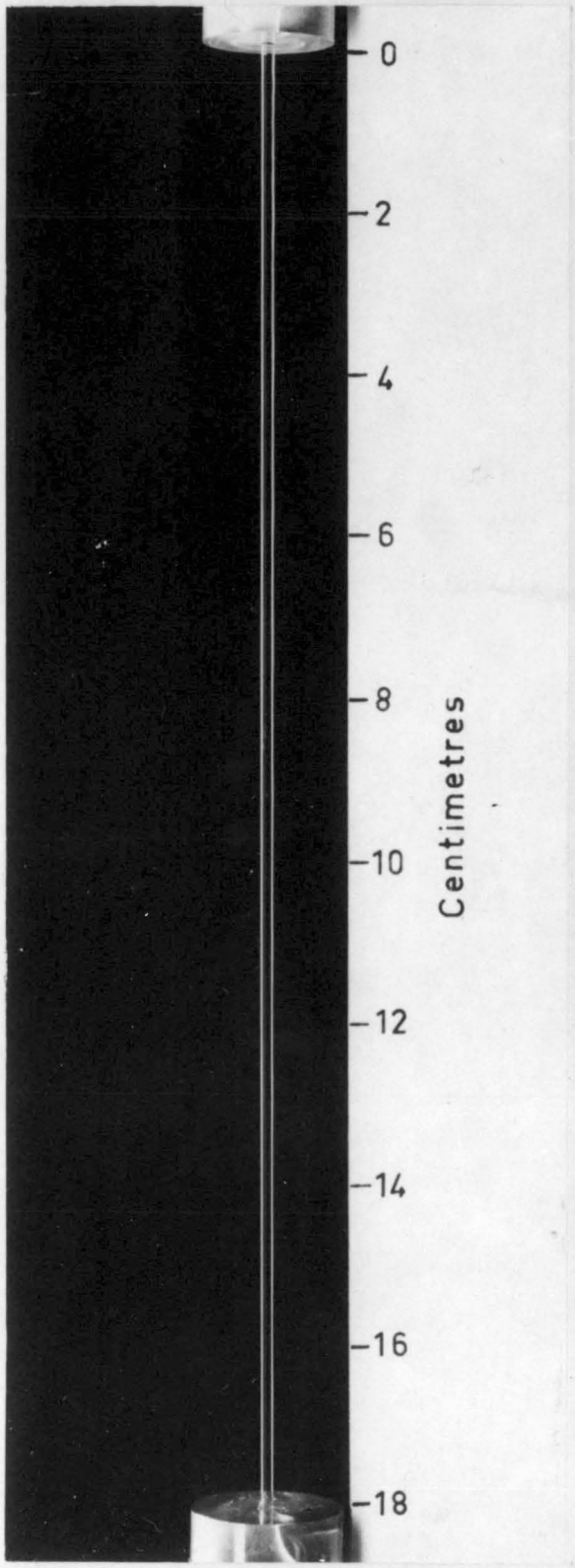

(a)

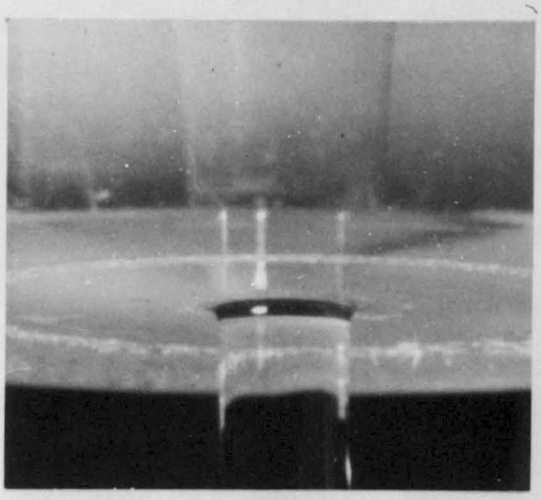

(b)

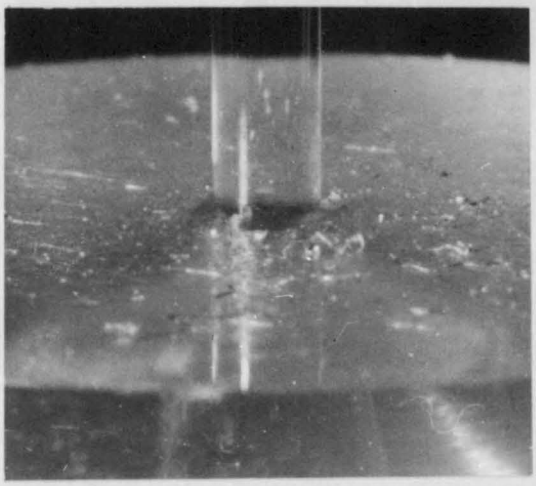

(c)

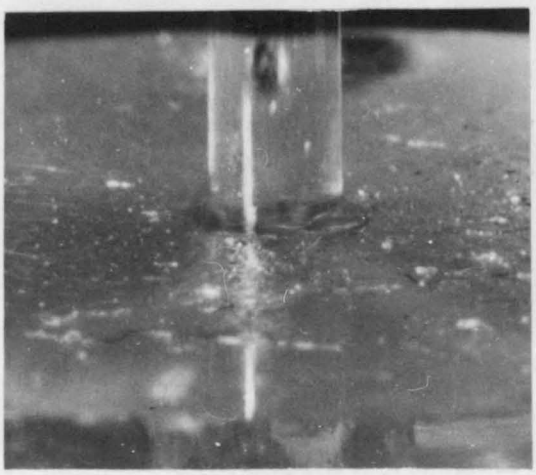

(d)

part of the mandrel, then the resulting nozzle is little different from a double cubic and the increase in X_1/X_4 can be allowed for by suitable mandrel design. The following procedure was finally adopted.

The mandrel (Table 6.2), made from AISI Type No.310 steel ('25-20 stainless'), was mounted on a brass rod (Figure 6.3) and highly

TABLE 6.2 COMPARISON OF MANDREL AND NOZZLE DIMENSIONS

Dimension	Mandrel	Nozzle
D_1 (cm)	0.780	0.84
D_2 (cm)	0.156	0.1574 (excluding radius)
X_1 (cm)	0.468	0.7 (est.)
X_2 (cm)	1.872	1.872
X_3 (cm)	0.094	0.094
X_4 (cm)	2.340	2.6 (est.)
Constant a	0.609	0.3 (est.)
Constant b	0.0381	0.038 (est.)

polished. Its profile was checked using a two-way travelling microscope and the results (Table 6.3) indicated good agreement with the designed profile. A 40 cm length of thick-walled pyrex glass tubing, I.D. = 0.84 cm, was chosen for the circularity of its bore and the sequence of operations to collapse it onto the mandrel are depicted in Figure 6.4. Two necks were drawn near one end (a), care being taken that the mandrel, when placed in the tube, contacted the glass smoothly and symmetrically and as far as possible from its lower

Figure 6.4

Figure 6.4

Sequence of Operations in the Construction

of the Glass Nozzle

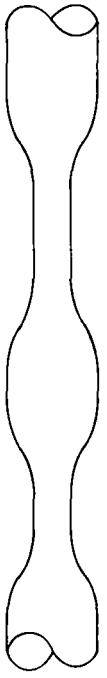

(a)

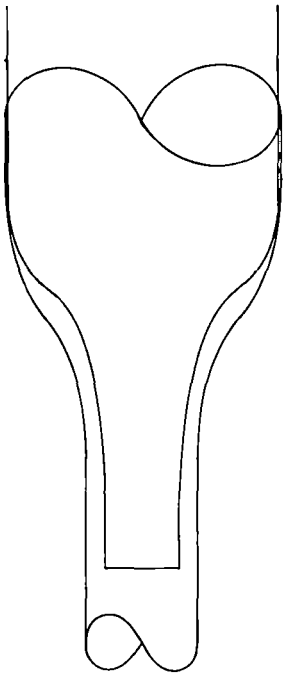

(b)

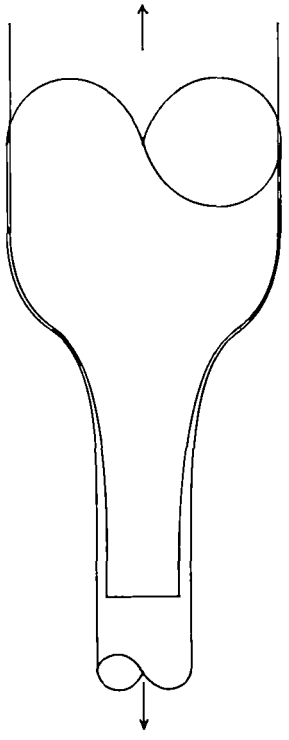

(c)

(d)

TABLE 6.3 DESIGNED AND MEASURED MANDREL DIAMETERS

x (cm)	Diameter (cm)		x (cm)	Diameter (cm)	
	Designed	Measured		Designed	Measured
0	0.780	0.780	1.3	0.242	0.244
0.1	0.779	0.778	1.4	0.219	0.221
0.2	0.770	0.772	1.5	0.201	0.203
0.3	0.747	0.748	1.6	0.187	0.189
0.4	0.702	0.701	1.7	0.176	0.177
0.5	0.631	0.631	1.8	0.168	0.168
0.6	0.557	0.557	1.9	0.163	0.162
0.7	0.492	0.490	2.0	0.159	0.160
0.8	0.434	0.436	2.1	0.157	0.157
0.9	0.386	0.386	2.2	0.156	0.157
1.0	0.339	0.338	2.3	0.156	0.157
1.1	0.301	0.300	2.4	0.156	0.157
1.2	0.269	0.268	2.42	0.156	0.155

end (b). The upper neck and the mandrel were heated separately to about 400°C and the mandrel was placed in the tube. This was then held vertically in tension in a horizontal flame and the glass stretched over the shoulder of the mandrel (c). While not allowing this section to cool below about 500°C, the lower end was sealed and the tube was suspended vertically with its upper end connected to a vacuum system (d). Working downwards from the shoulder, the glass was slowly collapsed onto the remainder of the mandrel. To obtain

a uniform collapse it was necessary to exert a strong downward force on the lower end of the tube. The tube was then disconnected from the vacuum system and the mandrel removed immediately.

To make the inside edge at the nozzle face as sharp and as square as possible, the following procedure was adopted. The nozzle tip was cut to within 0.2 cm of the required length and the nozzle was mounted in a spring-loaded jig in a lathe. A large diameter metal disc with a smoothly machined face was held in the lathe tailstock perpendicular to the nozzle axis. A sheet of silicon carbide paper (120 grits/sq in) was then soaked in water and held against the slowly rotating nozzle with the disc as a backing, the spring ensuring a light, even pressure. Gouging of the glass was avoided by continuous movement of the paper and the nozzle was ground to within about 0.05 cm of the required length. This was reduced to about 0.005 cm by successive use of finer papers (320 and 600 grits/sq in) and finally to length with 600 grit paper whose cutting power had been reduced by rubbing against another sheet of the same paper. The edge produced in this way contained chips no greater than 0.001 cm in diameter but which nevertheless caused noticeable instability of a jet. The nozzle face was then polished with cerium oxide paste on a plate glass backing. This produced a small radius (approx. 0.002 cm) at the inside edge, but this was later shown to have a tolerable effect on jet hydronamics. The final dimensions of the nozzle are compared with those of the mandrel in Table 6.2. To minimize wetting of the nozzle face a very thin coating (<0.0001 cm) of paraffin wax was condensed on the face.

As a final check on the precision of construction, the bore of the nozzle was measured at three diameters mutually inclined at 120°. The results, given in Table 6.4 as the averages of ten independent readings for each diameter, were even better than could reasonably be expected from the method of construction. An average value of 0.1574 cm was taken for D_o.

TABLE 6.4 CIRCULARITY OF THE JET NOZZLE

$D_{o,1}$	$D_{o,2}$	$D_{o,3}$
0.1574	0.1573	0.1574

6.2 ANALYSIS OF JET HYDRONAMICS

Several water jets with different flow rates were formed in the glass nozzle and the diameter of each was measured at a number of downstream points. A travelling microscope, fitted with an image-splitting eyepiece previously calibrated against a standard stage micrometer, was used at a magnification of 28X. The accuracy of measurement depended on the definition of the image and this was maximized by illuminating the jet through a slit whose width was approximately the same as the jet diameter. The reproducibility of each measurement was ±0.0002 cm and the results are given in Table 6.5.

For flow rates of 3.5 to 6.0 cc/sec, jets were stable over a length of approximately 20 cm. At lower flows surface tension effects produced instability: at 3.0 cc/sec the stable length decreased to about 10 cm and a family of standing waves approximately 0.001 cm

TABLE 6.5 MEASURED AND CALCULATED JET DIAMETERS

L	Q = 3.5 cc/sec		Q = 4.0 cc/sec		Q = 5.0 cc/sec		Q = 6.0 cc/sec	
(cm)	Meas.	Calc.	Meas.	Calc.	Meas.	Calc.	Meas.	Calc.
0	0.1581	0.1581	0.1578	0.1578	0.1573	0.1574	0.1569	0.1568
0.1	0.1557	0.1556	0.1555	0.1556	0.1554	0.1554	0.1552	0.1552
0.2	0.1546	0.1546	0.1546	0.1546	0.1546	0.1546	0.1546	0.1546
0.5	0.1527	0.1526	0.1529	0.1528	0.1531	0.1531	0.1533	0.1533
1.0	0.1504	0.1504	0.1508	0.1508	0.1514	0.1514	0.1519	0.1519
1.5	0.1491	0.1492	0.1500	0.1499	0.1506	0.1506	0.1512	0.1510
2.0	0.1485	0.1484	0.1491	0.1493	0.1502	0.1502	0.1506	0.1507
3.0	0.1466	0.1468	0.1478	0.1480	0.1493	0.1493	0.1502	0.1501
4.0	0.1453	0.1452	0.1466	0.1467	0.1483	0.1484	0.1493	0.1494
5.0	0.1440	0.1438	0.1457	0.1455	0.1478	0.1476	0.1489	0.1488
6.0	0.1426	0.1424	0.1445	0.1444	0.1470	0.1468	0.1485	0.1483
7.0	0.1409	0.1411	0.1432	0.1433	0.1459	0.1460	0.1478	0.1477
8.0	0.1396	0.1398	0.1421	0.1422	0.1453	0.1453	0.1470	0.1471
9.0	0.1387	0.1386	0.1413	0.1412	0.1445	0.1446	0.1466	0.1465
10.0	0.1373	0.1375	0.1402	0.1403	0.1438	0.1439	0.1459	0.1460
11.0	0.1364	0.1364	0.1394	0.1393	0.1432	0.1432	0.1455	0.1455
12.0	0.1354	0.1353	0.1385	0.1384	0.1426	0.1425	0.1451	0.1450

high appeared between 0 and 2 cm downstream from the nozzle. At higher flows there was some evidence of turbulence although this was not appreciable below about 9 cc/sec.

If a jet with a flat velocity profile accelerates uniformly from point 1 to point 2 over a length L then

$$V_2^2 = V_1^2 + 2a_j.L \qquad (6.1)$$

Continuity requires that

$$Q = V_1A_1 = V_2A_2 = V_1D_1^2/4 = V_2D_2^2/4 \qquad (6.2)$$

and this gives

$$(1/D_2^4 - 1/D_1^4) = a_j.L/8Q^2 = 1.234a_j.L/Q^2 \qquad (6.3)$$

As a first analysis of jet hydronamics, a plot was made of $1/D^4$ against L for all the flow rates (Graph 6.1). From this it was seen that for lengths of 1.5 to 12 cm, agreement with equation (6.3) was excellent for all flows. This was taken to indicate that a flat velocity profile existed after 1.5 cm of travel. The equations of the lines, fitted by the method of least squares, were:

$$Q = 3.5; \quad 1/D^4 = 1878 + 92.08\ L$$

$$Q = 4.0; \quad 1/D^4 = 1872 + 71.20\ L$$

$$Q = 5.0; \quad 1/D^4 = 1873 + 46.19\ L$$

$$Q = 6.0; \quad 1/D^4 = 1874 + 32.50\ L$$

and diameters calculated from these equations did not differ by more than 0.0002 cm from measured values (Table 6.5).

Equating the slopes of the lines to $1.234a_j/Q^2$ in accordance with equation (6.3) gave the acceleration of each jet. The results are shown in Table 6.6 and are plotted in Graph 6.2 and the increasing

Graph 6.1

Graph 6.1

Analysis of Measured Jet Diameters:

Jet Lengths 1.5 to 12 cm

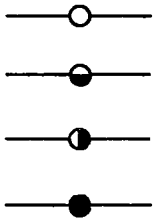

Q = 3.5 cc/sec

" 4.0 "

" 5.0 "

" 6.0 "

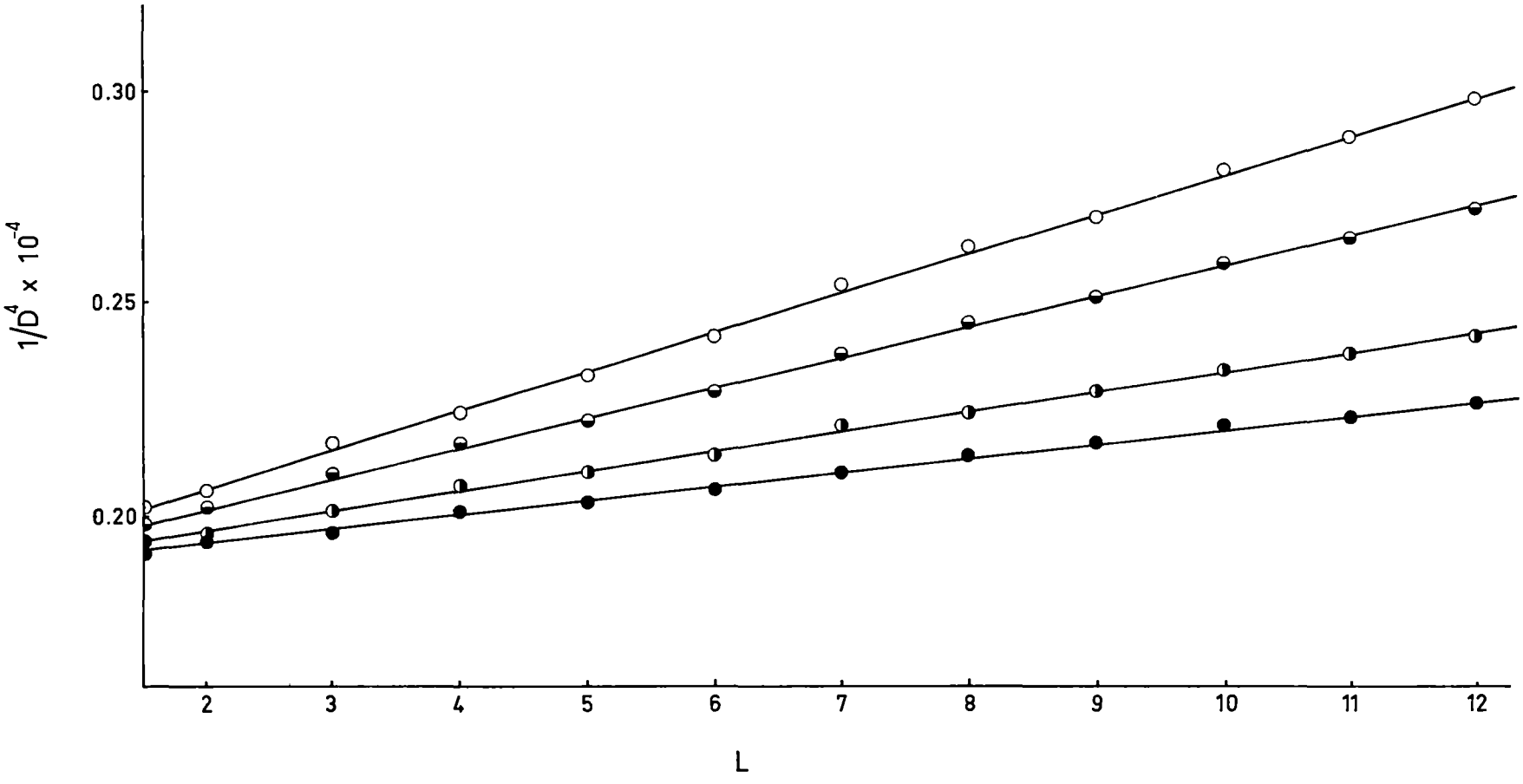
0.30
0.25
0.20
$1/D^4 \times 10^{-4}$
2
3
4
5
6
7
8
9
10
11
12
L

Graph 6.2

Graph 6.3

Graph 6.2

Jet Accelerations

Graph 6.3

Analysis of Measured Jet Diameters:

Jet Lengths 0 to 1.5 cm

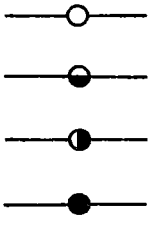

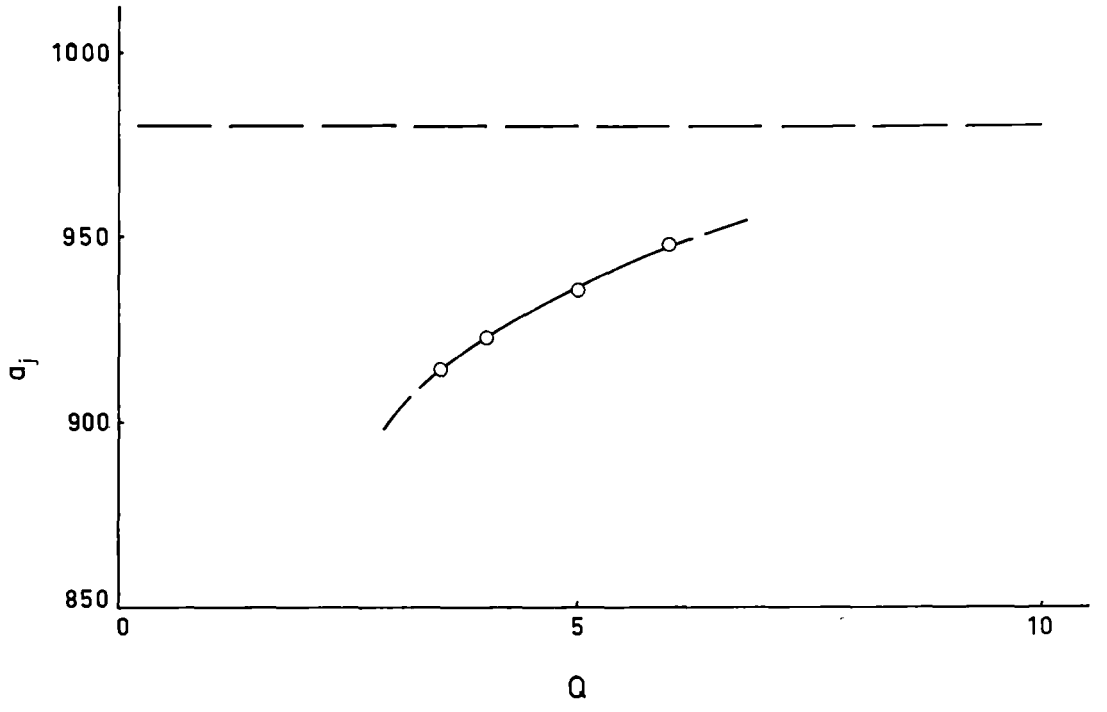
1000
950
900
850
a_j
0
5
10
Q

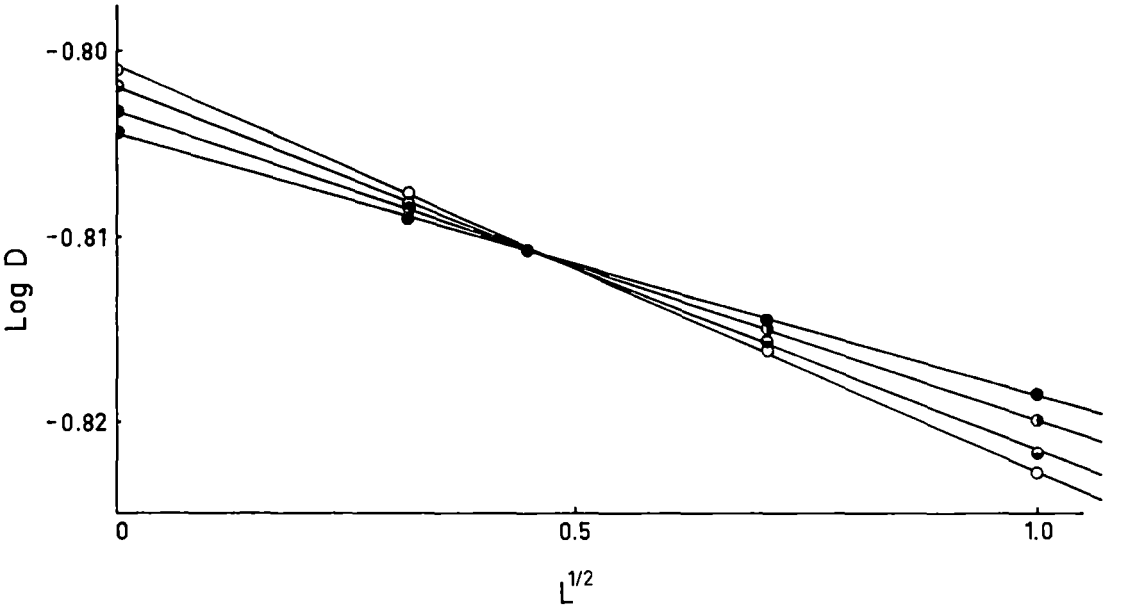
-0.80
-0.81
-0.82
Log D
0
0.5
1.0
$L^{1/2}$

effect of surface tension at decreasing flows is clearly evident. It appears that if the jets remained laminar at higher flows, their accelerations would approach a limiting value, no doubt less than 981 cm/sec^2 due to both surface tension and viscous effects.

TABLE 6.6 JET ACCELERATIONS

Q (cc/sec)	a_j (cm/sec^2)
3.5	914
4.0	923
5.0	936
6.0	948

That the jets did not attain a uniform acceleration until 1.5 cm of travel was taken to indicate the existence of a boundary layer at the nozzle exit. To estimate the thickness of this boundary layer the method described by Scriven and Pigford [8,9,244] (Appendix 4) was used. This required jet diameters as accurate as possible and measured diameters in the interval 0 to 1.5 cm were smoothed by plots of $\log_{10}D$ against the square root of jet length (Graph 6.3). The lines of best fit were evaluated by the method of least squares and the equations obtained were:

$$Q = 3.5; \quad -\log D = 0.8010 + 0.02175\, L^{\frac{1}{2}}$$

$$Q = 4.0; \quad -\log D = 0.8019 + 0.01974\, L^{\frac{1}{2}}$$

$$Q = 5.0; \quad -\log D = 0.8033 + 0.01664\, L^{\frac{1}{2}}$$

$$Q = 6.0; \quad -\log D = 0.8046 + 0.01395\, L^{\frac{1}{2}}$$

Although there is no theoretical basis for such a correlation, the excellent agreement between measured and calculated diameters (Table 6.5) was considered to justify its use. Measured values of the jet radii are plotted in Graph 6.4 in which the curves correspond to the linear relationships of Graphs 6.1 and 6.3.

Estimates of the dimensionless boundary layer thickness from equation (A.4.2) (Table 6.7) appeared to indicate that the thickness

TABLE 6.7 ESTIMATED BOUNDARY LAYER THICKNESSES

L	Q = 3.5		Q = 4.0		Q = 5.0		Q = 6.0	
(cm)	D	b	D	b	D	b	D	b
0.2	0.1546	0.065	0.1546	0.067	0.1546	0.070	0.1546	0.072
0.5	0.1526	0.105	0.1528	0.106	0.1531	0.105	0.1533	0.103
1.0	0.1504	0.143	0.1508	0.144	0.1514	0.141	0.1519	0.134
1.5	0.1492	0.152	0.1499	0.149	0.1506	0.151	0.1510	0.151
2.0	0.1484	0.150	0.1493	0.147	0.1502	0.149	0.1507	0.151
3.0	0.1468	0.147	0.1480	0.145	0.1493	0.149	0.1501	0.149

was independent of flow rate. However, the model used to obtain these estimates does not consider imperfections in nozzle construction. For example, it was observed that the jets contained very small surface tension 'rollers' at the nozzle face. These had been observed on a smaller scale in the jets formed in the plastic nozzles and they were thought to be magnified by the radius at the inside edge of the nozzle. A small stream of dye (aqueous potassium permanganate solution) was allowed to run down the outside of the nozzle

Graph 6.4

Graph 6.4

Measured and Smoothed Jet Radii

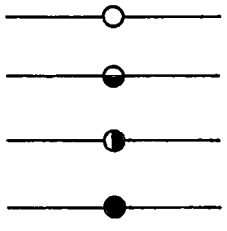

Q = 3.5 cc/sec

" 4.0 "

" 5.0 "

" 6.0 "

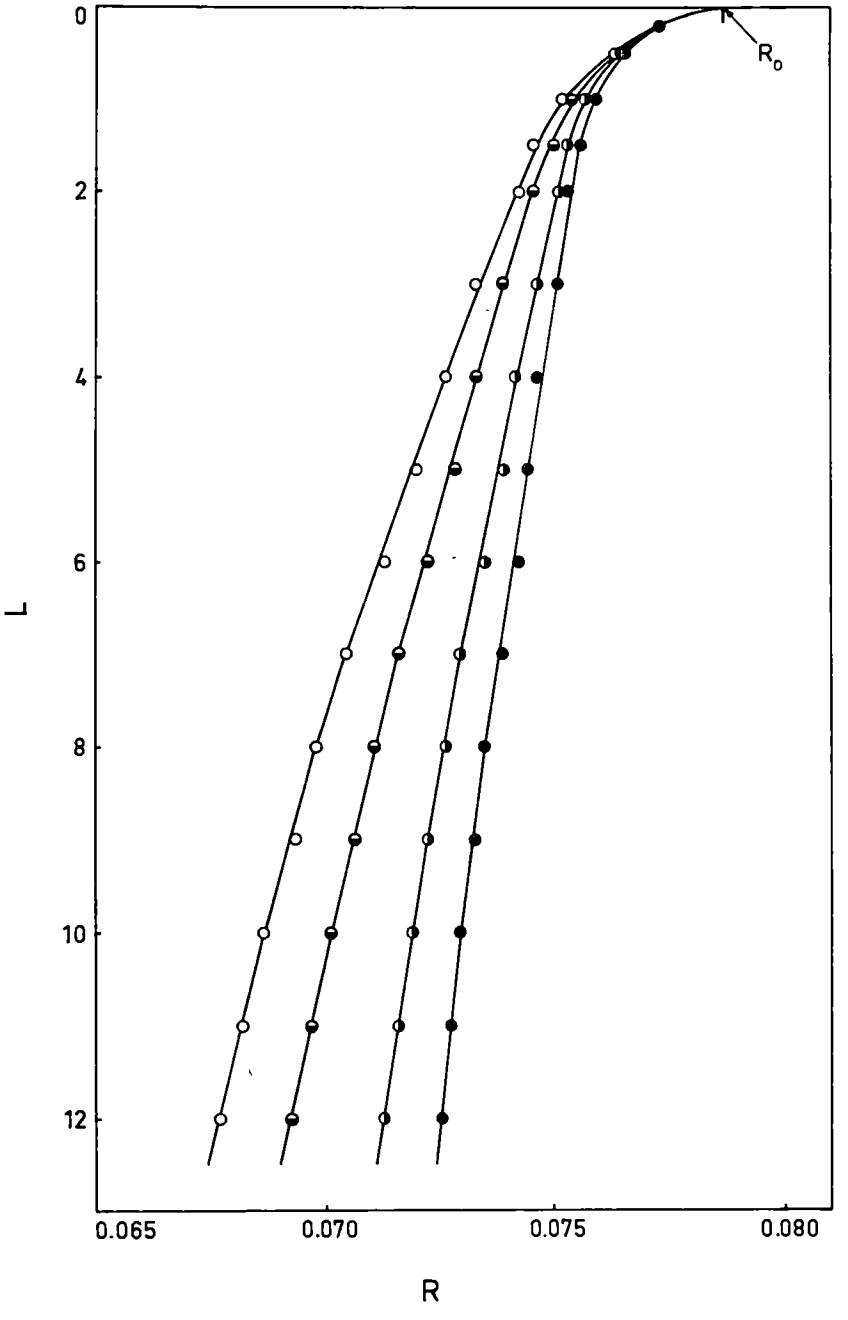
0
2
4
6
8
10
12
L
0.065
0.070
0.075
0.080
R
R_0

into the 'rollers' and a microscopic examination showed that they were in very lazy flow. Because of this and their very small size, it was considered that, while they would have a negligible effect on the absorption characteristics of the jets, little significance could be attached to the apparent independence of flow rate of the calculated boundary layer thicknesses. On the other hand, the near constancy of these estimates for lengths of 1.5 cm or more was taken to confirm the previous conclusion that the jets were accelerating uniformly with flat velocity profiles after 1.5 cm of travel.

That the boundary layer thicknesses were greater than those calculated for the plastic nozzles was attributed to the less precise construction of the glass nozzle. Nevertheless the jets were considered suitable for the absorption studies and this was subsequently confirmed by the absorption results obtained.

6.3 CORRECTION FACTORS FOR ABSORPTION RATES

For reasons given in Section 8.1, all absorption measurements obtained in this investigation were for jet flows between 3.4 and 3.6 cc/sec. To simplify the subsequent calculations, all the necessary parameters were estimated for a flow of 3.50 cc/sec and it can be shown (e.g. Tables 6.5 to 6.7) that this introduced negligible errors.

As a first step in the interpretation of the measurements, a relationship was established between absorption rates for non-ideal jets and those that would be obtained with an ideal jet. This allowed measured absorption rates to be corrected to values that

would have been obtained if the jet used had been ideal. Equations (5.1) to (5.4) could then be used to analyse the data. The required correction factors were estimated as follows.

The relevant jet parameters were calculated and are shown in Table 6.8.

TABLE 6.8 JET PARAMETERS

Parameter	Value	Reference
Q (cc/sec)	3.50	-
D_o (cm)	0.1574	Table 4.8
b	0.148	Table 4.11
$V_{o,av}$ (cm/sec)	180	$V_{o,av} = 4Q/\pi D_o^2$
$V_{o,c}$ (cm/sec)	203	Equation (A.4.10)
ν (cm^2/sec)	0.0101	Water at 20°C
ℓ (cm)	0.127	Equation (A.4.7)

Values of X were chosen arbitrarily and values of F_a were calculated using equation (A.4.15). A graphical procedure was used to estimate the constant B in equation (A.4.17) (see Graph 6.5) as $0.096[16\ell D V_{o,c}]$ and values of F_b were calculated using equations (A.4.16) and (A.4.17). Corresponding values of F_j were then calculated from equation (A.4.14). The results are given in Table 6.9 in the groups in which they were subsequently used in a numerical integration procedure. This procedure, for which an Elliott 503 Computer was used, required algebraic relationships between X and F_j and between X and D. These were established, again with the aid

Graph 6.5

Graph 6.5

Evaluation of The Constant F_b in Hydronamic Analysis

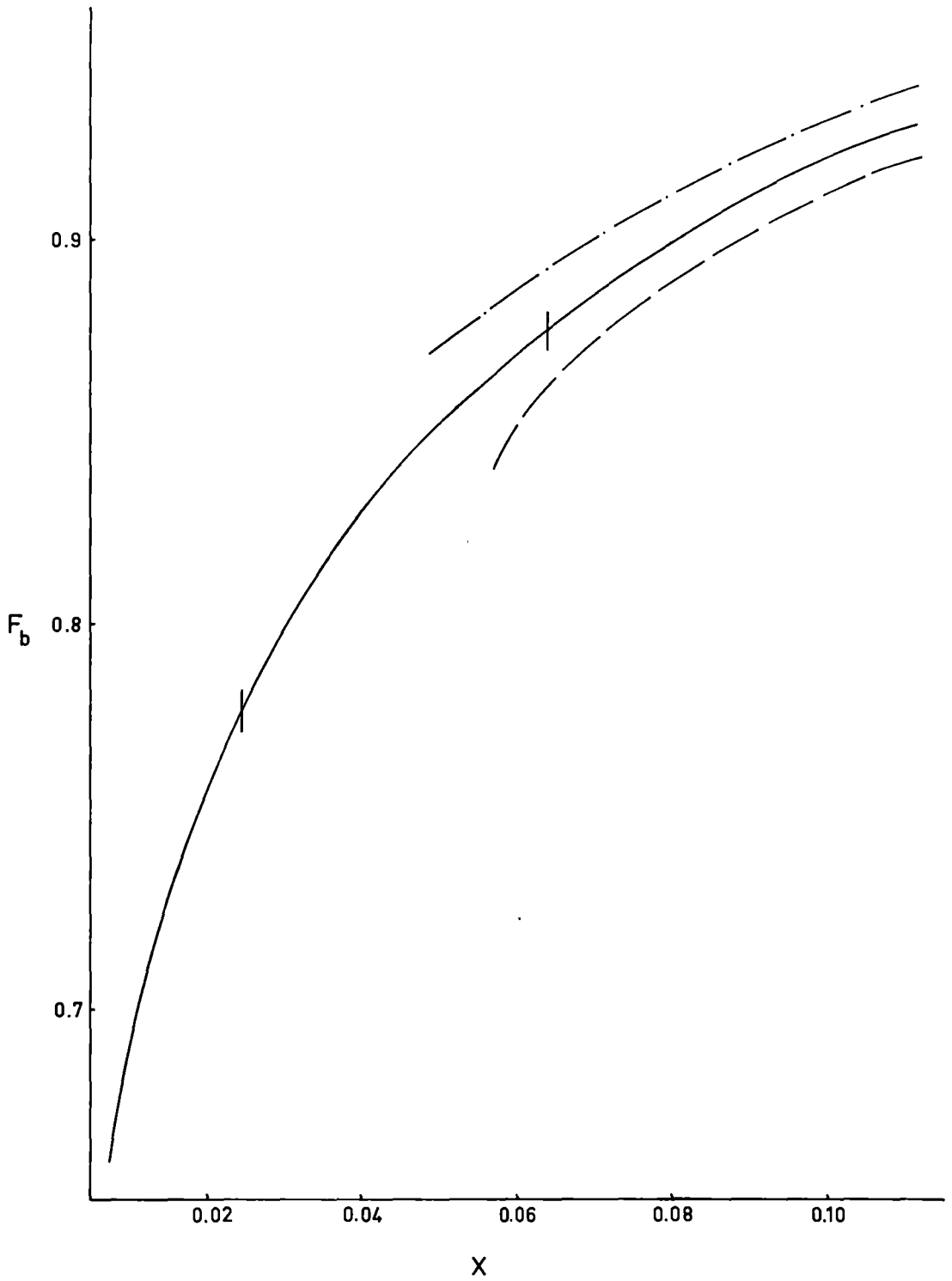
0.9
0.8
0.7
F_b
0.02
0.04
0.06
0.08
0.10
X

TABLE 6.9 CALCULATED VALUES OF F_a, F_b and F_j

X	F_a	F_b	F_j	X	F_a	F_b	F_j
	Group 1				Group 4		
0	1.000	0	0	0.5360	1.011	1.008	1.019
0.0013	1.000	0.343	0.343	1.072	1.022	1.024	1.046
0.0053	1.000	0.628	0.628	1.607	1.033	1.030	1.063
0.0107	1.000	0.697	0.697	2.143	1.044	1.033	1.077
0.0161	1.000	0.736	0.736	2.679	1.054	1.034	1.088
0.0214	1.000	0.763	0.763		Group 5		
0.0241	1.000	0.775	0.775	2.679	1.054	1.034	1.088
	Group 2			3.500	1.069	1.035	1.104
0.0241	1.000	0.775	0.775	4.500	1.087	1.036	1.123
0.0247	1.000	0.777	0.777	5.358	1.102	1.037	1.139
0.0643	1.001	0.872	0.873	6.500	1.122	1.037	1.159
0.0804	1.002	0.890	0.892		Group 6		
0.1071	1.002	0.914	0.916	6.500	1.122	1.037	1.159
	Group 3			7.000	1.130	1.037	1.167
0.1071	1.002	0.914	0.916	8.000	1.147	1.037	1.184
0.1607	1.003	0.947	0.950	9.000	1.162	1.037	1.199
0.2143	1.005	0.966	0.971	10.000	1.178	1.038	1.216
0.2679	1.006	0.977	0.983	11.000	1.193	1.038	1.231
0.5360	1.011	1.008	1.019	12.000	1.208	1.038	1.246

of the Elliott Computer (Appendix 6: Algol Program 'Chebfit'), by a technique [264] in which a smooth curve is fitted to the data. The equation to this curve is an n-degree polynomial in which the coefficients are calculated by minimizing the differences between input and calculated values of the independent variable. The maximum value of n is two less than the number of inpoint data points.

From equations (5.2) and (A.4.14), by identifying V_{id} with $V_{o,av}$, we get

$$N_X = (C_o - C_L)\left[\frac{\mathcal{D}.\ V_{o,av}}{\pi X}\right]^{\frac{1}{2}} F_j \qquad (6.4)$$

From equation (5.1)

$$\Phi = (C_o - C_L)[\pi \mathcal{D} V_{o,av}]^{\frac{1}{2}} \int_{X=X_1}^{X=X_2} D(X).F_j(X).X^{-\frac{1}{2}}dX \qquad (6.5)$$

and by comparison with equation (5.3)

$$\frac{\Phi_{id}}{\Phi} = F_h = \frac{2X_2^{\frac{1}{2}} D_o}{\int_{X=X_1}^{X=X_2} D(X).F_j(X).X^{-\frac{1}{2}}dX} \qquad (6.6)$$

The integral in equation (6.6) was evaluated numerically (Appendix 6) using Simpson's Rule with intervals in X of 0.0001 cm. The results are given in Table 6.10. Values of F_h were plotted against $X^{\frac{1}{2}}$ (Graph 6.6) and values of F_h required in the analysis of absorption data were interpolated from this curve.

Identification of V_{id} with $V_{o,av}$ is consistent with the derivation

Graph 6.6

Graph 6.6

Evaluation of The Constant F_h in Hydronamic Analysis

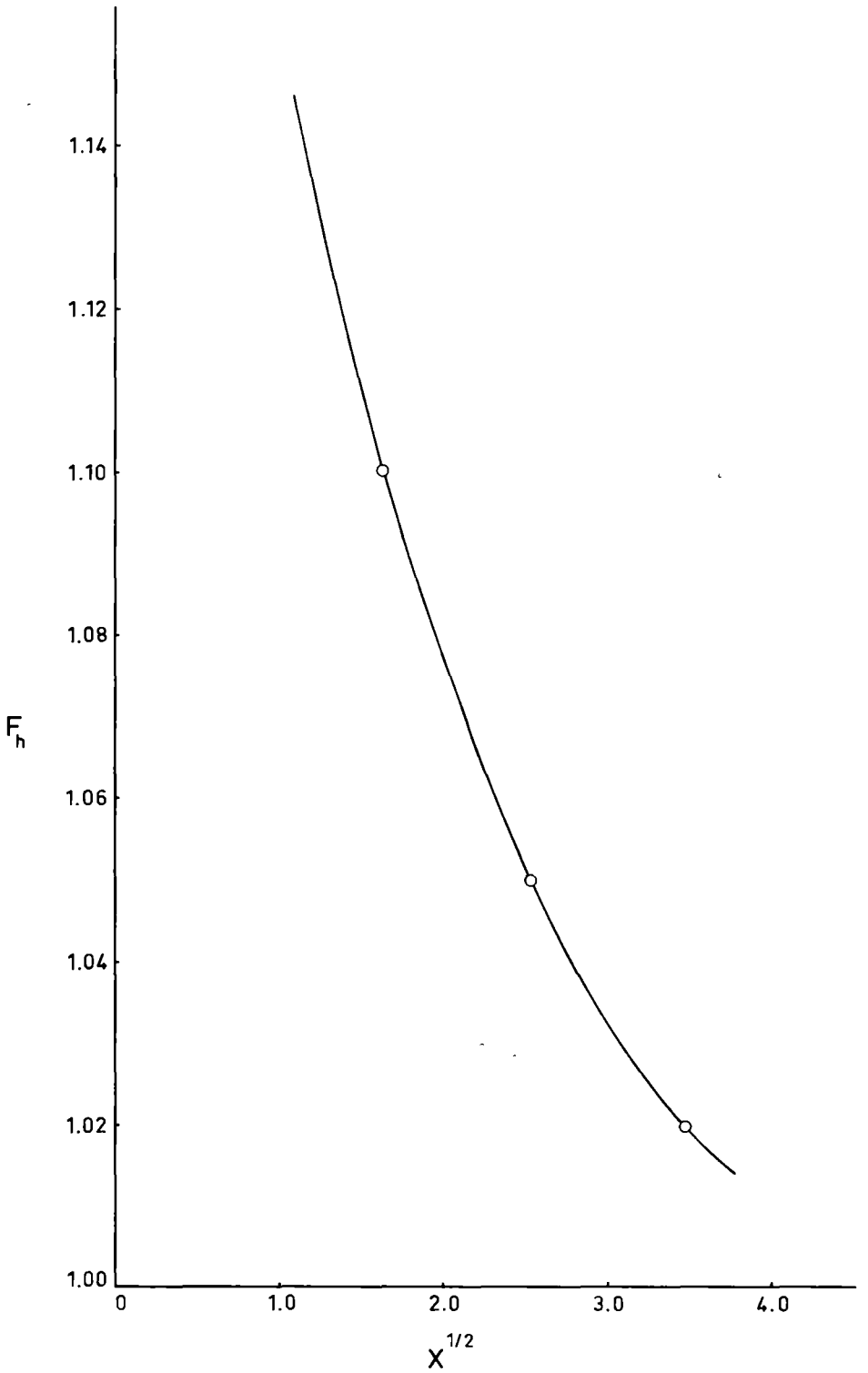
1.14
1.12
1.10
1.08
1.06
1.04
1.02
1.00
F_h
0
1.0
2.0
3.0
4.0
$X^{1/2}$

of equation (A.4.12). However, it should be noted that in similar calculations Scriven and Pigford [8,9,244] estimated V_{id} from the relationships

$$V_{id} = V_X - 2a_j X^{\frac{1}{2}} \tag{6.7}$$

and

$$V_X = 4Q/\pi D_X^2 \tag{6.8}$$

TABLE 6.10 CALCULATED VALUES OF F_h

X_1	X_2	$X_2^{\frac{1}{2}}$	$2X_2^{\frac{1}{2}}D_o$	$\int$	$\Sigma\int$	$F_h = \Phi_{id}/\Phi$
0	0.0241	0.1552	0.0489	0.0259	0.0259	1.888
0.0241	0.1071	0.3273	0.1030	0.0461	0.0720	1.431
0.1071	0.5360	0.7321	0.2305	0.1217	0.1937	1.190
0.5360	2.679	1.637	0.5153	0.2744	0.4681	1.101
2.679	6.500	2.550	0.8027	0.2961	0.7642	1.050
6.500	12.00	3.464	1.0905	0.3045	1.0687	1.020

where the D_X were real jet diameters downstream of the boundary layer disappearance and the V_{id} were taken as the average of several values. This procedure is not consistent with the derivation of equation (A.4.12) and gives higher values of F_h (for the present jet it gives a value for F_h at L = 12.00 of about 1.04). Scriven and Pigford would have obtained much better agreement between theory and experiment had they used the procedure given here.

CHAPTER 7 ABSORPTION MEASUREMENTS

7.1 PRINCIPLE OF MEASUREMENT

A schematic diagram of the absorption apparatus is shown in Figure 7.1. Liquid from a head tank was gravity fed at a constant rate to the jet nozzle mounted in an absorption chamber. The jet was caught cleanly and without gas entrainment at the bottom of the chamber and its length could be varied between 0 and 20 cm. Sulphur dioxide, either pure or mixed with nitrogen, was saturated with water vapour at the same temperature as the jet and passed through the chamber. The rates of flow of sulphur dioxide entering, nitrogen entering, and total gas leaving, were measured accurately for each jet length used and the absorption rate corresponding to each length was calculated on the assumption of negligible nitrogen absorption. Absorption rates measured in this way were shown to be more reliable than those based on chemical analysis of the liquid leaving the chamber.

7.2 DESCRIPTION OF APPARATUS

7.2.1 ABSORPTION CHAMBER

Plate 7.1 is a photograph of the absorption chamber and its mountings and a side view is sketched in Figure 7.2. Details of more important sections are shown in Figure 7.3. The chamber was made from a 9 inch length of 3 inch O.D., 8 gauge brass tube which was closed at the top by a flat piece of 1/4 inch brass plate and at the bottom by a dish-shaped piece of 1/4 inch perspex.

Figure 7.1

Figure 7.1

Absorption Equipment: Schematic

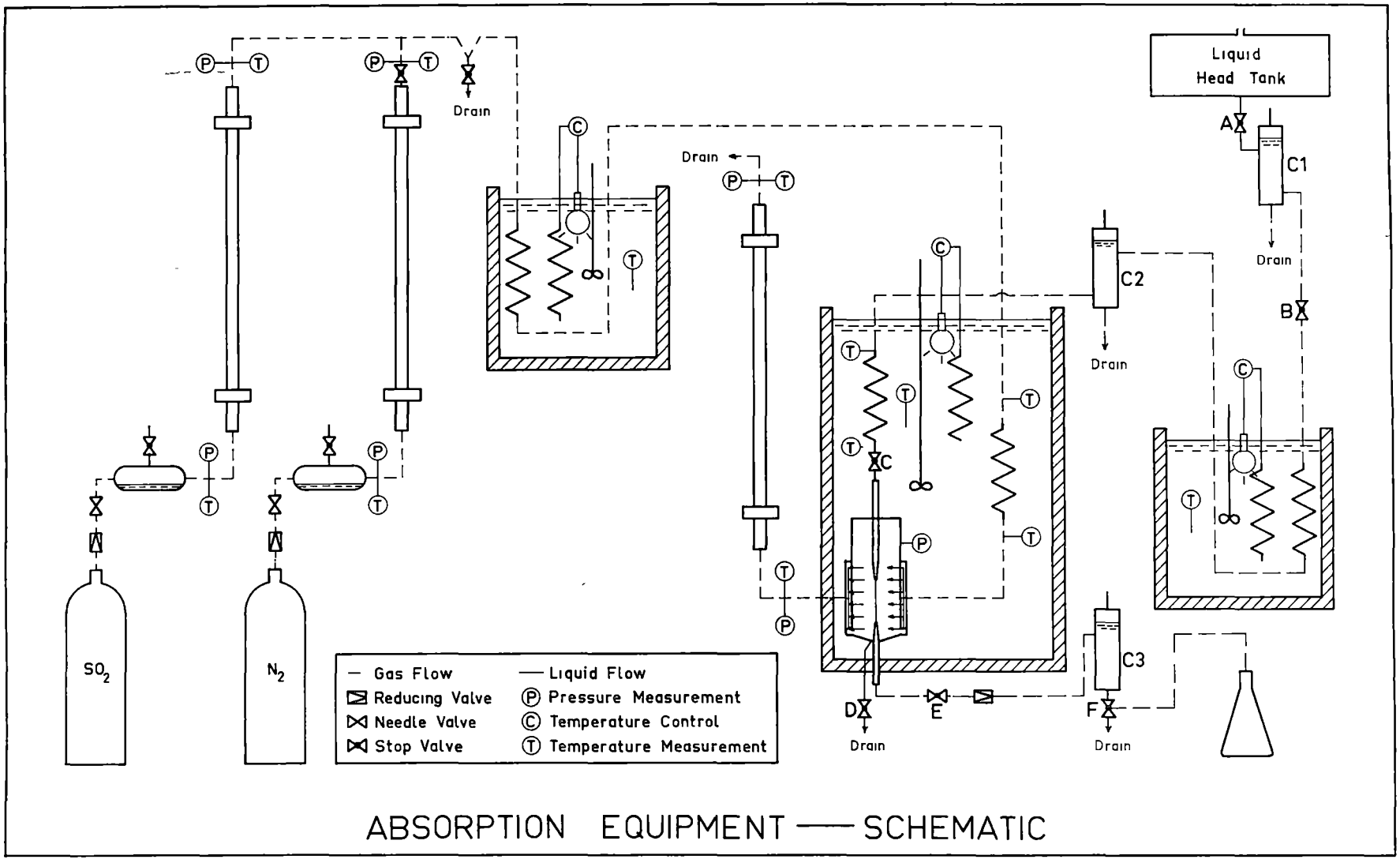

ABSORPTION EQUIPMENT — SCHEMATIC

Plate 7.1

Plate 7.1

Absorption Chamber and Mountings

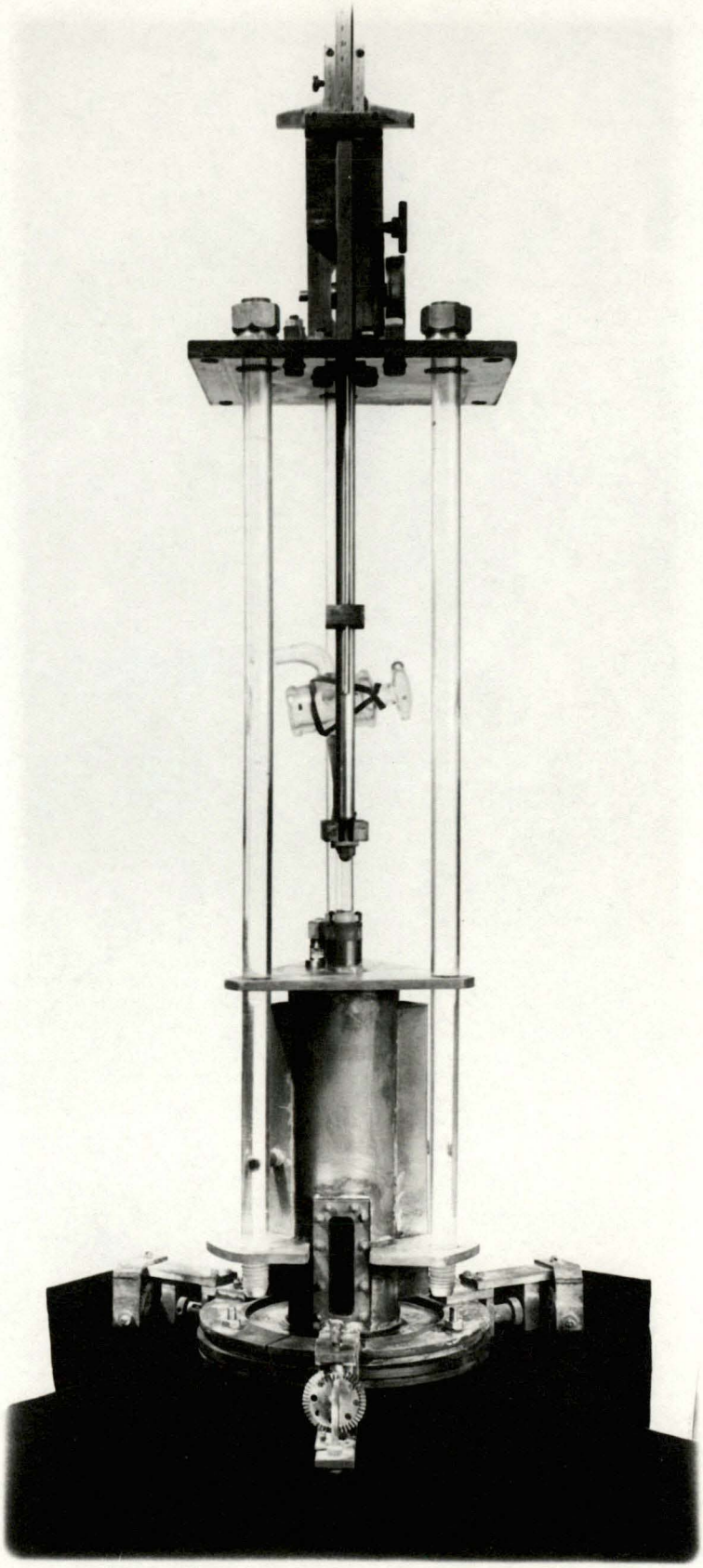

Figure 7.2

Figure 7.2

Absorption Chamber and Mountings

(a) Vernier Scale

(b) Brass Mounting

(c) Locking Pin

(d) Rack and Pinion

(e) Brass Adjusting Nuts

(f) 1 inch dia. Perspex Rods

(g) Rubber Cushion

(h) Manometer Connection

(j) Chamber Top - 1/4 inch Brass Plate

(k) Chamber Body - 3 inch O.D., 8 gauge Brass Tube

(l) Jet Nozzle

(m) Gas Inlet

(n) Laminar Jet

(o) Window

(p) Gear Trains

(q) Jet Receiver

(r) Bottom of Thermostat Bath

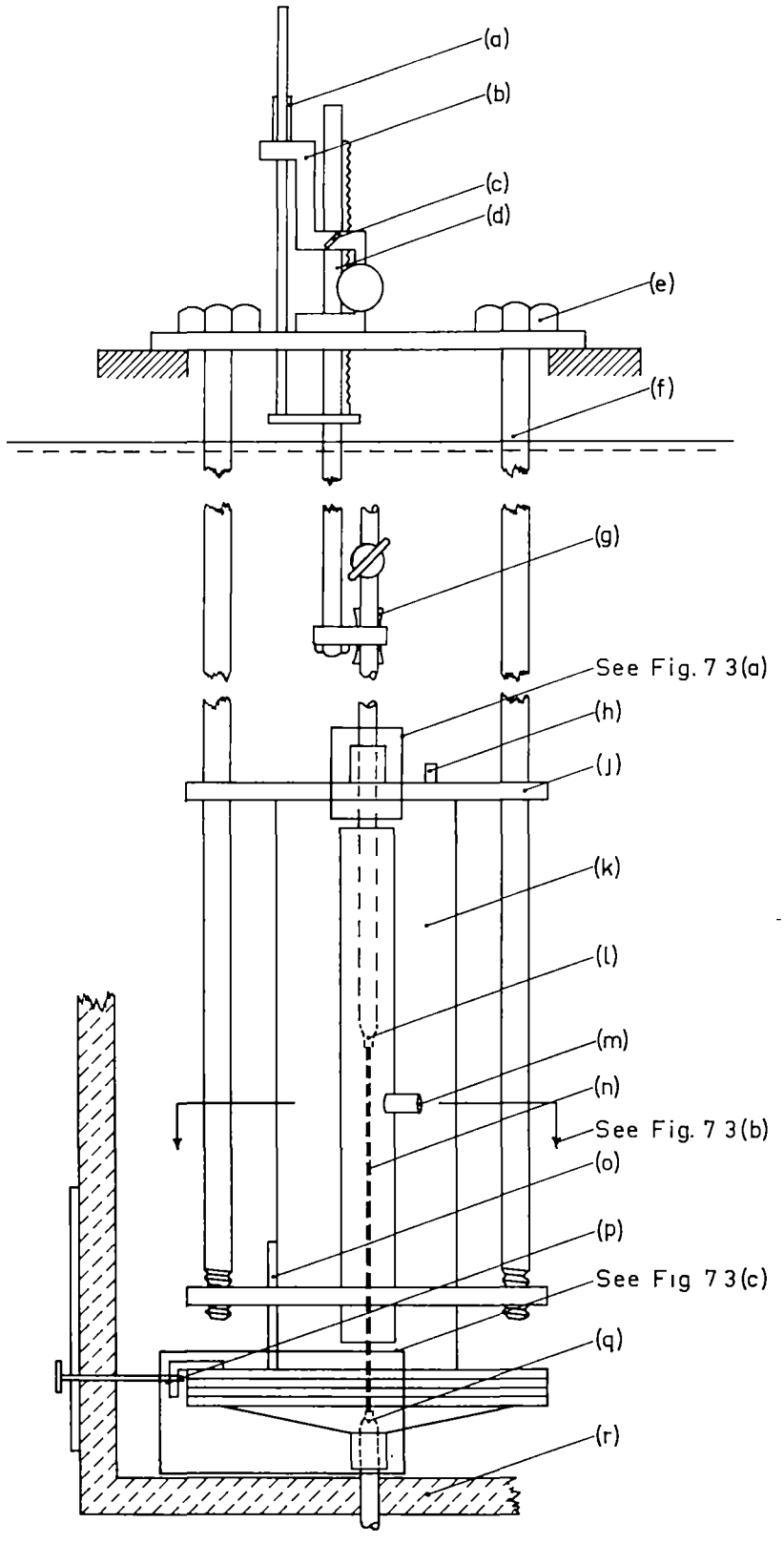

ABSORPTION CHAMBER AND MOUNTINGS

Figure 7.3

Figure 7.3

Absorption Chamber Details

Fig. 7.3 (a): Nozzle Mounting

(a) Brass Containing Srews (3)

(b) Nozzle

(c) Brass Cap

(d) '0' Ring

(e) Brass Mounting

(f) Chamber Top

(g) '0' Ring

(h) Brass Containing Screws (3)

(j) Brass Cap

Fig. 7.3 (b): Section Through Chamber

(a) Perspex Rods

(b) Gas Outlet

(c) Deflector Plate

(d) Window

(e) Nozzle

(f) Deflector Plate

(g) Gas Inlet

Fig. 7.3 (c): Chamber Bottom

(a) Chamber Body

(b) From Gear Trains

(c) '0' Ring

(d) Jet Receiver

(e) Perspex Bottom and Receiver Holder

(f) Annular Groove for Liquid Spill-Over

(g) Liquid Spill-Over Outlet

(h) I.C.I. Tensol 6 Cement

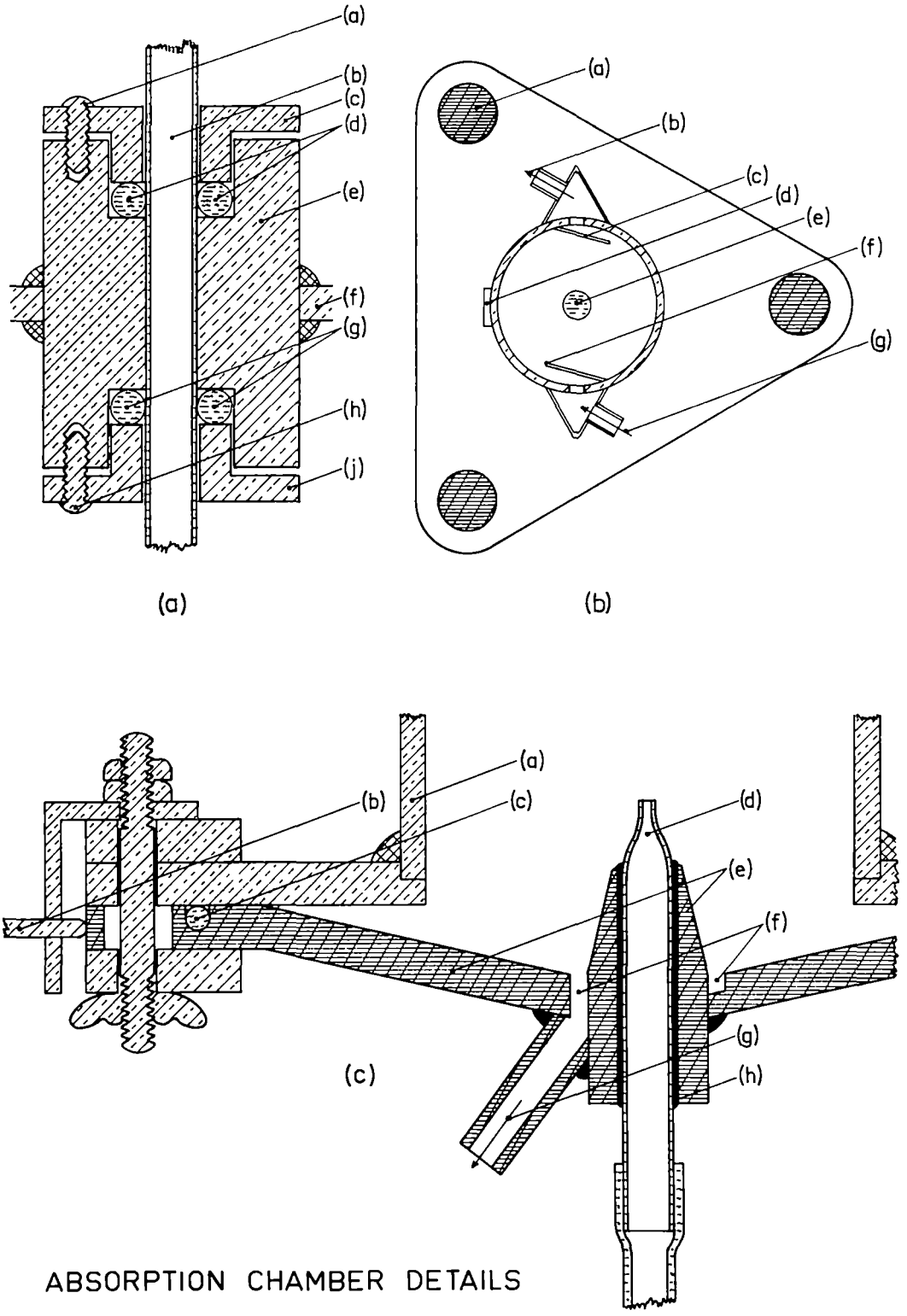

ABSORPTION CHAMBER DETAILS

The jet nozzle was mounted with a free-sliding, gas-tight fit through two 'O' rings in the top of the chamber (Figure 7.3, Section 'A'). Small adjustments in the alignment of the nozzle could be made by varying the tensions of the 'O' ring containing screws. The jet receiver (Figure 7.3, Section 'B') was cut from a glass nozzle which had been ground to give an opening of 0.16 cm and was cemented into the bottom of the chamber. By using this shape of receiver, instead of a cylindrical throat (capillary tube), the probability of gas entrainment during small variations in jet flow was substantially reduced. Preliminary investigations with the plastic nozzles had shown that, for jet lengths greater than 15 cm, catching the jet was made increasingly difficult by small disturbances in the gas phase. This is demonstrated in Plate 6.1 (c) which shows conditions at the receiver for a 15 cm jet and in Plate 6.1 (d) which is a similar photograph for an 18 cm jet. It was initially decided to limit the maximum jet length to 15 cm but it was subsequently found necessary (Section 8.1) to reduce this even further. Three probes, 120° apart, were mounted through gear trains around the bottom of the chamber. These could be operated outside the water bath and allowed fine adjustment to be made to the position of the chamber bottom and hence to that of the receiver. Any liquid spilled from the receiver during start-up was drained through a small sloping anular groove at the base of the receiver.

A rack and pinion assembly was clamped to the nozzle through a rubber cushion and was used to vary the height of the nozzle. After the nozzle had been set at a pre-determined height it was fixed in

position by a small locking pin. A depth gauge with a vernier scale was mounted on the rack and allowed jet lengths to be measured to ±0.005 cm. Some difficulty was experienced with slipping of the rubber cushion but it was found that if jet lengths were progressively decreased during a run (i.e. the nozzle was only moved downwards) and if the zero setting was noted at the end of the run, then satisfactory results could be obtained. Small changes in the zero setting explain the slightly different jet lengths tabulated in Appendix 5.

Gas was admitted to the chamber through a 6" x 1/4" slit in its side and a deflector plate (Figure 7.3, Section 'C') directed the gas into a circular motion around the jet. This eliminated interference with the jet and allowed a rough estimation to be made of the gas flow pattern in the vicinity of the jet. This estimation was necessary only in the case of absorption from nitrogen mixtures. Gas left the chamber through a similar slit in its opposite side and the pressure in the chamber was measured by a mercury manometer.

The chamber and its associated equipment were suspended in the main water bath by three 1 inch diameter rods which were made of perspex to minimize changes in jet settings due to temperature changes in the bath. Adjustments to the lengths of these rods, together with adjustments to the alignment of the nozzle and to the position of the receiver, ensured that the jet fell vertically. The jet was considered to be vertical when it entered the receiver symmetrically for all combinations of length and flow rate.

The jet and receiver were illuminated by a 12 volt, 6 watt lamp placed beneath the chamber. Judicious placement of this lamp caused the light to strike the jet at such an angle that any perturbations of the jet surface were immediately apparent. Because of the critical nature of its flow, the jet was extremely sensitive to small disturbances and for this reason the bath was mounted on a steel frame, on a concrete floor, in the basement of the Chemistry Department building. Under these conditions the jet flowed smoothly and could be caught for prolonged periods of time without either spill-over or gas entrainment.

7.2.2 LIQUID FLOW

All solutions were prepared from distilled water and were gravity fed to the absorption chamber from a 60 litre head tank situated approximately 8 feet above the chamber. They were fed through 5/16 inch I.D. nylex tubing to an all-glass constant head device (Figure 7.4), through a pre-heating coil to another similar constant head device and finally through a heating coil in the main bath to the absorption chamber. Liquid left the chamber through the jet receiver and passed to a collector via an orifice restriction and a third constant head device.

Both heating coils consisted of 10 feet of 3/8 inch O.D. stainless steel tubing. The temperature of the pre-heating bath depended on the ambient temperature and was adjusted so that the temperature of liquid entering the main heating coil did not differ by more than 1°C from that of the main bath. In this way the

Figure 7.4

Figure 7.4

Constant Head Device - All Glass

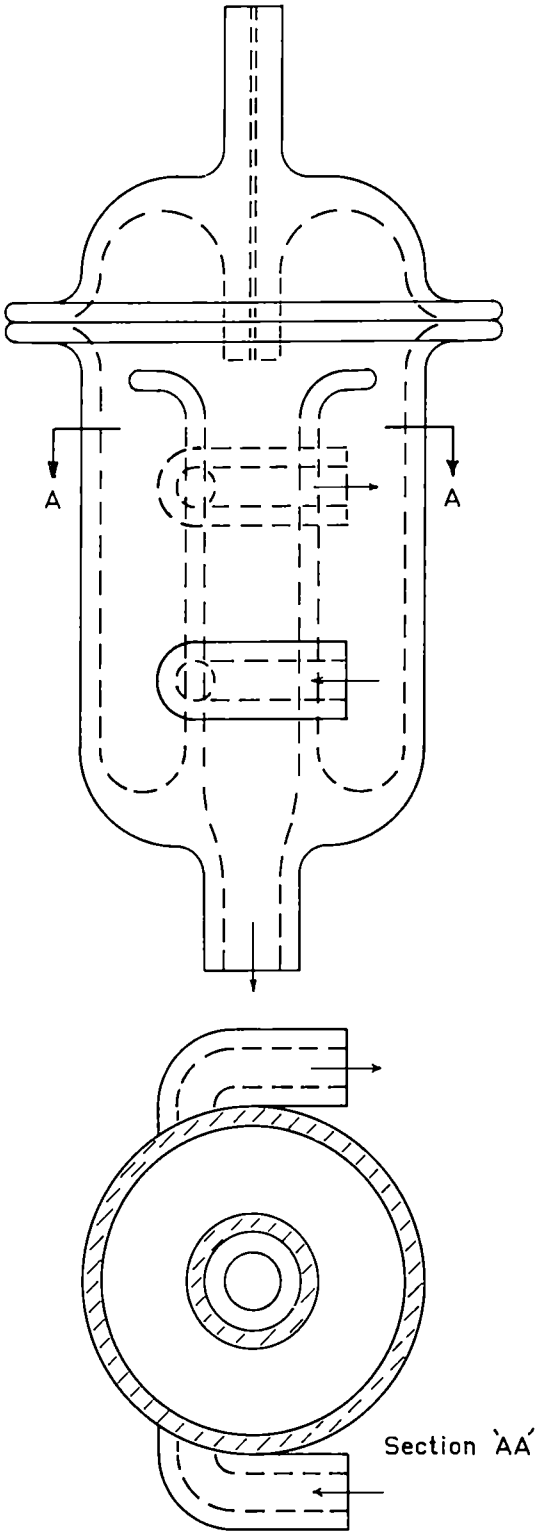

CONSTANT HEAD DEVICE

temperature of liquid flowing into the jet nozzle was maintained to within 0.2°C of that of the bath.

The three constant head devices were mounted on a vertical rack and their heights could be adjusted to within 0.02 cm. C2 was adjusted relative to the nozzle to maintain a constant jet flow and C1 was adjusted relative to C2 to maintain a constant flow through the pre-heating coil. The jet receiver operated most satisfactorily when the liquid surface in C3 was level with the top of the receiver and the orifice diameter was such that this occurred for jets of 6 to 7 cm. For other jet lengths, small adjustments were made to the height of C3. The liquid flow rate was measured by collecting the effluent from C3 in a calibrated 3 litre flask.

Preliminary measurements indicated that the rate of absorption of sulphur dioxide into water is not affected by any air dissolved in the water and this is not surprising in view of the relatively low solubility of air and the very slow rate of reaction between sulphur dioxide and oxygen [120-122]. However, it was observed that when aerated water contacted the nylex feed tubes, slow desorption of the air resulted in small bubbles adhering to the inside walls of the tubes and these affected measurements in two ways. Firstly, the amount of desorption increased during a run and caused a measurable decrease in flow rate. Secondly, bubbles occasionally broke free and disturbed the jet. Consequently all water used to prepare solutions was first de-aerated by stirring under vacuum for several hours.

7.2.3 GAS FLOW

Sulphur dioxide was stored in liquid form in steel cylinders and, before use, approximately 5 percent of the contents of each cylinder was purged to remove any non-condensible gases.

Gas, whose flow rate was coarsely adjusted by a pressure regulator and controlled by a small needle valve, flowed to the absorption chamber through a saturator, a flowmeter, a preheating coil and a further heating coil in the main bath. After leaving the chamber it passed to the atmosphere via another flowmeter. Both heating coils were made from 8 feet of 3/8 inch O.D. stainless steel tube and the temperature of the gas entering the chamber was again maintained to within 0.2°C of that of the main bath by controlling the preheating bath temperature.

The time required to obtain all the necessary measurements for a particular jet length was about 15 minutes and precautions were taken to ensure that, during this time, the rate of flow of gas to the absorption chamber did not vary by more than 0.2 percent. All connecting lines were of 5/16 inch nylex tubing and these, together with the perspex components in the absorption chamber, had a marked affinity for adsorbing sulphur dioxide. Hence, before each run, the equipment was purged for several days with gas of the same composition with which measurements were to be made. Variations in the sulphur dioxide pressure during a run were so small that this treatment reduced the adsorption effects to negligible proportions. The saturator, which was insulated with cotton wool and contained

approximately 300 ml of water, consisted of a 12 inch length of 3 inch I.D. glass tube lying on its side. The water was saturated with sulphur dioxide during the purging process. Any absorption or desorption from this solution during the required 15 or so minutes was small and its rate was essentially constant. Consequently there was no measurable change in the rate of flow of gas leaving the saturator.

It was expected that, under the conditions of the absorption experiments, it would be necessary to measure mass rates of gas flow with a precision of ±0.5 percent. This was accomplished by using volumetric flow meters and by carefully measuring the temperatures and pressures of the gases entering and leaving the meters.

The meters (Figure 7.5) were constructed from 100 ml burettes and were used to measure the time required for a soap film to move between two fixed points in the burette. A photo-electric cell (OCP 71) was mounted at each fixed point and a 2.2 volt, 25 amp, pre-focussed lamp was placed directly opposite each cell (Figure 7.5). When the film interrupted the light beam at the first point, a switching circuit (Figure 7.6) started a 50 cps pulse counter (scaler) and this was switched off when the film reached the second point. The meters were calibrated by passing air through them at a constant rate and measuring this rate by displacement with water. The pressure drop across the film was negligible and it was found that, if the film was formed evenly and the time between formation of successive films was carefully regulated, volumetric flow rates

Figure 7.5

Figure 7.5

Gas Flowmeter

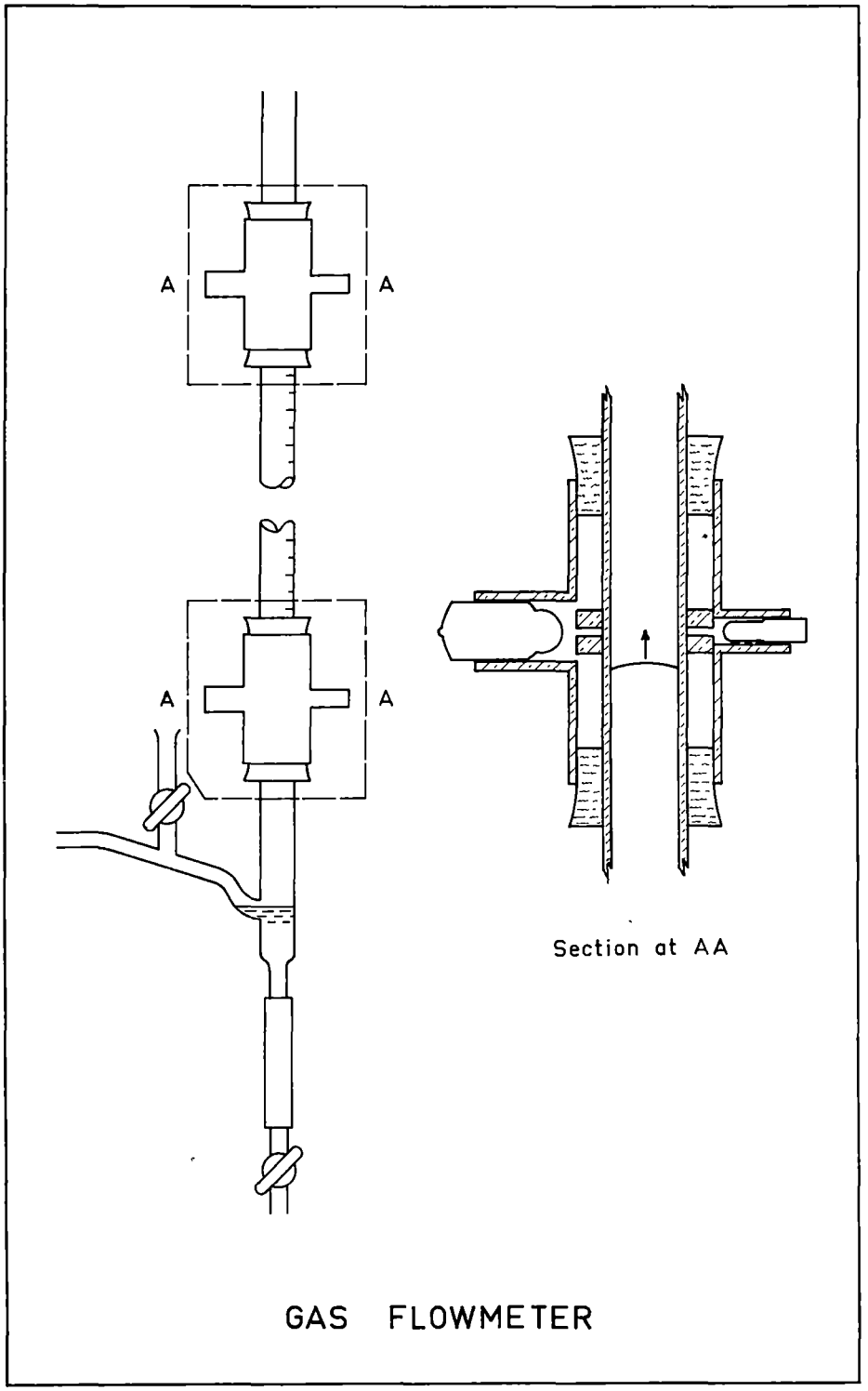
A
A
A
A
Section at AA
GAS FLOWMETER

Figure 7.6

Figure 7.6

Gas Flowmeter: Circuit Diagram

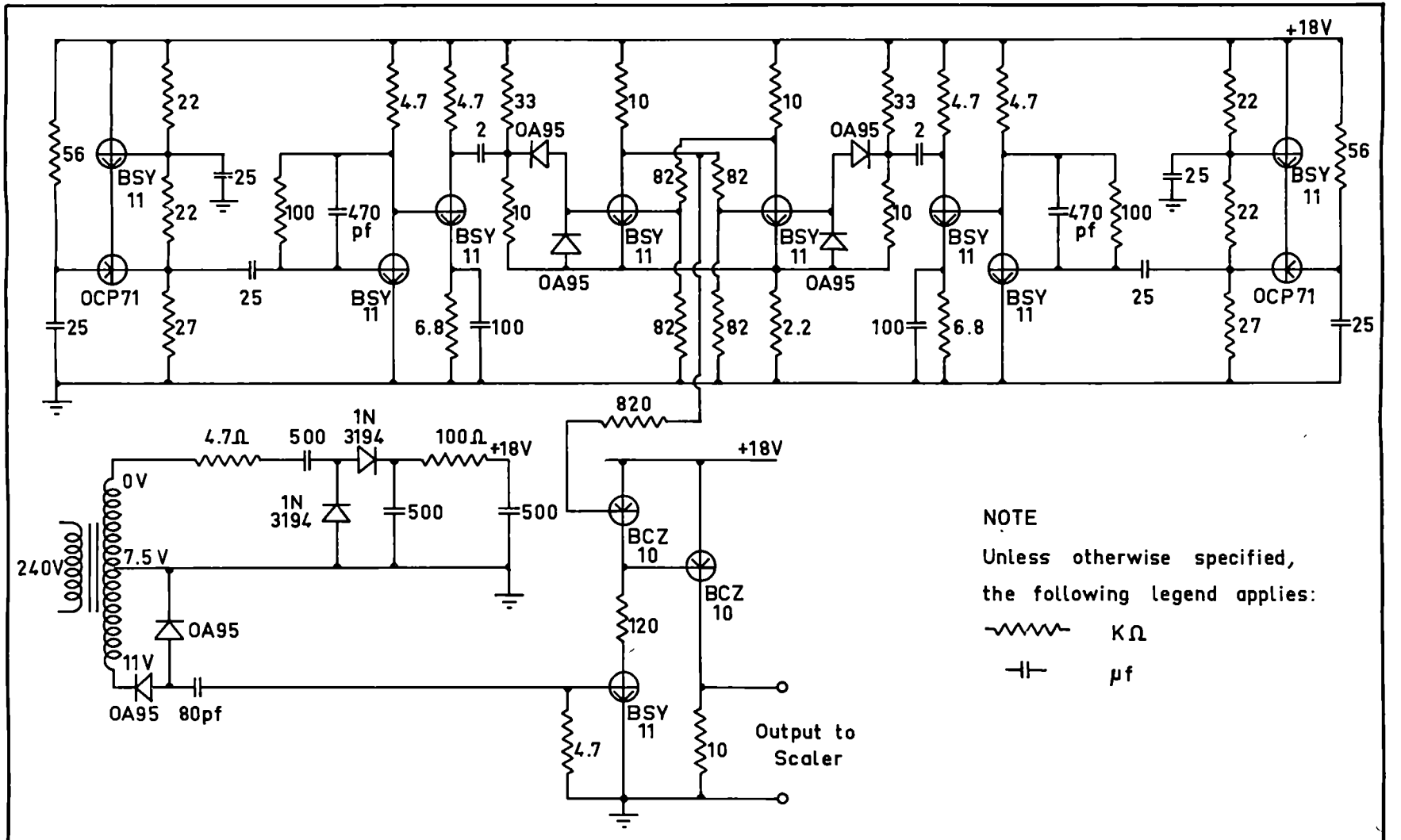

GAS FLOWMETER CIRCUIT DIAGRAM

in the range 1 to 15 cc/sec could be measured to within 0.2 percent.

For use with sulphur dioxide in the absorption measurements, a 5 percent v/v solution of sodium linear-alkylbenzene sulphonate (50% active) in water with 1 percent v/v of glycerol gave a stable film. This solution was saturated with sulphur dioxide during purging and any absorption or desorption was again shown to introduce negligible errors. The temperature of gas entering a meter during these measurements never differed by more than 2°C from that of gas leaving and the average for any meter never differed by more than 3°C from the temperature in the absorption chamber. It was estimated that the mass rates of flow calculated from these averages had the required maximum error of 0.5 percent.

7.2.4 TEMPERATURE MEASUREMENT

The choice of a method of temperature measurement was influenced by accuracy and ease and speed of measurement and by the geometry of the equipment in which it was required to obtain measurements. Three measuring devices were considered (resistance thermometer, thermocouple and thermistor) and the final choice of thermistors was determined by the availability of suitable ancillary equipment.

Several types of thermistor were tested and that considered most suitable was an S.T.C. Type F14 supplied by S.T.C. Ltd. of Sydney. Figure 7.7 shows the construction of these thermistors which, for protection during use, were mounted as shown in Figure 7.8. A 2 kilocycle A.C. bridge, incorporating constantan decade resistances of range 0 to 100 K ohms, was used to measure resistances.

Figure 7.7

Figure 7.8

Figure 7.7

S.T.C. Type F14 Thermistor

(a) Sensing Element

(b) Pt Wire

(c) CuNiFe Leads

(d) Glass Bead

(e) CuNiFe Leads

Figure 7.8

Thermistor Mounting

(a) Rubber Cork

(b) Rigid P.V.C. Tube

(c) Flexible Nylex Tube

(d) Thermistor

(e) Flexible Nylex Tube

(f) Insulated CuNiFe Leads

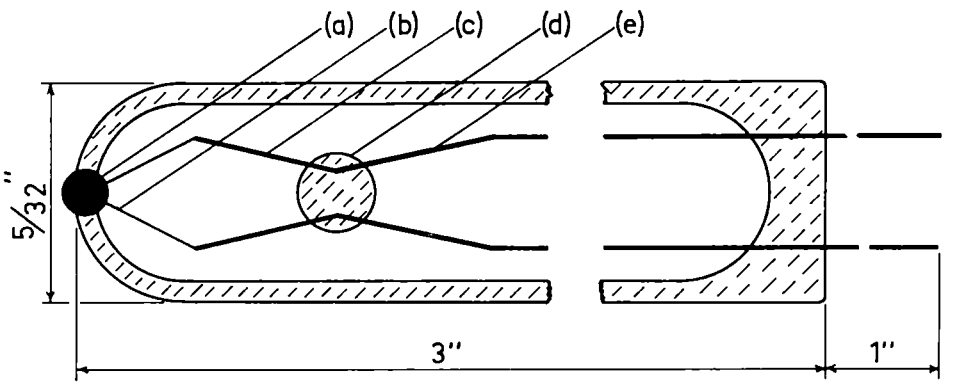

S.T.C. TYPE F14 THERMISTOR

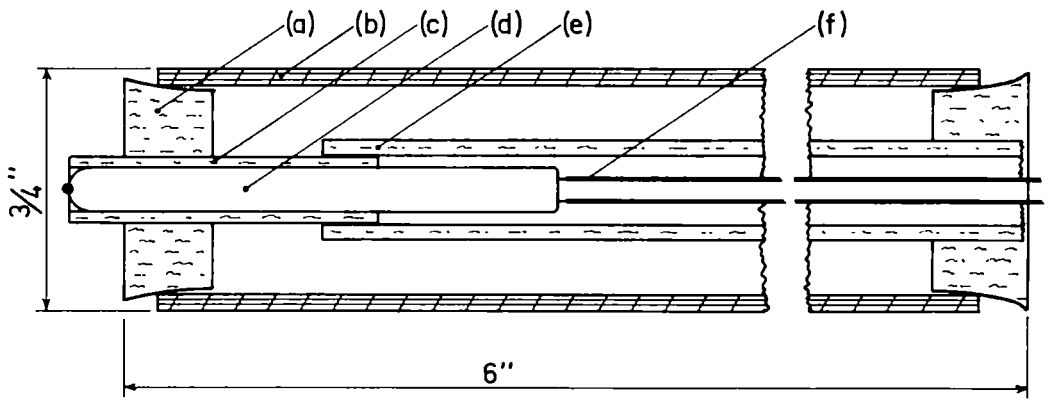

THERMISTOR MOUNTING

The nominal resistance of a Type F14 thermistor is 10,000 ohms at 20°C with a corresponding temperature coefficient of 400 ohms per °C. Errors in measurement caused by variations in ambient temperature were consequently negligible.

As bought from the manufacturers the thermistors exhibited instability, their resistances increasing by an average of approximately 1.5 ohms per day. However, preliminary tests showed that artificial aging (holding at 100°C for prolonged periods of time) gave increased stability and that a minimum aging time of 1000 hours should give acceptable stability. After aging for 1500 hours, fifteen thermistors were held for 28 days in a water bath in which the temperature was maintained at a constant 20 ± 0.05°C. For each thermistor, all resistances measured during this time were within 3 ohms of the mean value. The slope of the line of best fit (calculated by the method of least squares) to a plot of resistance versus time was not significantly different from zero. The thermistors were consequently considered to be stable and this was verified by the fact that, after completing the absorption measurements, further tests revealed no significant changes in resistance.

All thermistors were calibrated against a mercury in glass thermometer which had been calibrated by The National Physics Laboratory, England and which could be read to within ±0.02°C.

7.2.5 TEMPERATURE CONTROL

The thermostats used to control all water bath temperatures included a toluene-mercury regulator, an electronic relay and a 200

watt light globe used as a heating element. The regulators consisted of a glass head mounted on a copper coil and their method of operation is obvious from Figure 7.9. The coil, made from 8 feet of 1/2 inch O.D. copper tube, contained approximately 200 ml of toluene and the regulators responded to temperature changes of less than 0.01°C. However, the precision of control depended on the efficiency with which the baths were stirred. Tests using a thermistor probe showed that, with the stirring methods used, the temperature at any point in a bath never changed by more than 0.05°C.

7.3 EXPERIMENTAL METHOD

7.3.1 TYPES OF MEASUREMENT

The different types of measurement that were made are listed in Table 7.1.

7.3.2 ANALYSIS OF SOLUTIONS

All solutions were prepared in the head tank and analysed before use. As a check on the uniformity of mixing, samples were taken from three different locations in the tank and, in the case of the aqueous sulphur dioxide solution, were withdrawn through rubber sealing caps with a 2 ml, calibrated hypodermic syringe. Volumetric methods were used and the analyses were carried out in A-grade, calibrated equipment. The analytical methods used were as follows:

(i) Aqueous Sodium Chloride. Excess silver nitrate was added to the acidified (HNO_3) sample. Nitrobenzene was used as a coagulant and the residual silver nitrate was titrated with ammonium thiocyanate using ferric alum as an indicator. The primary standard was A.R.

Figure 7.9

Figure 7.9

Thermostat Head

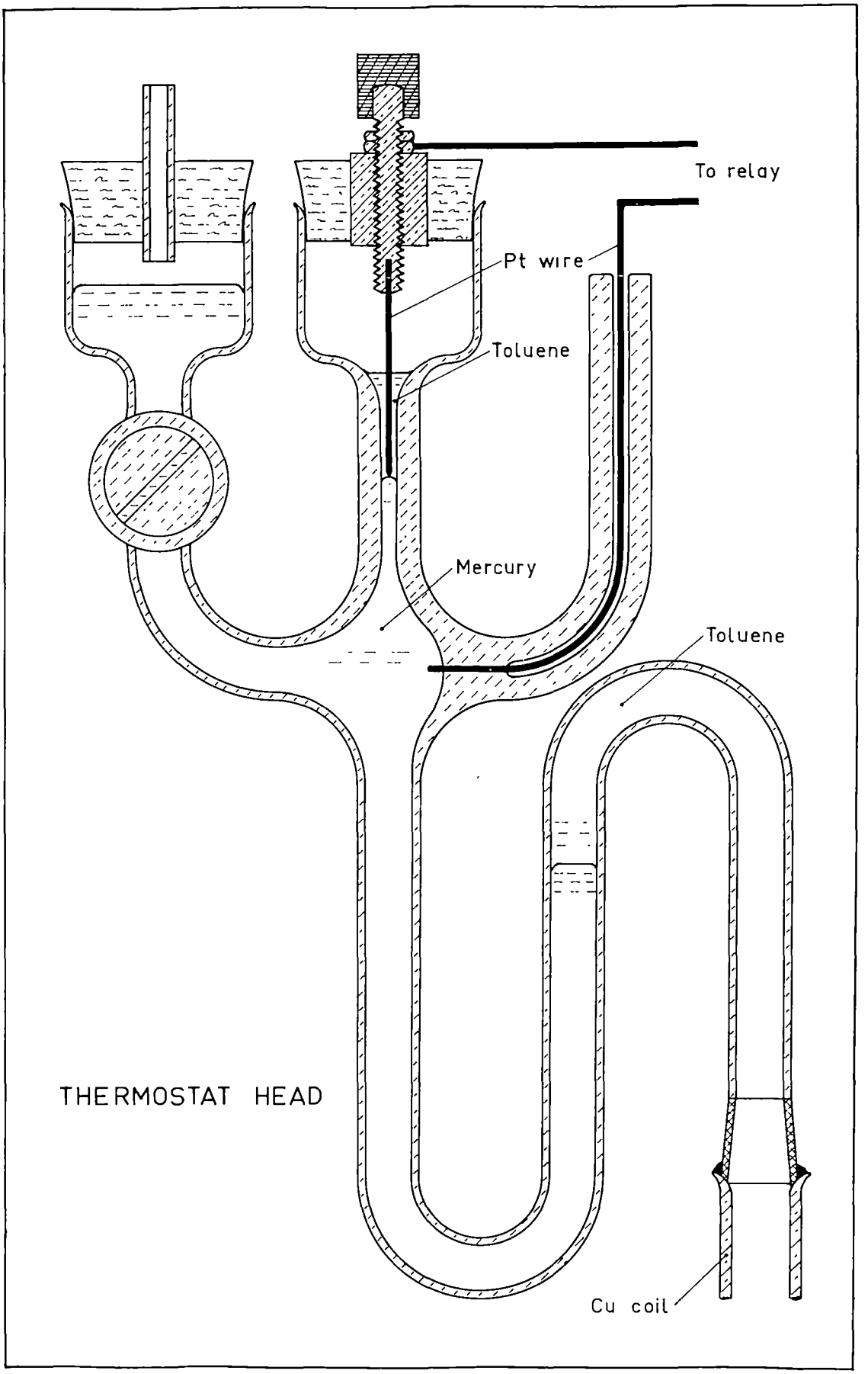
To relay
Pt wire
Toluene
Mercury
Toluene
THERMOSTAT HEAD
Cu coil

TABLE 7.1 CONDITIONS OF ABSORPTION MEASUREMENTS

Gas	Solution	Temperature (°C)
SO_2	Water	20
SO_2	1.053 M aq. NaCl	20
SO_2	0.028 M aq. HCl	20
SO_2	0.113 M aq. HCl	20
SO_2	0.481 M aq. HCl	20
SO_2	1.100 M aq. HCl	20
SO_2	0.735 M aq. SO_2	20
SO_2	0.287 M aq. NaOH	20
SO_2	0.472 M aq. NaOH	20
80% SO_2 in N_2	Water	20
60% SO_2 in N_2	Water	20

silver nitrate.

(ii) Aqueous Hydrochloric Acid and Sodium Hydroxide. A carbonate-free sodium hydroxide solution was prepared and standardized against A.R. potassium hydrogen phthalate using phenolphthalein indicator. Hydrochloric acid samples were titrated with sodium hydroxide with methyl orange indicator and sodium hydroxide samples were titrated directly with the potassium hydrogen phthalate.

(iii) Aqueous Sulphur Dioxide. A standard solution of A.R. potassium iodate was prepared. Solutions of iodine (in aqueous potassium iodide) and sodium thiosulphate were prepared and successively standardized. The samples were added to excess, acidified (HCl) iodine solution and the excess iodine was determined with the sodium thiosulphate using 'Thiodene' indicator.

All titrations were performed at least three times and the maximum difference between any two corresponding titres was about 0.3 percent.

7.3.3 OPERATING PROCEDURE

In the following description of procedure all notation refers to Figure 7.1.

(i) Cocks A to F were closed and the apparatus was purged with gas.

(ii) The main bath temperature was checked and the preheating bath temperatures were adjusted according to the ambient temperature.

(iii) The nozzle height was set to give a jet length of about 12 cm (Section 8.1); C1 and C2 were adjusted accordingly

and C3 was lowered as far as possible.

(iv) The head tank was placed in position.

(v) Cocks A to F were opened in the order A,B,F,E,D,C and the liquid feed system was thoroughly flushed with solution.

(vi) Cocks A to F were closed in the order C,D,E,F,B,A.

(vii) The expected absorption rate was estimated and the gas flow rate was adjusted so that the flow from the chamber during absorption would be about 1 cc/sec.

(viii) Cocks A to F were opened as in (v) and the position of C3 was adjusted to give a clean jet cut-off. Any liquid spill-over was allowed to drain from the chamber, cock D was closed and sufficient time was allowed for thermal equilibrium to be established.

(ix) The temperatures of gas and liquid to the chamber were measured.

(x) Volumetric gas flow rates and associated temperatures and pressures were measured and the absorption rate was calculated.

(xi) Cock F was adjusted and the liquid flow rate was measured. This required about 15 minutes and, during this time, constant checks were made to ensure that the jet flowed undisturbed and that the jet cut-off remained clean.

(xii) Steps (ix) and (x) were repeated and the two calculated absorption rates were compared. If these agreed within one percent, equilibrium was considered to have been established and the results were averaged. If the results differed by

more than one percent, steps (ix) and (x) were repeated until two successive results gave the required agreement.

(xiii) A different (smaller) jet length was selected and the positions of C1, C2 and C3 and the gas flow rate were adjusted accordingly.

(xiv) Steps (ix) and (x) were repeated until two successive measurements of the absorption rate, taken five minutes apart, again gave the required agreement.

(xv) Steps (xiii) and (xiv) were repeated until the jet length had been reduced to about 2.5 cm and eight to ten sets of measurements had been obtained.

(xvi) The liquid flow rate was again measured.

(xvii) Cocks C,F,E,B,A were closed in that order and the gas flow was turned off.

(xviii) The nozzle was carefully lowered until it just touched the receiver and this zero position was noted. Subsequent examination of the nozzle showed that this procedure did not damage the nozzle or significantly disturb the paraffin coating.

(xix) The head tank was removed and, if necessary, emptied and flushed with distilled water.

A run was considered to have been successful if

(a) the temperatures of gas and liquid to the absorption chamber had been maintained in the range 19.8 to 20.2°C;

(b) the two measured liquid flow rates agreed within 0.5

percent and

(c) no liquid spill-over or gas entrainment in the receiver had occurred.

The only run which presented any difficulty was that involving the aqueous sulphur dioxide solution. This arose because the nylex feed lines adsorbed sulphur dioxide from solution. Because of the limited volume of liquid available, continuous purging, as used for the gas lines, was not possible and the problem was solved as follows. A solution was prepared in the head tank and steps (i) to (vi) above were carried out. The liquid was held in the feed lines and the head tank was sealed to minimize desorption of gas. After several days the procedure was repeated and this was continued until the head tank was about half empty. A fresh solution, whose concentration was adjusted as closely as possible to that of the first, was prepared and was used to fill the feed lines once more. It was analysed immediately before the absorption measurements were commenced and, to minimize the effects of desorption while these measurements were being made, the number of jet lengths used was restricted to four. Because of the considerable time involved, absorption rates were measured for only one sulphur dioxide concentration but subsequent analysis of these measurements showed that this was sufficient to obtain the required information.

CHAPTER 8 ANALYSIS OF ABSORPTION MEASUREMENTS

8.1 INTRODUCTION

The results of all the absorption measurements are tabulated in Appendix 5 and the calculations made to analyse the data are shown in the accompanying 'typical calculations'.

It can be seen from the results that all measurements were restricted to jet flows of 3.4 to 3.6 cc/sec and the maximum jet length used was approximately 12.3 cm. These restrictions were necessary because at higher flows and longer lengths there was a marked tendency for turbulence to occur on the jet surface during absorption. When it did occur, the method of illuminating the jet made it immediately apparent. It could not be detected for the restricted conditions. The low flow rates used also had the advantage of conserving liquid feed.

That a laminar jet may become unstable during mass transfer is not surprising in view of the highly critical nature of the jet flow. Such instability does not appear to have been directly observed before, but Brian et al. [265] suggested that it may have occurred in their own and other jet experiments.

8.2 ABSORPTION INTO WATER

Results for the absorption of sulphur dioxide into water are shown in Graph 8.1 as a plot of Φ against $4(QL)^{\frac{1}{2}}$. For these and other results where a linear relationship was indicated, the straight line was fitted by the method of least squares. All

Graph 8.1

Graph 8.1

Absorption of Sulphur Dioxide into Water at 20°C

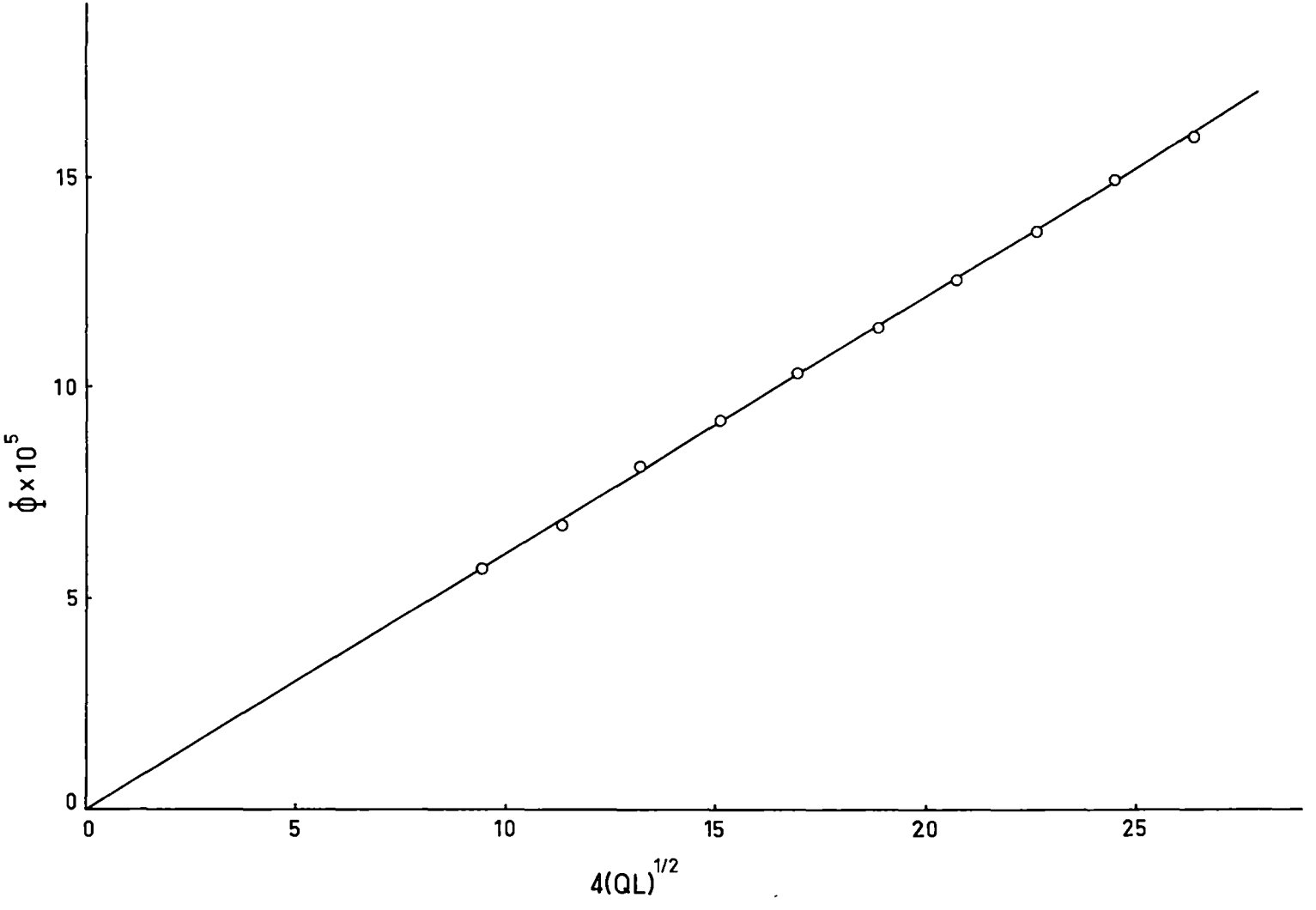
15
10
5
0
$\Phi \times 10^5$
0
5
10
15
20
25
$4(QL)^{1/2}$

calculations were performed with an Elliott 503 Computer using the Algol programme 'Curvefit' (Appendix 6).

The linear relationship agrees with the results of previous investigators [e.g. 7,19,106] and was taken to confirm the analysis of jet hydronamics. It can be interpreted in one of two ways.

(i) According to equation (5.4) it can be interpreted to mean that the absorption is a physical process and that the rate of ionization of sulphur dioxide in water is very slow compared with the rate of diffusion. This requires that any concentration dependence of $\mathcal{D}_u$ has a negligible influence on the absorption rate and means that the slope of the line is a measure of $C_{u,s}.\overline{\mathcal{D}}_u^{\frac{1}{2}}$. Values of this quantity, measured in this and other investigations, are compared in Table 8.1. In view of the difficulties in experimental techniques noted in Chapter 5, the agreement between results is rather surprising.

TABLE 8.1 MEASURED VALUES OF $C_{u,s}.\overline{\mathcal{D}}_u^{\frac{1}{2}}$

Investigator	Method	$C_{u,s}.\overline{\mathcal{D}}_u^{\frac{1}{2}}$ (moles/cm.sec) x 10^2
Lynn et al. [7]	W.W. Column	0.593
Chiang and Toor [19,106]	Laminar Jet	0.593
Norman and Sammak [109]	Laminar Jet	0.601
Groothuis and Kramers [111]	Still Liquid	0.581
Takeuchi and Namba [123]	Laminar Jet	0.604
This work	Laminar Jet	0.604

From the solubility measurements described in Chapter 3, a value of 1.360 moles/litre was obtained for $C_{u,s}$ at p_{SO_2} = 76.0 cm Hg. For $C_{u,s}.\overline{\mathcal{D}}_u^{\frac{1}{2}}$ = 0.604, this gives $\overline{\mathcal{D}}_u$ = 1.97 x 10^{-5} cm^2/sec. This is approximately 35 percent higher than the average value predicted by semi-empirical relationships (Table 2.4) and approximately 20 percent higher than the average experimental value listed in Table 2.5 (b).

(ii) According to equations (1.12) and (1.15), the linear relationship can also be interpreted in terms of a very fast ionization reaction. This requires either that the effects of concentration on both $\mathcal{D}_u$ and $\mathcal{D}_i$ are negligible or, alternatively, that these effects are cancelled by the concentration dependence of the ratio $\mathcal{D}_i/\mathcal{D}_u$. If one of these requirements is met, the slope of the line in Graph 8.1 is now a measure of $C_{u,s}.\overline{\mathcal{D}}_u^{\frac{1}{2}}.F_{Rl}$. A value of 0.63 for $\mathcal{D}_i/\mathcal{D}_u$ was interpolated from the data of Eriksen [119] and, using the Elliott Computer with Algol programme 'F Value' (Appendix 6), the value of F_{Rl} was calculated as 1.092. This gives $C_{u,s}.\overline{\mathcal{D}}_u^{\frac{1}{2}}$ = 0.553 and $\overline{\mathcal{D}}_u$ = 1.66 x 10^{-5} cm^2/sec. This is only about 12 percent higher than the average value predicted by the semi-empirical relationships and only about 3 percent higher than the average of the experimental values.

The above analysis appears to favour a fast ionization reaction. However, because it involves many assumptions which cannot be justified, and because of the uncertainties surrounding both measured and calculated diffusion coefficients, the evidence is by no means

conclusive and further information was sought.

8.3 ABSORPTION INTO AQUEOUS SODIUM CHLORIDE

In subsequent measurements it was necessary to use solutions whose viscosities were different from that of water, for which the jet had been calibrated. In order to assess the effects of viscosity on jet hydronamics, rates of absorption of sulphur dioxide into an aqueous solutions of sodium chloride were measured. The solution, which was 1.053 molar, had a viscosity of 1.098, cp. [124], and the measurements were obtained using the same head of liquid in the jet as was used for water. The results are shown in Graph 8.2.

Now, if the increased viscosity had significantly altered the jet hydronamics, it could have done so in three ways:

(i) by decreasing the jet flow;

(ii) by producing a thicker boundary layer;

(iii) by decreasing the jet acceleration;

and it is necessary to consider the possible effects of these changes on both the slope and intercept of a plot of Φ against $4(QL)^{\frac{1}{2}}$. The effect of decreased flow on the slope was allowed for in the calculations and it has already been noted (Section 6.2) that, because the flow remained in the range 3.4 to 3.6 cc/sec, the decrease would have a negligible effect on the intercept. A close examination of the analysis in Appendix 4 shows that a thicker boundary layer would affect the intercept more noticeably than the slope and the

Graph 8.2

Graph 8.2

Absorption of Sulphur Dioxide into 1.053 M Aqueous NaCl at 20°C

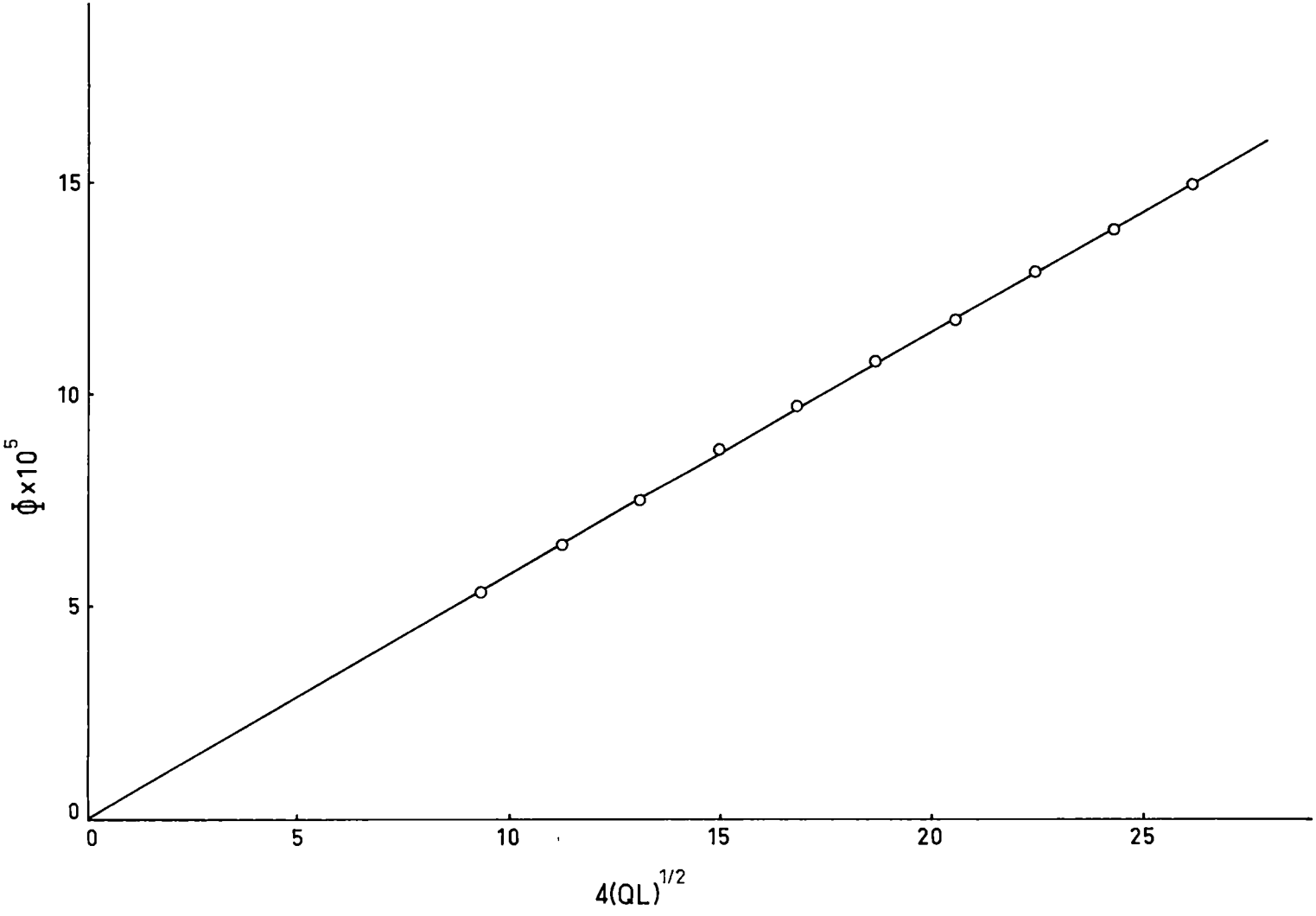
15
10
5
0
$\Phi \times 10^5$
0
5
10
15
20
25
$4(QL)^{1/2}$

decreased acceleration would affect the slope more than the intercept. Statistical analysis showed that the intercept in Graph 8.2 differs from zero no more significantly than that for water and it was concluded that any increase in boundary layer thickness had a negligible effect on the absorption measurements. If the slope of the line in Graph 8.2 had not been affected by decreased jet acceleration, its value could be predicted as follows. For absorption into water write

$$(\text{slope})_w = (C_{t,s})_w . (\overline{\mathcal{D}}_t^{\frac{1}{2}})_w$$

For absorption into aqueous sodium chloride write

$$(\text{slope})_n = (C_{t,s})_n . (\overline{\mathcal{D}}_t^{\frac{1}{2}})_n$$

Then

$$(\text{slope})_n = (\text{slope})_w . \frac{(C_{t,s})_n}{(C_{t,s})_w} . \left[\frac{(\overline{\mathcal{D}}_t)_n}{(\overline{\mathcal{D}}_t)_w}\right]^{\frac{1}{2}}$$

From equation (2.1)

$$\frac{(C_{t,s})_n}{(C_{t,s})_w} = 0.985$$

From the simple Stokes-Einstein relationship*

$$\left[\frac{(\overline{\mathcal{D}}_t)_n}{(\overline{\mathcal{D}}_t)_w}\right]^{\frac{1}{2}} = \left[\frac{\eta_w}{\eta_n}\right]^{\frac{1}{2}} = 0.956$$

---

*Ratcliffe and Holdcroft [181] measured diffusion coefficients for carbon dioxide in various aqueous electrolyte solutions and showed that the effect of viscosity was slightly different from that predicted by the simple Stokes-Einstein relationship. However, their measured coefficients for sodium chloride were better correlated by this relationship than by the one they derived.

Hence $(\text{slope})_n = 0.604 \times 0.985 \times 0.956 = 0.569$

The slope of the line in Figure 8.2 is 0.568 and it was concluded that any decrease in jet acceleration was so small that it had a negligible effect on jet hydronamics and hence on absorption rates.

In subsequent measurements the viscosities of all solutions were confined to the range 1.00 to 1.10 cp and diffusion coefficients used in the analysis of these measurements were calculated from the simple Stokes-Einstein relationship.

8.4 ABSORPTION INTO AQUEOUS HYDROCHLORIC ACID

The results of these measurements are shown in Graph 8.3. The slopes of the lines in this graph, and their 95 percent confidence limits are plotted against acid concentration in Graph 8.4.

Now if the rate of ionization of sulphur dioxide in water is very slow compared with diffusion, the slopes of these lines will be a measure of $C_{u,s}.\overline{\mathcal{D}}_u^{\frac{1}{2}}$ and values of this quantity were predicted as follows. $\overline{\mathcal{D}}_u$ was taken as 1.97×10^{-5} cm^2/sec for water (Section 8.2) and estimated for different acid concentrations using the Stokes-Einstein relationship. Values of $C_{u,s}$ were interpolated from Graph 3.4. The calculated values of $C_{u,s}.\overline{\mathcal{D}}_u^{\frac{1}{2}}$ are shown in Table 8.2 and a smooth curve showing the predicted relationship between this quantity and acid concentration is drawn in Graph 8.4.

On the other hand, if the rate of ionization of sulphur dioxide is fast compared with diffusion, the slopes of the lines in Graph

TABLE 8.2 PREDICTED VALUES OF $C_{u,s}.\overline{\mathcal{D}}_u^{\frac{1}{2}}$ FOR A SLOW IONIZATION REACTION

[HCl]	$C_{u,s}$	$\left[\frac{\eta_{HCl}}{\eta_{H_2O}}\right]^{\frac{1}{2}}$ [124]	$\overline{\mathcal{D}}_u^{\frac{1}{2}}$	$C_{u,s}.\overline{\mathcal{D}}_u^{\frac{1}{2}}$
0	1.360	1.000	0.444	0.604
0.05	(1.338)	1.001	0.444	0.594
0.10	1.339	1.002	0.443	0.593
0.25	1.354	1.006	0.442	0.598
0.40	1.375	1.010	0.440	0.605
0.70	1.415	1.017	0.437	0.618
1.00	1.451	1.024	0.434	0.630
1.30	1.483	1.032	0.431	0.639

8.3 are a measure of $C_{u,s}.\overline{\mathcal{D}}_u^{\frac{1}{2}}.F_{Rl}$. Values of this quantity were predicted as follows. $\mathcal{D}_u$ was taken as 1.66×10^{-5} cm^2/sec for water (Section 8.2) and estimated for different acid concentrations using the Stokes-Einstein relationship. Values of $C_{u,s}$ were interpolated from Graph 3.4. In accordance with the calculations of the concentrations of unionized sulphur dioxide molecules in hydrochloric acid solutions (Section 3.4.2), the apparent ionization constants for sulphur dioxide in these solutions were estimated on the basis of a simple common-ion effect. In other words, the concentrations of ionized species were calculated from the relationship

Graph 8.3

Graph 8.3

Absorption of sulphur dioxide into hydrochloric acid solutions

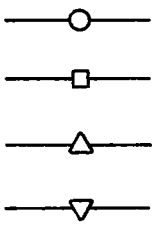

M HCl = 0.028

M HCl = 0.113

M HCl = 0.481

M HCl = 1.100

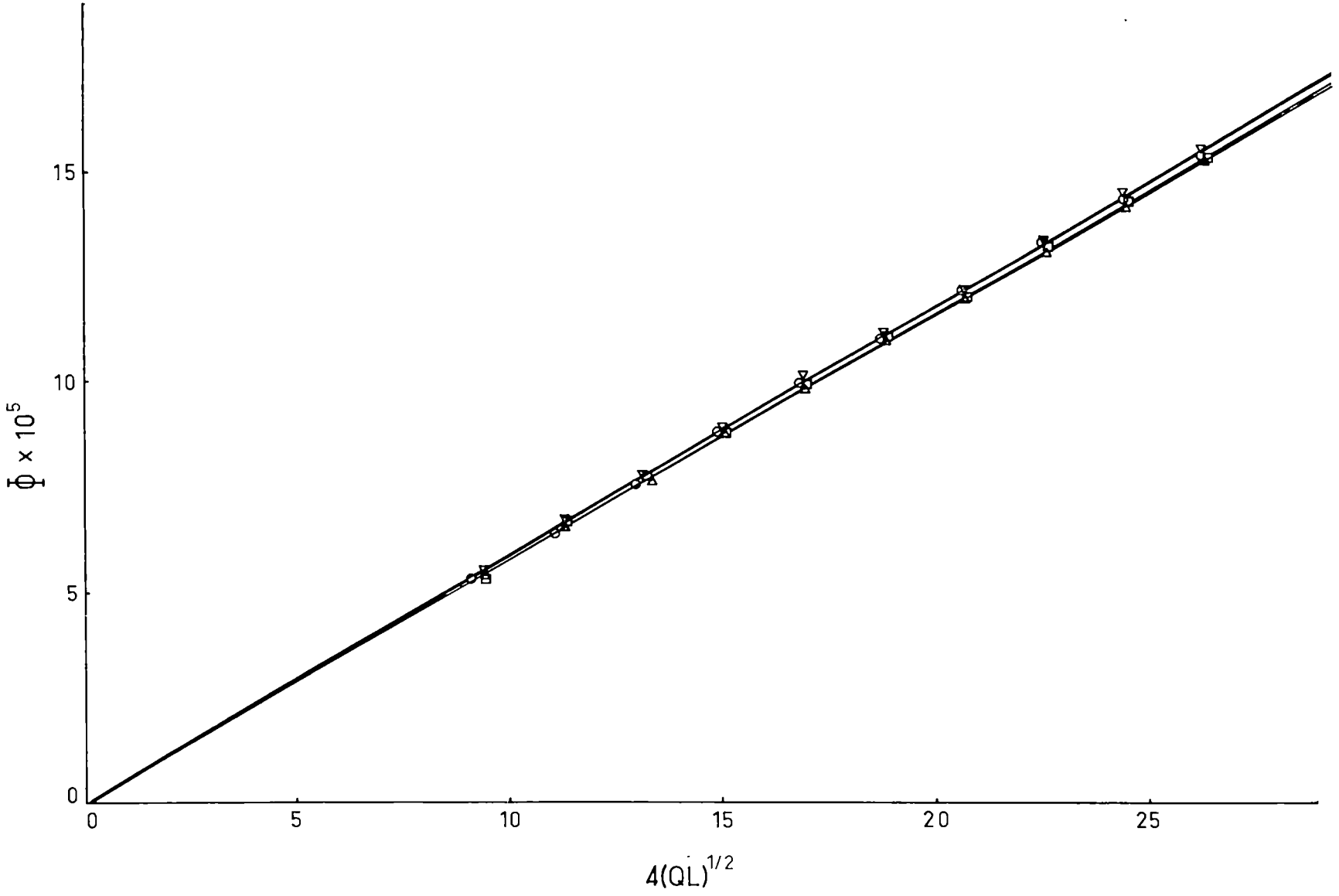
15
10
5
0
Φ x 10^5
0
5
10
15
20
25
4(QL)^1/2

Graph 8.4

Graph 8.4

$C_{u,s}.\overline{D}_u^{\frac{1}{2}}$ or $C_{u,s}.\overline{D}_u^{\frac{1}{2}}.F_{Rl}$ as a function of

hydrochloric acid concentration

— — — predicted for a slow ionization reaction

——————— predicted for a fast ionization reaction

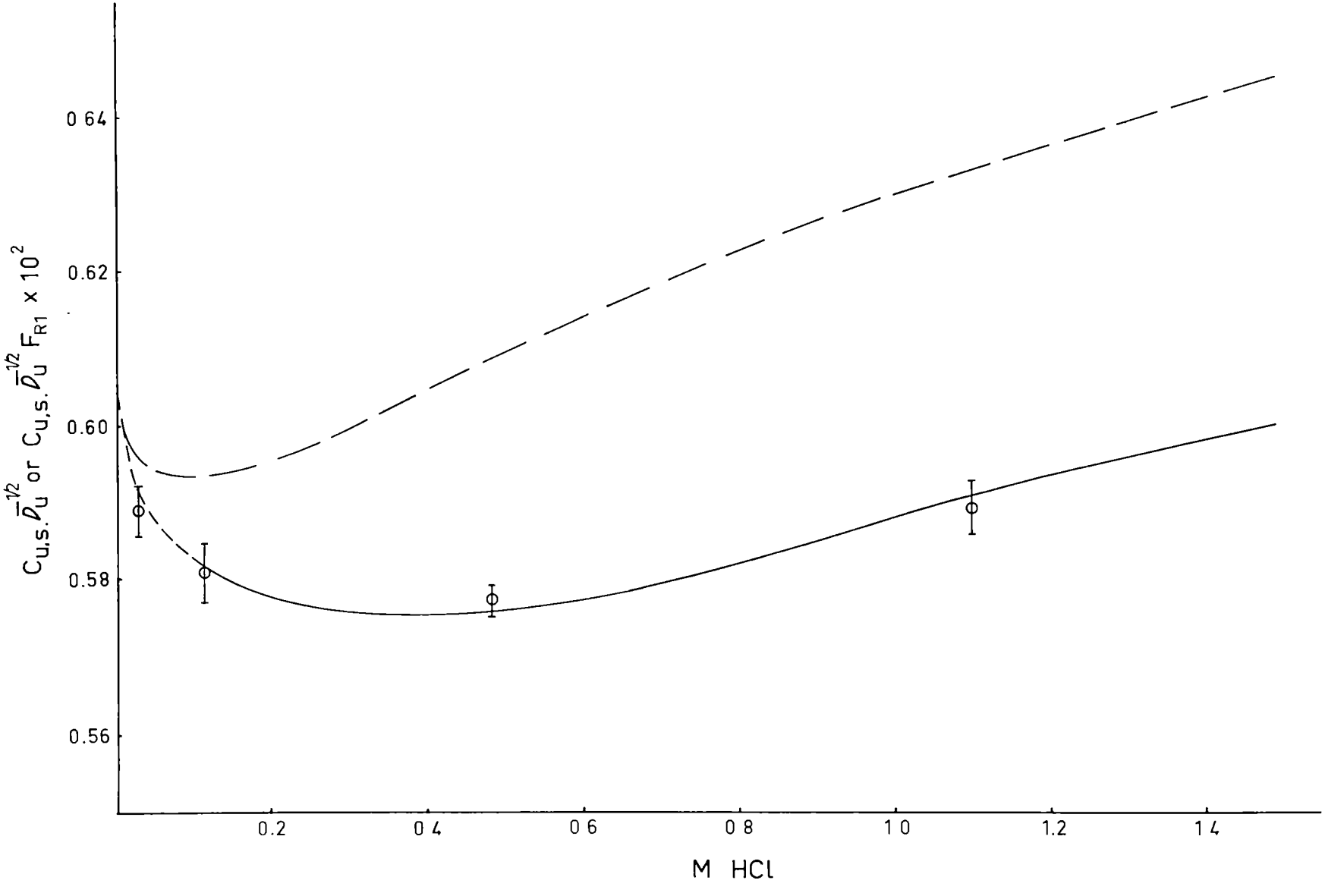
0 64
0.62
0.60
0.58
0.56
$C_{u,s.}\bar{\rho}_u^{1/2}$ or $C_{u,s.}\bar{\rho}_u^{1/2} F_{R1} \times 10^2$
0.2
0 4
0 6
0 8
1 0
1.2
1 4
M HCl

$$C_i = \tfrac{1}{2}\{-[H^+_{HCl}] + ([H^+_{HCl}]^2 + 4K_c.C_u)^{\frac{1}{2}}\} \quad (8.1)$$

and the apparent ionization constants were calculated from the relationship

$$K' = [C_i]^2 / [C_u] \quad (8.2)$$

The value of 0.63 for $\mathcal{D}_i/\mathcal{D}_u$ (Section 8.2) was assumed to be unaffected by the acid and this, together with the values of $C_{u,s}$ and K', was used to calculate values of F_{Rl} for different acid concentrations. The results of all these calculations are shown in Table 8.3 and a curve showing the relationship between the quantity $C_{u,s}.\overline{\mathcal{D}}_u^{\frac{1}{2}}.F_{Rl}$ and acid concentration is drawn in Graph 8.4. The excellent agreement between measured and predicted values of $C_{u,s}.\overline{\mathcal{D}}_u^{\frac{1}{2}}.F_{Rl}$ was taken as conclusive evidence that the ionization of water is very fast. Subsequent absorption measurements were interpreted on this basis.

8.5 ABSORPTION INTO AQUEOUS SULPHUR DIOXIDE SOLUTIONS

It has already been suggested (Section 4.1) that the discrepancies between diffusion coefficients for sulphur dioxide reported in the literature (Table 2.5 (b)) may have arisen, at least partly, from a concentration dependence of these coefficients. A technique by which absorption measurements can be used to determine such a concentration dependence has been described by Tang and Himmelblau [188]. They showed that if the differential coefficient $\mathcal{D}(C)$ is a linear function of concentration,

$$\text{i.e. if} \quad \mathcal{D}(C) = \mathcal{D}(0)[1 + p.C] \quad (8.3)$$

TABLE 8.3 PREDICTED VALUES OF $C_{u,s}.\overline{D}_u^{\frac{1}{2}}.F_{Rl}$ FOR A FAST IONIZATION REACTION

[HCl]	$[H^+]$	$C_{u,s}$	$(K')^{\frac{1}{2}}$	F_{Rl}	$[\frac{\eta_{HCl}}{\eta_{H_2O}}]^{\frac{1}{2}}$ [124]	$\overline{D}_u^{\frac{1}{2}}$	$C_{u,s}.\overline{D}_u^{\frac{1}{2}}.F_{Rl}$
0	0	1.360	0.150	1.092	1.000	0.407	0.604
0.05	0.048	(1.338)	0.131	1.082	1.001	0.406	0.588
0.10	0.094	1.339	0.116	1.072	1.002	0.405	0.582
0.25	0.224	1.354	0.082	1.051	1.006	0.404	0.576
0.40	0.345	1.375	0.063	1.039	1.010	0.403	0.576
0.70	0.575	1.415	0.043	1.029	1.017	0.401	0.579
1.00	0.782	1.451	0.033	1.020	1.024	0.397	0.588
1.30	0.970	1.483	0.028	1.017	1.032	0.394	0.595

then the integral coefficient measured in unsteady state absorption experiments is given, to a first approximation, by

$$\overline{\mathcal{D}}^{\frac{1}{2}} = [1 + (\tfrac{1}{2} - \tfrac{1}{\pi}).q.(C_s - C_L)] \qquad (8.4)$$

where the parameter q is given by

$$q = -p/(1 + p.C_s) \qquad (8.5)$$

Thus if a gas is absorbed into different concentrations of its aqueous solution, and the measured integral coefficients are plotted against corresponding values of $(C_s - C_L)$, the resulting curve will be a straight line whose intercept and slope will be given by the relationships:

$$\text{Intercept} = \mathcal{D}_s^{\frac{1}{2}} \qquad (8.6)$$

$$\text{and Slope} = \mathcal{D}_s^{\frac{1}{2}}.q.(\tfrac{1}{2} - \tfrac{1}{\pi}) \qquad (8.7)$$

As discussed in Section 7.3.3, data at only one value of C_L were obtained in this investigation. These are shown as a plot of Φ against $4(QL)^{\frac{1}{2}}$ in Graph 8.5 and the calculations made to estimate $\overline{\mathcal{D}}_u^{\frac{1}{2}}$ from these data and those for water are summarized in Table 8.4. The estimates of accuracy shown in this table are 90 percent confidence limits.

TABLE 8.4 CALCULATION OF $\overline{\mathcal{D}}_u^{\frac{1}{2}}$ FROM ABSORPTION DATA

$C_{t,s}$	$C_{t,L}$	$C_{u,s}$	$C_{u,L}$	$(C_{t,s} - C_{t,L})\overline{\mathcal{D}}_t^{\frac{1}{2}}$	F_{Rl}	$\overline{\mathcal{D}}_u^{\frac{1}{2}}$
1.535	0.0	1.360	0.0	0.6044 ± 0.0032	1.092	0.4069 ± 0.0016
1.535	0.735	1.360	0.617	0.3140 ± 0.0019	1.061	0.3984 ± 0.0024

Graph 8.5

Graph 8.5

Absorption of Sulphur Dioxide into a 0.735 M Solution of Sulphur Dioxide

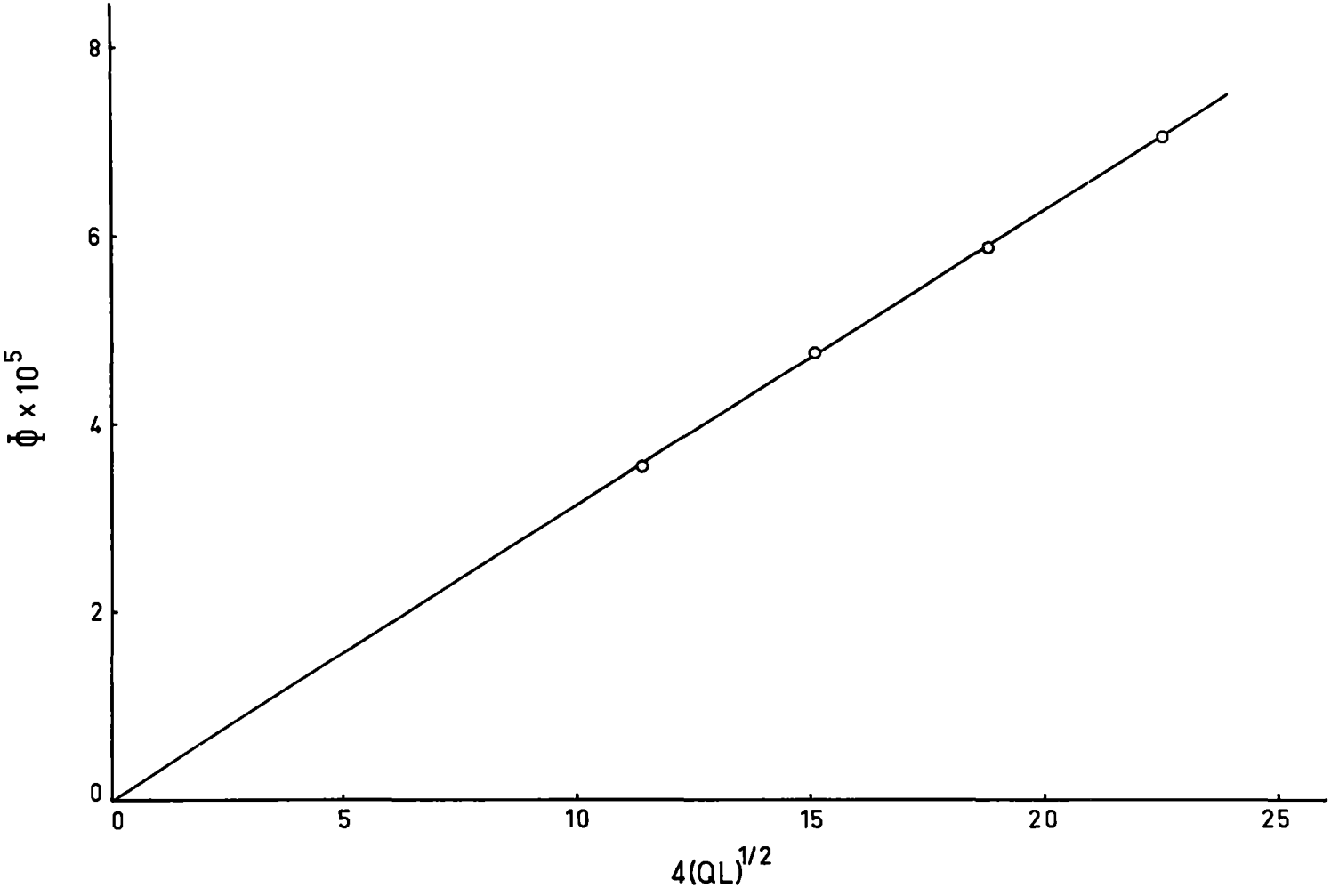
8
6
4
2
0
Φ x 10^5
0
5
10
15
20
25
4(QL)^1/2

Now Eriksen [119] has reported a value of 1.45×10^{-5} cm^2/sec for the diffusion coefficient in an aqueous solution of sulphur dioxide saturated at 1 atmosphere and 20°C. From the description of his apparatus, it appears that this measurement can be regarded as a weighted mean coefficient $\mathcal{D}_t$ defined by

$$\overline{\mathcal{D}}_t.C_t = \overline{\mathcal{D}}_u.C_u + \overline{\mathcal{D}}_i.C_i \qquad (8.8)$$

For $C_t = 1.535$, $C_u = 1.360$, $C_i = 0.175$ and $\mathcal{D}_i/\mathcal{D}_u = 0.63$, this gives $\overline{\mathcal{D}}_u = 1.51 \times 10^{-5}$ cm^2/sec or $\overline{\mathcal{D}}_u^{\frac{1}{2}} = 0.3886 \times 10^{-2}$.

The values of $\overline{\mathcal{D}}_u^{\frac{1}{2}}$ listed in Table 8.4, together with that calculated from Eriksen's result, are plotted, with their 90 percent confidence limits, against $(C_{u,s} - C_{u,L})$ in graph 8.6. The confidence limits indicate that the conclusion of a concentration dependence is significant only at the 90 percent level. That a higher level of significance cannot be attached to this conclusion arises largely from the errors in Eriksen's measurement.

It was assumed that a concentration dependence does exist (and this will be seen to be justified) and the results were analysed as follows:

$$\text{from Graph 8.6, Intercept} = \mathcal{D}_{u,s}^{\frac{1}{2}} = 0.3884 \times 10^{-2}$$

$$\text{Slope} = 0.0135 \times 10^{-2}.$$

$$\text{This gives } q = 0.191,$$

$$p = -0.152,$$

$$\mathcal{D}_{u,o} = 1.90 \times 10^{-5}, \quad \mathcal{D}_{u,s} = 1.51 \times 10^{-5}$$

$$\text{and } \mathcal{D}_u(C) \times 10^5 = 1.90\,[1 - 0.152\,C_u] \qquad (8.9)$$

Corresponding values of $\mathcal{D}_t(C)$ and $\mathcal{D}_i(C)$ were calculated from

Graph 8.6

Graph 8.6

$\overline{v}_u^{\frac{1}{2}}$ as a function of $(C_{u,s} - C_{u,L})$

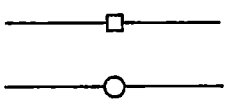

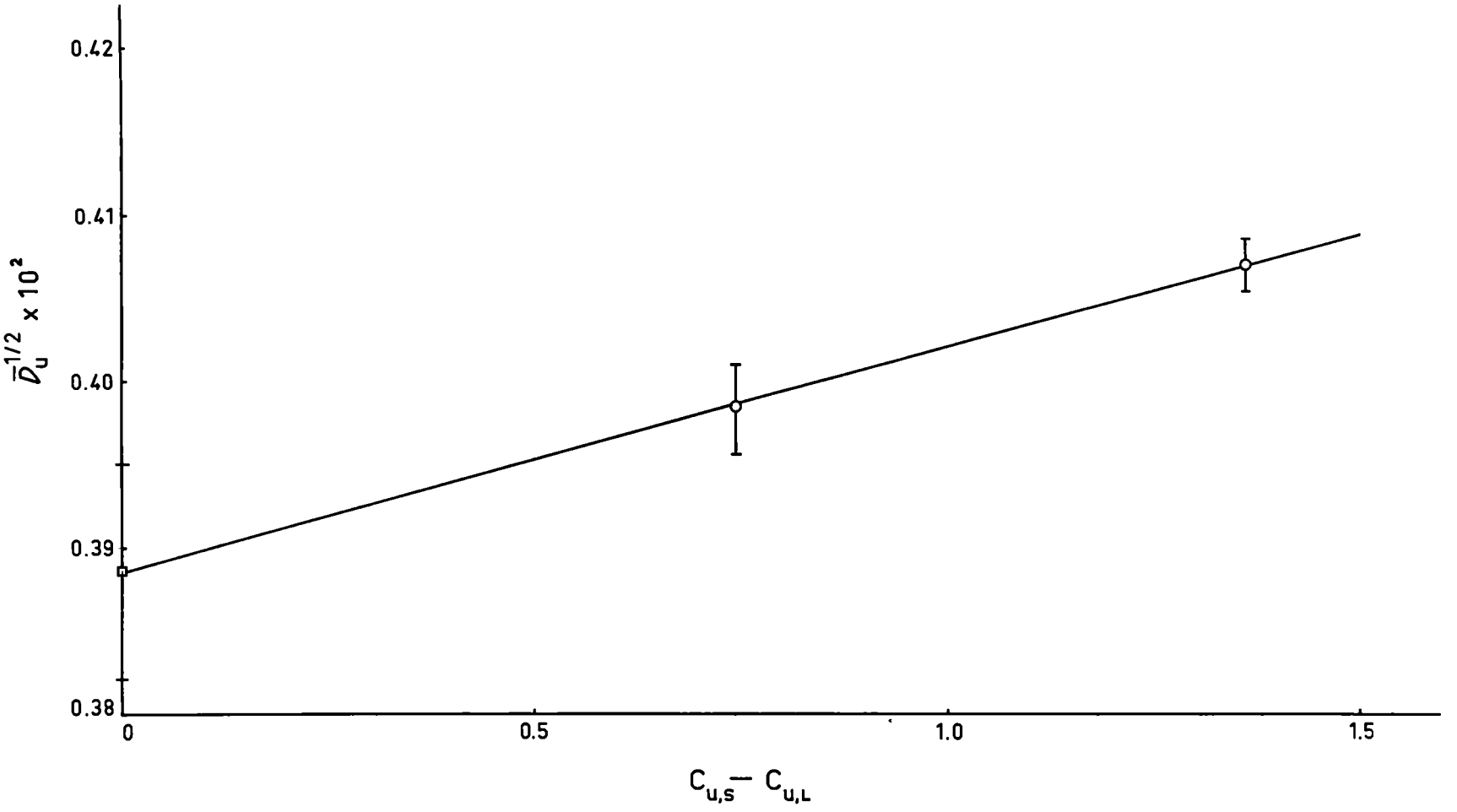
0.42
0.41
0.40
0.39
0.38
$\bar{D}_u^{1/2} \times 10^2$
0
0.5
1.0
1.5
$C_{u,s} - C_{u,L}$

equation (8.8) and the relationship $\mathcal{D}_i = 0.63\ \mathcal{D}_u$, and values of the three coefficients are plotted against C_t in Graph 8.7.

To compare the coefficients in Graph 8.7 with those listed in Table 2.5 (b) it is first necessary to examine the conditions under which the latter results were obtained. The value of 1.78×10^{-5} cm^2/sec which has been quoted in the literature [e.g. 7,119] as having been obtained by Kolthoff and Miller [189] at 20°C is, in fact, a calculated value based on the result obtained by these investigators at 25°C. Using a polarographic technique, Kolthoff and Miller measured a diffusion coefficient for aqueous solutions of sodium bisulphite, containing nitric acid. The average bisulphite concentration was 0.0012 molar and the nitric acid concentration was 0.092 molar. They tacitly assumed that the reactions

$$NaHSO_3 \rightarrow Na^+ + HSO_3^-$$

and

$$HSO_3^- + H^+ \rightarrow SO_2 + H_2O$$

occurred to completion and quoted the measured coefficient (2.04×10^{-5} cm^2/sec) as being that for unionized sulphur dioxide molecules. However, calculations based on a common ion effect and a value for K_c of 0.0203 at 25°C (Table 1.1) show that, at equilibrium, the concentrations of all the species in solution will be

$$Na^+ = 0.0012$$

$$H^+ = 0.0906$$

$$SO_2 = 0.00098$$

$$HSO_3^- = 0.00022$$

Graph 8.7

Graph 8.7

Concentration Dependence of Diffusion Coefficients in Aqueous Sulphur Dioxide Solutions

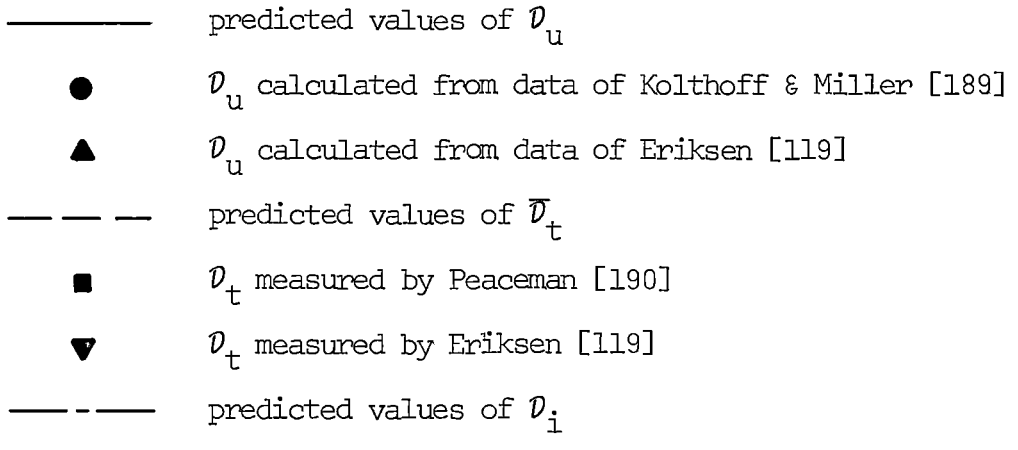

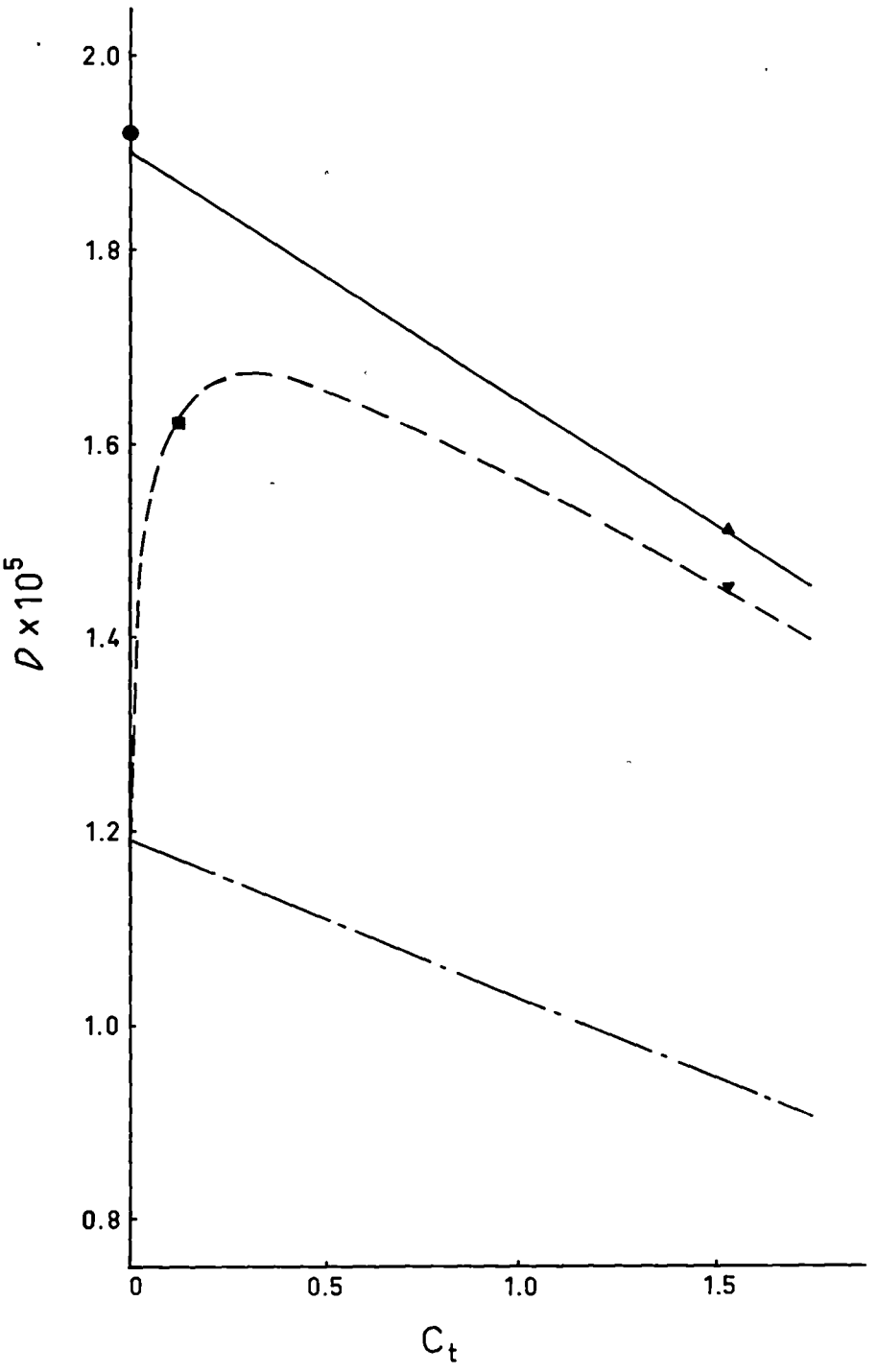
2.0
1.8
1.6
1.4
1.2
1.0
0.8
D x 10^5
0
0.5
1.0
1.5
C_t

In other words, both unionized sulphur dioxide and bisulphite ions may be expected to have been reduced at the mercury electrode. Consequently the diffusion coefficient measured was an effective coefficient for both species. If it is assumed that this is the same as the weighted coefficient defined by equation (8.8), a value of 2.19×10^{-5} cm^2/sec can be calculated for $\mathcal{D}_u(0)$ at 25°C. Using values of 0.894 and 1.005 cp for the viscosities of the solutions at 25 and 20°C (i.e. neglecting the effects of the solutes), and applying the Stokes-Einstein relationship to this result, gives a value of 1.92×10^{-5} cm^2/sec for $\mathcal{D}_u(0)$ at 20°C. This is in excellent agreement with the value of 1.90 cm^2/sec calculated from the absorption measurements in this investigation (Graph 8.7).

The value of 1.62×10^{-5} cm^2/sec was obtained by Peaceman [190] using aqueous sulphur dioxide solutions in a diaphragm cell under the conditions shown below. Two separate measurements of the diffusion coefficient for 'total' sulphur dioxide gave the results

Chamber	C_t
Lower	Start = 0.0; Finish = 0.04
Upper	Start = 0.23; Finish = 0.21

1.61 and 1.63 cm^2/sec. If the average of 1.62 cm^2/sec is regarded as a measure of $\mathcal{D}_t$ at the average cell concentration (0.12 molar), it can be seen from Graph 8.7 that the agreement with the corresponding value of $\mathcal{D}_t$ predicted from the absorption measurements is again excellent.

There is, of course, no justification for assuming that $\mathcal{D}_u$ and $\mathcal{D}_i$ are linearly dependent on concentration; nor is there any justification for assuming that the ratio $\mathcal{D}_i/\mathcal{D}_u$ is independent of concentration. However, the close agreement between measured and predicted coefficients indicates that the extent of concentration dependence for both coefficients is of the order shown in Graph 8.7.

Values of the quantity $\mathcal{D}_u.\eta$ at different concentrations are shown in Table 8.5 and these indicate that the Stokes-Einstein relationship does not describe the concentration dependence of this coefficient. It should also be noted that both the measured and predicted values of $\mathcal{D}_u$ at infinite dilution are much greater than those calculated from semi-empirical relationships (Table 2.4). Any attempt to explain these results would be largely conjecture. However, it is suggested that the high values of $\mathcal{D}_u(0)$ may arise from the dipole moment of the unionized sulphur dioxide molecules. According to Eriksen [119] this will distort the surrounding water

TABLE 8.5 $\mathcal{D}_u.\eta$ AS A FUNCTION OF C_t

C_t	0	0.25	0.50	0.75	1.00	1.25	1.50
$\mathcal{D}_u.\eta \times 10^5$	1.92	1.91	1.88	1.84	1.79	1.74	1.68

structure and may cause a decrease in 'local' viscosities. The concentration dependence of the diffusion coefficients may also arise, at least partly, from this effect but a much better understanding of the structure of aqueous solutions is required before any definite conclusion can be drawn.

8.6 ABSORPTION INTO AQUEOUS SODIUM HYDROXIDE SOLUTIONS

When sulphur dioxide is dissolved in an aqueous solution of sodium hydroxide, several reactions may occur [69,118], viz:

$$SO_2 + H_2O \rightleftarrows H^+ + HSO_3^- \quad (1)$$

$$H^+ + OH^- \rightleftarrows H_2O \quad (2)$$

$$SO_2 + OH^- \rightleftarrows HSO_3^- \quad (3)$$

$$HSO_3^- + OH^- \rightleftarrows SO_3^= + H_2O \quad (4)$$

$$SO_2 + 2OH^- \rightleftarrows SO_3^= + H_2O \quad (5)$$

$$2HSO_3^- \rightleftarrows S_2O_5^= + H_2O \quad (6)$$

$$SO_3^= + SO_2 \rightleftarrows S_2O_5^= \quad (7)$$

$$2SO_2 + 2OH^- \rightleftarrows S_2O_5^= + H_2O \quad (8)$$

It should be noted that, although the mechanisms are different, reactions (1), (2) and (4) or (3) and (4) give the same overall result as reaction (5), and that reactions (3) and (6) or (5) and (7) give the same result as reaction (8).

It was noted in Section 1.4.2 that Takeuchi and Namba [123] absorbed sulphur dioxide into laminar jets of aqueous sodium hydroxide and interpreted their results on the assumption that only reaction (5) occurred - i.e. they assigned a value of 2.0 to the parameter m in equation (1.16). This led to the conclusion that the diffusion coefficient for sodium hydroxide was constant in the concentration range 0 to 3 molar and had a value of 4.35×10^{-5} cm^2/sec at 20°C. Recent measurements of $\mathcal{D}_{NaOH}$ (Table 8.6) suggest that the value estimated by Takeuchi and Namba may be too high and that their interpretation of the absorption mechanism may be wrong.

TABLE 8.6 DIFFUSION COEFFICIENTS FOR NaOH

Ref.	$\mathcal{D}(25°C) \times 10^5$	$\mathcal{D}(20°C) \times 10^5$ (Calculated from Stokes-Einstein relationship)
[233]	2.3	2.0
[258]	2.5	2.2

Alternatively, if their interpretation of the mechanism is correct, it is desirable to explain the high value of the diffusion coefficient.

It was also noted in Section 1.4.2 that the estimates of F_{R2} made by Takeuchi and Namba show considerable scatter. Consequently, it was considered necessary to check their measurements and additional data were obtained in this investigation. These are shown in Graph 8.8 and the relationship between F_{R2} and sodium hydroxide concentration (Table 8.7) is shown in Graph 8.9.

TABLE 8.7 RELATIONSHIP BETWEEN F_{R2} AND SODIUM HYDROXIDE CONCENTRATION

Ref.	M NaOH	F_{R2}
[123]	0.290	1.185
[123]	0.527	1.340
This work	0.287	1.175
This work	0.472	1.321

The results attributed to Takeuchi and Namba were obtained as follows. A close examination of their data shows that the scatter is much more pronounced for the shorter jet and that, for the longer jet,

Graph 8.8

Graph 8.8

Absorption of Sulphur Dioxide into Aqueous Sodium Hydroxide Solutions

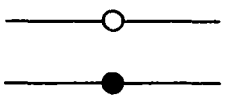

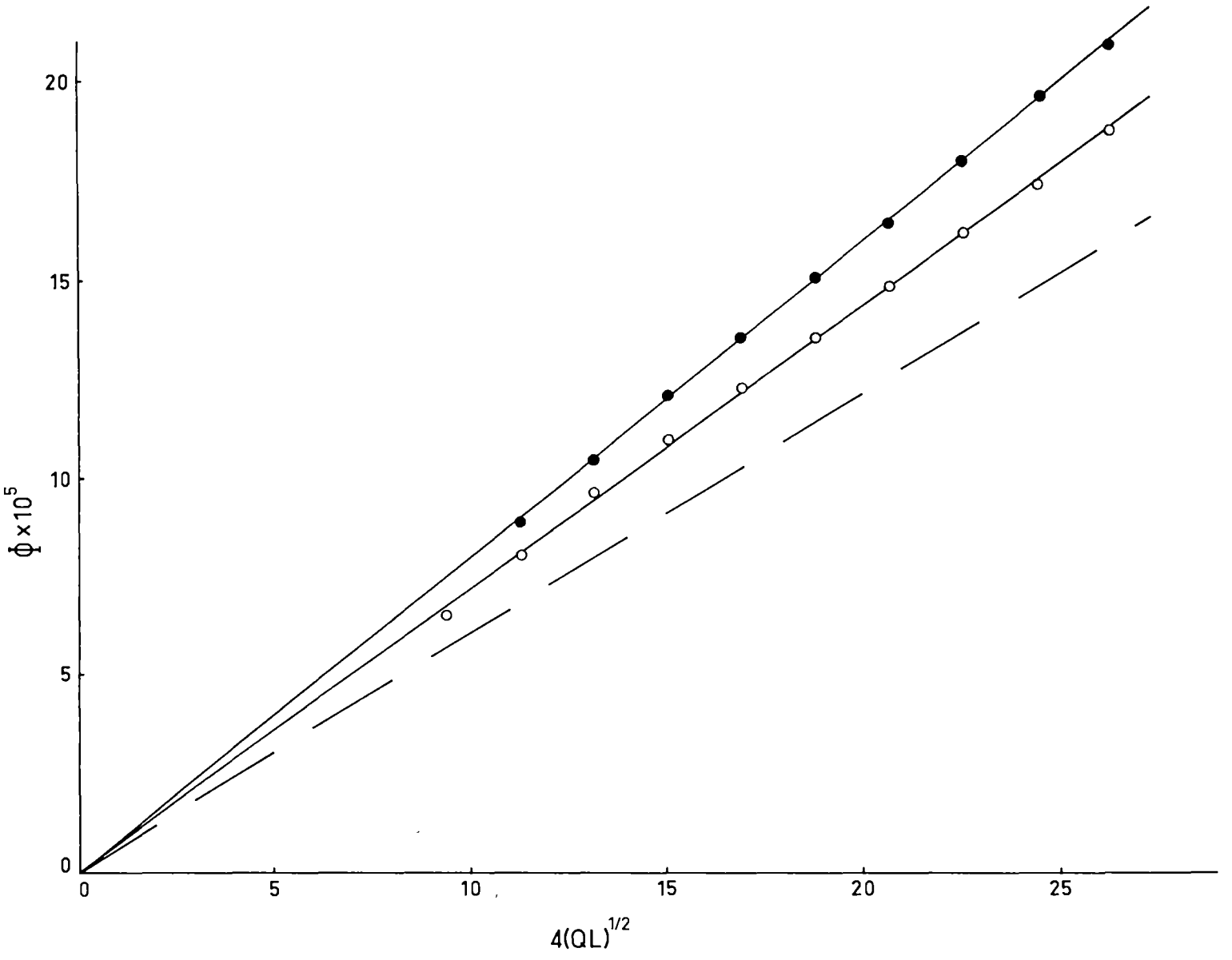
20
15
10
5
0
$\Phi \times 10^5$
0
5
10
15
20
25
$4(QL)^{1/2}$

Graph 8.9

Graph 8.9

Relationship Between F_{R2} and Sodium Hydroxide Concentration

□ Takeuchi and Namba [123]

○ This investigation

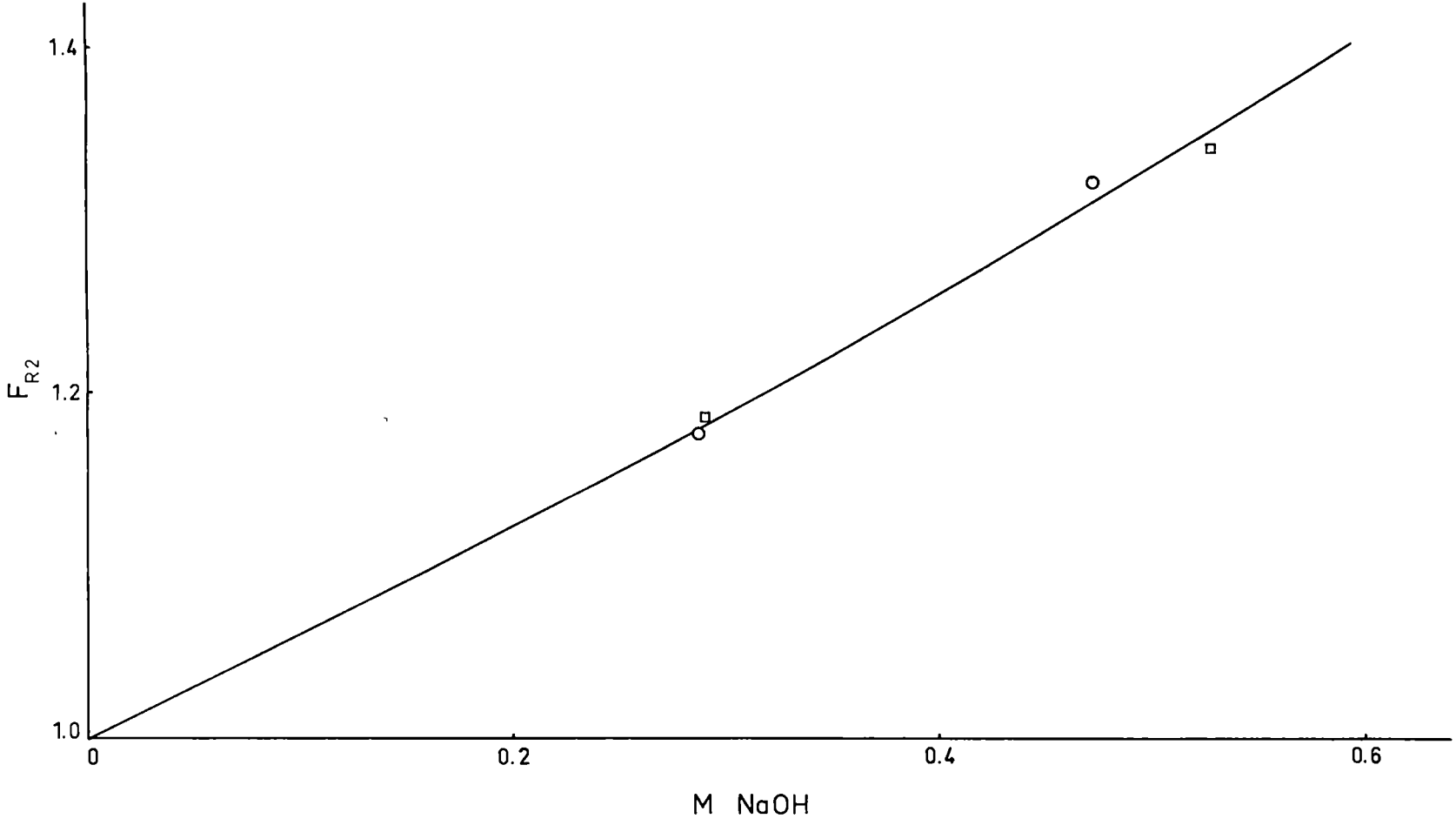
1.4
1.2
1.0
F_{R2}
0
0.2
0.4
0.6
M NaOH

it occurred mainly for very high and very low jet flow rates. The measurements obtained under these conditions were rejected because of

(a) the greater influence of viscosity on hydronamic correction factors for the short jet

(b) the possibility of ripples at low jet flows and

(c) the possibility of turbulence at high jet flows.

The remaining estimates of F_{R2} (four for each concentration) did not differ by more than 2 percent from their mean and it is these means which are given in Table 8.7. The agreement between these results and those obtained in this investigation, as shown in Graph 8.9, is good and the curve in this graph gives equal weight to both sets of results.

Before attempting to analyse these results, it is necessary to consider the heat effects accompanying the absorption process. It will subsequently be argued that the two reactions which may occur during the process are:

$$SO_2(aq) + 2NaOH(aq) \rightleftarrows Na_2SO_3(aq) + H_2O(\ell); \quad \Delta H = -27.8 \text{ kcals}$$

and $$SO_2(aq) + Na_2SO_3(aq) \rightleftarrows Na_2S_2O_5(aq); \quad \Delta H = -2.0 \text{ kcals}.$$

These reactions occur in a reaction zone which is moving away from the gas-liquid interface and equations (1.32) to (1.36) are not strictly applicable. However, if, as a first approximation, it is assumed that the reactions do occur at the interface, equation (1.35) gives $K_1 \simeq 0.92$ and equation (1.36) gives $K_2 \simeq 1.03$. Now it seems reasonable to expect that the movement of the reaction zone away from the interface will have a greater tendency to increase K_1

than to decrease K_2. In other words, it can be assumed that this movement will cause only a small change in the effect of the temperature rise on diffusion and expansion of the liquid; on the other hand, it will have a greater effect on the temperature rise at the interface. This means that with the moving zone, the product of K_1 and K_2 will be closer to 1.0 than is the value of 0.95 calculated for an interfacial reaction. For this reason, heat effects were neglected in the following interpretation of the absorption mechanisms. In view of the fact that this interpretation is essentially qualitative, this was considered to be justified.

In the following discussion, the ionization of sulphur dioxide in water is neglected and its possible effect on the absorption mechanism is discussed later. Table 8.8 shows values of F_{R2} calculated from equations (1.28) and (1.29) for four different mechanisms. These were based on the following conditions:

1. The overall reaction between sulphur dioxide and sodium hydroxide was assumed to be very fast compared with diffusion. This permits the use of equations (1.28) and (1.29).

2. After the first instant of contact, the interface will contain, not hydroxyl ions, but reaction products. It follows that for this, and other absorption processes in which a moving reaction zone is involved (Figure 1.2), the equilibrium solubility of the dissolving gas is determined, not by the concentration of the reacting solute as is commonly supposed [e.g. 123,256], but by the interfacial concentration of the reaction products. This will decrease with time as the products diffuse away from the interface and it is

TABLE 8.8 CALCULATED VALUES OF F_{R2} FOR DIFFERENT ABSORPTION MECHANISMS

Mechanism	m	[NaOH]	$\overline{\mathcal{D}}_t \times 10^5$	$\overline{\mathcal{D}}_{NaOH} \times 10^5$	C_t	F_{R2} (Uncorrected)	$\left[\frac{\eta_{NaOH}}{\eta_{H_2O}}\right]^{\frac{1}{2}}$	F_{R2} (Corrected)
1	1.0	0.20	1.55	2.10	1.535	1.14	1.02	1.12
		0.40	1.55	2.10	1.535	1.28	1.04	1.23
		0.60	1.55	2.10	1.535	1.42	1.06	1.34
2	2.0	0.20	1.55	2.10	1.535	1.07	1.02	1.05
		0.40	1.55	2.10	1.535	1.14	1.04	1.10
		0.60	1.55	2.10	1.535	1.21	1.06	1.14
3	2.0	0.20	1.55	4.20	1.535	1.08	1.02	1.06
		0.40	1.55	4.20	1.535	1.16	1.04	1.12
		0.60	1.55	4.20	1.535	1.25	1.06	1.18
4	2.0	0.20	1.55	8.40	1.535	1.09	1.02	1.07
		0.40	1.55	8.40	1.535	1.20	1.04	1.15
		0.60	1.55	8.40	1.535	1.30	1.06	1.23

not possible to predict its effect on the equilibrium solubility. Consequently the solubility was assumed to be the same as for water.

3. Heat effects were neglected.

4. The value of 1.55×10^{-5} cm^2/sec used for $\overline{D}_t$ was calculated from the results given in Table A.5.4 using the relationship

$$C_t.\overline{D}_t^{\frac{1}{2}} = \Phi/4(QL)^{\frac{1}{2}}$$

5. The value of 2.1×10^{-5} cm^2/sec used for the diffusion coefficient of hydroxyl ions in the sodium hydroxide solutions is the mean of the values given in Table 8.6.

6. Concentration effects were allowed for on the basis of the Stokes-Einstein relationship using values for η_{NaOH} given in Ref., [124] and values for η_{H_2O} given in Ref. [125]. It is most probable that the correction factors calculated in this way are not very accurate but, in view of the relatively small factors involved, this should not have introduced any significant errors.

The relationships between the calculated values of F_{R2} and alkali concentration are shown as smooth curves in Graph 8.10. From this it can be seen that if $\overline{D}_t$ is constant and the parameter m has a value of 2.0, the value of $\overline{D}_{NaOH}$ must be increased by a factor much greater than 4. That Takeuchi and Namba [123] were able to assign a value of 2.0 to m and conclude that $\overline{D}_{NaOH}$ must be increased by a factor of only about 3, arises from the fact that they assumed equilibrium solubilities to be related to alkali concentration. Their calculated values of F_{R2} were based on these solubilities but their experimental values were based on the solubility in water.

Graph 8.10

Graph 8.10

Predicted Values of F_{R2} for Different Absorption Mechanisms

—— —— —— Curve Through Experimental Results (Graph 8.9)

———————— Predicted for Different Mechanisms

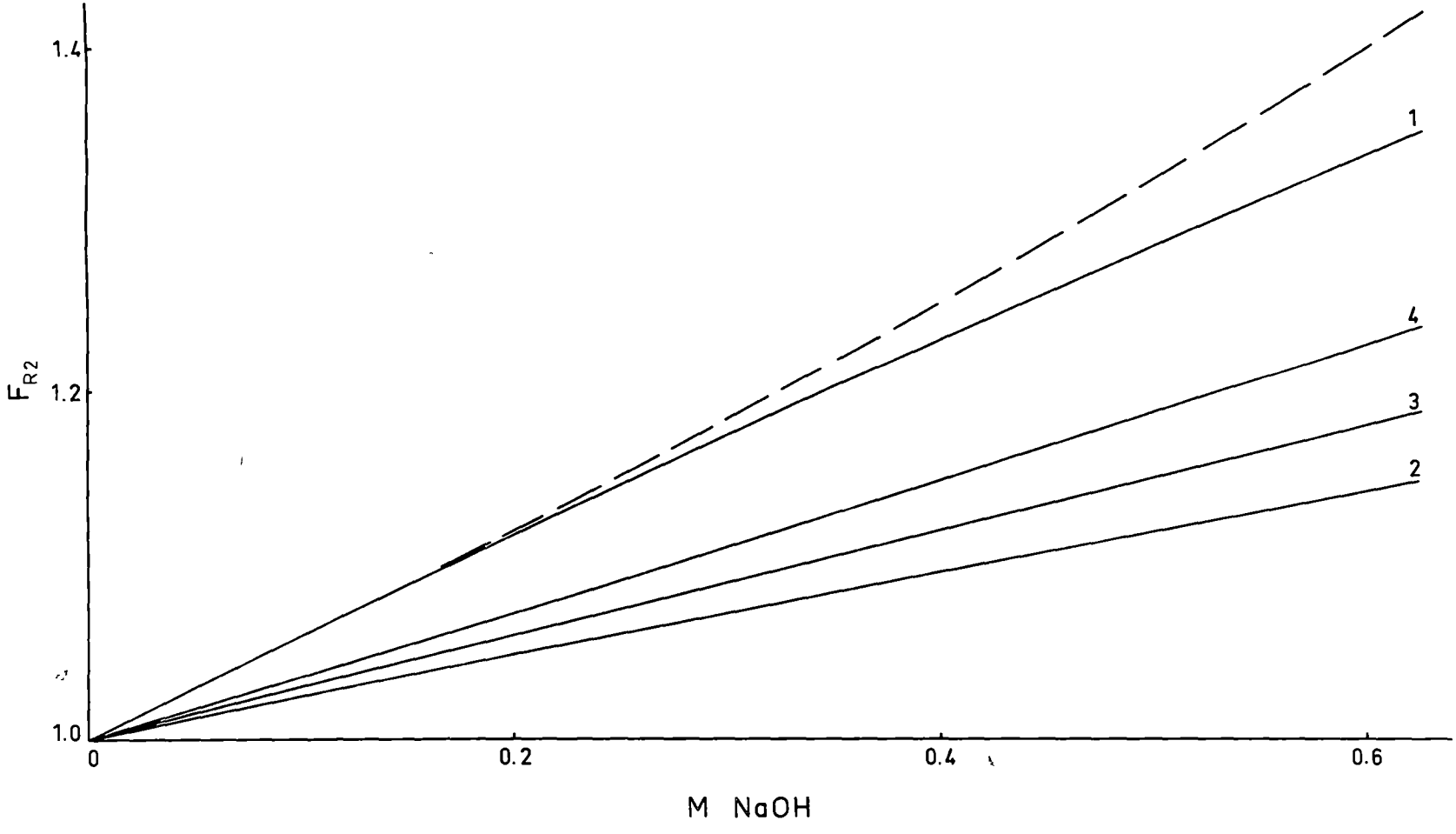
1.4
1.2
1.0
F_{R2}
0
0.2
0.4
0.6
M NaOH
1
4
3
2

Consequently, the two sets of values are not comparable. The conditions under which $\overline{\mathcal{D}}_{NaOH}$ can be increased are discussed below and it will be seen that an increase by a factor of more than 4 is most unlikely. It is reasonable to conclude, then, that either m cannot have a value of 2.0 or else the increased absorption rates result from factors which have not yet been considered.

Now Sherwood and Wei [266] have shown that, for steady state conditions, interactions between diffusing ionic species may lead to absorption rates much greater than those predicted by theoretical relationships based on molecular diffusion concepts. They state that 'in a system of mixed ions, as in the simultaneous diffusion of hydrogen chloride and sodium chloride, the faster moving H^+ may move ahead of its Cl^- partner, essential electrical neutrality being maintained by the presence of the slower moving Na^+ ions, which now lag behind their own Cl^- partners. At very low H^+ concentration in a solution of sodium chloride the electrical potential in the direction of diffusion may cause the effective diffusivity of H^+ to be even greater than that of the free hydrogen ion.'

It is on this basis that any increase in $\overline{\mathcal{D}}_{NaOH}$ may be explained. If m = 2.0, reaction (5) must occur at the reaction boundary and, in this region, sodium hydroxide will be diffusing in the presence of ionized sodium sulphite. The diffusion coefficient for free OH^- ions at 20°C is approximately 3.8×10^{-5} cm^2/sec [266] and, because of the relatively high concentrations of the solutions being considered here, this may define the upper limit of $\overline{\mathcal{D}}_{NaOH}$; certainly a value greater

than 8.4×10^{-5} cm^2/sec is most unlikely.

Now, because about 10 percent of the sulphur dioxide in an aqueous solution is ionized, it is possible that interactions between H^+, HSO_3^-, Na^+ and $SO_2^=$ ions may increase the effective value of $\overline{\mathcal{D}}_t$. This would have a much greater effect on the absorption rate than would a corresponding increase in $\overline{\mathcal{D}}_{NaOH}$. Such an interaction would be very complex, involving, among other considerations, the ionization equilibrium of the sulphur dioxide. It is not possible, therefore, to estimate the likely magnitude of any increase in $\overline{\mathcal{D}}_t$ but it is suggested that, if reaction (5) does occur at the reaction boundary, any analysis of the absorption mechanism should consider the possibility of such an increase.

Reference to Graph 8.10 shows that the absorption measurements may also be interpreted by assigning a value of 1.0 to m and explaining the discrepancies at higher alkali concentrations as again being due to interactions between the diffusing species. This would mean that one of reactions (1), (3) or (8) occurs and would require that HSO_3^- (reactions (1) and (3)) or $S_2O_5^=$ (reaction (8)) ions are relatively stable in the presence of hydroxyl ions. The writer has been unable to find any relevant kinetic data but it may be argued that, by analogy with the bicarbonate ion [22,237,262], the bisulphite ion will not be stable. On the other hand it seems reasonable to argue that, because of the higher valency of the pyrosulphite ion, the reaction

$$S_2O_5^= + 2OH^- \rightleftarrows 2SO_3^= + H_2O$$

may be slowed by a decrease in the frequency of collision between the ions. This, of course, is conjecture but the possibility that the absorption process involves essentially reaction (8) cannot be dismissed *a priori*.

The preceding discussion indicates that the absorption of sulphur dioxide into aqueous sodium hydroxide solutions may be a complex process. It can only be concluded that considerably more experimental data will be required before the mechanisms of the process can be elucidated.

8.7 ABSORPTION INTO WATER FROM MIXTURES WITH NITROGEN

As discussed in Section 1.2.2, Arnold [31] suggested that gas-phase transfer during unsteady state absorption cannot be described in terms of Fick's law coefficients. He derived a set of theoretical relationships to describe the transfer process but attempts to verify these experimentally were not very satisfactory due to lack of precision in the experimental data.

In terms of the nomenclature used in this thesis, these relationships can be written, for physical absorption in the liquid phase, as

$$N = \frac{(P_G - P_0)}{R_c T}\left[\frac{\mathcal{D}_G}{\pi\theta F_g}\right]^{\frac{1}{2}} = (C_0 - C_L)\left[\frac{\mathcal{D}_L}{\pi\theta}\right]^{\frac{1}{2}} \qquad (8.10)$$

where F_g is 'a factor used to correct the [gas-phase] diffusivity calculated on the assumption that Fick's law is valid.'

F_g is defined by the relationship

$$F_g = \frac{P_0' - P_G'}{\phi\pi^{\frac{1}{2}}}^2 \qquad (8.11)$$

where the parameter ϕ is defined by the relationship

$$\frac{P_0' - P_G'}{1 - P_0'} = \pi^{\frac{1}{2}}.\phi \exp(\phi^2) \operatorname{erfc}(\phi) \qquad (8.12)$$

Writing equation (8.10) in terms of the variables associated with a laminar jet, and integrating to obtain total absorption rates, gives (cf. equation (5.4))

$$\Phi_{id} = 4\left(\frac{P_G - P_0}{R_c T}\right)\left(\frac{\mathcal{D}_G}{F_g}\right)^{\frac{1}{2}}(QL)^{\frac{1}{2}} = 4(C_0 - C_L)\mathcal{D}_L^{\frac{1}{2}}(QL)^{\frac{1}{2}} \qquad (8.13)$$

or

$$\frac{\Phi_{id}}{4(QL)^{\frac{1}{2}}} = \left(\frac{P_G - P_0}{R_c T}\right)\left(\frac{\mathcal{D}_G}{F_g}\right)^{\frac{1}{2}} = (C_0 - C_L)\mathcal{D}_L^{\frac{1}{2}} \qquad (8.14)$$

Putting $C_L = 0$ and writing $C = H.p$ gives

$$\left(\frac{P_G - P_0}{R_c T}\right)\left(\frac{\mathcal{D}_G}{F_g}\right)^{\frac{1}{2}} = H.p_0.\mathcal{D}_L^{\frac{1}{2}} \qquad (8.15)$$

which reduces to

$$\frac{P_G - P_0}{P_0} = \frac{1}{1 + \left(\frac{\mathcal{D}_G}{\mathcal{D}_L}\right)^{\frac{1}{2}} / R_c THF_g^{\frac{1}{2}}} \qquad (8.16)$$

For absorption of sulphur dioxide into water, the right hand side of equation (8.14), with $C_L = 0$, becomes $C_u.F_{Rl}.\bar{\mathcal{D}}_u^{\frac{1}{2}}$. Writing, now, $C_u = H.p$, equation (8.16) becomes

$$\frac{P_G - P_0}{P_0} = \frac{1}{1 + \left(\frac{\mathcal{D}_G}{\bar{\mathcal{D}}_u}\right)^{\frac{1}{2}} / R_c THF_{Rl}.F_g^{\frac{1}{2}}} \qquad (8.17)$$

For $R_c = 6.24 \times 10^3$ cm Hg/gm. mole °K

$T = 293$°K

$H = (1.360/76.0) \times 10^{-3}$ gm. mole/cm Hg. cc (Graph 3.2)

equation (8.7) becomes

$$\frac{P_G - P_0}{P_0} = \frac{1}{1 + 32.7\left(\frac{\mathcal{D}_G}{\mathcal{D}_u}\right)^{\frac{1}{2}} / F_{Rl} . F_g^{\frac{1}{2}}} \qquad (8.18)$$

Since F_g is a function of p_0' (and hence of p_0) equation (8.18) can only be solved by successive approximations. It was solved for different values of p_G for absorption of SO_2 from nitrogen and values of $\Phi/4(QL)^{\frac{1}{2}}$ predicted using equation (8.14) are compared with those calculated for no gas phase resistance in Table 8.9 and Graph 8.11.

Experimental results obtained for the absorption of SO_2 from two mixtures with nitrogen are shown in Tables A.5.9 and A.5.10 and in Graph 8.12. Three different gas flow rates were used for each mixture and, for each mixture, the results were corrected to a common sulphur dioxide partial pressure by assuming a linear relationship between inlet pressure and absorption rate. In view of the very small corrections involved, this was considered to introduce negligible errors.

The slopes of the curves in Graph 8.12 ($\Phi/4(QL)^{\frac{1}{2}}$) decrease with increasing jet length, the rate of change of the slopes decreasing with increasing gas flow rate. If the results for each mixture are corrected to a common, average SO_2 pressure, based on the inlet and outlet pressures, the curves for lower flow rates still fall below those for higher flows. This suggests that the decreasing slopes in Graph 8.12 are caused, not only by decreasing SO_2 pressures, but also by some characteristic of the gas flow pattern. The obvious conclusion

TABLE 8.9 PREDICTED VALUES OF $\Phi/4(QL)^{\frac{1}{2}}$ WITH AND WITHOUT GAS-PHASE RESISTANCE

P = 76.0 cm Hg; $\mathcal{D}_G$ = 0.123 cm^2/sec

P_G	P_O	$C_{u,s}$	$\overline{\mathcal{D}}_u^{\frac{1}{2}}$ [Eqn.(8.4)]	F_{Rl}	$\frac{\Phi}{4(QL)^{\frac{1}{2}}}$ $(=C_{u,s}.\overline{\mathcal{D}}_u^{\frac{1}{2}}.F_{Rl})$	F_g	P_O	$C_{u,s}$	$\overline{\mathcal{D}}_u^{\frac{1}{2}}$ [Eqn.(8.4)]	F_{Rl}	$\frac{\Phi}{4(QL)^{\frac{1}{2}}}$ $(=C_{u,s}.\overline{\mathcal{D}}_u^{\frac{1}{2}}.F_{Rl})$
76.0	76.0	1.360	0.407	1.092	0.604						
70.0	70.0	1.253	0.409	1.096	0.562						
65.0	65.0	1.164	0.412	1.100	0.527						
60.0	60.0	1.075	0.414	1.104	0.491	0.056	54.4	0.975	0.416	1.109	0.450
55.0	55.0	0.986	0.416	1.108	0.454						
50.0	50.0	0.897	0.418	1.113	0.417						
45.0	45.0	0.807	0.420	1.119	0.379	0.195	37.5	0.674	0.423	1.131	0.322
40.0	40.0	0.718	0.422	1.127	0.341						
35.0	35.0	0.629	0.424	1.135	0.302						
30.0	30.0	0.540	0.425	1.145	0.263						

Graph 8.11

Graph 8.11

Predicted Values of $\Phi/4(QL)^{\frac{1}{2}}$

With and Without Gas-Phase Resistance

———— predicted for no gas-phase resistance

——-—— predicted for a gas-phase resistance
based on corrected diffusion coefficients

● experimental results

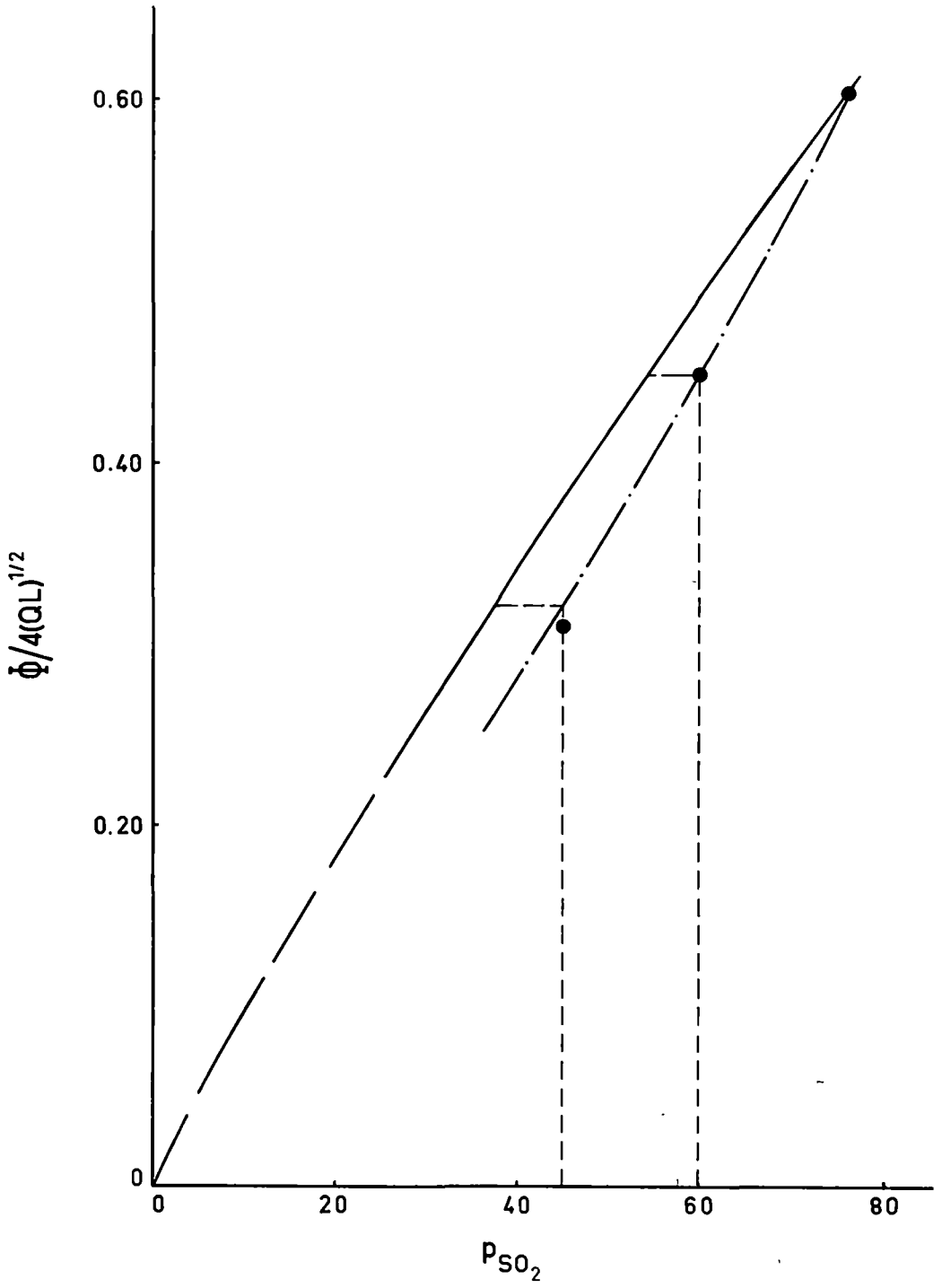
0.60
0.40
0.20
0
0
20
40
60
80
$\Phi/4(QL)^{1/2}$
p_{SO_2}

Graph 8.12

Graph 8.12

Absorption into Water from Mixtures with Nitrogen

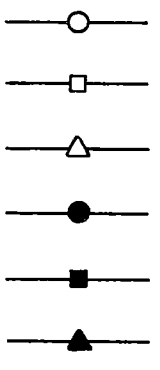

SO_2 = 80% v/v; Gas Inlet Flow = 4.1 cc/sec

SO_2 = 80% v/v; Gas Inlet Flow = 5.9 cc/sec

SO_2 = 80% v/v; Gas Inlet Flow = 8.7 cc/sec

SO_2 = 60% v/v; Gas Inlet Flow = 2.7 cc/sec

SO_2 = 60% v/v; Gas Inlet Flow = 4.1 cc/sec

SO_2 = 60% v/v; Gas Inlet Flow = 6.6 cc/sec

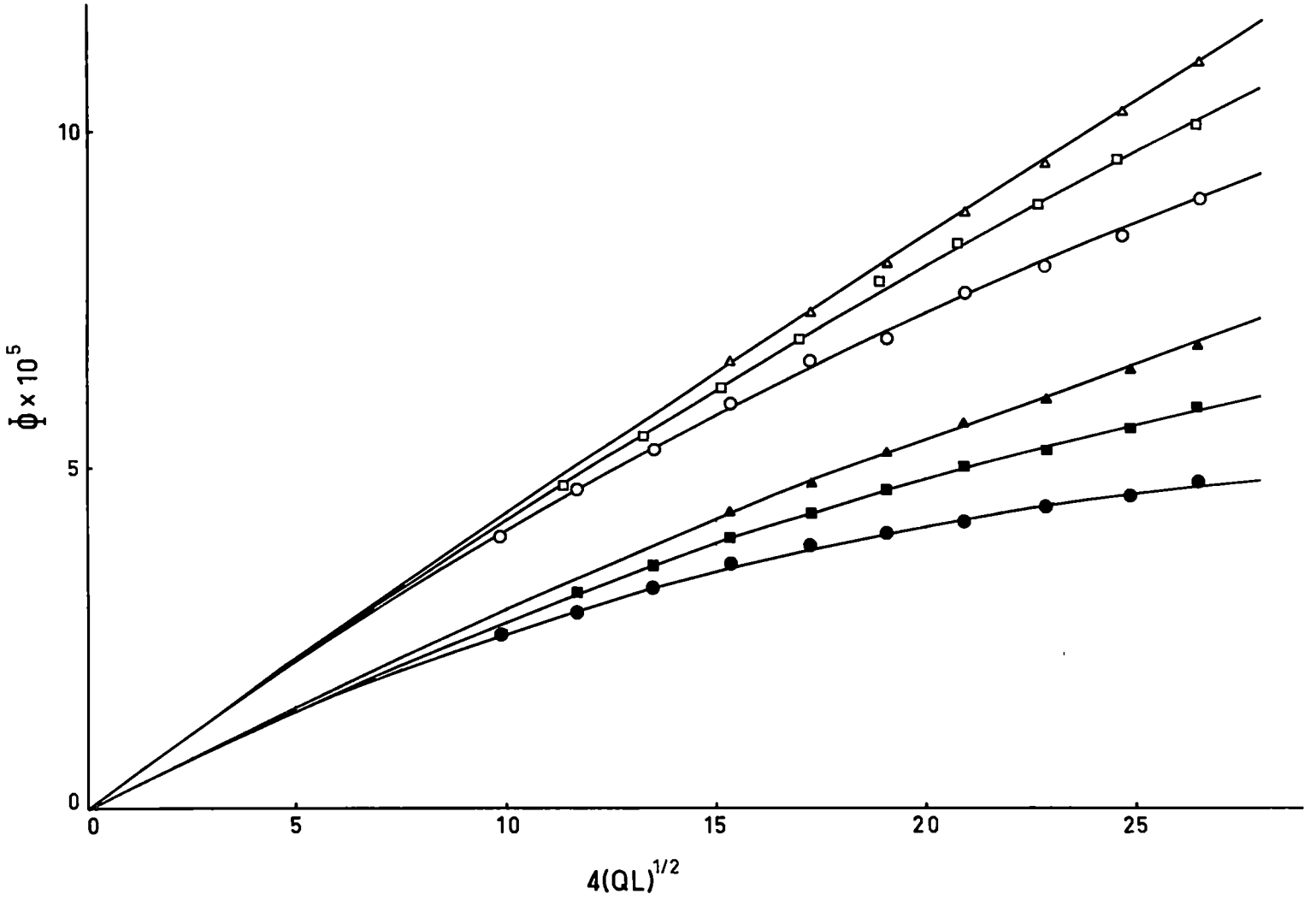
10
5
0
$\Phi \times 10^5$
0
5
10
15
20
25
$4(QL)^{1/2}$

to be reached is that the fast moving jet is surrounded by a gas-phase boundary layer and that the resistance to transfer in this layer is related to the SO_2 concentration. However, the unknown nature of the gas flow pattern prevents any exact analysis being made.

Graph 8.13 shows that, within experimental error, the relationship between the quantities $[\Phi/4(QL)^{\frac{1}{2}}]^{\frac{1}{2}}$ and $4(QL)^{\frac{1}{2}}$ can be regarded as linear. This, again because of the ill-defined gas hydronamics, is difficult to explain. However, it can be seen that, for each mixture, straight lines through the experimental points (from which the curves in Graph 8.12 were drawn) extrapolate to almost the same point on the ordinate (Table 8.10). This indicates that the curves

TABLE 8.10 LIMITING VALUES OF $\Phi/4(QL)^{\frac{1}{2}}$

SO_2 Conc^n % v/v	Gas Inlet Flow cc/sec.	$\left[\frac{\Phi}{4(QL)^{\frac{1}{2}}}\right]^{\frac{1}{2}} \times 10^2$	$\frac{\Phi}{4(QL)^{\frac{1}{2}}} \times 10^5$
80	4.1	0.2123	0.451
80	5.9	0.2116	0.448
80	8.7	0.2108	0.444
			Average 0.448
60	2.7	0.1760	0.310
60	4.1	0.1755	0.308
60	6.6	0.1758	0.309
			Average 0.309

Graph 8.13

Graph 8.13

Limiting Values of $\Phi/4(QL)^{\frac{1}{2}}$.

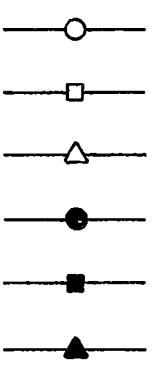

SO_2 = 80% v/v; Gas Inlet Flow = 4.1 cc/sec

SO_2 = 80% v/v; Gas Inlet Flow = 5.9 cc/sec

SO_2 = 80% v/v; Gas Inlet Flow = 8.7 cc/sec

SO_2 = 60% v/v; Gas Inlet Flow = 2.7 cc/sec

SO_2 = 60% v/v; Gas Inlet Flow = 4.1 cc/sec

SO_2 = 60% v/v; Gas Inlet Flow = 6.6 cc/sec

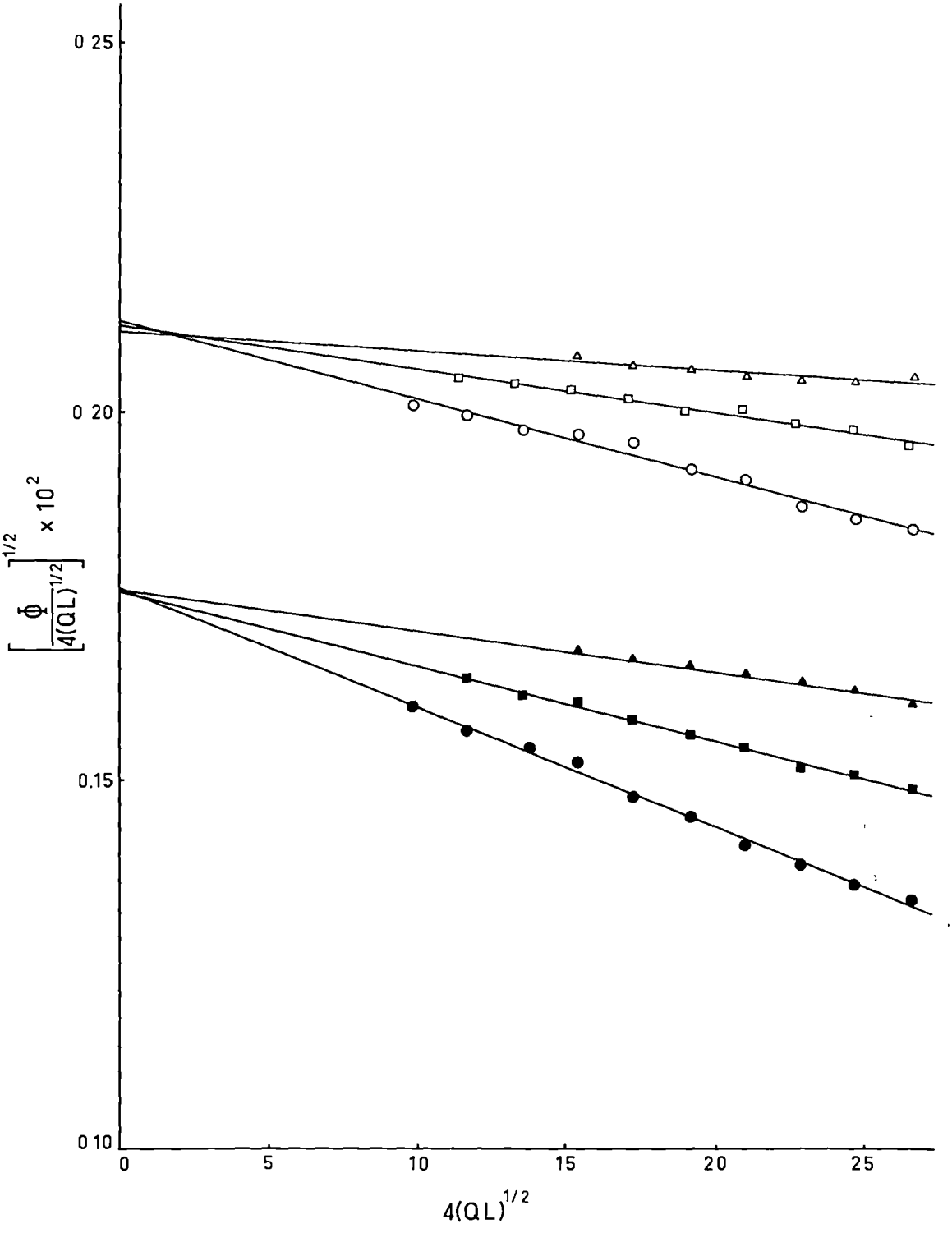
0 25
0 20
0.15
0 10
0
5
10
15
20
25
$\left[\frac{\Phi}{4(QL)^{1/2}}\right]^{1/2} \times 10^2$
$4(QL)^{1/2}$

in Graph 8.12 have the same limiting slope at zero jet length and it seems reasonable to assume that the extrapolation eliminates the effects of reduced SO_2 pressure and gas hydronamics.

If these limiting slopes (Table 8.10) are compared with those predicted theoretically (Table 8.9 and Graph 8.11), the agreement is seen to be good. The experimentally measured slope at the lower SO_2 concentration is about 4% lower than the corresponding predicted value, and this most probably arises from the method used to correct for jet hydronamics. This involved neglecting the gas-phase resistance and assuming that liquid-phase hydronamic factors could be applied without further correction. This gives values of $\Phi/4(QL)^{\frac{1}{2}}$ which are too low and introduces errors which increase with decreasing SO_2 concentration. It was for this reason that lower SO_2 concentrations were not investigated.

The writer suggests that penetration-theory concepts may be extended to the study of gas-phase transfer in industrial absorption equipment. In particular it may be profitable to develop theories analogous to those that have been developed for liquid-phase transfer [5,24-27]. The essential difference between the mechanisms in the two phases would be that the Fick's law diffusion coefficients used to describe gas-phase transfer would need to be corrected, as described above, to allow for changes in the partial pressure of the solute gas.

8.8 CONCLUSIONS

During the last twenty years it has been established that the overall chemical reaction between sulphur dioxide and water can be described, to a good first approximation, by the classical equation

$$SO_2 + H_2O \rightleftharpoons H^+ + HSO_3^- \qquad (1)$$

However, the only two attempts to measure the rate constant for this reaction have yielded very conflicting results and, consequently, measured rates of absorption of sulphur dioxide into water have been interpreted in two different ways. Many of these measurements were made under unsteady-state conditions using a variety of experimental techniques, and they all appeared to indicate a process of physical absorption. In some cases this was interpreted to mean that the reaction is so slow that it has no effect on the absorption process: in these cases the absorption measurements were used to estimate diffusion coefficients for un-ionized sulphur dioxide molecules. In other cases it was suggested that if the reaction is fast, the diffusion coefficients estimated in this way would be some 'effective' coefficient for all the diffusing spcies - i.e. for un-ionized sulphur dioxide molecules and $H^+.HSO_3^-$ ion-pairs.

In this investigation a laminar-jet technique was used

and unsteady-state measurements were made of the rates of absorption of sulphur dioxide into different aqueous solutions. Inasmuch as absorption into water appears to be a physical process, the results support the conclusions reached in the previous studies and the diffusion coefficient calculated on the basis of physical absorption theory - i.e. simple penetration theory - agrees very well with the coefficients similarly calculated in these studies.

To examine the effect of reaction (1) on the absorption process a mathematical model was established in which the reaction was assumed to be pseudo first order and the two extreme cases of a very slow reaction and a very fast reaction were considered. The model was used to interpret measured rates of absorption into hydrochloric acid solutions and the results clearly indicated the reaction to be very fast.

The model also indicated that the value of the 'effective' diffusion coefficient, estimated from results for absorption into water, will depend on the conditions of measurement. In particular, because the diffusion coefficient for the $H^+.HSO_3^-$ ion-pair is much lower than that for un-ionized sulphur dioxide molecules, and because the ratio $[H^+].[HSO_3^-] / [SO_2]$ increases with decreasing sulphur dioxide concentration, the estimate will depend on the concentration of sulphur dioxide at the gas-liquid

interface. That different investigations have yielded similar estimates arises from the fact that similar interfacial concentrations were used in each investigation.

In addition, the estimate will be affected by the interfacial concentration if either of the diffusing species exhibits any concentration-dependence. This was investigated by absorbing sulphur dioxide into its aqueous solution and the former effect was allowed for by analysing the measurements in terms of the mathematical model for a very fast reaction. This gave estimates of the 'effective' diffusion coefficient at different sulphur dioxide concentrations as well as estimates of the differential coefficients for both un-ionized sulphur dioxide molecules and the $H^+.HSO_3^-$ ion-pair. The results obtained have three important consequences:

(i) previous estimates of the diffusion coefficient for un-ionized sulphur dioxide molecules in water, obtained from data other than absorption rates, do not appear to agree very well and many authors have commented on this. However, a close examination of the original data shows that the discrepancies arise from differences in experimental conditions. If suitable allowances are made for these differences, the coefficients agree extremely well with the estimates made in this investigation. One notable feature of these estimates

is that they indicate a much higher coefficient in dilute solutions than is predicted by semi-empirical relationships; this is thought to be due to the dipole moment of the molecule.

(ii) all estimates of diffusion coefficients were made using solubility data obtained in this investigation; the good agreement between different estimates discussed in (i) is considered to reflect favourably on the precision of the solubility measurements.

(iii) the 'effective' diffusion coefficient is shown to exhibit a marked concentration-dependence at low sulphur dioxide concentrations. This becomes important when it is considered that most industrial absorption processes are carried out at these concentrations and that the concentration of sulphur dioxide in the gas outlet of an absorption tower is usually much lower than in the gas inlet. This demonstrates the need for extreme caution when using laboratory absorption data to evaluate the performance of industrial equipment. This may apply not only to sulphur dioxide absorption but also to other processes, such as the absorption of chlorine, in which a chemical reaction occurs between a relatively soluble gas and its absorbent. It is suggested that it may be profitable to re-evaluate many of the absorption

experiments that have been carried out under these conditions.

The studies involving absorption of pure sulphur dioxide were concluded with an investigation of the absorption into aqueous sodium hydroxide solutions. The process was regarded as one involving a moving reaction zone, for which a mathematical model is available, and the absorption measurements were analysed in an attempt to determine the reaction mechanism in this zone; three possible reactions were considered, viz.

$$SO_2 + NaOH \rightarrow Na^+ + HSO_3^- \qquad (2)$$

$$2SO_2 + 2NaOH \rightarrow 2Na^+ + S_2O_5^{=} + H_2O \qquad (3)$$

$$SO_2 + 2NaOH \rightarrow 2Na^+ + SO_3^{=} + H_2O \qquad (4)$$

The model predicts the same absorption rates if reactions (2) or (3) occur and lower rates if reaction (4) occurs. Measured rates fell between the two sets of predicted values and it could be argued that both reactions (2) and (4), or (3) and (4), occur. However, the model is based on many simplifying assumptions and it is very difficult to assess the errors that these may introduce. In particular, it does not consider the effect of interactions between diffusing ionic species. Crude theoretical estimates indicate that this effect may be considerable during steady-state absorption with a moving reaction zone but the author suspects that to refine the method of estimation and apply it to unsteady-state conditions may well

be an intractable problem. It is suggested that a more profitable approach may be to elucidate the reaction mechanism in some other way and then to use absorption studies to measure the effects of ionic interactions.

Two other important points which arose from studying the sulphur dioxide - aqueous sodium hydroxide system should also be noted. First, had it been shown that either reaction (2) or (3) occurs in the reaction zone, it would have been possible to distinguish between them only on the basis of kinetic data for the two reactions; such data do not appear to be available. Second, if a gas is absorbed into an aqueous electrolyte and it reacts with the dissolved solute, measured absorption rates are usually interpreted using theoretical solubility data for the gas in the electrolyte; arguments have been advanced in this thesis to show that it would be more accurate to use the solubility data for water.

Since 1950 there has been a marked increase in the number of studies of the effects of liquid-phase hydronamic conditions in industrial absorption equipment. Despite the fact that gas-phase conditions may considerably affect absorption rates in many processes, such as the absorption of sulphur dioxide into water, this has received little attention. The results of the liquid-phase studies suggest that absorption processes may be described by a surface-renewal model of penetration theory. It would be convenient to extend this model to the gas phase but this would require that penetration thoery equations are

applicable to gas-phase transfer. Theoretical considerations indicate that if Fick diffusion equations are used to describe unsteady-state gas-phase transfer, they must be corrected to allow for changes in the partial pressure of the solute gas. This can be achieved by inserting a correction factor into the penetration theory equations but the resulting equations had not been tested experimentally with any precision. In the last part of this investigation sulphur dioxide was absorbed into water from mixtures with nitrogen and the measured absorption rates were shown to agree very well with theoretically predicted values.

The method used to measure absorption rates in this investigation did not permit a study of those dilute mixtures of sulphur dioxide which are of practical importance; from this point of view the value of this investigation is limited. However, it has been shown that techniques established to investigate liquid-phase absorption mechanisms can be adapted to studies of gas-phase transfer without the need to closely define gas-phase hydronamic conditions. It is suggested that this may be of considerable importance in designing further experimental studies of gas-phase transfer.

APPENDIX 1

REFERENCES

1. Whitman, W.G., Chem. & Met. Eng., 29, 146 (1923). Quoted by Ref. 2.
2. Lewis, W.K. & Whitman, W.G., Ind. Eng. Chem., 16, 1215 (1924).
3. Sherwood, T.K. & Pigford, R.L., 'Absorption and Extraction', 2nd ed., McGraw-Hill, New York (1952).
4. Norman, W.S., 'Absorption, Distillation and Cooling Towers', Longmans, Green & Co., London (1961).
5. Danckwerts, P.V., Ind. Eng. Chem., 43, 1460 (1951).
6. Higbie, R., Trans. Am. Inst. Chem. Engrs., 31, 365 (1935).
7. Lynn, S., Straatemeier, J.R. & Kramers, H., Chem. Eng. Sci., 4, 49, 58, 63 (1955).
8. Scriven, L.E., Ph.D. Dissert., Univ. of Delaware, U.S.A. (1956).
9. Scriven, L.E. & Pigford, R.L., Am. Inst. Chem. Engrs. J., 4, 439 (1958).
10. Cullen, E.J. & Davidson, J.F., Chem. Eng. Sci., 6, 49 (1956).
11. Wendel, M.M. & Pigford, R.L., Am. Inst. Chem. Engrs. J., 4, 249 (1958).
12. Vielstich, W., Chem. Ing. Tech., 28, 543 (1956).
13. Raimondi, P., Ph.D. Dissert., Carnegie Inst. Technol., U.S.A. (1957).
14. Raimondi, P. & Toor, H.L., Am. Inst. Chem. Engrs. J., 5, 86 (1959).
15. Harvey, E.A. & Smith, W., Chem. Eng. Sci., 10, 274 (1959).

16. Cullen, E.J. & Davidson, J.F., Trans. Far. Soc., 53, 113 (1957).

17. Davidson, J.F. & Cullen, E.J., Trans. Inst. Chem. Engrs., 35, 51 (1957).

18. Nijsing, R.A.T.O., Ph.D. Thesis, Univ. of Delft, Holland (1957).

19. Chiang, S.H., Ph.D. Dissert., Carnegie Inst. Technol., U.S.A. (1958).

20. Chiang, S.H. & Toor, H.L., Am. Inst. Chem. Engrs. J., 5, 165 (1959).

21. Rehm, T.R., Ph.D. Dissert., Univ. of Washington, U.S.A. (1960).

22. Rehm, T.R., Moll, A.J. & Babb, A.L., Chem. Eng. Prog., 58, 52 (1962); Am. Inst. Chem. Engrs. J., 9, 760 (1963).

23. Govindan, T.S. & Quinn, J.A., Am. Inst. Chem. Engrs.,J., 10, 35 (1964).

24. Danckwerts, P.V. & Kennedy, A.M., Trans. Inst. Chem. Engrs., 32, 49, 53 (1954).

25. Kishinevskii, M.Kh., Zhur. Priklad. Khim., 27, 382 (1954).

26. Toor, H.L. & Marchello, J.M., Am. Inst. Chem. Engrs. J., 4, 97 (1958).

27. Harriott, P., Chem. Eng. Sci., 17, 149 (1962).

28. Olander, D.R., Am. Inst. Chem. Engrs. J., 6, 233 (1960).

29. Danckwerts, P.V., Trans. Far. Soc., 46, 701 (1950).

30. Dhillon, S.S. & Perry, R.H., Am. Inst. Chem. Engrs. J., 8, 389 (1962).

31. Arnold, B.H., Trans. Am. Inst. Chem. Engrs., 40, 361 (1944).

32. Woods, D.R., Ph.D. Dissert., Univ. of Winsconsin, U.S.A. (1961).

33. Danckwerts, P.V., Research (London), 2, 494 (1949); quoted by Ref. 20.

34. Killefer, D.H., Ind. Eng. Chem., 29, 1293 (1937).

35. Cryder, D.S. & Maloney, J.O., Trans. Am. Inst. Chem. Engrs., 37, 827 (1941).

36. Davies, J.T., Trans. Inst. Chem. Engrs., 38, 289 (1960).

37. Emmert, R.E., Ph.D. Dissert., Univ. of Delaware, U.S.A. (1954).

38. Emmert, R.E. & Pigford, R.L., Chem. Eng. Progr., 50, 87 (1954).

39. Edwards, G.R., Robertson, F., Rumford, F. & Thomson, J., Trans. Inst. Chem. Engrs., 32, 6 (1954).

40. Delaney, L.J., Ph.D. Dissert., Univ. of Philadelphia, U.S.A. (1961).

41. Delaney, L.J. & Eagleton, L.C., Am. Inst. Chem. Engrs.,J., 8, 418 (1962).

42. Matsuyama, T., Chem. Eng. (Japan), 14, 245 (1950); Mem. Fac. Eng., Kyoto Univ. (Japan), 15, 142, 151 (1953).

43. Goodgame, T.H. & Sherwood, T.K., Chem. Eng. Sci., 3, 37 (1954).

44. Davies, J.T., Kilner, A.A. & Ratcliffe, G.A., Chem. Eng. Sci., 19, 583 (1964).

45. Chiang, S.H. & Toor, H.L., Am. Inst. Chem. Eng. J., 6, 539 (1960).

46. Vrentas, J.S., Ph.D. Dissert., Univ. of Delaware, U.S.A.(1963).

47. Blank, M., Ph.D. Thesis, Univ. of Cambridge, England (1959).

48. Goodridge, F. & Bricknell, D.J., Trans. Inst. Chem. Engrs., 40, 54 (1962).

49. Goodridge, F. & Robb, I.D., Ind. Eng. Chem. Fund., 4, 49 (1965).

50. Plevan, R.E. & Quinn, J.A., Am. Inst. Chem. Eng. J., 12, 894 (1966).

51. Whitaker, S. & Pigford, R.L., Am. Inst. Chem. Eng. J., 12, 741 (1966).

52. Sternling, C.V. & Scriven, L.E., Am. Inst. Chem. Eng. J., 5, 514 (1959).

53. Ellis, S.R.M. & Biddulph, M., Chem. Eng. Sci., 21, 1107 (1966).

54. Chiang, S.H. & Toor, H.L., Am. Inst. Chem. Eng. J., 10, 398 (1964).

55. Wright, R.J., J. Chem. Soc., 105, 2907 (1914).

56. Garrett, C.S., J. Chem. Soc., 107, 1324 (1915).

57. Schaffer, K. & Kohler, W., Z. anorg. u. allgem. Chem., 104, 212 (1918).

58. Baly, E.C.C. & Bailey, R.A., J. Chem. Soc., 121, 1813 (1922).

59. Dietzel, R. & Galanos, S., Z. Electrochem., 31, 466 (1925).

60. Getman, F.H., J. Phys. Chem., 30, 266 (1926).

61. Ley, H. & Konig, E., Z. physik. Chem., B41, 365 (1938).

62. Harkins, W.D., Gans, D.M. & Bowers, H.E., Nature, 125, 464 (1930).

63. Dickinson, R.G. & West, S.S., Phys. Rev., 35, 1126 (1930).

64. Bhagavantam, S., Nature, 126, 995 (1930).

65. Gerding, H. & Nivjeld, W.J., Nature, 137, 1070 (1936).

66. Fadda, P., Nuovo Cimento, 9, 168 (1932); quoted by Chem. Abs. 27, 230.

67. Nisi, H., Japan. J. Phys., 6, 1 (1930); quoted by Chem. Abs. 25, 4794.

68. Rao, B.P., Proc. Indian Acad. Sci., 20A, 292 (1944).

69. Simon, A. & Waldmann, K., Z. anorg. u. allgem. Chem., 283, 359 (1956).

70. DeMaine, P.A.D., J. Chem. Phys., 26, 1049 (1957).

71. Jones, L.H. & McLaren, E., J. Chem. Phys., 28, 995 (1958).

72. Falk, M. & Giguere, P.A., Can. J. Chem., 36, 1121 (1958).

73. Ratkowsky, D.A., Ph.D. Dissert., Univ. of Washington, U.S.A. (1960).

74. Ratkowsky, D.A. & McCarthy, J.L., J. Phys. Chem., 66, 516 (1962).

75. Eigen, M., Kustin, K. & Maass, G., Z. physik. Chem., 30, 130 (1961).

76. Ellis, A.J. & Anderson, D.W., J. Chem. Soc., 1961, 1765.

77. Dzhabagin, T.K., Roi, D.K. & Semenov, P.A., Khim. Prom., 1963, 870.

78. Rabe, A.E. & Harris, J.F., J. Chem. Eng. Data, 8, 333 (1963).

79. Sherrill, M.S. & Noyes, A.A., J. Am. Chem. Soc., 48, 1861 (1926).

80. Campbell, W.B. & Maass, O., Can. J. Research, 2, 42 (1930).

81. Morgan, O.M. & Maass, O., Can. J. Research, 5, 162 (1931).

82. Johnstone, H.F. & Leppla, P.W., J. Am. Chem. Soc., 56, 2233 (1934).

83. Tartar, H.V. & Garretson, H.H., J. Am. Chem. Soc., 63, 808 (1941).

84. Wang, J.C. & Himmelblau, D.M., Am. Inst. Chem. Engrs. J., 10, 574 (1964).

85. Whitney, R.P. & Vivian, J.E., Chem. Eng. Prog., 45, 323 (1949).

86. Chertkov, B.A., Khim. Prom., 1959, No.7, 586; Chem. Abs., 55, 6956h.

87. Haslam, R.T., Ryan, W.P. & Weber, H.C., Trans. Am. Inst. Chem. Engrs., 15, 177 (1923).

88. Adams, F.W., Trans. Am. Inst. Chem. Engrs., 28, 162 (1932).

89. Johnstone, H.F. & Singh, A.D., Ind. Eng. Chem., 29, 286 (1937).

90. Jenness, L.C. & Caulfield, J.G.L., Paper Trade J., 109, 26, 37 (1939); quoted by Ref. 86.

91. Whitney, R.P. & Han, S.T., Tappi, 35, 569 (1952).

92. Whitney, R.P., Han, S.T. & Davis, J.C., Tappi, 36, 172 (1952).

93. Guyer, A., Richarz, W. & Guyer, A. Jr., Helv. Chem. Acta, 38, 1192 (1955).

94. Parkinson, R.V., Tappi, 39, 522 (1956); Chem. Abs. 50, 13440e.

95. Kafarov, V.V. & Trofinov, V.I., Zh. Priklad. Khim., 31, 1809 (1958); Chem. Abs. 53, 13685e.

96. Lunde, K.E., Ind. Eng. Chem., 50, 293 (1958).

97. Bretsznajder, S., Kawecki, W. & Kotowska, W., Bull. acad. polon. sci., 7, 691 (1959); Chem. Abs. 54, 17982e.

98. Gasyuk, G.N., Bolshakov, A.G., Kortnev, A.V. & Krainii, P.Ya., Zh. Priklad. Khim., 32, 95 (1959).

99. Bettelheim, J., Klimicek, R., Struad, M. & Chlimsky, F., Chem. prumsyl., 10, 281 (1960); Chem. Abs. 54, 23488f.

100. Chertkov, B.A., Khim. Prom., 1960, 47; Chem. Abs. 54, 21939b; Khim. Prom., 1960, 223; Chem. Abs. 56, 5457c; Khim. Prom., 1962, 67; Chem. Abs. 58, 258d; Khim. Prom., 1963, 537; Chem. Abs. 60, 2558f.

101. Chertkov, B.A., Zh. Priklad. Khim., 37, 2437 (1964).

102. Chertkov, B.A., Pucklina, D.L. & Pekareva, T.I., Zh. Priklad. Khim., 32, 1385 (1959); Chem. Abs. 53, 19353e.

103. Thomas, W.J., Trans. Inst. Chem. Engrs., 42, 3, 7 (1964).

104. Vivian, J.E. & Whitney, R.P., Chem. Eng. Prog., 43, 691 (1947).

105. Pearson, D.A., Lundberg, L.A., West, F.B. & McCarthy, J.L., Chem. Eng. Prog., 47, 257 (1951).

106. Toor, H.L. & Chiang, S.H., Am. Inst. Chem. Engrs. J., 5, 339 (1959).

107. Stephens, E.J. & Morris, G.A., Chem. Eng. Prog., 47, 232 (1951).

108. Novella, E.C. & Simo, J.B., Anales Real Soc. Espan., Fis. Y Chim., 57B, 321, 333 (1961).

109. Norman, W.S. & Sammak, F.Y.Y., Trans. Inst. Chem. Engrs., 41, 109 (1963).

110. Ternovskaya, A.N. & Belopolskii, A.P., Zh. Fiz. Khim., 24, 43 (1950).

111. Groothuis, H. & Kramers, H., Chem. Eng. Sci., 4, 17 (1955).

112. Nijising, R.A.T.O., Hendriksz, R.H. & Kramers, H., Chem. Eng. Sci., 10, 88 (1959).

113. Manogue, W.H., Ph.D. Dissert., Univ. of Delaware, U.S.A. (1957).

114. Manogue, W.H. & Pigford, R.L., Am. Inst. Chem. Engrs. J., 6, 494 (1960).

115. Kramers, H., Blind, M.P.P. & Snoeck, E., Chem. Eng. Sci., 14, 115 (1961).

116. Hikita, H., Nakanishi, K. & Kataoka, T., Chem. Eng. (Tokyo), 23, 459 (1959); Chem. Abs., 53, 18561b.

117. Elenkov, D., Ikonopisov, S. & Nankov, N., Compt. Rend. Acad. Bulgare Sci., 16, 266 (1963); Chem. Abs., 62, 3456a.

118. Simon, A. & Waldmann, K., Z. anorg. u. allgem. Chem., 284, 36 (1956).

119. Eriksen, T., Chem. Eng. Sci., 22, 727 (1967).

120. Coughanowr, D.R., Ph.D. Dissert., Univ. of Illinois, U.S.A. (1956).

121. Johnstone, H.F. & Coughanowr, D.R., Ind. Eng. Chem., 50, 1169 (1958).

122. Pritchett, P.W., Ph.D. Dissert., Univ. of Delaware, U.S.A. (1960).

123. Takeuchi, N. & Namba, Y., Hiroshima Daigaku Kogakubu Kenky Hokoku, 12, 241 (1964).

124. International Critical Tables, Vol. 3, McGraw-Hill, New York (1928).

125. Hodgman, C.D. (ed.), 'Handbook of Chemistry and Physics', 38th ed., Chemical Rubber Publishing Co., Cleveland, U.S.A. (1958).

126. Perry, J.H. (ed.), 'Chemical Engineer's Handbook', McGraw-Hill, New York, 4th ed. (1963).

127. Seidell, A., 'Solubilities of Inorganic and Metal Organic Compounds', van Nostrand, New York, 3rd ed. (1940); Supplement (1951).

128. Stephen, H. & Stephen, T., (eds.), 'Solubilities of Inorganic and Organic Compounds', Pergamon Press, London (1963).

129. Kaye, G.W.C. & Laby , T.H., 'Tables of Physical and Chemical Constants', Longmans, Green & Co., London (1955).

130. Lange, N.A. (ed.), 'Handbook of Chemistry', McGraw-Hill, New York, 10th ed. (1961).

131. Sherwood, T.K., Ind. Eng. Chem., 17, 745 (1925).

132. Plummer, A.W., Chem. Eng. Progr., 46, 369 (1950).

133. Beuschlein, W.L. & Simenson, L.O., J. Am. Chem. Soc., 62, 610 (1940).

134. Fox, C.J.J., Z. physik. Chem., 41, 458 (1902); quoted by Ref.127.

135. van Krevelen, D.W. & Hoftyser, P.J., Chim. Industr., 21st Congress Inst. Chim. Ind., 1948, p 168.

136. Fick, A., Pogg. Ann., 94, 59 (1855); Phil. Mag., 10. 30 (1855); quoted by Ref.137).

137. Tyrrel, H.J.V., J. Chem. Educ., 41, 397 (1964).

138. Colè, A.F.W., & Gordon, A.R., J. Phys. Chem., 40, 733 (1936).

139. Crank, J., 'The Mathematics of Diffusion', O.U.P. (1956).

140. Hwang, J.L., J. Chem. Phys., 20, 1320 (1952).

141. Friedmann, N.E., Trans. Am. Soc. Mech. Engrs., 80, 635 (1958).

142. Macey, R.I., Bull, Math., Biophys., 21, 19 (1959); quoted by Ref.188.

143. Yang, K.T., & Szewczyk, A., Trans. Am. Soc. Mech. Engrs., 81C, 251 (1959); quoted by Ref.188.

144. Tsang, T., Ind. Eng. Chem., 52, 707 (1960); J. App. Phys., 32, 1518 (1961).

145. Phillips. J.R., Nature, 185, 233 (1960); Aust. J. Phys., 13, 1 (1960).

146. Greenfield, H., J. Soc. Industr. App. Math., 10, 424 (1962).

147. Heaslet, M.A., & Alksne, A., J. Soc. Industr. App. Math., 9, 584 (1961).

148. Anderson, R.B., Bayer, J. & Hofer, L.J.E., Ind. Eng. Chem., Proc. Des. and Dev., 4, 167 (1965).

149. Duda, J.L. & Vrentas, J.S., Ind. Eng. Chem. Fund., 5, 69 (1966).

150. Stefan, J., Ann. Physik., 41, 723 (1890); quoted by Refs.173, 174.

151. Maxwell, J.C., Phil. Mag., 35, 185 (1868); quoted by Ref.174.

152. Vogel, Ann. Physik., 43, 1235 (1914); quoted by Ref.173.

153. Sutherland, W., Phil. Mag., 36, 507 (1893); quoted by Ref.173.

154. Jeans, J.H., 'The Dynamical Theory of Gases', Longmans, Roberts & Green Co., London (1939).

155. Chapman, S., Trans. Roy. Soc., (London), 211, 479 (19121); quoted by Ref.173.

156. Chapman, S. & Cowling, T.G., 'The Mathematical Theory of Non-Uniform Gases', Cambridge University Press, New York (1952).

157. Hirschfelder, J.O., Curtiss, C.F. & Bird, R.B., 'Molecular Theory of Gases and Liquids', Wiley & Son, New York (1954).

158. Wilke, C.R. & Lee, C.Y., Ind. Eng. Chem., 47, 1253 (1955).

159. Hirschfelder, J.O., Bird., R.B. & Spotz, E.L., Chem. Rev., 44, 205 (1949); Trans. Am. Soc. Mech. Engrs., 72, 921 (1949).

160. Bromley, L.A. & Wilke, C.R., Ind. Eng. Chem., 43, 1641 (1951).

161. Chen, N.H. & Othmer, D.F., J. Chem. Eng. Data, 7, 37 (1962).

162. Stiel, L.I. & Thodos, G., J. Chem. Eng. Data, 7, 234 (1962).

163. Fair, J.R. & Lerner, B.J., Am. Inst. Chem. Engrs., J., 2, 13 (1956).

164. Monchick, L. & Mason, E.A., J. Chem. Phys., 35, 1676 (1961).

165. Stiel, L.I. & Thodos, G., Am. Inst. Chem. Engrs. J., 10, 266 (1964).

166. Mason, E.A. & Monchick, L., J. Chem. Phys., 36, 2746 (1962).

167. Giddings, J.C. & Seager, S.L., Ind. Eng. Chem. Fund., 1, 277 (1962).

168. Holsen, J.N. & Strunk, M.R., Ind. Eng. Chem. Fund., 3, 143 (1964).

169. Walker, R.E. & Westernberg, A.A., J. Chem. Phys., 26, 1753 (1957); 29, 1139, 1147 (1958); 31, 519 (1959); 32, 486 (1960).

170. Mueller, C.R. & Cahill, R.W., J. Chem. Phys., 40, 651 (1964).

171. Reid, R.C. & Sherwood, T.K., 'The Properties of Gases and Liquids', McGraw-Hill, New York, 1958.

172. Andrew, S.P.S., Chem. Eng. Sci., 4, 269 (1955).

173. Arnold, J.H., Ind. Eng. Chem., 22, 1091 (1930).

174. Gilliland, E.R., Ind. Eng. Chem., 26, 681 (1934).

175. Othmer, D.F. & Chen, H.T., Ind. Eng. Chem., Proc. Des. & Dev., 1, 249 (1962).

176. Slattery, J.C. & Bird, R.B., Am. Inst. Chem. Engrs. J., 4, 137 (1958).

177. Ibrahim, S.H. & Kuloor, N.R., Brit. Chem. Eng., 6, 862 (1961).

178. Scott, D.S., Ind. Eng. Chem. Fund., 3, 278 (1964).

179. Himmelblau, D.M., Chem. Rev., 64, 527 (1964).

180. Baird, M.H.I. & Davidson, J.F., Chem. Eng. Sci., 17, 467, 473 (1962).

181. Ratcliffe, G.A. & Holdcroft, J.G., Trans. Inst. Chem. Engrs., 41, 315 (1963).

182. Onda, K., Okamato, T. & Yamaji, Y., Chem. Eng. (Japan), 24, 918 (1960); Mem. Fac. Eng., Nagoya Univ., 13, 138 (1961).

183. Tang, Y.P. & Himmelblau, D.M., Am. Inst. Chem. Engrs. J., 9, 630 (1963).

184. Thomas, W.J. & Furzer, I.A., Chem. Eng. Sci., 17, 115 (1962).

185. Goodridge, F. & Gartside, G., Trans. Inst. Chem. Engrs., 43, 74 (1965).

186. Thomas, W.J. & Adams, M.J., Trans. Far. Soc., 61, 668 (1965).

187. TAng, Y.P., Ph.D. Thesis, Univ. of Texas, U.S.A. (1963).

188. Tang, Y.P. & Himmelblau, D.M., Chem. Eng. Sci., 20, 7 (1965).

189. Kolthoff, I.M. & Miller, C.S., J. Am. Chem. Soc., 63, 2818 (1941).

190. Peaceman, D.W., Sc.D. Thesis, Mass. Inst. of Technol., (1951).

191. Arnold, J.H., J. Am. Chem. Soc., 52, 3937 (1930).

192. Wilke, C.R., Chem. Eng. Progr., 45, 218 (1949).

193. Longsworth, L.G., J. Am. Chem. Soc., 74, 4155 (1952).

194. Othmer, D.F. & Thakar, M.S., Ind. Eng. Chem., 45, 589 (1953).

195. Schiebel, E.G., Ind. Eng. Chem., 46, 2007 (1954).

196. Wilke, C.R. & Chang, Pin, Am. Inst. Chem. Engrs.,J., 1, 264 (1955).

197. Innes, K.K. & Albright, L.F., Ind. Eng. Chem., 49, 1793 (1957).

198. Ibrahim, S.H. & Kuloor, N.R., Brit. Chem. Eng., 5, 795 (1960).

199. Crank, J. & Henry, M.E., Trans, Far. Soc., 45, 636 (1949).

200. Rhodes, E., Ind. Eng. Chem. Fund., 5, 146 (1966).

201. Gordon, A.R., J. Chem. Phys., 5, 522 (1937).

202. Glasstone, S., Laidler, K.J. & Eyring, H., 'The Theory of Rate Processes', McGraw-Hill Book Co., New Ysrk (1941).

203. Darken, L.S., Trans. Am. Inst. Min. (Metall.) Engrs., Metals Div., 175, 184 (1948(; quoted by Ref.188.

204. Gosting, L.J. & Morris, M.S., J. Am. Chem. Soc., 71, 1998 (1949).

205. Hartley, G.S. & Crank, J., Trans. Far. Soc., 45, 801 (1949).

206. Horrocks, J.K. & McLaughlin, E., Trans. Far. Soc., 58, 1357 (1962).

207. Gibbs, R.K. & Himmelblau, D.M., Ind. Eng. Chem. Fund., 2, 55 (1963).

208. Dymond, J. & Hildebrand, J.H., Ind. Eng. Chem. Fund., 6, 130 (1967).

209. Owen, B.B. & Sweeton, F.H., J. Am. Chem. Soc., 63, 2811 (1941).

210. Choppin, G.R. & Buijs, K., J. Chem. Phys., 39, 2042 (1963).

211. Robinson, R.A. & Stokes, R.H., 'Ele ctrolyte Solutions', Butterworths, London (1956).

212. Haslam, R.T., Hershen, R.L. & Keen, R.H., Ind. Eng. Chem., 16, 1224 (1924).

213. Greenwalt, C.H., Ind. Eng. Chem., 18, 1291 (1926).

214. Chilton, C.H. & Colburn, A.P., Ind. Eng. Chem., 26, 1183 (1934).

215. Cooper, C.M., Drew, T.B. & McAdams, W.H., Ind. Eng. Chem., 26, 428 (1934).

216. Gilliland, E.R. & Sherwood, T.K., Ind. Eng. Chem., 26, 516 (1934).

217. Chambers, F.S. & Sherwood, T.K., Ind. Eng. Chem., 29, 1415 (1937).

218. Friedman, S.J. & Miller, C.O., Ind. Eng. Chem., 33, 885 (1941).

219. Kapitsa, P.L., Zhur. Exp. Teor. Fiz., 18, 3 (1948); quoted by Ref.227.

220. Duckler, A.E. & Bergelin, O.P., Chem. Eng. Progr., 48, 557 (1952).

221. Jackson, M.L., A.I.Ch.E.J., 1, 231 (1955).

222. Stirba, C. & Hurt, D.M., A.I.Ch.E.J., 1, 178 (1955).

223. Belkin, B.H.H., MacLeod, A.A., Monrad, C.C. & Rothfus, R.R., A.I.Ch.E.J., 5, 245 (1959).

224. Thomas, W.J. & Portalski, S., Ind. Eng. Chem., 50, 1081 (1958).

225. Duckler, A.E., Chem. Eng. Progr., 55, (10), 62, (1959).

226. Tailby, S.R. & Portalski, S., Trans. I.Ch.E., 38, 324 (1960); 39, 328 (1961).

227. Wilkes, J.O. & Nedderman, R.M., Chem. Eng. Sci., 17, 177 (1962).

228. Portalski, S., Ph.D. Thesis, Univ. of London, England (1960); Chem. Eng. Sci., 18, 787 (C963); ibid. 19, 575 (1964); A.I.Ch.E.J., 10, 584, 586, 597 (1964); Ind. Eng. Chem. Fund., 3, 49 (1964).

229. Davis, E.J., Chem. Eng. Sci., 20, 265 (1965).

230. Bond, J. & Donald, M.B., Chem. Eng. Sci., 6, 237 (1957).

231. Nysing, R.A.T.O. & Kramers, H., Chem. Eng. Sci., 8, 81 (1958).

232. Dekker, W.A., Snoeck, E. & Kramers, H., Chem. Eng. Sci., 11, 61 (1959).

233. Vivian, J.E. & Peaceman, D.W., A.I.Ch.E.J., 2, 437 (1956).

234. Gilliland, E.R., Baddour, E.R. & Brian, P.L.T., A.I.Ch.E.J., 4, 223 (1958).

235. Brian, P.L.T., Vivian, J.E. & Habib, A.G., A.I.Ch.E.J., 8, 205, (1962).

236. Emmert, R.E. & Pigford, R.L. A.I.Ch.E.J., 8, 171, 702 (1962).

237. Roberts, D. & Danckwerts, P.V., Chem. Eng. Sci., 17, 961 (1962).

238. Jaymond, M., Chem. Eng. Sci., 14, 126 (1961).

239. Savinova, E.V. & Tovbin, M.V., Ukrain. Khim. Zhur., 25, 32 (1959).

240. Dirken, MN.J. & Mook, H.W., Biochem. Z., 219, 452 (1930).

241. Uhara, I., Bull. Chem. Soc. (Japan), 18, 412, 429 (1943).

242. Hofmeister, H.K. & Kohlhaas, R., Ber. Bun. Physik. Chem., 69, 232 (1965).

243. Yano, T. & Kawai, K., Chem. Eng. (Japan), 21, 413 (1957).

244. Scriven, L.E. & Pigford, R.L., A.I.Ch.E.J., 5, 397 (1959).

245. Sharma, M.M. & Danckwerts, P.V., Chem. Eng. Sci., 18, 729 (1963); 19, 991 (1964).

246. Clarke, J.K.A., Ind. Eng. Chem. Fund., 3, 239 (1964).

247. Hatch, T.F. & Pigford, R.L., Ind. Eng. Chem. Fund., 1, 209 (1962).

248. Spalding, C.W., A.I.Ch.E.J., 8, 685 (1962).

249. Astarita, G., M.Ch.E. Dissert., Univ. of Delaware, U.S.A. (1960).

250. Astarita, G., Chem. Eng. Sci., 16, 202 (1961).

251. Briggs, D.K.H. & Thompson, G.H., J. App. Chem., 11, 464 (1961).

252. Jeffreys, G.V. & Bull, A.F., Trans. I.Ch.E., 42, 118 (1964);

253. Southwell, "Relaxation Methods", Clarendon Press, Oxford (1946), p.222; quoted by Ref.16.

254. Novella, E.C., Sala, A.L. & Simo, J.B., Anales Real Soc. Espan. Fix. y Quim., B58, 227, 243, 251 (1962).

255. Yoshida, F. & Koyanagi, T., Ind. Eng. Chem., 50, 365 (1958).

256. Yoshida, F. & Miura, Y., A.I.Ch.E.J., 9, 331 (1963).

257. Howkins, J.E. & Davidson, J.F., A.I.Ch.E.J., 4, 324 (1958).

258. Davidson, J.F., Cullen, E.J., Hansen, D. & Roberts, D., Trans. I.Ch.E., 37, 122 (1959).

259. Ratcliffe, G.A. & Reid, K.J., Trans. I.Ch.E., 40, 69 (1962).

260. Ratcliffe, G.A. & Holdcroft, J.G., Chem. Eng. Sci., 15, 100 (1961).

261. Becker, H.G., Ind. Eng. Chem., 16, 1220 (1924).

262. Danckwerts, P.V. & Kennedy, A.M., Chem. Eng. Sci., 8, 201 (1958).

263. Rouse, H. & Hassan, M.M., Mech. Eng., 71, 213 (1949).

264. Boothroyd, J.R., Comm. ACM, 10, 801 (1967).

265. Brian, P.L.T., Vivian, J.E. & Matiatos, D.C., Am. Inst. Chem. Engrs. J., 13, 28 (1967).

266. Sherwood, T.K. & Wei, J.C., Am. Inst. Chem. Engrs. J., 1, 522 (1955).

APPENDIX 2

NOMENCLATURE

A: cross-sectional area of jet in equation (6.2).

A: parameter in equation (A.4.2.); $A = (\pi^2 a_j R_o^4)/4Q^2$.

a: constant in equation (1.33) indicating the effect of a temperature change on the interfacial concentration; defined by $C_{o,h} = C_o + a.\Delta t_i$.

a: parameter defined by equation (1.13).

a: constant in nozzle design; see Fig. 6.1.

a_j: jet acceleration; cm/sec^2.

a_1: dimensionless constant in equation (A.4.5); $a_1 = 1.2262$.

a_2: dimensionless constant in equation (A.4.5); $a_2 = 0.9631$.

a_3: dimensionless constant in equation (A.4.5); $a_3 = 2.2068$.

a_4: dimensionless constant in equation (A.4.6); $a_4 = 0.1873$.

a_5: dimensionless constant in equation (A.4.6); $a_5 = 0.0176$.

B: parameter in equation (A.4.17); evaluated graphically in the present study (see Graph 6.5).

b: constant in nozzle design; see Fig. 6.1.

b: parameter defined by equation (1.14).

b: dimensionless boundary layer thickness; $b = \delta/R_o$.

C: concentration of dissolved gas; gm moles/litre. N.B. when using concentration terms to calculate diffusion coefficients, it is necessary to express C in units of gm moles/cc.

C_i: concentration of unionized species; H^+ of HSO_3^- in the present study; concentration at the gas-liquid interface only in equation (1.30).

C_L: concentration in the body of the liquid.

C_0 or C_S: concentration at the gas-liquid interface; saturation concentration.

$C_{0,h}$: saturation concentration at the gas-liquid interface in the presence of heat effects.

C_p: specific heat of the absorbing liquid; cals/gm.°C.

C_P: concentration of species P.

C_R: concentration of species R.

C_t: concentration of 'total' sulphur dioxide; $C_t = C_u + C_i$.

C_u: concentration of unionized sulphur dioxide.

D: jet diameter; cm.

D_1, D_2: specification in nozzle design; see Fig. 6.1.

D_o: nozzle diameter at nozzle face; cm.

d: depth below liquid surface; cm.

$\mathcal{D}$: 'differential' diffusion coefficient defined by equation (2.4); cm^2/sec.

$\bar{\mathcal{D}}$: 'integral' diffusion coefficient defined by equation (2.5); cm^2/sec.

$\mathcal{D}_G$: diffusion coefficient for gaseous sulphur dioxide.

$\mathcal{D}_i$: diffusion coefficient for ionized species; H^+ and HSO_3^- in the present study.

$\mathcal{D}_t$: diffusion coefficient for 'total' sulphur dioxide; defined by $\mathcal{D}_t = (C_i\mathcal{D}_i + C_u\mathcal{D}_u)/C_t$.

$\mathcal{D}_u$: diffusion coefficient for unionized species; unionized sulphur dioxide in the present study.

$\mathcal{D}(0)$: differential diffusion coefficient at infinite dilution.

F_a: dimensionless parameter, defined by equation (A.4.15), indicating the effect of jet acceleration on local absorption rates.

F_b: dimensionless parameter, defined by equations (A.4.16) and (A.4.17), indicating the effect of the jet boundary layer on local absorption rates.

F_g: Factor to correct gas-phase Fick diffusion coefficients for unsteady state absorption.

F_h: dimensionless parameter, defined by equation (6.6), indicating the effect of jet hydronamics on total absorption rates.

F_j: dimensionless parameter, defined by equation (A.4.14), indicating the total effect of jet hydronamics on local absorption rates.

F_{R1}: factor, defined by equation (1.15), indicating the effect of a first order reaction on total absorption rates.

F_{R2}: factor, defined by equations (1.27) and (1.28), indicating the effect of a second order reaction on total absorption rates.

G: gas.

g: acceleration due to gravity; g = 981 cm/sec^2.

H: Henry's law constant; ergs/gm mole in equation (1.31) and mm Hg. litre/gm mole in solubility measurements.

H_s: total heat change accompanying absorption; sum of heat of solution and heat of reaction; cals/gm mole.

K: equilibrium constant for a first order, reversible reaction with two products; defined by equation (1.10).

K_1: constant defined by equation (1.35).

K_2: constant defined by equation (1.36).

K_a: thermodynamic ionization constant for the reaction

$$SO_2 + H_2O \rightleftarrows H^+ + HSO_3^-;$$

defined by

$$K_a = \frac{\gamma_\pm^2 . C_i^2}{\gamma_u . C_u} : \text{moles per litre.}$$

K_c: concentration ionization constant for the reaction

$$SO_2 + H_2O \rightleftarrows H^+ + HSO_3^-;$$

defined by

$$K_c = \frac{C_i^2}{C_u} ; \text{ moles per litre.}$$

k: thermal cibductivity of absorbing liquid in equations (1.32), (1.33) and (1.35); cals/°C.cm.sec.

k: Boltzmann's constant in equation (2.7); 1.380×10^{-16} ergs/°C.

k_G: gas-phase mass transfer coefficient; moles cm Hg/cm^2.sec.

k_i: interfacial mass transfer coefficient; cm/sec.

k_L: liquid-phase mass transfer coefficient; cm/sec.

k_{LR}: liquid-phase mass transfer coefficient when absorption is accompanied by a chemical reaction.

L: jet length; cm.

ℓ: length of flat plate required to produce a boundary layer of thickness δ; cm.

M: molecular weight or molarity.

m: number of moles of gas G which reacts with solute S.

N, N_A: local (instantaneous) absorption rate; gm moles/cm^2.sec.

N_h: local absorption rate in the present of heat effects; defined by equation (1.34).

N_X: local absorption in a real jet at a point X cm downstream.

$N_{X,id}$: local absorption rate in an ideal jet at a point X cm downstream.

n: subscript denoting sodium chloride in Section 8.3.

P: section of the jet at which the boundary layer disappears.

P: total gas pressure in absorption chamber; cm Hg.

P: product species for a first order reaction in equation (1.10) ($C_P = C_{P_1} = C_{P_2}$), or a second order reaction in equation (1.16).

P_1,P_2: products of a first order reaction in equation (1.9).

p: partial pre-sure of solute gas; cm Hg.

p: constant defined by equation (8.3).

p_G: partial pressure of solute gas in the body of the gas phase.

p_G': dimensionless partial pressure (mole fraction) of solute gas in the body of the gas phase; $p_G' = p_G/P$.

p_0: partial pressure of solute gas at the gas-liquid interface.

p_0': dimensionless partial pressure (mole fraction) of solute gas at the gas-liquid interface; $p_0' = p_0/P$.

Q: jet flow rate; cc/sec.

q: constant defined by equation (8.5).

R: species undergoing first order reaction in equation (1.9).

R: jet radius; cm.

R_c: gas constant; 6.236×10^3 cm Hg/gm mole.°K.

R_o: nozzle radius at the nozzle face; cm.

r: molecular radius in equation (2.7); cm.

r: dimensionless parameter in equation (A.4.2); $r = R_o/R$.

S: dissolved solute which reacts with an absorbing gas according to a second order reaction; cf. equation (1.16).

T: absolute temperature; °K.

t: temperature; °C.

Δt_i: temperature change at the gas-liquid interface; °C.

V: velocity; cm/sec.

V_{id}: uniform velocity of an ideal jet.

$V_{o,av}$: average jet velocity at nozzle face.

$V_{o,c}$: velocity in jet core at nozzle face.

$V_{o,Y}$: axial component of velocity in jet boundary layer at nozzle face.

V_s: velocity of jet surface.

$V_{s,X}$: velocity of jet surface at a point X cm downstream.

V_u: velocity of undisturbed fluid flowing past a flat plate.

V_w: velocity of fluid in the wake directly behind a flat plate.

V_X: axial component of jet velocity.

V_Y: radial component of jet velocity.

W: width of wake behind a flat plate; cm.

w: subscript denoting water in Section 8.3.

X: distance measured from nozzle face in direction of jet flow; cm.

X_1, X_2, X_3, X_4: specifications in nozzle design; see Fig. 6.1.

x (or X): direction of diffusion.

Y: distance into jet, measured at nozzle face perpendicular to direction of jet flow; cm.

α: condensation coefficient (fraction of gas molecules striking a liquid surface which actually condense) in equation (1.31).

α: degree of ionization.

β: dimensionless parameter defined by equation (1.33).

$\gamma^{\pm}$: mean activity coefficient of the ionized species.

γ_u: activity coefficient of the unionized species.

δ: thickness of the jet boundary layer at the nozzle face; cm.

η: dynamic viscosity; gm/cm.sec - poise.

θ: time; secs.

θ: parameter used in Appendix 3; cm^2.

κ: specific conductance; $ohms^{-1}.cm^{-1} \times 10^3$.

Λ: equivalent conductance; $ohms^{-1}.cm^2$.

Λ_o: equivalent conductance at infinite dilution.

$\Lambda_{o,c}$: equivalent conductance at infinite dilution for a solution that otherwise has the same properties as one whose concentration is C.

ν: kinematic viscosity; cm^2/sec.

ξ: dimensionless parameter in equations (A.4.5) and (A.4.6); $\xi = (X/4\ell)^{1/3}$.

ρ: density of absorbing liquid; gm/cc.

ρ_m: molal density of absorbed gas; gm moles/cc.

σ: parameter defined by equations (1.28) and (1.29).

Φ: total absorption rate over the surface of a real jet; in Appendix 5 denotes measured absorption rates which have been corrected to a common temperature and pressure and to which hydronamic corrections have also been made; gm moles/sec.

Φ_{id}: total absorption rate over the surface of an ideal jet.

Φ': measured absorption rates which have been corrected to an interfacial temperature of 20°C and a gas partial pressure of 76.0 cm Hg.

Φ'': measured absorption rates.

APPENDIX 3

ABSORPTION ACCOMPANIED BY A FAST, REVERSIBLE, FIRST ORDER REACTION

Consider the reaction

$$R \rightleftarrows P_1 + P_2 \qquad \text{(A.3.1)}$$

If the products P_1 and P_2 are univalent ions of opposite sign, they will diffuse together as an ion pair with a diffusion coefficient $\mathcal{D}_P$. If the reaction is very fast compared with the rate of diffusion, equilibrium conditions will be approached at all points along the diffusion path and the concentrations of reactant and product can be related by

$$K = \frac{[P_1][P_2]}{[R]} = \frac{[P]^2}{[R]} \quad \text{for all } x \qquad \text{(A.3.2)}$$

Hereafter, for convenience, [P] will be written as P and [R] as R.

Consider a slab of thickness dx in the diffusion path. A materials balance for both components gives

$$\mathcal{D}_R \frac{\partial^2 R}{\partial x^2} + \mathcal{D}_P \frac{\partial^2 P}{\partial x^2} = \frac{\partial}{\partial t}(R + P) \qquad \text{(A.3.3)}$$

Since $P = (KR)^{\frac{1}{2}}$, equation (A.3.3) becomes

$$\mathcal{D}_R \frac{\partial^2}{\partial x^2}\left[R + \frac{\mathcal{D}_P}{\mathcal{D}_R}(KR)^{\frac{1}{2}}\right] = \frac{\partial}{\partial t}\left[R + (KR)^{\frac{1}{2}}\right] \qquad \text{(A.3.4)}$$

Write $\theta = \mathcal{D}_R t$; $\gamma = K^{\frac{1}{2}} \frac{\mathcal{D}_P}{\mathcal{D}_R}$

Then

$$\frac{\partial^2}{\partial x^2}\left[R + \gamma R^{\frac{1}{2}}\right] = \frac{\partial}{\partial \theta}\left[R + (KR)^{\frac{1}{2}}\right] \qquad \text{(A.3.5)}$$

The appropriate boundary conditions are;

$t = 0,\ R = R_L$ for all x : $\theta = 0,\ R = R_L$ for all x

$x = \infty,\ R = R_L$ for all t : $x = \infty,\ R = R_L$ for all θ

$x = 0,\ R = R_0$ for all t : $x = 0,\ R = R_0$ for all θ

Assume $R = R\left(\frac{x}{\sqrt{\theta}}\right) = R(\eta)\ ;\quad \eta = \frac{x}{\sqrt{\theta}}$

Then $$\frac{\partial R}{\partial x} = \frac{dR}{d\eta} \cdot \frac{\partial \eta}{\partial x} = \frac{1}{\sqrt{\theta}} \cdot \frac{dR}{d\eta}\ ,$$

$$\frac{\partial^2 R}{\partial x^2} = \frac{1}{\sqrt{\theta}} \cdot \frac{d^2R}{d\eta^2} \cdot \frac{\partial \eta}{\partial x} = \frac{1}{\theta}\frac{d^2R}{d\eta^2}\ ,$$

$$\frac{\partial R}{\partial \theta} = \frac{dR}{d\eta} \cdot \frac{\partial \eta}{\partial \theta} = -\frac{\eta}{2\theta} \cdot \frac{dR}{d\eta}$$

and equation (A.3.5) becomes

$$\frac{d^2}{d\eta^2}\left[R + \gamma R^{\frac{1}{2}}\right] + \frac{\eta}{2} \cdot \frac{d}{d\eta}\left[R + (KR)^{\frac{1}{2}}\right] = 0 \qquad \text{(A.3.6)}$$

Case 1. $\mathcal{D}_P = \mathcal{D}_R$

In this case $\gamma = K^{\frac{1}{2}}$ and equation (A.3.6) becomes

$$\frac{d^2}{d\eta^2}\left[R + (KR)^{\frac{1}{2}}\right] + \frac{\eta}{2} \cdot \frac{d}{d\eta}\left[R + (KR)^{\frac{1}{2}}\right] = 0$$

which gives

$$\frac{d}{d\eta}\left[R + (KR)^{\frac{1}{2}}\right] = C_1 \exp\left[-\int_0^{\eta} \frac{\eta}{2}\, d\eta\right] = C_1 \exp\left(-\frac{\eta^2}{4}\right)$$

and

$$\left[R + (KR)^{\frac{1}{2}}\right] = C_2 + C_1 \int_0^{\eta} \exp\left(-\frac{x^2}{4}\right) dx$$

At $\eta = 0$, $R = R_0$

$$\therefore \quad C_2 = R_0 + (KR_0)^{\frac{1}{2}}$$

At $\eta = \infty$, $R = R_L$

$$\therefore \quad R_L + (KR_L)^{\frac{1}{2}} = R_0 + (KR_0)^{\frac{1}{2}} + C_1 \int_0^{\eta} \exp\left(-\frac{x^2}{4}\right) dx$$

$$\therefore \quad R_L - R_0 + K^{\frac{1}{2}}(R_L^{\frac{1}{2}} - R_0^{\frac{1}{2}}) = C_1 \sqrt{\pi}$$

$$\therefore \quad C_1 = \frac{1}{\sqrt{\pi}}\left[(R_L - R_0) + K^{\frac{1}{2}}(R_L^{\frac{1}{2}} - R_0^{\frac{1}{2}})\right]$$

Now $$N(t) = -\mathcal{D}_R\left(\frac{\partial R}{\partial x}\right)_{x=0} - \mathcal{D}_P\left(\frac{\partial P}{\partial x}\right)_{x=0}$$

$$\therefore \quad N(t) = -\mathcal{D}_R\left[\frac{\partial}{\partial x}\,(R + K^{\frac{1}{2}}R^{\frac{1}{2}})\right]_{x=0}$$

$$= -\left[\frac{\mathcal{D}_R}{t}\right]^{\frac{1}{2}}\left[\frac{\partial}{\partial \eta}(R + K^{\frac{1}{2}}R^{\frac{1}{2}})\right]_{\eta=0}$$

But $$\left[\frac{\partial}{\partial \eta}(R + K^{\frac{1}{2}}R^{\frac{1}{2}})\right]_{\eta=0} = \left[\frac{\partial}{\partial \eta}\left(C_2 + C_1 \int_0^{\eta} \exp\left(-\frac{x^2}{4}\right) dx\right)\right]$$

$$= \left[C_1 \exp\left(-\frac{\eta^2}{4}\right)\right]_{\eta=0}$$

$$= C_1$$

$$\therefore \quad N(t) = \left[\frac{\mathcal{D}_R}{\pi t}\right]^{\frac{1}{2}}[R_0 - R_2]\left[1 + \frac{K^{\frac{1}{2}}}{R_0^{\frac{1}{2}} + R_L^{\frac{1}{2}}}\right] \qquad (A.3.7)$$

and

$$\Phi = \left[\frac{\mathcal{D}_R t}{\pi}\right]^{\frac{1}{2}}[A(R_0 - R_L)]\left[1 + \frac{K^{\frac{1}{2}}}{R_0^{\frac{1}{2}} + R_L^{\frac{1}{2}}}\right] \qquad (A.3.8)$$

It is thus seen that the factor

$$F = \left[1 + \frac{K^{\frac{1}{2}}}{R_0^{\frac{1}{2}} + R_L^{\frac{1}{2}}}\right] \qquad (A.3.9)$$

indicates the effect of the chemical reaction on the absorption rate.

Case 2. $\mathcal{D}_P \neq \mathcal{D}_R$

The appropriate boundary conditions for equation (A.3.6) are:

$\theta = 0, \quad R = R_L$ for all x
$x = \infty, \quad R = R_L$ for all θ } ; $\quad \eta = \infty, \quad R = R_L$

$x = 0, \quad R = R_0$ for all θ; $\quad \eta = 0, \quad R = R_0$

Now $$\frac{d}{d\eta}(R^{\frac{1}{2}}) = \frac{1}{2} R^{-\frac{1}{2}} \frac{dR}{d\eta}$$

and $$\frac{d^2}{d\eta^2}(R^{\frac{1}{2}}) = \frac{1}{2} R^{-\frac{1}{2}} \frac{d^2A}{d\eta^2} - \frac{1}{4} R^{-3/2}\left(\frac{dR}{d\eta}\right)^2$$

$\therefore$ in equation (A.3.6)

$$\frac{d^2R}{d\eta^2} + \frac{\gamma R^{-\frac{1}{2}}}{2} \cdot \frac{d^2R}{d\eta^2} - \frac{\gamma R^{-3/2}}{4}\left(\frac{dR}{d\eta}\right)^2 + \frac{\eta}{2}\frac{dR}{d\eta} + \frac{K^{\frac{1}{2}} \eta R^{-\frac{1}{2}}}{4}\frac{dR}{d\eta} = 0$$

$$\therefore \quad \frac{d^2R}{d\eta^2} + \left(\frac{\eta R^{\frac{1}{2}} + \frac{K^{\frac{1}{2}}\eta}{2} - \frac{\gamma}{2R}\frac{dR}{d\eta}}{2R^{\frac{1}{2}} + \gamma}\right)\frac{dR}{d\eta} = 0 \qquad \text{(A.3.10)}$$

Now $$N(t) = -\mathcal{D}_R\left(\frac{\partial R}{\partial x}\right)_{x=0} - \mathcal{D}_P\left(\frac{\partial P}{\partial x}\right)_{x=0}$$

$$\therefore \quad N(t) = -\mathcal{D}_R\left[\frac{\partial}{\partial x}(R + \gamma R^{\frac{1}{2}})\right]_{x=0}$$

Now $$\left(\frac{\partial A}{\partial x}\right)_{x=0} = \frac{1}{\theta^{\frac{1}{2}}}\left(\frac{\partial A}{\partial \eta}\right)_{\eta=0}$$

and $$\left(\frac{\partial}{\partial x}R^{\frac{1}{2}}\right)_{x=0} = \frac{1}{\theta^{\frac{1}{2}}} \cdot \frac{1}{2}\left(R^{-\frac{1}{2}} \cdot \frac{dR}{d\eta}\right)_{\eta=0}$$

$$= \frac{R_0^{\frac{1}{2}}}{2\theta^{\frac{1}{2}}}\left(\frac{dR}{d\eta}\right)_{\eta=0}$$

$$\therefore \quad N(t) = -\frac{\mathcal{D}_R}{\theta^{\frac{1}{2}}}\left(1 + \frac{\gamma R_0^{-\frac{1}{2}}}{2}\right)\left(\frac{dR}{d\eta}\right)_{\eta=0}$$

$$\therefore \quad N(t) = -\left(\frac{\mathcal{D}_R}{t}\right)^{\frac{1}{2}}\left(\frac{2R_0^{\frac{1}{2}} + \gamma}{2R_0^{\frac{1}{2}}}\right)\left(\frac{dR}{d\eta}\right)_{\eta=0} \qquad \text{(A.3.11)}$$

From equation (A.3.10) we have

$$\frac{d^2R}{d\eta^2} + F(\eta)\frac{dR}{d\eta} = 0 \qquad \text{(A.3.12)}$$

where $$F(\eta) = \frac{\eta R^{\frac{1}{2}} + \frac{K^{\frac{1}{2}}\eta}{2} - \frac{\gamma}{2R} \cdot \frac{dR}{d\eta}}{2R^{\frac{1}{2}} + \gamma} \qquad \text{(A.3.13)}$$

This gives

$$\frac{dR}{d\eta} = C_1 \exp\left(-\int_0^{\eta} F(x)dx\right) \qquad \text{(A.3.14)}$$

and

$$R = C_2 + C_1 \int_0^{\eta} \exp\left(-\int_0^{y} F(x)dx\right)dy \qquad \text{(A.3.15)}$$

From the boundary condition $\eta = 0$, $R = R_0$, equation (A.3.14) gives

$$\left(\frac{dR}{d\eta}\right)_{\eta=0} = C_1 \qquad \text{(A.3.16)}$$

and equation (A.3.15) gives

$$R_0 = C_2$$

From the other boundary condition $\eta = \infty$, $R = R_L$, equation (A.3.15) gives

$$R_L - R_0 = C_1 \int_0^{\infty} \exp\left[-\int_0^{y} F(x)dx\right]dy$$

Now expand $F(\eta)$ in a Maclaurin's series and consider only the first two terms.

$$F(\eta) = F(0) + F'(0)_{\eta} + \ldots$$

Then

$$F(0) = -\frac{\frac{\gamma}{2R_0}\left(\frac{dR}{d\eta}\right)_{\eta=0}}{2R_0^{\frac{1}{2}} + \gamma}$$

$$\therefore \quad F(0) = -\frac{\gamma C_1}{2R_0(2R_0^{\frac{1}{2}} + \gamma)} \qquad \text{(A.3.17)}$$

$$\text{and } F'(\eta) = \frac{[2R^{\frac{1}{2}} + \gamma][R^{\frac{1}{2}} + \frac{\eta R^{-\frac{1}{2}}}{2} \cdot \frac{dR}{d\eta} + \frac{K^{\frac{1}{2}}}{2} - \frac{\gamma}{2R} \cdot \frac{d^2R}{d\eta^2} + \frac{\gamma}{2R^2}\left(\frac{dR}{d\eta}\right)^2]}{[2R^{\frac{1}{2}} + \gamma]^2}$$

$$- \frac{[\eta R^{\frac{1}{2}} + \frac{K^{\frac{1}{2}}\eta}{2} - \frac{\gamma}{2R}\frac{dR}{d\eta}][R^{-\frac{1}{2}}\frac{dR}{d\eta}]}{[2R^{\frac{1}{2}} + \gamma]^2}$$

$$\therefore F'(\eta) = \frac{[2R^{\frac{1}{2}} + \gamma][R^{\frac{1}{2}} + \frac{K^{\frac{1}{2}}}{2}] + [\gamma - K^{\frac{1}{2}}][\frac{\eta R^{-\frac{1}{2}}}{2}]\frac{dR}{d\eta}}{[2R^{\frac{1}{2}} + \gamma]^2}$$

$$- \frac{\frac{\gamma}{2R}[2R^{\frac{1}{2}} + \gamma]\frac{d^2R}{d\eta^2} + \frac{\gamma}{2R^2}[3R^{\frac{1}{2}} + \gamma][\frac{dR}{d\eta}]^2}{[2R^{\frac{1}{2}} + \gamma]^2} \qquad \text{(A.3.18)}$$

From equation (A.3.12) we have

$$\left(\frac{d^2R}{d\eta^2}\right)_{\eta=0} = -F(0)\left(\frac{dR}{d\eta}\right)_{\eta=0}$$

$$\therefore \left(\frac{d^2R}{d\eta^2}\right)_{\eta=0} = \frac{\gamma C_1}{2R_0(2R_0^{\frac{1}{2}} + \gamma)}$$

$$\text{and } F'(0) = \frac{(2R_0^{\frac{1}{2}} + \gamma)(R_0^{\frac{1}{2}} + \frac{K^{\frac{1}{2}}}{2}) - \frac{\gamma^2 C_1^2}{4R_0^2} + \frac{\gamma C_1^2}{2R_0^2}(3R_0^{\frac{1}{2}} + \gamma)}{(2R_0^{\frac{1}{2}} + \gamma)^2}$$

$$\therefore F'(0) = \left(\frac{R_0^{\frac{1}{2}} + \frac{K^{\frac{1}{2}}}{2}}{2R_0^{\frac{1}{2}} + \gamma}\right) + \frac{\gamma^2 C_1^2}{4R_0^2} \cdot \frac{(\frac{6R_0^{\frac{1}{2}}}{\gamma} + 1)}{(2R_0^{\frac{1}{2}} + \gamma)^2} \qquad \text{(A.3.19)}$$

Now

$$\int_0^y F(x)dx \simeq \int_0^y [F(0) + x\,F'(0)]dx$$

$$\simeq F(0)y + F'(0)\,\frac{y^2}{2}$$

$$\therefore \int_0^\infty \exp\,[-\int_0^y F(x)dx]dy \simeq \int_0^\infty \exp - [\frac{F'(0)}{2} \cdot y^2 + F(0)y]dy$$

$$= \int_0^\infty \exp - [\frac{F'(0)}{2}\{y^2 + \frac{2F(0)}{F'(0)} \cdot y\}]dy$$

$$= \int_0^\infty \exp - [(\frac{F'(0)}{2})\{(y + \frac{F(0)}{F'(0)})^2 - (\frac{F(0)}{F'(0)})^2\}]dy$$

$$= \exp \frac{\{F(0)\}^2}{2F'(0)} \int_{\frac{F(0)}{F'(0)}}^\infty \exp\,\{-\frac{F'(0)}{2} \cdot z^2\}dz$$

where $z = y + \frac{F(0)}{F'(0)}$

$$= \exp \frac{\{F(0)\}^2}{2F'(0)}\,[\int_0^\infty \exp\,\{-\frac{F'(0)}{2} \cdot z^2\}dz - \int_0^{\frac{F(0)}{F'(0)}} \exp\,\{-\frac{F'(0)}{2} \cdot z^2\}dz\,]$$

$$= \exp \frac{\{F(0)\}^2}{2F'(0)}\,[\,(\frac{\pi}{2F'(0)})^{\frac{1}{2}} - (\frac{2}{F'(0)})^{\frac{1}{2}} \int_0^{\frac{F(0)}{(2F'(0))^{\frac{1}{2}}}} \exp\,(-w^2)dw\,]$$

$$= \exp\frac{(F(0))^2}{2F'(0)}\left[\left(\frac{\pi}{2F'(0)}\right)^{\frac{1}{2}} - \left(\frac{2}{F'(0)}\right)^{\frac{1}{2}} \cdot \frac{\pi^{\frac{1}{2}}}{2}\,\mathrm{erf}\left(\frac{F(0)}{(2F'(0))^{\frac{1}{2}}}\right)\right]$$

$$= \left(\frac{\pi}{2F'(0)}\right)^{\frac{1}{2}} \cdot \exp\frac{(F(0))^2}{2F'(0)}\left[1 - \mathrm{erf}\left(\frac{F(0)}{(2F'(0))^{\frac{1}{2}}}\right)\right]$$

$$= \left(\frac{\pi}{2F'(0)}\right)^{\frac{1}{2}} \exp\frac{(F(0))^2}{2F'(0)}\,\mathrm{erfc}\left(\frac{F(0)}{(2F'(0))^{\frac{1}{2}}}\right)$$

$$\therefore\quad R_L - R_0 = C_1\left(\frac{\pi}{2F'(0)}\right)^{\frac{1}{2}} \exp\frac{(F(0))^2}{2F'(0)}\,\mathrm{erfc}\left(\frac{F(0)}{(2F'(0))^{\frac{1}{2}}}\right)$$

$$\therefore\quad C_1 = \frac{R_L - R_0}{\left(\frac{\pi}{2F'(0)}\right)^{\frac{1}{2}} \exp\frac{(F(0))^2}{2F'(0)}\,\mathrm{erfc}\left(\frac{F(0)}{(2F'(0))^{\frac{1}{2}}}\right)}$$

Writing $F(0) = a$ and $2F'(0) = b$, we have

$$C_1 = \frac{R_L - R_0}{\left(\frac{\pi}{b}\right)^{\frac{1}{2}} \exp\left(\frac{a^2}{b}\right)\mathrm{erfc}\left(\frac{a}{b^{\frac{1}{2}}}\right)}$$

Now from equations (A.3.11) and (A.3.16) we have

$$N(t) = -\left(\frac{\mathcal{D}_R}{t}\right)^{\frac{1}{2}}\left(\frac{2R_0^{\frac{1}{2}} + \gamma}{2R_0^{\frac{1}{2}}}\right) C_1$$

whence

$$N(t) = \left[\frac{\mathcal{D}_R}{\pi t}\right]^{\frac{1}{2}}[R_0 - R_1]\left[\frac{R_0^{\frac{1}{2}} + \frac{\gamma}{2}}{\left(\frac{R_0}{b}\right)^{\frac{1}{2}} \exp\left(\frac{a^2}{b}\right) \operatorname{erfc}\left(\frac{a}{b^{\frac{1}{2}}}\right)}\right] \qquad (A.3.20)$$

which gives

$$\Phi = \left[\frac{\mathcal{D}_R t}{\pi}\right]^{\frac{1}{2}}[A(R_0 - R_L)]\left[\frac{R_0 + \frac{\gamma}{2}}{\left(\frac{R_0}{b}\right)^{\frac{1}{2}} \exp\left(\frac{a^2}{b}\right) \operatorname{erfc}\left(\frac{a}{b^{\frac{1}{2}}}\right)}\right] \qquad (A.3.21)$$

where

$$a = \frac{\gamma(R_0 - R_L)}{2R_0(2R_0^{\frac{1}{2}} + \gamma) \exp\left(\frac{a^2}{b}\right) \operatorname{erfc}\left(\frac{a}{b^{\frac{1}{2}}}\right)} . \qquad (A.3.22)$$

$$b = \frac{R_0^{\frac{1}{2}} + \frac{K^{\frac{1}{2}}}{2}}{R_0^{\frac{1}{2}} + \frac{\gamma}{2}} + 2a^2\left(\frac{6R_0^{\frac{1}{2}}}{\gamma} + 1\right) \qquad (A.3.23)$$

$$\text{and} \quad \gamma = K^{\frac{1}{2}} \cdot \frac{\mathcal{D}_P}{\mathcal{D}_R} \qquad (A.3.24)$$

The results given in equations (A.3.21) to (A.3.24) are the same as those given by Olander [28] except that the expression defining the parameter b in equation (A.3.23) is multiplied by a factor of two. Professor Olander kindly submitted his derivations of his equations (86) to (88) and the writer wishes to acknowledge that the preceding derivation is based largely on his work. The discrepancy between the two expressions for the parameter b arises from the fact that Olander used a wrong expression for the Maclaurin's series.

The third term on the right hand side of equation (A.3.21) is a measure of the effect of the reaction on absorption rates and is denoted by F. The precision with which this factor allows for reaction effects can be estimated by comparing values of F calculated in this way (see Appendix 6, Procedure F Value) with those calculated from equation (A.3.9) for the special case $\mathcal{D}_P = \mathcal{D}_R$. The results of these calculations are shown in Table A.3.1 for conditions of interest in this investigation. It can be seen that the precision is not good and this no doubt results from terminating the Maclaurin series after two terms. The writer was unable to find any analytical technique which would improve the precision, and values of F calculated from equations (A.3.21) to (A.3.24) were arbitrarily corrected by replacing the factor 2 in equation (A.3.23) by the factor $6.60(R_0 - R_L)/R_0$. This was chosen by a trial and error procedure and, of course, cannot be justified except in so far as it preserves the general form of the solution and, in any case, the values of F are comparatively small. Values of F calculated using this correction factor are also shown in Table A.3.1 and it can be seen that, in general, the maximum discrepancy between calculated and required values is 0.2 percent; for very small ranges of conditions this rises to 0.8 percent. The corrected form of equation (A.3.23) together with equations (A.3.20), (A.3.21) and (A.3.24) are quoted in Section 1.2.1.2 of this thesis and were used to analyse absorption measurements.

TABLE A.1.1 CALCULATED VALUES OF THE REACTION FACTOR F FOR $\mathcal{D}_P/\mathcal{D}_R = 1.0$

(a) R_0, R_L Fixed; K Variable (Absorption of SO_2 into Water and Aqueous HCl)

R_0	R_L	$K^{\frac{1}{2}}$	F		
			Required	Before Correction	After Correction
1.400	0.0	0.010	1.009	1.006	1.008
1.400	0.0	0.030	1.025	1.018	0.025
1.400	0.0	0.050	1.042	1.030	1.041
1.400	0.0	0.070	1.059	1.041	1.058
1.400	0.0	0.090	1.076	1.053	1.075
1.400	0.0	0.110	1.093	1.065	1.092
1.400	0.0	0.130	1.110	1.077	1.109

TABLE A.1.1 (Cont.)

(b) R_0, K Fixed; R_L Variable (Absorption of SO_2 into Water and Aqueous SO_2)

R_0	R_L	$K^{\frac{1}{2}}$	F		
			Required	Before Correction	After Correction
1.360	0.00	0.150	1.129	1.090	1.128
1.360	0.20	0.150	1.093	1.084	1.105
1.360	0.40	0.150	1.083	1.079	1.089
1.360	0.60	0.150	1.077	1.075	1.079
1.360	0.80	0.150	1.073	1.071	1.072
1.360	1.00	0.150	1.069	1.068	1.070
1.360	1.20	0.150	1.066	1.066	1.066

TABLE A.1.1 (Cont.)

(c) R_L, K Fixed; R_0 Variable (Absorption of SO_2 into Water from Other Gases)

R_0	R_L	$K^{\frac{1}{2}}$	F		
			Required	Before Correction	After Correction
0.20	0.0	0.150	1.335	1.235	1.346
0.40	0.0	0.150	1.237	1.166	1.241
0.60	0.0	0.150	1.194	1.135	1.195
0.80	0.0	0.150	1.168	1.117	1.168
1.00	0.0	0.150	1.150	1.105	1.150
1.20	0.0	0.150	1.137	1.096	1.137
1.40	0.0	0.150	1.127	1.089	1.126

APPENDIX 4

ANALYSIS OF LAMINAR JET HYDRONAMICS

A.4.1 VELOCITY DISTRIBUTION AND BOUNDARY LAYER THICKNESS

Assume that the velocity distribution in the jet can be represented as shown in Fig. A.4.1. At the nozzle face, the velocity within a central core is uniformly flat; outside the core there is an anular boundary layer in which the velocity distribution can be represented by the equation:

$$\frac{V_{o,y}}{V_{o,c}} = 1.5 \left[\frac{Y}{\delta}\right] - 0.5 \left[\frac{Y}{\delta}\right]^3 \qquad (A.4.1)$$

Downstream of the nozzle the jet is affected simultaneously by its acceleration and momentum interchange between the core and the boundary layer. The result of this interchange is that the boundary layer thickness gradually decreases; finally, at some downstream section P, the boundary layer vanishes and the velocity distribution across the entire jet section becomes uniformly flat.

Write equations for conservation of mass and momentum and solve to obtain the relationship:

$$b = 2.094 \left[r^2 - 1 - AX \left\{\frac{1 + r}{r}\right\}^2\right] \qquad (A.4.2)$$

Estimate b for increasing values of X. As P is approached these estimates will approach a constant value; the value of X for which they become constant can be taken as the jet length required for the boundary layer to disappear.

Figure A.4.1

Figure A.4.1

Velocity Distribution in a Laminar Jet

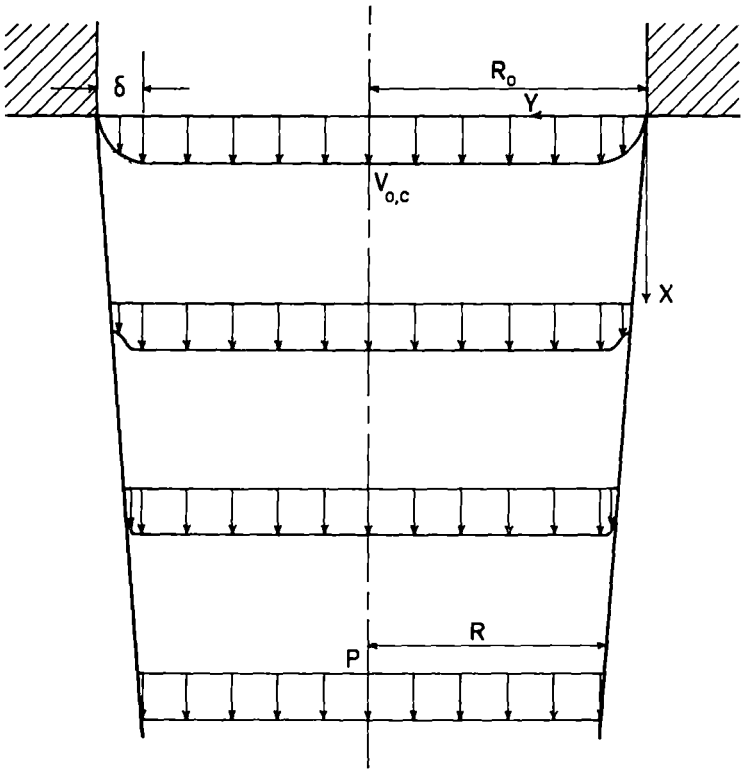
δ
R_o
Y
$V_{o,c}$
X
R
P

A.4.2 SURFACE VELOCITY OF THE JET

(a) Due to Gravity

In the absence of boundary layer effects write

$$\frac{V_{s,x}}{V_{o,av}} = \left[1 + \frac{2gX}{V_{o,av}^2}\right]^{\frac{1}{2}} \qquad (A.4.3)$$

(b) Due to Boundary Layer Effects

Assume the effect on surface velocity of the boundary layer is independent of gravitational effects.

(i) Consider an infinitely thin plate of length ℓ placed in a fluid moving in laminar flow parallel to the direction of flow. The width of wake produced is given by

$$W = \left[\frac{280}{13}\frac{\nu\ell}{V_u}\right]^{\frac{1}{2}} \qquad (A.4.4)$$

and the velocity distribution in the wake is described by an equation of the same form as equation (A.4.1). The fluid velocity in the wake at a distance X directly behind the plate is approximated by the relationships

$$\frac{V_w}{V_u} = a_1\xi(1 - a_2\xi^3 + a_3\xi^6) \; ; \; \xi^3 \leqslant 0.0486 \qquad (A.4.5)$$

and

$$\frac{V_w}{V_u} = 1 - \frac{a_4}{(\xi^3 + 0.13)^{\frac{1}{2}}} - \frac{a_5}{(\xi^3 + 0.13)} \; ; \; \xi^3 \geqslant 0.125 \qquad (A.4.6)$$

(ii) Assume that the jet boundary layer can be treated as two

dimensional and that the two problems are analogous. Then W can be replaced by , V_u by $V_{o,c}$ and V_w by V_s; i.e. write

$$\delta = \left[\frac{280}{13} \frac{\nu \ell}{V_{o,c}} \right] \tag{A.4.7}$$

$$\frac{V_s}{V_{o,c}} = a_1 \xi (1 - a_2 \xi^3 + a_3 \xi^6) \; ; \quad \xi^3 < 0.0486 \tag{A.4.8}$$

and

$$\frac{V_s}{V_{o,c}} = 1 - \frac{a_4}{(\xi^3 + 0.13)^{\frac{1}{2}}} - \frac{a_5}{(\xi^3 + 0.13)} \; ; \quad \xi^3 > 0.125 \tag{A.4.9}$$

Further, it can be shown that

$$V_{o,c} = \frac{V_{o,av}}{(1 - 3b/4 - b^2/5)} \tag{A.4.10}$$

A.4.3 SOLUTION OF THE DIFFUSION EQUATION FOR VARIABLE SURFACE VELOCITY

Consider an elemental volume in the boundary layer and carry out a mass balance. By neglecting second order terms it can be shown that the diffusion equation in the boundary layer reduces to

$$V_y \frac{\partial C}{\partial X} + V_x \frac{\partial C}{\partial Y} = \mathcal{D} \frac{\partial^2 C}{\partial Y^2} \tag{A.4.11}$$

The solution to this equation is given as

$$\frac{N_x}{N_{x,id}} = 2f(X) \left[\frac{\mathcal{D}X}{V_{o,av}} \right]^{\frac{1}{2}} \tag{A.4.12}$$

where

$$f(X) = \frac{V_s}{[B + 4\mathcal{D}\int V_s . dX]^{\frac{1}{2}}} \qquad (A.4.13)$$

is a function which accounts for the effect of radial velocity components in terms of the surface velocity.

The actual surface velocity cannot be calculated but equations (A.4.3), (A.4.8) and (A.4.9) are combined in the following way: Write

$$\frac{N_x}{N_{x,id}} = -1 + F_a + F_b = F_j \qquad (A.4.14)$$

By combining equations (A.4.12) and (A.4.13) separately with equations (A.4.3), (A.4.8) and (A.4.9), equations (A.4.15), (A.4.16) and (A.4.17) can be obtained:

$$F_a = \left[\frac{1 + \frac{2gX}{V_{o,av}}}{1 + \frac{2gX}{4V_{o,av}} - \frac{2gX}{24\,V_{o,av}^2}} \right]^{\frac{1}{2}} \qquad (A.4.15)$$

$$F_b = [1 - a_2\xi^3 + a_3\xi^6] \left[\frac{4a_1 V_{o,c}\xi}{(3V_{o,av})(1 - 4a_2\xi^3/7 + 2a_3\xi^6/5)} \right]^{\frac{1}{2}} ;$$

$$\xi^3 \leqslant 0.0486 \qquad (A.4.16)$$

$$F_b = \left[\frac{V_{o,c}}{V_{o,av}} \right]^{\frac{1}{2}} \frac{1 - a_4/(\xi^3 + 0.13)^{\frac{1}{2}} - a_5/(\xi^3 + 0.13)}{[1 - 1/\xi^3\{2a_4(\xi^3 + 0.13)^{\frac{1}{2}} + a_5 \ell n(\xi^3 + 0.13) - B/16\ell\mathcal{D}V_{o,c}\}]^{\frac{1}{2}}} ;$$

$$\xi^3 \geqslant 0.125 \qquad (A.4.17)$$

where B is evaluated by trial and error to give smooth transition from equation (A.4.16) in the region $0.0486 \leqslant \xi^3 \leqslant 0.125$.

APPENDIX 5

TABLE A.5.1 SOLUBILITY OF SULPHUR DIOXIDE IN WATER

20°C		30°C	
P_{SO_2} cm Hg	gm SO_2 per 100 gm H_2O	P_{SO_2} cm Hg	gm SO_2 per 100 gm H_2O
7.8	1.29	18.8	2.03
14.5	2.23	24.9	2.67
22.0	3.17	32.6	3.45
27.8	3.95	39.6	4.20
34.8	4.96	48.3	4.97
41.8	5.86	54.2	5.58
51.0	7.08	62.4	6.33
61.4	8.42	68.4	6.99
70.9	9.67	74.8	7.51
77.9	10.60	82.2	8.33

TABLE A.5.2 SOLUBILITY OF SULPHUR DIOXIDE IN AQUEOUS HCl AT 20°C

HCl = 0.120M		HCl = 0.323M		HCl = 0.614M		HCl = 1.31M	
P_{SO_2} mm Hg	gm SO_2 per 100 gm H_2O	P_{SO_2} mm Hg	gm SO_2 per 100 gm H_2O	P_{SO_2} mm Hg	gm SO_2 per 100 gm H_2O	P_{SO_2} mm Hg	gm SO_2 per 100 gm H_2O
221	2.89	290	3.80	394	5.04	224	2.86
364	4.75	373	4.86	537	6.93	371	4.82
473	6.25	468	6.02	652	8.41	482	6.33
572	7.50	568	7.25	748	9.67	588	7.72
666	8.71	664	8.49	857	11.06	694	9.15
798	10.42					802	10.54

TABLE A.5.3 VISCOSITIES OF AQUEOUS SULPHUR DIOXIDE SOLUTIONS AT 20°C

$$\eta = K_v.\theta.(\rho_B - \rho_L)$$

$K_v = 0.00912$; $\rho_B = 2.405$ gm/cc

C_t	ρ_L [81]	$\rho_B - \rho_L$	θ	η (cp)
0	0.998	1.407	78.36	1.005
0.178	1.003	1.402	80.88	1.034
0.382	1.010	1.395	82.60	1.051
0.518	1.014	1.391	83.65	1.061
0.792	1.023	1.382	85.36	1.076
1.050	1.031	1.374	86.90	1.089
1.146	1.034	1.371	87.60	1.095

TABLE A.5.4 ABSORPTION INTO WATER

Q	L	$4[QL]^{\frac{1}{2}}$	$\Phi'' \times 10^5$	$\Phi' \times 10^5$	$\Phi \times 10^5$
3.57	1.56	9.44	4.84	5.02	5.67
3.57	2.25	11.34	5.84	6.06	6.72
3.57	3.06	13.22	7.15	7.42	8.10
3.57	4.00	15.12	8.22	8.52	9.18
3.57	5.06	17.00	9.32	9.66	10.28
3.57	6.25	18.90	10.46	10.84	11.40
3.57	7.56	20.78	11.62	12.04	12.53
3.57	9.00	22.67	12.80	13.26	13.68
3.57	10.56	24.56	14.07	14.55	14.91
3.57	12.25	26.45	15.09	15.60	15.90

TABLE A.5.5 ABSORPTION INTO 1.053M AQUEOUS NaCl

Q	L	$4[QL]^{\frac{1}{2}}$	$\Phi'' \times 10^5$	$\Phi' \times 10^5$	$\Phi \times 10^5$
3.53	1.56	9.39	4.50	4.72	5.33
3.53	2.25	11.28	5.51	5.78	6.41
3.53	3.06	13.15	6.50	6.81	7.44
3.53	4.00	15.03	7.69	8.06	8.68
3.53	5.06	16.91	8.69	9.11	9.69
3.53	6.25	18.79	9.76	10.23	10.76
3.53	7.56	20.67	10.75	11.27	11.73
3.53	9.00	22.-5	11.89	12.47	12.87
3.53	10.56	24.42	12.90	13.52	13.86
3.53	12.25	26.30	14.00	14.68	14.96

TABLE A.5.6 ABSORPTION INTO AQUEOUS HCl

(a) HCl = 0.0280M

Q	L	$4[QL]^{\frac{1}{2}}$	$\Phi'' \times 10^5$	$\Phi' \times 10^5$	$\Phi \times 10^5$
3.57	1.45	9.10	4.48	4.65	5.27
3.57	2.14	11.06	5.50	5.71	6.36
3.57	2.95	12.98	6.59	6.85	7.50
3.57	3.89	14.91	7.82	8.12	8.76
3.57	4.95	16.82	8.95	9.30	9.90
3.57	6.14	18.73	10.04	10.43	10.98
3.57	7.45	20.63	11.21	11.65	12.14
3.57	8.89	22.54	12.36	12.84	13.26
3.57	10.45	24.43	13.42	13.94	14.29
3.57	12.14	26.33	14.44	15.00	15.29

TABLE A.5.6 (Cont.)

(b) HCl = 0.113M

Q	L	$4[QL]^{\frac{1}{2}}$	$\Phi'' \times 10^5$	$\Phi' \times 10^5$	$\Phi \times 10^5$
3.57	1.56	9.44	4.52	4.70	5.31
3.57	2.25	11.34	5.78	6.01	6.67
3.57	3.06	13.22	6.80	7.07	7.72
3.57	4.00	15.12	7,80	8.10	8.72
3.57	5.06	17.00	8.92	9.27	9.86
3.57	6.25	18.90	10.11	10.50	11.05
3.57	7.56	20.78	11.09	11.52	11.99
3.57	9.00	22.67	12.29	12.77	13.18
3.57	10.56	24.56	13.41	13.93	14.28
3.57	12.25	26.45	14.41	14.97	15.25

TABLE A.5.6 (Cont.)

(c) HCl = 0.481M

Q	L	$4[QL]^{\frac{1}{2}}$	$\Phi'' \times 10^5$	$\Phi' \times 10^5$	$\Phi \times 10^5$
3.55	1.56	9.41	4.57	4.77	5.39
3.55	2.25	11.30	5.65	5.89	6.53
3.55	3.06	13.18	6.62	6.92	7.56
3.55	4.00	15.07	7.74	8.09	8.71
3.55	5.06	16.95	8.77	9.16	9.75
3.55	6.25	18.84	9.92	10.39	10.93
3.55	7.56	20.72	10.97	11.49	11.96
3.55	9.00	22.61	12.03	12.62	13.02
3.55	10.56	24.49	13.12	13.76	14.10
3.55	12.25	26.38	14.22	14.92	15.20

TABLE A.5.6 (Cont.)

(d) HCl = 1.100M

Q	L	$4[QL]^{\frac{1}{2}}$	$\Phi'' \times 10^5$	$\Phi' \times 10^5$	$\Phi \times 10^5$
3.53	1.56	9.39	4.70	4.90	5.54
3.53	2.25	11.28	5.81	6.06	6.72
3.53	3.06	13.15	6.76	7.06	7.71
3.53	4.00	15.03	7.85	8.20	8.83
3.53	5.06	16.91	9.13	9.54	10.15
3.53	6.25	18.79	10.12	10.58	11.13
3.53	7.56	20.67	11.20	11.70	12.18
3.53	9.00	22.55	12.32	12.90	13.31
3.53	10.56	24.42	13.51	14.14	14.49
3.53	12.25	26.30	14.47	15.15	15.44

TABLE A.5.7 ABSORPTION INTO AQUEOUS SO_2

$C_{t,L} = 0.735, \quad C_{u,L} = 0.615$

Q	L	$4(QL)^{\frac{1}{2}}$	$\Phi'' \times 10^5$	$\Phi' \times 10^5$	$\Phi \times 10^5$
3.50	2.32	11.40	3.09	3.19	3.54
3.50	4.07	15.10	4.30	4.44	4.78
3.50	6.32	18.81	5.41	5.59	5.88
3.50	9.07	22.54	6.62	6.84	7.06

TABLE A.5.8 ABSORPTION INTO AQUEOUS NaOH

(a) NaOH = 0.287M

Q	L	$4[QL]^{\frac{1}{2}}$	$\Phi'' \times 10^5$	$\Phi' \times 10^5$	$\Phi \times 10^5$
3.55	1.56	9.41	5.53	5.76	6.51
3.55	2.25	11.30	6.93	7.21	8.00
3.55	3.06	13.18	8.46	8.81	9.62
3.55	4.00	15.07	9.76	10.16	10.94
3.55	5.06	16.95	11.04	11.49	12.23
3.55	6.25	18.84	12.34	12.85	13.52
3.55	7.56	20.72	13.69	14.22	14.80
3.55	9.00	22.61	15.06	15.65	16.15
3.55	10.56	24.49	16.32	16.96	17.38
3.55	12.25	26.38	17.67	18.36	18.71

TABLE A.5.8 (Cont.)

(b) NaOH = 0.472M

Q	L	$4[QL]^{\frac{1}{2}}$	$\Phi'' \times 10^5$	$\Phi' \times 10^5$	$\Phi \times 10^5$
3.54	2.25	11.29	7.72	7.97	8.84
3.54	3.06	13.17	9.25	9.56	10.44
3.54	4.00	15.05	10.81	11.17	12.03
3.54	5.06	16.93	12.28	12.69	13.50
3.54	6.25	18.82	13.83	14.29	15.03
3.54	7.56	20.70	15.25	15.75	16.40
3.54	9.00	22.58	16.84	17.40	17.96
3.54	10.56	24.45	18.48	19.09	19.57
3.54	12.25	26.34	19.79	20.44	20.83

TABLE A.5.9 ABSORPTION INTO WATER FROM NITROGEN

SO_2 = 80% v/v

(a) Gas Inlet Flow = 4.1 cc/sec

Q	L	$4(QL)^{\frac{1}{2}}$	Inlet P_{SO_2}	$\Phi'' \times 10^5$	$\Phi' \times 10^5$	$\Phi_\cdot \times 10^5$	$\Phi \times 10^5$ $P_{SO_2} = 60.0$
3.56	1.70	9.84	59.8	3.46	3.50	3.96	3.97
3.56	2.39	11.67	59.8	4.13	4.18	4.64	4.65
3.56	3.20	13.50	59.7	4.73	4.79	5.23	5.26
3.56	4.14	15.36	59.7	5.45	5.51	5.93	5.96
3.56	5.20	17.21	59.8	6.11	6.18	6.58	6.60
3.56	6.39	19.08	59.8	6.59	6.66	7.01	7.03
3.56	7.70	20.94	59.8	7.23	7.30	7.60	7.62
3.56	9.14	22.81	59.8	7.64	7.71	7.96	7.98
3.56	10.70	24.68	59.8	8.14	8.21	8.42	8.45
3.56	12.39	26.56	59.8	8.71	8.79	8.96	8.99

TABLE A.5.9 (Cont.)

(b) Gas Inlet Flow = 5.9 cc/sec

Q	L	$4(QL)^{\frac{1}{2}}$	Inlet P_{SO_2}	$\Phi'' \times 10^5$	$\Phi' \times 10^5$	$\Phi \times 10^5$	$\Phi \times 10^5$ $P_{SO_2} = 60.0$
3.57	2.25	11.33	60.4	4.25	4.30	4.77	4.74
3.57	3.06	13.22	60.5	5.01	5.07	5.54	5.49
3.57	4.00	15.11	60.4	5.75	5.82	6.27	6.23
3.57	5.06	17.00	60.4	6.47	6.55	6.97	6.92
3.57	6.25	18.89	60.4	7.14	7.23	7.61	7.56
3.57	7.56	20.78	60.4	7.97	8.07	8.40	8.34
3.57	9.00	22.67	60.4	8.60	8.70	8.98	8.92
3.57	10.56	24.56	60.4	9,29	9.40	9.64	9.58
3.57	12.25	26.45	60.4	9.86	9.98	10.17	10.10

TABLE A.5.9 (Cont.)

(c) Gas Inlet Flow = 8.7 cc/sec

Q	L	$4(QL)^{\frac{1}{2}}$	Inlet P_{SO_2}	$\Phi'' \times 10^5$	$\Phi' \times 10^5$	$\Phi \times 10^5$	$\Phi \times 10^5$ $P_{SO_2} = 60.0$
3.56	4.14	15.36	60.5	6.14	6.17	6.65	6.59
3.56	5.20	17.21	60.6	6.92	6.95	7.39	7.31
3.56	6.39	19.08	60.6	7.71	7.75	8.15	8.07
3.56	7.70	20.94	60.6	8.46	8.52	8.87	8.78
3.56	9.14	22.81	60.6	9.24	9.30	9.60	9.50
3.56	10.70	24.68	60.6	10.05	10.12	10.37	10.27
3.56	12.39	26.56	60.6	10.95	10.92	11.13	11.02

TABLE A.5.10 ABSORPTION INTO WATER FROM NITROGEN

SO_2 = 60% v/v

(a) Gas Inlet Flow = 2.7 cc/sec

Q	L	$4(QL)^{\frac{1}{2}}$	Inlet P_{SO_2}	$\Phi'' \times 10^5$	$\Phi' \times 10^5$	$\Phi \times 10^5$	$\Phi \times 10^5$ P_{SO_2} = 45.0
3.56	1.70	9.84	45.3	2.23	2.25	2.54	2.52
3.56	2.39	11.67	45.3	2.59	2.61	2.89	2.87
3.56	3.20	13.50	45.3	2.95	2.97	3.24	3.22
3.56	4.14	15.36	45.3	3.30	3.33	3.59	3.57
3.56	5.20	17.21	45.3	3.53	3.56	3.79	3.76
3.56	6.39	19.08	45.3	3.83	3.85	4.05	4.02
3.56	7.70	20.94	45.3	4.02	4.04	4.21	4.18
3.56	9.14	22.81	45.3	4.25	4.28	4.42	4.39
3.56	10.70	24.68	45.3	4.45	4.48	4.59	4.56
3.56	12.39	26.56	45.3	4.67	4.70	4.79	4.76

TABLE A.5.10 (Cont.)

(b) Gas Inlet Flow = 4.1 cc/sec

Q	L	$4(QL)^{\frac{1}{2}}$	Inlet P_{SO_2}	$\Phi'' \times 10^5$	$\Phi' \times 10^5$	$\Phi \times 10^5$	$\Phi \times 10^5$ $P_{SO_2} = 45.0$
3.56	2.39	11.67	45.8	2.86	2.88	3.19	3.13
3.56	3.20	13.50	45.8	3.26	3.28	3.58	3.52
3.56	4.14	15.36	45.9	3.73	3.75	4.04	3.96
3.56	5.20	17.21	45.9	4.10	4.12	4.38	4.30
3.56	6.39	19.08	45.9	4.48	4.51	4.74	4.65
3.56	7.70	20.94	45.9	4.87	4.90	5.10	5.00
3.56	9.14	22.81	45.8	5.14	5.17	5.34	5.25
3.56	10.70	24.68	45.9	5.55	5.58	5.72	5.61
3.56	12.39	26.56	46.0	5.87	5.91	6.02	5.89

TABLE A.5.10 (Cont.)

(c) Gas Inlet Flow = 6.6 cc/sec

Q	L	$4(QL)^{\frac{1}{2}}$	Inlet P_{SO_2}	$\Phi'' \times 10^5$	$\Phi' \times 10^5$	$\Phi \times 10^5$	$\Phi \times 10^5$ $P_{SO_2} = 45.0$
3.56	4.14	15.36	45.0	3.98	4.01	4.32	4.32
3.56	5.20	17.21	45.0	4.43	4.46	4.75	4.75
3.56	6.39	19.08	45.1	4.95	4.98	5.24	5.23
3.56	7.70	20.94	45.1	5.41	5.45	5.67	5.66
3.56	9.14	22.81	45.1	5.86	5.90	6.09	6.08
3.56	10.70	24.68	45.1	6.29	6.33	6.49	6.48
3.56	12.39	26.56	45.1	6.66	6.71	6.84	6.82

TYPICAL CALCULATIONS

Absorption of Sulphur Dioxide into 1.100 M Aqueous Hydrochloric Acid

		Run 1	Run 2
Jet length (cm)		12.25	12.25
Jet Flow (cc/sec)		3.53	3.53
$4(QL)^{\frac{1}{2}}$		26.30	26.30
Total gas flow rates: Flowmeter volumes (cc):			
Inlet = 99.7			
Outlet = 39.9			
Flow times (sec):	Inlet	24.44	24.39
	Outlet	76.2	75.0
Flow rates: To absorption		4.075	4.090
From absorption		0.524	0.532
Gas temperatures (°C):			
To inlet meter		19.2	19.2
From inlet meter		20.8	20.8
Average		20.0	20.0
To outlet meter		19.8	19.8
From outlet meter		21.3	21.3
Average		20.6	20.6
Gas pressures (cm Hg):			
Gas to absorption		76.2	76.2
Absorption chamber		76.2	76.2
Gas from absorption		76.2	76.2

	1	2	Avge.
Water vapour pressures:			
Gas to absorption	1.7	1.7	
Gas from absorption	1.8	1.8	
Sulphur dioxide flow rates (cc/sec at N.T.P.):			
To absorption	3.718	3.728	
From absorption	0.475	0.483	
Sulphur dioxide absorbed (cc/sec at N.T.P.):	3.243	3.245	3.244
(moles/sec x 10^5) (Φ'')			14.47
Liquid temperatures (°C):			
To nozzle			20.5
Interface			21.6
Water vapour pressure at interface (cm Hg)			2.0
Partial pressure of sulphur dioxide at interface (cm Hg)			74.2
Correction factors:			
Heat effects ($K_1.K_2$)			1.012
Temperature $\left[\frac{C_t.\overline{\vartheta}_t^{\frac{1}{2}}(20.0°C)}{C_t.\overline{\vartheta}_t^{\frac{1}{2}}(20.5°C)}\right]$			
(estimated from diffusion data in Ref.[179] and solubility data in Refs.[105,132])			
Pressure (76.0/74.2)			1.024
Total			1.047
Sulphur dioxide absorbed at 76.0 cm Hg and 20.0°C:			
(moles/sec x 10^5) (Φ')			15.15
Hydronamic correction factor (F_h)			1.019
Sulphur dioxide absorbed at 76.0 cm Hg and 20.0°C in an ideal jet (moles/sec x 10^5) (Φ)			15.44

APPENDIX 6

ALGOL PROGRAMME FOR NUMERICAL INTEGRATION

```
begin    integer i,dorder,forder,dplus1,fplus1;
         real a,b,x,integral; switch S:=next; sameline; freepoint(6);
         print ££1?TOTAL JET ABSORPTION INTEGRALS£12??;
next:    read a; if a<0.0 then stop;
         read b,dorder,forder;
         dplus1:=dorder+1; fplus1:=forder+1;
              begin real array D[1:dplus1],F[1:fplus1];
                   real procedure poly(x,a,n); value x,n; real x; integer n; array a;
                        begin integer i; real y;
                             y:=a[n+1];
                             for i:=n step -1 until 1 do y:=y*x+a[i];
                             poly:=y;
                        end;
                   real procedure function(x); value x; real x;
                        begin real y;
                             y:=poly(x,D,dorder)*poly(x,F,forder);
                             if x<0.0 then print ££1?FUNCTION ERROR?,stop;
                             if x<10^-4 then function:=0.0 else function:=y/sqrt(x);
                        end function;
```

ALGOL PROGRAMME FOR NUMERICAL INTEGRATION (continued)

```
                real procedure simps(f,x,a,b,eps); value a.b.eps; real f,x,a,b,eps;
                    begin real Z1,Z2,Z3,h,k; switch s:=again,done;
                        if a=b then begin h:=0.0; goto done end;
                        x:=a; Z1:=f; x:=b; Z1:=Z1+f; k:=(b-a)/2.0;
                        x:=a+k; Z2:=f; Z3:=Z1+4.0*Z2; Z1:=Z1+2.0*Z2;
again:                  Z2:=0; h:=k/2;
                        for x:=a+h step k until b do Z2:=Z2+f;
                        Z1:=Z1+4.0*Z2;
                        if Z1≠0 then begin if abs((Z1-2.0*Z3)/Z1)<eps then goto done end
                                else if abs((Z1-2.0*Z3)*h)/3.0<10^-8 then goto done ;
                        Z3:=Z1; Z1:=Z1-2.0*Z2; k:=h; goto again;
done:                   simps:=h*Z1/3.0
                    end simps;
                for i:=1 step 1 until dplus1 do read D[i];
                for i:=1 step 1 until fplus1 do read F[i];
                integral:=simps(function(x),x,a,b,10^-5);
                print ££1?FOR THE RANGE?,a,£ TO?,b,£ INTEGRAL IS?,integral;
            end of inner block;
        goto next;
end of program;
```

ALGOL PROGRAMME "CURVEFIT"

```
begin  integer n,m,nless1,mplus1;  sameline;  digits(3);  scaled(5);
       read n,m;  nless1:=n-1;  mplus1:=m+1;
          begin integer i,j;
             real f,x,y;
             real array X,FF,F,W[0:nless1],coeff[1:mplus1];
             switch SS:=lsfail,over;
             procedure LSQFIT3(x,y,w,N,R,nplus1,eps,exit);  value N,nplus1,eps;  integer N,nplus1;
             real eps;  real array x,y,R,w;  label exit;
                begin integer i,j,k;  real p,q,xk;  real array B[1:nplus1,1:nplus1];  integer
                                                                          array D[1:nplus1];
                      procedure ATOLU1(a,r,n,eps,singular);  value n,eps;  integer n;  real eps;
                                                                          real array a;
                      integer array r;  label singular;
                         begin integer i,j,k,piv,ri,rk;
                               real det,pivot,arki;
                               for i:=1 step 1 until n do r[i]:=i;
                               det:=1.0;
                               for i:=1 step 1 until n do
                                   begin piv:=i;  ri:=r[i];  pivot:=a[ri,i];
                                         for k:=i+1 step 1 until n do
                                         if abs(a[r[k],i])>abs(pivot) then begin piv:=k; pivot:=
                                                                          a[r[k],i] end;
```

ALGOL PROGRAMME "CURVEFIT" (continued)

```
                if abs(pivot)<eps then
                   begin  print ££12?MATRIX SINGULAR£1?OR ILL-CONDITIONED
                                                                £12??;
                          goto singular
                   end;
                det:=det*pivot;
                ri:=r[piv]; r[piv]:=r[i]; r[i]:=ri;
                for j:=i+1 step 1 untiln do a[ri,j]:=a[ri,j]/pivot;
                for k:=i+1 step 1 until n do
                    begin  rk:=r[k];  arki:=a[rk,i];
                           for j:=i+1 step 1 until n do a[rk,j]:=a[rk,j]-
                                                          arki*a[ri,j]
                           end k
            end i;
    end ATOLU1;
procedure LU1SOL(a,b,r,n); value n;  real array a,b;  integer array r;
                                                          integer n;
    begin integer i,j,ri,iless1;
          real procedure sigma(tk,k,a,b);  value a,b;  real tk;  integer k,a,b;
              begin real  sum;  sum:=0.0;
```

ALGOL PROGRAMME "CURVEFIT" (continued)

```
                for k:=a step 1 until b do sum:=sum+tk;  sigma:=sum
            end sigma;
        for i:=1 step 1 until n do
            begin  ri:=r[i];  iless1:=i-1;
                   b[ri]:=(b[ri]-sigma(a[ri,j]*b[r[j]],j, ,iless1))/a[ri,i]
            end;
        for i:=n-1 step -1 until 1 do
            begin  ri:=r[i];
                   b[ri]:=b[ri]-sigma(a[ri,j]*b[r[j]],j,i+1,n)
            end
    end LU1SOL;
procedure PERMB(b,r,n);  value n;  real array b;  integer array r;  integer n;
    comment rearranges the elements of b[1:n]
            so that b[i]:=b[r[i]],i=1,2,....,n;
    begin integer i,k;  real w;  switch S:=L;
        for i:= n step -1 until 2 do
            begin  k:=r[i];
        L:         if k≠i then
                       begin  if k>i then begin k:=r[k]; goto L end;
                              w:=b[i];  b[i]:=b[k];  b[k]:=w
                       end
```

ALGOL PROGRAMME "CURVEFIT" (continued)

```
                end i;
          end PERMB;
       for i:=1 step 1 until nplus1 do
          begin  R[i]:=0.0;  for j:=1 step 1 until ido B[i,j]:=0.0  end;
       for k:=0 step 1 until N do
          begin p:=w[k];  xk:=x[k];
                for i:=1 step 1 until nplus  do
                   begin q:=1.0;
                         for j:=1 step 1 until i do begin B[i,j]:=B[i,j]+p*q;
                                                          q:=q*xk end;
                         R[i]:=R[i]+p*y[k];  p:=p*xk
                   end
          end;
       for i:=2 step 1 until nplus1 do
         for j:=i-1 step -1 until 1 do
            B[j,i]:=B[i,j];
       A TO LU1(B,D,nplus1,eps,exit);
       LU1 SOL(B,R,D,nplus1);
       PERMB(R,D,nplus1)
end LSQFIT3;
```

ALGOL PROGRAMME "CURVEFIT" (continued)

```
            for i:=0 step 1 until nless1 do
               begin read X[i],F[i],W[i];
                     FF[i]:=F[i]
               end for i;
            LSQFIT3(X,F,W,nless1,coeff,mplus1,10^-6,lsfail); goto over;
lsfail:     print ££12?LEAST SQUARES FIT FAILURE?,stop;
over:       print ££12?CURVE FITTING WITH A POLYNOMIAL OF ORDER?,m,
            ££12?COEFFICIENTS ARE : £1t?POWER OF X £t2?COEFFICIENT?;
            for i:=1 step 1 until mplus1 do
            print ££1ts3??,(i-1),££t2??, coeff[i];
            print ££12?INPUT POINTS AND FITTED CURVE £12??,
            ££1t2?X£t2?INPUT£t2?CALC£t2?DIFF£1??;
            for i:=0 step 1 until nless1 do
               begin f:=FF[i];  x:=X[i];
                     y:=coeff[mplus1];
                     for j:=m step -1 until 1 do y:=x*y+coeff[j];
                     print ££1ts8??,x,££ts8??,f,££ts8??,y,££ts8??,(f-y);
               end for i;
         end inner block;
end of program
```

ALGOL PROGRAMME "CHEBFIT"

```
begin  integer i,j,m,n;  real x,sum;  switch s:=L;
       procedure chebfit(x,y,n,a,m);  value  n,m;
       array x,y,a;  integer n,m;
       begin  integer i,j,k,mplus1,ri,i1,imax,rj,j1;  switch s:=start,swap,fit;
              real d,h,ai1,rhi1,denom,ai,rhi,xj,hmax,
                   himax,xi,hi,abshi,nexthi,prevh;
              interger array r[0:m+1];  array rx,rh[0:m+1];
              mplus1:=m+1;  prevh:=0;
              comment index vector for initial reference set;
              r[0]:=1;  r[mplus1]:=n;
              d:=(n-1)/mplus1;  h:=d;
              for i:=1 step 1 until m do
              begin r[i]:=h+1;  h:=h+d end;
       start: h:=1.0;
              for i:=0 step 1 until mplus1 do
              begin ri:=r[i];
                    rx[i]:=x[ri];  a[i]:=y[ri];
                    rh[i]:=h:=-h
              end i;
```

ALGOL PROGRAMME "CHEBFIT" (continued)

```
for j:=0 step 1 until m do
begin i1:=mplus1;  ai1:=a[i1];
      rhi1:=rh[i1];
      for i:=m step -1 until j do
      begin denom:=rx[i1]-rx[i-j];
            ai:=a[i];  rhi:=rh[i];
            a[i1]:=(ai1-ai)/denom;
            rh[i1]:=(rhi1-rhi)/denom;
            i1:=i;  ai1:=ai;  rhi1:=rhi
      end i
end j;
h:=-a[mplus1]/rh[mplus1];
for i:=0 step 1 until mplus1 do
a[i]:= a[i]+rh[i]*h;
for j:=m-1 step -1 until 0 do
begin xj:=rx[j];  i:=j;  ai:=a[i];
      for i1:=j+1 step 1 until m do
      begin ai1:=a[i1];
            a[i]:=ai-xj*ai1;
            ai:=ai1;  i:=i1
```

ALGOL PROGRAMME "CHEBFIT" (continued)

```
      end i1
end j;
hmax:=abs(h);
if hmax<prevh then
begin a[mplus1]:=-hmax;  goto fit end;
a[mplus1]:=prevh:=hmax;  imax:=r[0];  himax:=h;
j:=0;  rj:=r[j];
for i:=1 step 1 until n do
if i≠rj then
begin xi:=x[i];  hi:=a[m];
      for k:=m-1 step -1 until 0 do
      hi:=hi*xi+a[k];
      hi:=hi-y[i];  abshi:=abs(hi);
      if abshi>hmax then
      begin hmax:=abshi;  himax:=hi;  imax:=i end
end
else
if j<mplus1 then
begin j:=j+1;  rj:=r[j] end;
if imax=r[0] then
begin for i:=0 step 1 until mplus1 do
```

ALGOL PROGRAMME "CHEBFIT" (continued)

```
      if imax<r[i] then goto swap;
      i:=mplus1;
swap: nexthi:= if i-i div 2*2=0 then h else -h;
      if himax*nexthi ≥ 0 then r[i]:=imax
      else
      if imax<r[0] then
      begin j1:=mplus1;
            for j:=m step -1 until 0 do
            begin r[j1]:=r[j];  j1:=j end;
            r[0]:=imax
      end
      else
      if imax>r[mplus1] then
      begin j:=0;
            for j1:=1 step 1 until mplus1 do
            begin r[j]:=r[j1];  j:=j1 end;
            r[mplus1]:=imax
      end
      else r[i-1]:=imax;
      goto start
```

ALGOL PROGRAMME "CHEBFIT" (continued)

```
            end;
      fit:
      end chebfit;
      sameline;  digits(2);  freepoint(8);
L:    read n;  if n=0 then print ££r5h??,stop;
      begin real array X,Y[1:n];  switch s:=L1;
            print ££l?TEST REVISED ACM 91?;
            for i:=1 step 1 until n do read X[i],Y[i];
L1:         read m;  if m=0 then goto L;
            begin real array A[0:m+1];
                  chebfit(X,Y,n,A,m);  print ££l?ORDER OF POLYNOMIAL m=?,m;
                  print ££l?COEFFICIENTS CONSTANT TERM FIRST?;
                  for i:=0 step 1 until m+1 do print ££l??,A[i];
                  print £  =MAXIMUM ERROR?;
                  print ££l?OBSERVED£t?COMP£t?ERROR?;
                  for i:=1 step 1 until n do
                  begin x:=X[i];  sum:=A[m];
                        for j:=m-1 step -1 until 0 do
                        sum:=sum*x+A[j];
                        print ££l??,Y[i],££t??,sum,££t??,Y[i]-sum
```

ALGOL PROGRAMME "CHEBFIT" (continued)

```
                    end;
                    goto L1
                end
            end
        end of programme;
```

ALGOL PROGRAMME "F VALUE"

```
begin  real A,B,K,C,X,Y,a,lowa,higha,b,rootb,rootA,eps,F,zero;
       switch S:=next,error,over;
       real procedure erfc(x);  value x;  real x;
            begin real poly;
                 if x>4.0 then erfc:=0.0
                 else begin poly:=1.0+x*(7.0523078₁₀-2+x*(4.22820123₁₀-2+x*(9.2705272₁₀-3+x*(1.520143₁₀
                                                                    -4+x*(2.765672₁₀-4+x*(4.30638₁₀-5))))));
                           poly:=poly*poly;
                           poly:=poly*poly;
                           erfc:=1.0/(poly*poly)
                      end
            end;
       real procedure a value(a);  value a;  real a;
       comment determines value of a;
            begin real pi,rootpi,KC,G,function;  switch S:= out;
                 pi:=3.14159;  rootpi:= sqrt(pi);  rootA:= sqrt(A);
                 KC:=K*C;  X:=(rootA+K/2.0)/(rootA+KC/2.0);
                 Y:=((rootA*6.0)/(KC)+1.0);  b:=(X+2.0*a*a*Y);  rootb:= sqrt(b);
                 G:= erfc(a/rootb);
```

```
                if G=0.0 then
                     begin print ££1?ERFC=0.0 FOR THESE DATA?;
                           function:=10+70;
                           goto out
                     end;
                function:= rootb*KC*(A-B);
                function:=function/(2.0*rootpi*A*(2.0*rootA+KC)* exp(a*a/b)*G;

out:    a value:=a-function;
           end;
        real procedure bisec(f,x,a,b,eps,error);  value a,b,eps;  real f,x,a,b,eps;  label error;
           begin real q;  x:=a;  q:=f;  x:=b;
                if f*q≥0 then goto error;
                q:=(b-a)*sign(q)/2.0;  x:=(a+b)/2.0;  eps:=eps/2.0;
                for q:=q/2.0 while abs(q)>eps do x:=x+(if f>0 then q else -q);
                bisec:=x
           end bisec;
        sameline;  scaled(6);
        read eps;
next:   read A;  if A<0.0 then stop;
        read B,C,K,lowa,higha;  print ££1? INPUT DATA=?,A,B,C,K;
        zero:=bisec(a value(a),a,lowa,higha,eps,error);
```

```
      goto over;
error: print ££1?BISEC ERROR?;  goto next;
over:  F:=(rootb*(rootA+(K*C/2.0)))/(rootA*exp(a*a/b)*erfc(a/rootb));
       print ££1?AA=?,a,££t?BB=?,b,££t?F=?,F;
       goto next;
end of program;
```

ACKNOWLEDGMENT

Many people have contributed to this project, some more than others. To list the contribution made by each would be fatuous but the author would like to record his very sincere gratitude for the assistance given by the following people: Mr. A.P. Beswick; Prof. H. Bloom; Mr. J.R. Boothroyd; Mr. D. Brooks; Dr. R.F. Cane; Dr. G.H. Cheesman; Messrs. B. Chinchella, A.R. Christian, K.R. Christian; R.M. Davies, and W.P.U. Dixon; Mrs. J. Edwards; Messrs. A.J. Finney, and E. Forsyth; Mr. J.C. Horner; Dr. F.H.C. Kelly; Messrs., D. Millwood, J. Moule and W.A. Neale; Prof. D.R. Olander; Miss T. Orlova; Prof. A.R. Oliver; Messrs. D. Paget and C.A. Richards; Dr. N.K. Roberts; Miss M.W. Smith; Dr. P.W. Smith; Mr. E.L. Valentine and Mrs. E. Wiley.